



**THESIS APPROVAL**  
**GRADUATE SCHOOL, KASETSART UNIVERSITY**

Master of Engineering (Advanced and Sustainable Environmental Engineering)  
**DEGREE**

Advanced and Sustainable Environmental Engineering      Engineering  
**FIELD**      **FACULTY**

**TITLE:** Marine Litter Transportation in the Phang-Nga Bay, Andaman Sea,  
Thailand

**NAME:** Miss Rungtip Junlah

**THIS THESIS HAS BEEN ACCEPTED BY**

**THESIS ADVISOR**

( Assistant Professor Pasinee Worachananant, Ph.D. )

**THESIS CO-ADVISOR**

( Mr. Sornthep Vannarat, Ph.D. )

**GRADUATE COMMITTEE  
CHAIRMAN**

( Associate Professor Thongchai Rohitatisha Srinophakun, Ph.D. )

**APPROVED BY THE GRADUATE SCHOOL ON** \_\_\_\_\_

**DEAN**

( Associate Professor Gunjana Theeragool, D.Agr. )

THESIS

MARINE LITTER TRANSPORTATION IN THE PHANG-NGA BAY,  
ANDAMAN SEA, THAILAND



RUNGTIP JUNLAH

A Thesis Submitted in Partial Fulfillment of  
the Requirements for the Degree of  
Master of Engineering (Advanced and Sustainable Environmental Engineering)  
Graduate School, Kasetsart University  
2015

Rungtip Junlah 2015: Marine Litter Transportation in the Phang-Nga Bay, Andaman Sea, Thailand. Master of Engineering (Advanced and Sustainable Environmental Engineering), Major Field: Advanced and Sustainable Environmental Engineering, Faculty of Engineering. Thesis Advisor: Assistant Professor Pasinee Worachananant, Ph.D. 196 pages.

Marine litter is defined as a pollutant in water body which reached the sea from both main land and off shore. Plastic has a large share in marine litter found in the sea because of its persistence and buoyancy properties. This study aims to investigate marine litter transportation, especially plastic and floating marine litter, based upon oceanic circulation in the Andaman Sea by applying Finite Volume Coastal and Oceanic Model (FVCOM) and particle tracking technique. The buoy test has been conducted to estimate actual marine litter movement in six study sites along the coastal Andaman Sea. Oceanic circulation in general tide and tide in coupled with 10-m wind in two monsoons, Northeast and Southwest monsoons are then simulated and the particle tracking analysis was performed. Results obtained from simulation are validated, and it has revealed a good agreement between observation and simulation. Overall, residual current in the Andaman Sea driven by only tide has very calm velocity except at the near shore and shallow water, and has various directions, whereas that in Northeast monsoon tends to have stronger currents' velocity moving westerly. Meanwhile, residual current during Southwest monsoon has tendency to move landwards. Particle tracking technique reveals that marine litter in Andaman Sea is dispersed out of the origins through either tide or tide coupled with wind driving. However, tide coupled with wind driving seems to transport floating marine particle farther than solely tidal force with maximum distance of 80-90 km within 90 days. The results from this study are valuable and beneficial for waste management along coastal line in Andaman Sea.

---

Student's signature

---

Thesis Advisor's signature

## ACKNOWLEDGEMENTS

I would like to express my deep gratitude to Dr. Pasinee Worachananant, my advisor, and Dr. Sornthep Vannarat in Large Scale Simulation Research Laboratory, National Electronics and Computer Technology Center, Thailand, my co-advisor, as well as the rest of my committee members, for their benevolence, support, and advice. I also would like to express my gratitude towards Assoc. Prof. Yoshimura Chihiro, Department of Civil Engineering, Tokyo Institute of Technology, Japan, for devoting his time to give me kind and invaluable advice. During my experimental learning, I have also received very kind valuable advices from Mr. Saifhon Tomkratoke and Dr. Sirod Sirisup; I, therefore, would like to express my deep gratitude to both of them. Working under their supervision has been a very honorably memorable experience as there were many significant discussions and revealing knowledge.

I would like to sincerely thank my committee chairman, Asst. Prof. Dr. Wirong Chanthorn and Dr. Pinsak Suraswadi for their valuable guidance during my examination session. My gratitude is also extended to other related people for their mentally and spiritually support during my difficulties. My grateful expression also goes to Advanced and Sustainable Environmental Engineering of Thailand Advanced Institute of Science and Technology and Tokyo Institute of Technology, National Science and Technology Development Agency, Thailand for the greatest opportunities given to me. Special thanks also go to the Phuket Marine Biological Center for useful available resources during my fieldtrip experiment and Marine Department and Hydrographic Department for contributed information.

Last but not least, I could not fail to mention the kindness and unconditionally support from my family and beloved friends. Their love and enthusiastic encouragement have truly motivated and inspired me in the rough times.

Rungtip Junlah

December 2014

## TABLE OF CONTENTS

	<b>Page</b>
TABLE OF CONTENTS	i
LIST OF TABLES	ii
LIST OF FIGURES	v
LIST OF ABBREVIATIONS	xii
INTRODUCTION	1
OBJECTIVES	5
LITERATURE REVIEW	7
MATERIALS AND METHODS	25
Materials	25
Methods	27
RESULTS AND DISCUSSION	40
CONCLUSION AND RECOMMENDATIONS	161
Conclusion	161
Recommendations	163
LITERATURE CITED	164
APPENDICES	170
Appendix A Floating buoy experiment	171
Appendix B Tidal harmonic analysis obtained from T_Tide Package	174
Appendix C Linear Regression summary of tidal validation	191
CURRICULUM VITAE	196

## LIST OF TABLES

<b>Table</b>		<b>Page</b>
1	Example of marine litter categorized by origins	8
2	Analyzing food wrapper and its label to detect their potential sources	15
3	Study site for this buoy experiment	27
4	Buoys observation at Patong Beach and theirs velocities	44
5	Buoys observation at Yao Noi island and their velocities	48
6	Buoy observation at Panyee island and their velocities	52
7	Buoys observation at Phi Phi islands and their velocities	54
8	Buoys observation at Saphan Hin and their velocities	59
9	Buoys observation at Kuraburi and their velocities	63
10	Tidal amplitude (m) and its percent reduction difference of harmonic constituents of tidal amplitude	68
11	Tidal phase ( $^{\circ}$ ) and its error statistic of harmonic constituents of tidal elevation	69
12	Form number for tidal characteristic at four stations	77
13	Displacement profile of marine particles at Phang-Nga bay	98
14	Displacement profile of marine particles originated from coastal line of mainland	104
15	Displacement profile of marine particles originated from Phuket	112
16	Displacement profile of marine particles originated from Yao islands	120
17	Displacement profile of marine particles originated from Phi Phi islands	127
18	Displacement profile of marine particles originated from Racha Yai island	134
19	Displacement profile of marine particles originated from Racha Noi island	141
20	Displacement profile of marine particles originated from Lanta Yai island	148

### LIST OF TABLES (Continued)

<b>Table</b>	<b>Page</b>
21 Displacement profile of marine particles originated offshore	157
 <b>Appendix Table</b>	
B1 Tidal amplitude and phase with 95% CI estimates of observation data at Ao Por station	175
B2 Tidal amplitude and phase with 95% CI estimates of simulation data at Ao Por	177
B3 Tidal amplitude and phase with 95% CI estimates of observation data at Kuraburi station	179
B4 Tidal amplitude and phase with 95% CI estimates of simulation data at Kuraburi station	181
B5 Tidal amplitude and phase with 95% CI estimates of observation data at Tapao Noi Station	183
B6 Tidal amplitude and phase with 95% CI estimates of simulation data at Tapao Noi Station	185
B7 Tidal amplitude and phase with 95% CI estimates of observation data at Tarutao Station	187
B8 Tidal amplitude and phase with 95% CI estimates of simulation data at Tarutao Station	189
C1 Residuals of tidal elevation linear regression between observation and simulation at Ao Por	192
C2 Coefficients of tidal elevation linear regression between observation and simulation at Ao Por	192
C3 Residuals of tidal elevation linear regression between observation and simulation at Tapao Noi	193

**LIST OF TABLES (Continued)**

<b>Appendix Table</b>	<b>Page</b>
C4 Coefficients of tidal elevation linear regression between observation and simulation at Tapao Noi	193
C5 Residuals of tidal elevation linear regression between observation and simulation at Kuraburi	194
C6 Coefficients of tidal elevation linear regression between observation and simulation at Kuraburi	194
C7 Residuals of tidal elevation linear regression between observation and simulation at Tarutao	195
C8 Coefficients of tidal elevation linear regression between observation and simulation at Tarutao	195

## LIST OF FIGURES

Figure		Page
1	Scope of work	4
2	Schema represents lifecycle of marine litter	10
3	Decomposition rate of various marine litters in the ocean	11
4	Marine litter on the Beach at Lanta island taken on 13 July, 2007	13
5	Marine litter (expired date: 18 December, 2007) found at Kata Noi Beach, Phuket, on November 1, 2008	15
6	Monsoon in the Southeast Asia Region of the Andaman Sea where (a) is Northeast Monsoon and (b) is Southwest Monsoon, and the bold arrows indicate wind speed of 0.25-0.50 m/s	18
7	Comparison of water elevation in between analytic and computation simulated by FVCOM and POM	21
8	Basic classes of oceanic model grid where structured grid is used by POM, ECOM and ROMS and unstructured grid is used by ADCIRC (FE), SELFE (FE) and FVCOM	22
9	Schematic diagram of method used in this research	26
10	Light floatable Styrofoam is assumed to be a buoy	28
11	Study sites for buoy test	29
12	The topography of the Andaman Sea	31
13	Model configuration covered the Andaman Sea and bay of Bengal	32
14	Study boundary and model configuration	33
15	Winds that influence the Andaman Sea are (a) Northeast monsoon (February, 2013) and (b) Southwest monsoon (September, 2013)	36
16	Study sites for buoy test along the Andaman coast of southern Thailand covering places locating in Phang-Nga, Phuket and Krabi	40
17	Buoy test of Western current at Patong beach which located at the Southwest of Phuket.	41

## LIST OF FIGURES (Continued)

Figure		Page
18	Daily water level at Patong, Phuket represented by Tapao Noi island on 17 <sup>th</sup> November, 2013 (Hydrographic Department)	42
19	Floatable buoys at Patong beach at different locations and times where (a) is Buoy 1, (b) is Buoy 2 and (c) is Buoy 3	43
20	Buoy test was conducted at the North of Yao Noi island, Phang-Nga bay	45
21	Daily water level at Yao Noi island, Phang-Nga represented by Tapao Noi island on 20 <sup>th</sup> November, 2013 (Hydrographic Department)	46
22	Floatable buoys at Yao Noi island where (a) is Buoy 1, (b) is Buoy 2 and (c) Buoy 3 which was weighted by 240g lead at 50 cm depth at different times	47
23	Buoy test was conducted at Panyee island, located at Phang-Nga bay	49
24	Daily water level at Panyee island, Phang-Nga represented by Tapao Noi island on 21 <sup>st</sup> November, 2013 (Hydrographic Department)	50
25	Floatable buoys at Panyee island where (a) is Buoy 1, (b) is Buoy 2, (c) is Buoy 3 and (d) is Buoy 4 which was weighted by 240g lead at 50 cm depth at different times	51
26	Buoy test was conducted at Phi Phi Don, the Southwest of Phi Phi island	53
27	Daily water level at Phi Phi islands, Krabi represented by Tapao Noi island on 26 <sup>th</sup> November, 2013 (Hydrographic Department)	54
28	Three floatable buoys at Phi Phi Don at different time where (a) is Buoy 1, (b) is Buoy 2 and (c) is Buoy 3	55
29	Buoy test of the eastern current at Saphan Hin which is locate at the Southeast of Phuket	56

## LIST OF FIGURES (Continued)

Figure		Page
30	Daily water level at Saphan Hin, Phuket represented by Tapao Noi island on 28 <sup>th</sup> November, 2013 (Hydrographic Department)	57
31	Four floatable buoys at Sapha Hin at variable time where (a) is Buoy 1, (b) is Buoy 2, (c) is Buoy 3 and (d) is Buoy 4	58
32	Buoy test was conducted at the site where is facing open Andaman Sea at Kuraburi, Phang-Nga province	60
33	Daily water level at Kuraburi, Phang-Nga represented by Kuraburi on 30 <sup>th</sup> November, 2013 (Hydrographic Department)	61
34	Floatable buoys in Kuraburi at variable time where (a) is Buoy 1, (b) is Buoy 2, (c) is Buoy 3 and (d) is Buoy 4 which was weighted by 240g lead at 50 cm depth at different times	62
35	Comparison of time series tidal elevation at Ao Por for 41 days where black line is observation and red line is simulation	65
36	Comparison of time series tidal elevation at Tapao Noi for 41 days where black line is observation and red line is simulation	65
37	Comparison of time series tidal elevation at Kuraburi for 41 days where black line is observation and red line is simulation	66
38	Comparison of time series tidal elevation at Tarutao for 41 days where black line is observation and red line is simulation	67
39	Histogram of water level difference between observation and simulation for 328 sampling hours during 41 days at (a) Ao Por, (b) Tapao Noi, (c) Kuraburi and (d) Tarutao	71
40	Linear regression of water level between observation (m) and simulation (m) at (a) Ao Por, (b) Tapao Noi, (c) Kuraburi and (d) Tarutao	74
41	Tidal rotary current demonstrated its velocity, direction and water level at Saphan Hin, Phuket for four periods of tide.	78

## LIST OF FIGURES (Continued)

Figure		Page
42	Sea water level (m) of flood current during (a) high tide and (b) mean tide and ebb current during (c) mean tide and (d) low tide at Phang-Nga bay	79
43	Magnitude of residual surface current in (a) Andaman Sea and (b) Phang-Nga bay under the tidal dominated condition predicted by FVCOM	81
44	Directional vector of residual current in Andaman Sea during under tidal dominated condition predicted by FVCOM	82
45	Directional vector of residual current in Phang-Nga bay under tidal dominated condition predicted by FVCOM	83
46	Magnitude of residual surface current in (a) Andaman Sea and (b) Phang-Nga bay during Northeast monsoon predicted by FVCOM	85
47	Directional vector of residual current in the Andaman Sea during Northeast monsoon predicted by FVCOM	87
48	Directional vector of residual current in Phang-Nga bay during Northeast monsoon predicted by FVCOM	88
49	Magnitude of residual surface current in (a) the Andaman Sea and (b) Phang-Nga bay during Southwest monsoon predicted by FVCOM	90
50	Directional vector of residual current in the Andaman Sea during Southwest monsoon predicted by FVCOM	91
51	Directional vector of residual current in Phang-Nga during Southwest monsoon predicted by FVCOM	92
52	Locations of tracing marine litter movement in the Andaman Sea	93
53	Transportation of marine litters in Phang-Nga bay between (a) Day 1 and Day 90 under the condition of (b) tidal dominant, (c) Northeast monsoon and (d) Southwest monsoon	96

## LIST OF FIGURES (Continued)

Figure		Page
54	Histogram of particle displacement (m) at Phang-Nga bay in three case scenarios	99
55	Transportation of marine at coastal line of mainland between (a) Day 1 and Day 90 under the condition of (b) tidal dominant, (c) Northeast monsoon and (d) Southwest monsoon	102
56	Histogram of particle displacement (m) at coastal line of mainland in three case scenarios	105
57	Transportation path of marine litters originated from the coastal of Phang-Nga bay under the condition of (a) tidal dominant, (b) Northeast monsoon and (c) Southwest monsoon	106
58	Transportation of marine litters at Phuket between (a) Day 1 and Day 90 under the condition of (b) tidal dominant, (c) Northeast monsoon and (d) Southwest monsoon	110
59	Histogram of particle displacement (m) at Phuket in three case scenarios	113
60	Transportation path of marine litters originated from Phuket under the condition of (a) tidal dominant, (b) Northeast monsoon and (c) Southwest monsoon	114
61	Transportation of marine litters at Yao islands between (a) Day 1 and Day 90 under the condition of (b) tidal dominant, (c) Northeast monsoon and (d) Southwest monsoon	118
62	Histogram of particle displacement (m) at Yao islands in three case scenarios	121
63	Transportation path of marine litters originated at Yao islands under the condition of (a) tidal dominant, (b) Northeast monsoon and (c) Southwest monsoon	122

## LIST OF FIGURES (Continued)

Figure		Page
64	Transportation of marine litters at Phi Phi islands between (a) Day 1 and Day 90 under the condition of (b) tidal dominant, (c) Northeast monsoon and (d) Southwest monsoon	125
65	Histogram of particle displacement (m) at Phi Phi islands in three case scenarios	128
66	Transportation path of marine litters originated from Phi Phi islands under the condition of (a) tidal dominant, (b) Northeast monsoon and (c) Southwest monsoon	129
67	Transportation of marine litters at Racha Yai island between (a) Day 1 and Day 90 under the condition of (b) tidal dominant, (c) Northeast monsoon and (d) Southwest monsoon	132
68	Histogram of particle displacement (m) at Racha Yai island in three case scenarios	135
69	Transportation path of marine litters originated from Racha Yai island under the condition of (a) tidal dominant, (b) Northeast monsoon and (c) Southwest monsoon	136
70	Transportation of marine litters at Racha Noi island between (a) Day 1 and Day 90 under the condition of (b) tidal dominant, (c) Northeast monsoon and (d) Southwest monsoon	139
71	Histogram of particle displacement (m) at Racha Noi island in three case scenarios	142
72	Transportation path of marine litters originated from Racha Noi island under the condition of (a) tidal dominant, (b) Northeast monsoon and (c) Southwest monsoon	143
73	Transportation of marine litters at Lanta Yai island between (a) Day 1 and Day 90 under the condition of (b) tidal dominant, (c) Northeast monsoon and (d) Southwest monsoon	146

## LIST OF FIGURES (Continued)

<b>Figure</b>		<b>Page</b>
74	Histogram of particle displacement (m) at Lanta Yai island in three case scenarios	149
75	Transportation path of marine litters originated at Lanta Yai island under the condition of (a) tidal dominant, (b) Northeast monsoon and (c) Southwest monsoon	150
76	Transportation of marine litters at offshore between (a) Day 1 and Day 90 under the condition of (b) tidal dominant, (c) Northeast monsoon and (d) Southwest monsoon	155
77	Histogram of particle displacement (m) at Offshore of Phang-Nga bay at three case scenarios	158
78	Transportation path of marine litters originated from offshore of Phang-Nga bay under the condition of (a) tidal dominant, (b) Northeast monsoon and (c) Southwest monsoon	159
 <b>Appendix Figure</b>		
A1	Buoy was left freely floating on sea surface	172
A2	Buoy was driven and stuck at the fishing gears in coastal zone	172
A3	Buoy reached the muddy land during low tide	173
A4	Buoys were stuck on rocky cave during current driven	173

## LIST OF ABBREVIATIONS

A.M.	=	Ante Meridiem (before midday)
cm/s	=	Centimeter per second
EFDC	=	Environmental Fluid Dynamics Computer
EPA	=	Environmental Protection Agency
FVCOM	=	Finite Volume Coastal Oceanic Model
g	=	Gram
GEBCO	=	General Bathymetric Chart of the Oceans
GFS	=	Global Forecast System
GPS	=	Global Positioning System
K1	=	Amplitude of Luni-solar diurnal
KMO	=	Kommunenenes Internasjonale Miljøorganisasjon
M2	=	Amplitude of Principal lunar
m/s	=	Meter per second
NOAA	=	National Oceanic and Atmospheric Administration
NOMADS	=	NOAA Operational Model Archive and Distribution System
O1	=	Amplitude of Principal lunar diurnal
P.M.	=	Post meridiem (after midday)
PMBC	=	Phuket Marine Biological Center
POM	=	Princeton Ocean Model
ROMS	=	Regional Ocean Modeling System
S2	=	Amplitude of Principal solar
TMD	=	Tidal Model Driver
UNEP	=	United Nation for Environmental Program
WSPA	=	World Society for the Protection of Animals
WWF	=	World Wildlife Fund

# **MARINE LITTER TRANSPORTATION IN THE PHANG-NGA BAY, ANDAMAN SEA, THAILAND**

## **INTRODUCTION**

Marine litter is defined as solid materials of human activities that are discarded – accidentally or intentionally—at sea or reach the sea through waterways or through domestic and industrial outfalls (The United States Environmental Protection Agency [EPA], 2002). It could be found near the original source or, often, transported in long distance; it results in trans-boundary issue in some particular areas (United Nations Environment Programme [UNEP], 2005). The source of marine litter is simply categorized by either from land or from sea; they are called land-based and sea-based, respectively. Main-land base source is waste along the river basin, industrial facility, and municipal landfill and recreation activities. And the main sea-based source is shipping or cruise line, fishing line and gear, offshore oil and platforms.

Major source of marine litter is floatable litter such as plastic - including beverage bottles, packing containers and mixed plastic - because of its durability and persistence. Plastic is very persistence to natural bio-degradation; it is still doubtful how long it exactly lasts in the ocean, but it seems to durable 3-10 years (Jose, 2002). Due to its density which is closely to the density of seawater, it is easily to be carried by the currents (World Society for the Protection of Animals [WSPA], 2012). It has been found that 89 percent of floatable marine litter on the oceanic surface in the North Pacific is plastic.

The marine litter effects the conservation of species and local economic in tourism. Marine litter interferes fishing boat and gear; it also derogates the coastal scenery (WSPA, 2012). Plastic bag can be wrapped around boat's propellers and stuck in the engine. Even though there has no any catastrophic impact caused by marine litter in Thai coastal The Andaman Sea, it is clearly reported that high tourism value were affected by visual beauty (UNEP, 2009). Plastic litter, up to twenty-eight

percent, has been found in a marine mammal's stomach in South America (Pablo *et al.*, 2011). Some scientists believed that dolphin ingested plastic because they thought it was their prey, or it was an item they can play with.

Monitoring can clarify type, source and distribution mechanism of marine litter and it eventually leads to strategic plan and implementation by various management agencies. But according to many beach clean-up programs along the coastal zone in Thailand, it is unable to identify source and accumulated zone to pick up the rubbishes. There is very little detailed work on physical process of current pattern of the sea in East Asian region (UNEP, 2009). Therefore, to address marine litter in action, it is important to understand the ocean current pattern and marine litter's transport mechanism. Oceanic current pattern, wind and tide carry marine litter to many places and long-range transport before it deposited on shoreline or settle on the seabed.

Along the coastal of southern region of Thailand where is connected to the Andaman Sea, weather is classified into two monsoonal seasons which are affected by trade winds. The former is Northeast monsoon which causes dry environment, and it lasts from December to June. The latter is Southwest monsoon which is wet season and last from July to November. Simulation of current pattern in the Andaman Sea could provide a tool for better understanding on marine litter movement in The Andaman Sea along coastal Thailand. And by using oceanographic numerical model and particle tracking, we are possible to observe marine litter transportation over years with the suggestion of potential transportation path.

Finite Volume Coastal Oceanic Model (FVCOM) is an oceanic model; it is successfully applied in a number of estuarine, continental shelf and regional or open sea studies (Changsheng *et al.*, 2006) because of its unstructured grids. For example, water elevation from tidal solution compared very well with observed elevation and current data with M2 component of less than 3 cm in amplitude and 5° in phase. The similarly good performed result from simulation under tidal solution is also expressed at Rookey bay and Naples bay, Banks of Newfoundland, Gulf of Maine and New

England Shelf, East China Sea, Florida, Fukuoka bay in Japan, Gulf of Mexico, Chao Phraya River. Furthermore, there are evidences showing that FVCOM has well performed in developed model of particle tracking on sea surface (Wang and Shen, 2010). Particle tracking technique uses model's prediction of current velocity to calculate individual's movement in space and time. It serves set of recommendations for particle movement in ocean and estuary.

Accordingly, this study aims to investigate current pattern of The Andaman Sea which influences floatable marine litter transport mechanism by FVCOM. And it finally reveals the movement of marine litter on the sea surface in different scenarios based upon monsoonal seasons and the origins such as mainland and islands.

## SCOPE OF WORK

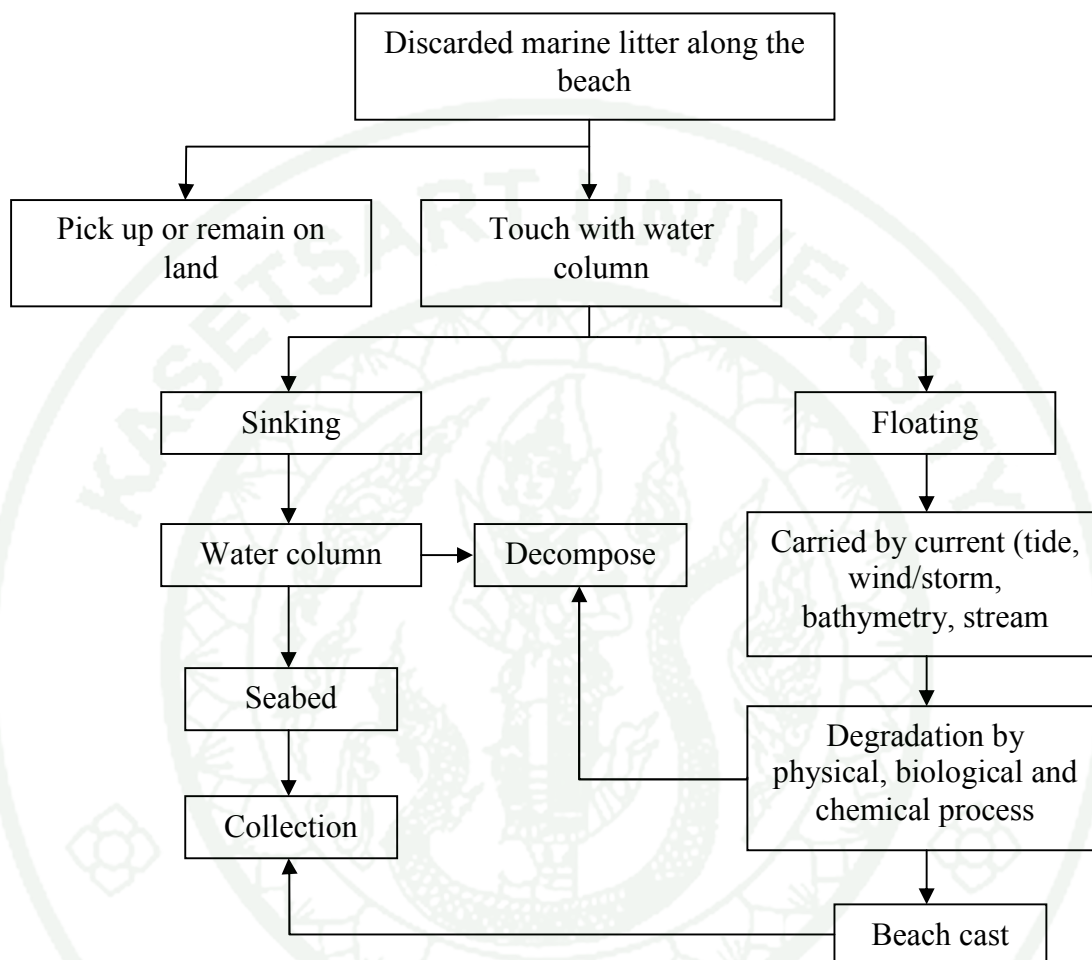


**Figure 1** Scope of work

## OBJECTIVES

Followings are the objectives of this study:

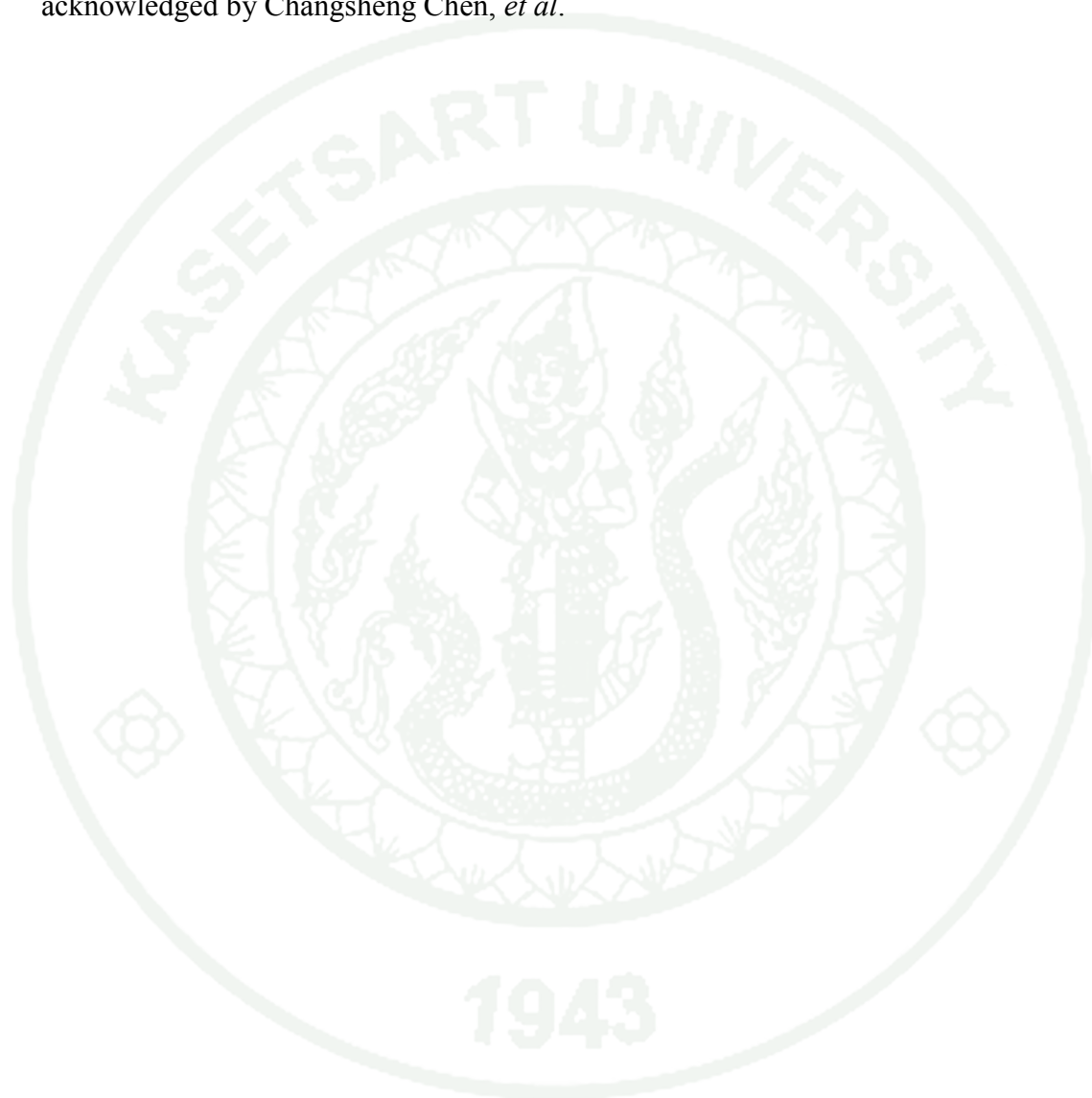
1. To study current characteristic and pattern at the Andaman Sea which influences to floating marine litter transportation by using oceanic modeling
2. To study and compare marine litter transportation on the water surface especially the coastal Andaman Sea in Thailand carried by tide and tide coupled with monsoons

### Scope of works

This research is mainly focused on transportation of floatable marine litter which originates from mainland and island at the coastal areas of the Andaman Sea in the southern part of Thailand. To perform long distance transport of floatable marine litter, FVCOM (Finite Volume Coastal Ocean Model) is used to determine current velocity as well as validated with collected data. Model is forced by tide obtained from TOPEX 7.2, Tidal Model Driver (TMD) and 10-m wind obtained from Global Forecast System (GFS) Model. Lastly, particle tracking technique is applied in order to visualize marine litter transportation in space and time. However, there are other several factors contributing to current pattern and transport of floating marine litter such as steams, meteorological condition and salinity; we have assumed the studied scenarios to be in the sea between litters' origin and destination. In addition, meteorological data such as rainfall, short wave energy and evaporation rate and salinity data is not continually collected all over the domain; hence, uniform forcing data would be inappropriate.

Water elevation at four stations along southern coast of Thailand is contributed with both genuine measurement and calculation. Gauge is deployed at Ao Por by Marine Department, whereas water level based upon tide at Kuraburi, Tapao Noi island and Tarutao island is calculated by Hydrographic Department. In real

environment, buoy is assumed to be a marine litter which floats on water surface; therefore, buoy experiment is conducted in order to observe its travelling pattern during a period of time. It is, then, used to compare the result with particle tracking obtained from FVCOM. Hydro dynamic model FVCOM is developed and acknowledged by Changsheng Chen, *et al.*



# LITERATURE REVIEW

## Marine litter

### 1. Definition and characteristic

Marine litter is first defined as solid materials of human origin that are discarded at sea or reach the sea through waterways or through domestic and industrial outfalls. It could be any persistent, manufactured or processed materials discarded or abandoned in the marine or coastal environment. It consists of items that have been made or used by human and littered into the sea, rivers or on beaches; brought indirectly to the sea by river, storm or wind; accidentally lost, including material lost at sea in bad weather such as fishing gear and net; or intentionally discarded by people on coastal line (UNEP, 2005).

In general, four main size of marine litter are classified as: mega-litter (>100mm diameter); macro-litter (20-100 mm diameter); meso-litter (5-20 mm diameter); and micro-litter (0.3-5 mm diameter) (Stevenson, 2011).

Marine litters are primarily from many sources. According to international beach clean-up activity which gained volunteers from 108 countries and locations around the world in 2009, it reports that 64% of picked marine litter is from shoreline and recreational activities, 25% of which is from smoking related activities and only 8% of marine litter is from waterway (Catherine and Kate, 2010).

Therefore, types of marine litter are also categorized by its source both from land-based and sea-based. The main sea-based source is shipping or cruise line, fishing line and gear, offshore oil and platforms. Main-land base source is waste along the river basin, industrial facility, and municipal landfill and recreation activities as described and exemplified in Table 1.

**Table 1** Example of marine litter categorized by origins

<b>land-based source</b>	<b>Sea-based source</b>
<u>Beachgoers:</u> Food packing, beverage containers, cigarette butts, toys	<u>Offshore oil and gas platform:</u> Any items that lost from offshore platform can become marine litter
<u>Improper trash disposal on land:</u> Discharge from rainfall and municipal wastewater that reaches sea by waterway. It contains any waste that come long the water as well as any trash that discarded carelessly.	<u>Military and Research Vessels:</u> Rubbish from vessels may be accidentally released into the water or may be deliberately thrown overboard.
<u>Industrial wastewater:</u> Production scarps, flawed products, packaging materials, plastic resin pellets	<u>Ship, boat and other vessel:</u> Fishing gears, nets, crab pots, fishing line, other type of fishing equipment
<u>Storm water discharges:</u> Storm drains collect runoff water which is generated during heavy rain.	<u>Recreational boat:</u> Bags, packaging, fishing gears

**Source:** Michelle *et al.* (1992)

Lost and discarded fishing gear is a primary cause for environmental, economic and public safety concern, but plastic is the most widespread of marine litter item which is ingested by marine animals and leads to major health issues and frequently death (UNEP, 2009). Plastic and polystyrene are consistently found to be main contributor to marine litter all over the world. In many regions, plastic materials constitute as much as 90 - 95% of the total amount of marine litter. For example, it is reported that 89 percent of floatable marine litter on the surface is plastic - including polystyrene, polyethylene, nylon, polypropylene, polycarbonate and polyvinyl chlorine –according to survey in 1998. This is because it is durable and persistent. Plastic is hardly broken down through chemical, physical and biological process. Its

highly buoyant allows them to transport a thousands of mile and persist to marine environment up to 600 years (UNEP, 2009).

## 2. Fate and distribution of marine litter

As mentioned earlier that marine litter is sourced from various activities both land-based and marine based. Fate of marine litter depends on density of the item. The item with density greater than seawater will sink into the water column and might transported with the internal wave or reach the seabed. The lighter material, which its density is lighter than seawater, drifts on the surface current.

Marine litter can be found not only in urban and extensive populated region, but also the area which far away from the sources (UNEP, 2005). It is a fact that dispersion of marine litter is contributed by large-scale and/or local surface current, bottom current, and wind from different sources and to different places. Because of those mentioned natural factors, a number of marine litters will remain visible by floating on the surface. It has been reported that floating marine litter such micro –plastic detected at southern California coastal water is found in water at 56 – 68% of sampling stations. Also, NOAA and the Joint Institute for Study of Atmosphere and the Ocean at University of Washington revealed that the amount of plastic in surface samples considerably base upon seasons and lotions (Stevenson, 2011). And unidentified numbers of marine litter will be mixed in water column and accumulated on the seabed because the floatable particle can be sunk if it is broken down to size of small grain of sand and slowly travel in vertical direction (Edyvane *et al.*, 2004). Consequently, it is very crucial to have as much knowledge as possible regarding to current pattern in general, current circulation and weather system in an area as a background for marine litter management on individual beaches and off-shore area.

To sum up, the fate of marine litter lifecycle is presented in Figure 2. Once marine litter touches sea environment, it will either float along the sea surface or sink in water column based upon the items' density. If the item floats, it can travel in a

long distance and might be physically and chemically broken down into fragments. It is also possible that the complete feature or fragment of marine litter will reach either the beach cast and be collected or sediment. But the worst case is marine litter traveling in long distance and gradually breaking down into small pieces before it caused death of marine faunas and other damages.

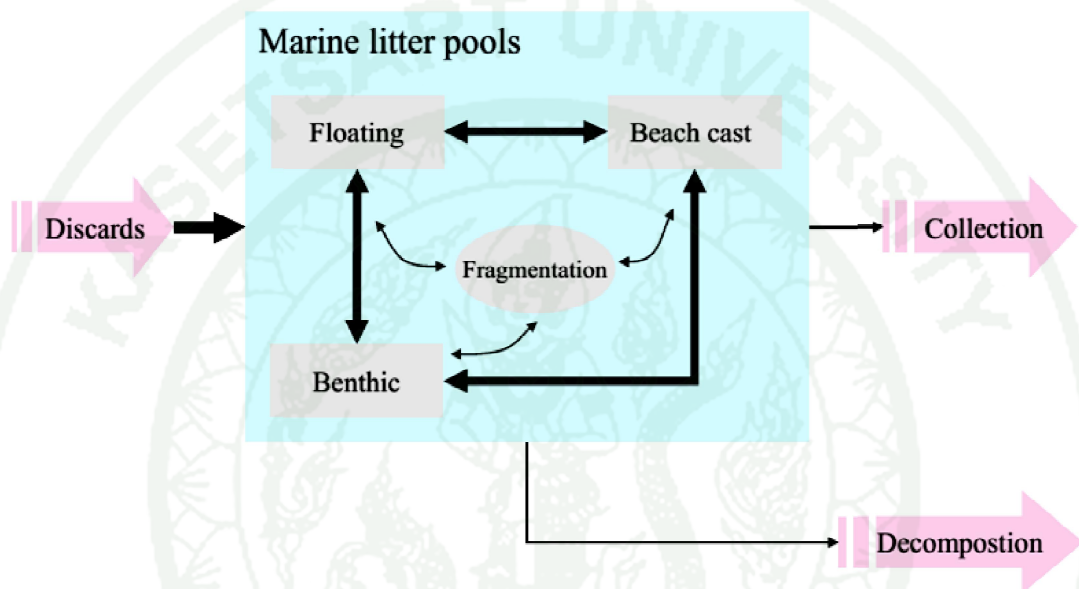


**Figure 2** Schema represents lifecycle of marine litter

**Source:** UNEP (2009)

The transport of objects in the ocean driven by current is technically referred to as drift. It can be dispersed across the Pacific Ocean. For instance, the litter from Fukushima's power plant hit by great tsunami in 2010 at Japan was predicted to drift in North Pacific Subtropical Gyre and reach Hawaiian islands in two year time. An oceanic model was used to project the oceanic current and buoyant particle in a period of time due to oceanic dynamic (Maximenko, 2011).

Item's characteristic that contributes to identify whether that item will float or sink is weight and volume. Objects will float in water if the weight is less than the same volume of water. On the other hand, if it is heavy than the same volume of

water, it sinks. Transportation of floating marine litter is contributed by surface currents and winds, complicating inferences about their origins (Iván and Martin, 2009).

Marine litter can be broken down by natural process in physical, chemical and biological mechanisms. The degradation period is identified by item's composition such as chemical composition, molecular weight and additives, environmental condition and other factors. It is reported that plastic takes longer degradation process in the ocean than on the land due to low temperature (Courtney, n.d.). In addition, degradation time for some items that are chiefly found in oceanic environment is demonstrated in Figure 3. Plastic bags would estimate to take up-to 20 years to degrade while plastic bottles would need 450 years to decompose in the oceanic environment.

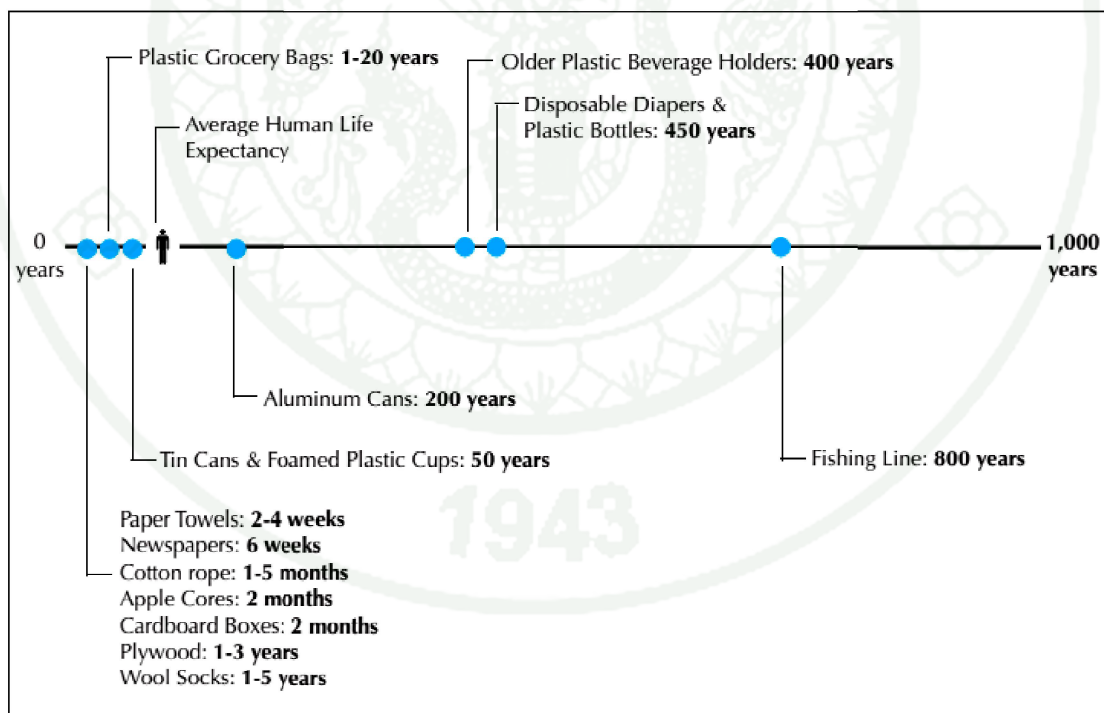


**Figure 3** Decomposition rate of various marine litters in the ocean

**Source:** Stevenson (2011)

### 3. Effect of marine litter

Discarding litter into the world's sea of ocean is substantial and represents a growing threat to marine environment and industry; it is, therefore, environmental, economic and anthropological problem. Some costs are transparent such as risk to community, property and livelihood, while beach-cleaning and suffering and death of wildlife are not so obvious and have only been recognized and discussed recently.

In socio-economic aspect, it causes the damages in loss of aesthetics and visual amenity, hazard to swimmer and drivers and loss for clean-up, recovery and disposal. Marine litter accumulated along the East coast of Sweden caused clean-up cost 1,125,000 Euros per year, more or less, even if 80 per cent of the litter did not originate in Sweden. Likewise, tourism industry in Thailand has got an impact due to marine litter as the litter derogates its beauty such as Lanta island at Krabi and Patong Beach at Phuket (Greenfins, 2007; WSPA, 2012).

In environmental aspect, wildlife such as whale, sea turtle and dolphin has suffered from marine plastic and litter. Effects to marine organism are entanglement and ingestion. Entanglement results in death of at least hundreds of thousands of marine animals and birds. It is generally because of abandoned fishing net and gear. It has been reported according to global beach clean-up activities (International Coastal Cleanup 25<sup>th</sup> Anniversary) that marine wildlife found entangled in marine litter including; 138 birds, 89 fishes, 55 invertebrates, 19 reptiles, 23 mammals and 12 amphibians (Catherine and Kate, 2010).

In Thailand, coral reef, which plays an important role as a fish nursery, in continental shelf of Chumporn and Nakornsrihammarat provinces is usually covered by fishing net discarded in the sea from fishing sector (Greenfins, 2007). Nevertheless, there is no report regarding to economic loss as well as ecological service loss because of fishing gears to coral reefs in this area.

#### 4. Marine litter in Thailand

Marine litter also unavoidably causes negative impact to economic sector especially tourism industry and coral ecosystem. It has been reported on news many times that marine animals and rare animal species have been destroyed from these marine litters (Stevenson, 2011). Damage from marine litter originated from both land and sea causes negative impacts to tourism industry is appeared at Lanta island (Figure 4), Patong beach in Phuket and Pattaya because it affects to visual amenity. Kommunenes Internasjonale Miljøorganisasjon or KIMO evidently suggested that people tend to avoid littered beach, and the UK residents spent 6.7 billion pound on holidays and day trip. This can aid to roughly estimate economic impact of marine litter to tourism industry (Tom, 2010).



**Figure 4** Marine litter on the Beach at Lanta island taken on 13 July, 2007

**Source:** Greenfins (2007)

Thailand's top five litter of year 2014 are plastic bag (17.18%), straw (11.48%), Styrofoam containers (8.28%), bottle lid (7.05%) and drink can (6.89%), according to beach cleaning up activities that have been tremendously promote by Department of Marine and Coastal Resource (Department of Marine and Coastal

Resources [DMCR], 2014). It is also reported that Bang-Sean beach, a famous tourist attraction at Chonburi, was accumulated marine litters which has not been produced in the local area. Even though many marine litters have been found in many places, it has not yet been identified both source of marine litter and its accumulation site (UNEP, 2009). In term of international cooperation, it can be considered as one of trans-boundary issue. It is not only the big issue like transportation across the ocean, but it is also adjacent area such as shared sea. For example, in Black Sea, half of marine litter sampled from Turkish beach in the West of Black sea coast was labeled in foreign languages (Topçu *et al.*, 2013).

In Thailand, there have been several plans in enhancing and studying more about marine litters. Recently, beach survey method has been developed among working group in Department of Marine Coastal and Resources. In addition, Thailand has joined International Beach Clean-up hosting by Ocean Conservancy. Lastly, during author's personal volunteering in Malaysia with AYVP (Asian Youth Volunteer Program), volunteers who stayed at Terengganu, the East side of Malaysian Peninsula has been running beach cleanup for 3 weeks. They revealed that the label of litters picked up on the beach were Thai, Bahasa and Indonesian. Even if there was no evident data on the litter quantity and type of litter, it clearly presents that marine litter along the coastal zone of Asian region is allowed to travel like other areas.

In Phuket, Thailand, Martin (2011) has been explored and counted marine litter on The Andaman coast, Phuket, Thailand, in late August 2008. While analyzing 1,127 food wrapper lables, 74% of single use plastic bags and food wrappers were of Thai origin, details as shown in Table 2. Moreover, a plastic wrap perished almost a year prior to beach survey has been found in perfect condition as exhibited in Figure 5.

**Table 2** Analyzing food wrapper and its label to detect their potential sources

Percent	Language	Country of origin
74%	Thai	Thailand
6.5%	Bahasa/others	Indonesia
3.5%	Malay/others	Malaysia
2%	Burmese/others	Myanmar
1.5%	Hindi	India
12.5%	unidentifiable	Unidentifiable

Source: Martin (2011)



**Figure 5** Marine litter (expired date: 18 December, 2007) found at Kata Noi Beach, Phuket, on November 1, 2008

Source: Martin (2011)

## Ocean

The coastal ocean (continental shelf and estuary zone) is where the community meets the sea, where freshwater mixes with seawater, where important biodiversity services such as mangrove forest and coral reef locate, and where commercial transportation and recreation belong (Robert *et al.*, 2004). Conversely, it is also where the negatively huge natural phenomena such as tsunami, storm surge and algae bloom occurred. For the importance of coastal utility itself, a numbers of researches regarding to coastal ecosystem and biodiversity, oceanography, air-sea interaction and numerical oceanic model have been continually and intensively studied in recent decades. There are many crucial factors contributing to characteristic of coastal zone. First of all, it is the earth crust of the geographically coastal zone which leads to different bathymetry and the level of complexity of shoreline. Secondly, sea and air are strongly related in heat and gas exchanging, mass transport through precipitation and evaporation process, wind driven current and vice versa. Lastly, with the uniquely environmental condition, particle transportation is dictated by those physical components.

### 1. The Andaman Sea

The Andaman Sea is located in the northeastern Indian Ocean. It is bounded with Myanmar in the North, Thailand and Peninsula Malaysia in the East, Sumatra island in the South and the Andaman and Nicobar on the West separated the Andaman and bay of Bengal. The Andaman and Nicobar islands are India's important coral reef resources and largest block of coral cover in South Asia. This area is regionally outstanding in terms of both species diversity and intact corals with approximately 200 coral species and 400 fish species have been recorded. Although the Andaman Sea composes only one third of Thailand's coastline, over half of country's coral reef are found in this waters with 210 coral species and over 100 fish species have been recorded. In Thailand, tens of thousands local small-scale fishermen have traditionally fished the Andaman Sea near shore waters for generations (World Wildlife Fund [WWF], n.d.).

In addition, dugongs have been reported throughout the region, as well as Irrawaddy dolphin. Whale sharks, coconut crabs, various dolphin and blue and sperm whale are some of the other marine animals that form this rich diversity of marine fauna in the Andaman Sea. However, it is reported that damage to species and habitats occur both from legal and illegal harvesting. It derived from poor management, pollution, uncontrolled tourism, destructive fisheries and poaching.

## **2. Physical characteristic of the Andaman Sea**

Surface circulation in the Andaman Sea is influenced by monsoon; tide also plays a greater role than trade wind sometimes. In addition, characteristic season and annual current pattern are driven by wind, as shown in Figure 6. The seasons in the Andaman Thai coast are classified into two seasons which are the dry season (December through June) and the wet season (July through November) with the early dry in November – December and the early wet in May – June. Moreover, The Andaman Sea is named as a productive sea because of upwelling phenomena during Northeast monsoon (Limpsaichol, n.d.; Wyrтки, 1973; Siripong, 1977; Potemra, 1990; Somkiat *et al.*, 1991). It typically carries nutrient rich water from deeper sea as well as colder and saltier water.

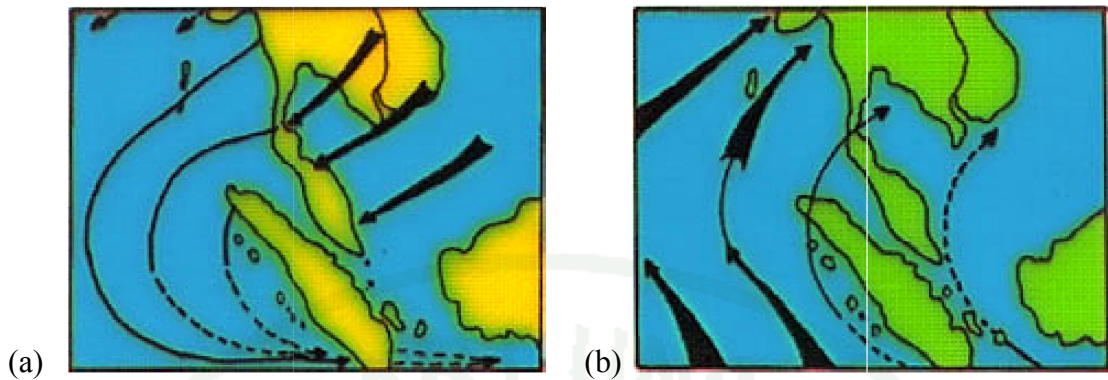


**Figure 6** Monsoon in the Southeast Asia Region of the Andaman Sea where (a) is Northeast Monsoon and (b) is Southwest Monsoon, and the bold arrows indicate wind speed of 0.25-0.50 m/s

**Source:** Limpsaichol (n.d.)

Tide is rise and fall of water caused by combination of gravitational force exerted with moon and sun force. Tides are very long-period waves that move through the oceans in response to the forces exerted by the moon and sun. Tides originate in the oceans and progress toward the coastlines where they appear as the regular rise and fall of the sea surface. This is naturally happened by nature and unique in individual areas. There are many tidal characteristic based on their nature namely tidal range and period. In the Andaman Sea, seawater amplitude is dominated by semidiurnal tide. Semidiurnal tide characteristic is composed of two high and two low tides during a day of almost equal amplitudes during neap tides. Semidiurnal tide with a mean tidal range of 1.8 m was found in Phang-Nga bay where is adjacent to Phuket eastwards (Sojisuporn *et al.*, 1994). The tidal current is found at near shore while off shore current is predominated by wind-driven (Somkiat, 2010)

### 3. Surface current in The Andaman Sea

Ocean current transports marine litter made of plastic, because they are able to float at or near the surface. Floating marine particle can contribute in tracing current pattern (Iván and Martin, 2009), and at the same time, current pattern can also

forecast the transportation of floating marine particles. Wind together with temperature, and salinity are prime factors in circulating water around the ocean. Wind caused the movement of water in horizontal layer and the net effect to low water is to move in a direction perpendicular to wind direction, so called Ekman transport. Salinity and temperature also affect the ocean circulation as the process of mixing called thermohaline circulation. In addition, earth rotation is taken into account as moving air and water are deflected clockwise in the Northern hemisphere and anti-clockwise in the Southern hemisphere, so called Coriolis Effect.

In the Andaman Sea, seasonal change of the wind plays an important role in surface circulation. During the Northeast monsoon, water mass moves toward the Andaman Sea from the North and leave the Andaman Sea in the South between the Andaman island and Sumatra island (Syamsul *et al.*, 2010). In the Strait of Malacca which connected to the Andaman Sea in the South East, the surface current always flows North-westward for both monsoon seasons. The velocity of surface current in the Southwest monsoon is stronger than Northeast monsoon and lower water elevation (Syamsul *et al.*, 2012).

In order to have a better understanding on physical oceanography, many researchers have been observing ocean in order to explain the dynamic changes of important components such as temperature, nutrient and particle transportation in the ocean. Nevertheless, observing large scale of ocean with a numbers of instruments is costly and time consuming. Therefore, many researchers try to develop numerical oceanic model to response to curiosity on complexity environment such ocean.

#### **4. Numerical Oceanic Modeling**

FVCOM was developed to cope with highly complex bathymetry and case studies where precise simulation is needed. It was composed with finite difference and finite element. The first is dealt with computational efficiency while the latter is put to geometric flexibility. The model resolves the governing equations by means and flux calculation over each grid control volume.

#### 4.1 Numerical oceanic model application

The governing equations are derived from the Reynolds-averaged Navier-Stokes under the hydrostatic assumption and the Boussinesq approximation. The primitive equation in Cartesian coordinate is consisted of momentum conservation and continuity equation as shown below;

$$\frac{\partial u}{\partial t} + u \frac{\partial u}{\partial x} + v \frac{\partial u}{\partial y} + w \frac{\partial u}{\partial z} - fv = -\frac{1}{\rho_0} \frac{\partial P}{\partial x} + \frac{\partial}{\partial z} (K_m \frac{\partial u}{\partial z}) + F_u \quad (1)$$

$$\frac{\partial v}{\partial t} + u \frac{\partial v}{\partial x} + v \frac{\partial v}{\partial y} + w \frac{\partial v}{\partial z} - fu = -\frac{1}{\rho_0} \frac{\partial P}{\partial y} + \frac{\partial}{\partial z} (K_m \frac{\partial v}{\partial z}) + F_v \quad (2)$$

$$\frac{\partial u}{\partial x} + \frac{\partial v}{\partial y} + v \frac{\partial w}{\partial z} + = 0 \quad (3)$$

where x, y and z are the East, North and vertical of the axes in Cartesian coordinate; u, v and w are the velocity of x, y and z component;  $\rho_0$  is the density of seawater which is the function of temperature and salinity; f is the Coriolis parameter which responses to angular velocity of the earth circulation and latitude;  $K_m$  is the eddy viscosity coefficient in vertical axis; P is the pressure. The current calculation is divided into two steps which are internal and external modes using two distinct time steps though the computation of numerical method called “mode splitting”. Full description of FVCOM can be reached in FVCOM manual.

#### 4.2 FVCOM and other oceanic models

Oceanic models such as Princeton Ocean Model (POM), Regional Ocean Modeling System (ROMS) and Finite Volume Coastal Ocean Model (FVCOM) and Environmental Fluid Dynamics Computer (EFDC) have successfully simulated transport and circulation process of coastal and estuary zone. Comparing the result from computation and observation data, POM, ROMS and FVCOM perform very well, yet there are some differences in detail because of their model grids and numerical scheme (Robert *et al.*, 2004). As shown in Figure 7, unstructured-grid

FVCOM seems to work very well on both amplitude and phase of water elevation (Changsheng, 2013).

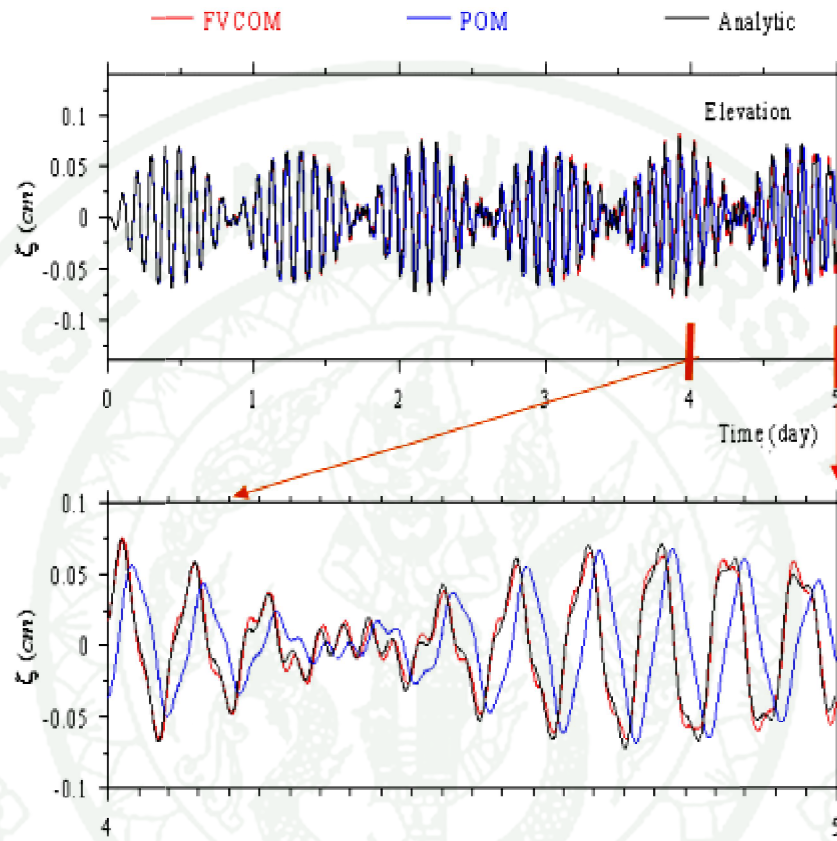


**Figure 7** Comparison of water elevation in between analytic and computation simulated by FVCOM and POM

**Source:** Changsheng (2013)

Moreover, sea-level variation at Fukuoka bay was simulated by using both FVCOM and POM. And the root-mean-square of the both model validation is 0.742 and 1.88, respectively. It well indicated that FVCOM is more accurate because it is replaced with high-resolution which also prove the difference of grid solution (Kazushiro and Atsuhiko, 2007) as shown in Figure 8. However, it is strongly emphasized that oceanic models are sensitive to their forcing data which means that better forcing data leads to better simulations as well.

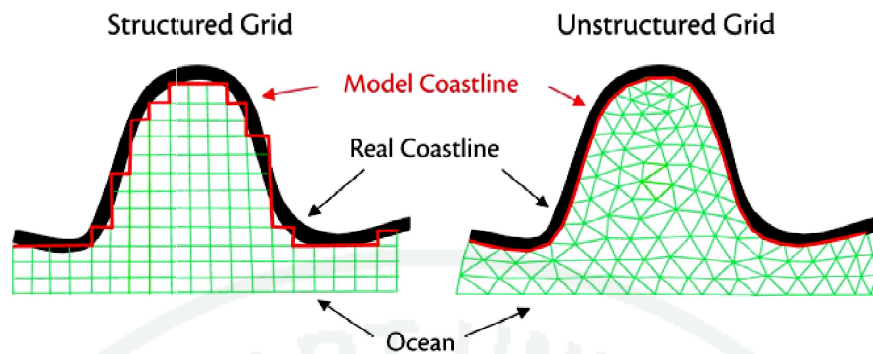


**Figure 8** Basic classes of oceanic model grid where structured grid is used by POM, ECOM and ROMS and unstructured grid is used by ADCIRC (FE), SELFE (FE) and FVCOM

**Source:** Changsheng *et al.* (2006)

FVCOM is run with unstructured triangular grid which is initiated by coastal and bathymetry data in area inside the boundary in which allow it to perform well under complex coastal line and bathymetry such as steep bottom geography and it additional provides more realistic flow disturbance at near shore. FVCOM is recently used as a new research tool regarding physical ocean modeling (Changsheng *et al.*, 2006). The resolution of triangular grid in boundary varies according to coastal geography and bathymetry (Lianyuan *et al.*, 2004). Through flux form of the governing equations in unstructured grid triangular and second-order accurate flux stream, it allows three-dimensional FVCOM to compute more precisely mass momentum, heat, and salt conservation.

Well determined of physical characteristic of important component in the interested area, Surface wind stress, heat flux, amount of precipitation and evaporation, tides, river discharge and ground water discharge, as well as grid coordinates of site studies are used as forcing driving FVCOM (Changsheng *et al.*, 2011).

### 4.3 FVCOM and its applications

A numbers of estuaries, continental shelf and open ocean studies have been successfully applied by using FVCOM. Water elevation from tidal solution compared very well with observed elevation and current data with  $M_2$  component of less than 3 cm in amplitude and  $5^\circ$  in phase (Changsheng *et al.*, 2011). The same well performed result from simulation under tidal solution is also expressed at Rookey bay and Naples bay (Zheng and Weisberg, 2010), Banks of Newfoundland (Guoqi *et al.*, 2011), Gulf of Maine and New England Shelf (Changsheng *et al.*, 2011), East China Sea (Xing *et al.*, 2013), Florida (Robert *et al.*, 2004), Fukuoka bay in Japan (Kazushiro and Atsuhiko, 2007) and Gulf of Mexico (Dubravko and Lixia, 2009).

Besides determining and correcting computational result with observatory data, it has been used to predict changes of important parameters in ocean according to coastal constructed development projects. For example, Oujiang River Estuary was determined a case scenario where a mouth river blocking project is constructed. Tide, current pattern and salinity variation were observed and considered for decision making process (Xing *et al.*, 2013). This does not only benefit to long-term stability and sustainability, it also makes advantages to aquaculture and biodiversity.

### 4.4 Particle tracking

Marine floating litter can be studied by many tools. One of those is deriving seattleite image of high spatial resolution of sea surface current (Elodie *et al.*, 2009). And the trajectory of item is, then, calculated accordingly. Another method is to conduct beach survey and clean-up and compared based on season, environmental factors and land-used (Luzhen *et al.*, 2009). Labeling on wrap and litter can be used to identify its origin or discarded time (Martin, 2011; Topçu *et al.*, 2013). In current study, there are many researches focusing on marine litter distribution model by applying a global ocean circulation model coupled with a Lagrangian particle tracking model. For simulate marine litter transportation for over 30 years, transportation and accumulation of marine litter can be displayed in global oceanic environment

(Lebreton *et al.*, 2012). The result revealed that dominance of the accumulation zones is in the northern hemisphere, while smaller seas surrounded by densely populated areas are also shown to have a high concentration of floating litter.

Particle tracking model uses predictions of movement of individual particles in space and time from three-dimensional models. It provides a set of recommendations for particle tracking in estuary and ocean modeling. In FVCOM, particle tracking or tracer-tracking equation incorporated is the same as the water temperature equation as shown below.

$$\frac{\partial DC}{\partial t} + \frac{\partial DuC}{\partial x} + \frac{\partial DvC}{\partial y} + \frac{\partial \omega C}{\partial \sigma} - \frac{1}{D} \frac{\partial}{\partial \sigma} (K_h \frac{\partial C}{\partial \sigma} - DF_c = DC_0(x, y, \sigma, t) \quad (4)$$

Where  $C$  is the concentration of the tracer,  $D$  is the total water depth,  $v$ ,  $u$  and  $\omega$  are the  $x$ ,  $y$  and  $\sigma$  components of the water velocity, is the vertical thermal diffusion coefficient,  $K_h$  is the vertical thermal diffusion coefficient,  $F_c$  is the horizontal diffusion term, and  $C_0$  is the concentration injected from a source point.

The Lagrangian particle tracking module consists of solving a non-linear system of ordinary differential equation or ODE as follows

$$\frac{d\vec{x}}{dt} = \vec{v}(\vec{x}(t), t) \quad (5)$$

Where  $\vec{x}$  is the particle position at a time  $t$ ,  $d\vec{x}/dt$  is the rate of change of the particle position in time and  $\vec{v}(\vec{x}, t)$  is the three-dimensional velocity field generated by the model. The complete explanation regarding to this section is described in FVCOM manual (Changsheng *et al.*, 2006).

## MATERIALS AND METHODS

### Materials

#### 1. Buoy experiment

1.1 GPS

1.2 Styrofoam

1.3 Glue

1.4 Stick

1.5 Red ribbon

#### 2. Simulation

Simulation experiment is performed with available computational resources at Large Scale Simulation Research Laboratory, National Electronics and Computer Technology Center, Thailand

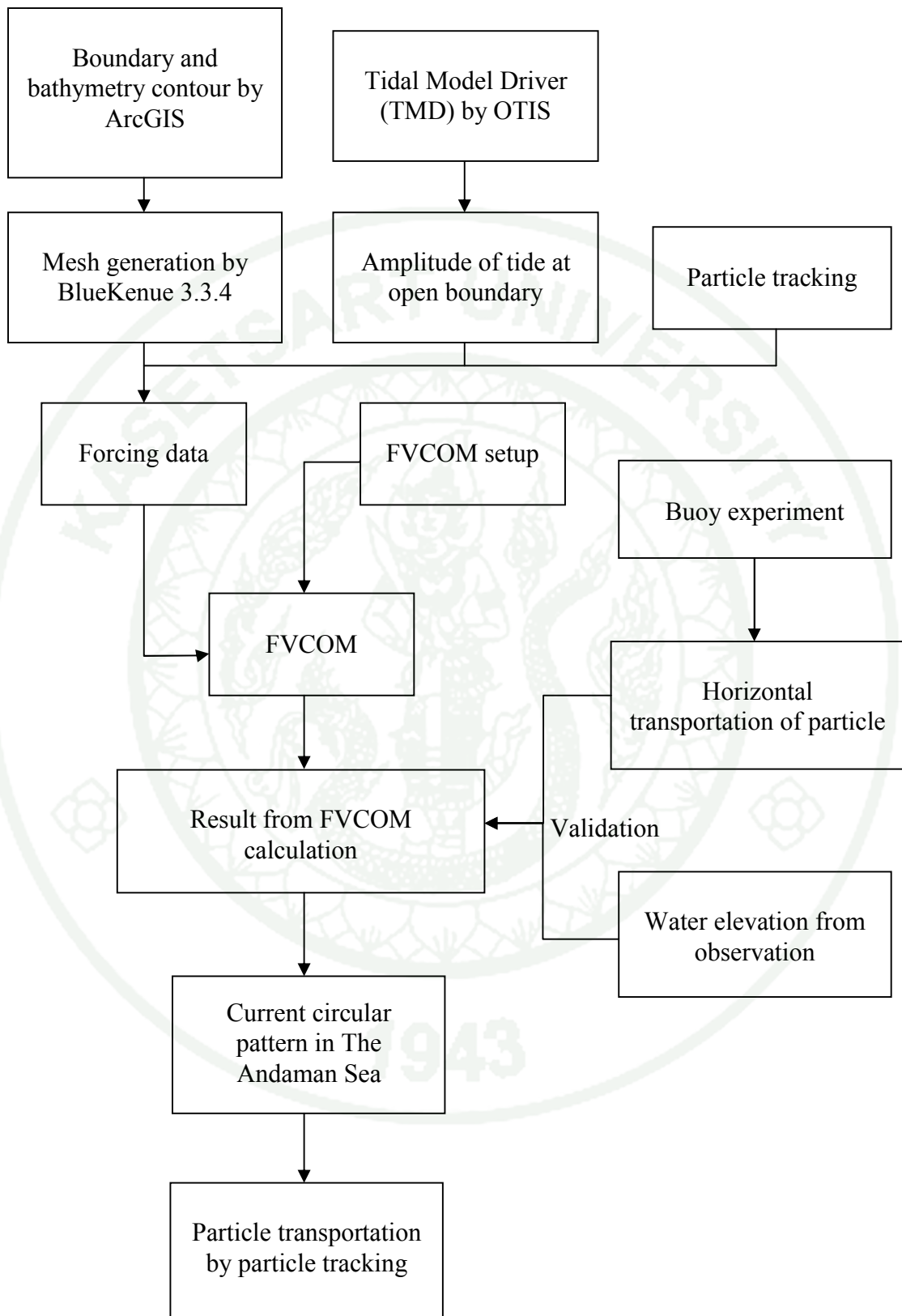


**Figure 9** Schematic diagram of method used in this research

## Methods

### 1. Buoy experiment

Data collection is field-based experiment which virtual marine litter was observed. In order to understand behavior of marine litter transportation, especially light and floatable litter, buoy experiment was conducted in order to observe transportation of floatable particle on oceanic surface. A buoy is presumed to be a marine litter driven by current velocity.

#### 1.1 Study sites

The criteria to choose study sites are land-use (tourist spot and adjacent areas) and location (near main land and isolated island). Therefore, six places along coastal line of southern Thailand were chosen to be study sites of current pattern as listed in Table 3 and their locations are also shown in Figure 11.

**Table 3** Study site for this buoy experiment

List	Name	Province	X	Y	Type of land-use
1	Patong	Phuket	420071	870576	Tourist destination
2	Yao Noi island	Phang-Nga	459923	905261	Tourist destination
3	Panyee island	Phang-Nga	447410	920363	Tourist destination
4	Phi Phi islands	Krabi	473787	853516	Tourist destination
5	Saphan Hin	Phuket	434284	868610	Small fisheries scale
6	Kuraburi	Phang-Nga	427530	1023452	Small fisheries scale

## 1.2 Data collection

Buoy test is generally given the initial idea of direction of floating particle movement on the water surface. Two to four buoys were left to float on the water surface of the study sites for approximately 4-6 hours continuously. To avoid external influences such as strong wind, wave from boat operation and bathymetry that caused vortex flow, buoys were chosen to leave at open oceanic and estuary area, not at the cave and off from boat transportation. The location of buoy after it has been left floating on water surface is recorded by GPS, and its location is plotted on map by SAGA. The result from buoy experiment is used to verify with current pattern simulated by FVCOM. Buoy is designed to be able to float along the current for long time and to easily catch the sight by red flag on top. To make it float with velocity of surface current, it is designed to be light; it, therefore, made of Styrofoam as shown in Figure 10.

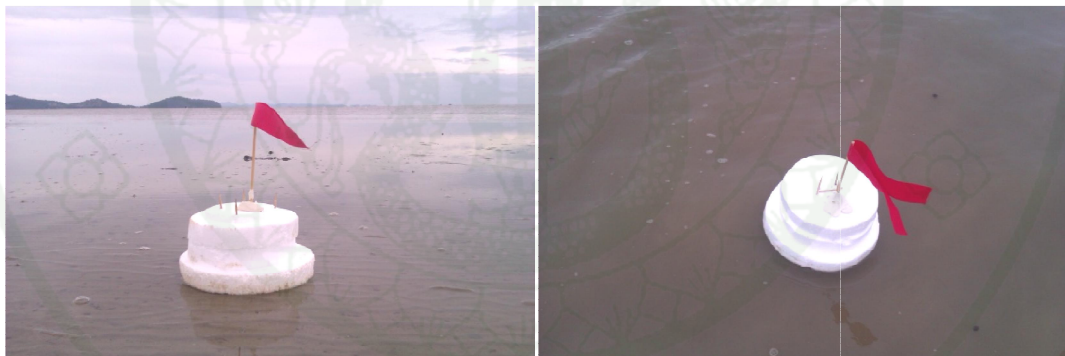


**Figure 10** Light floatable Styrofoam is assumed to be a buoy

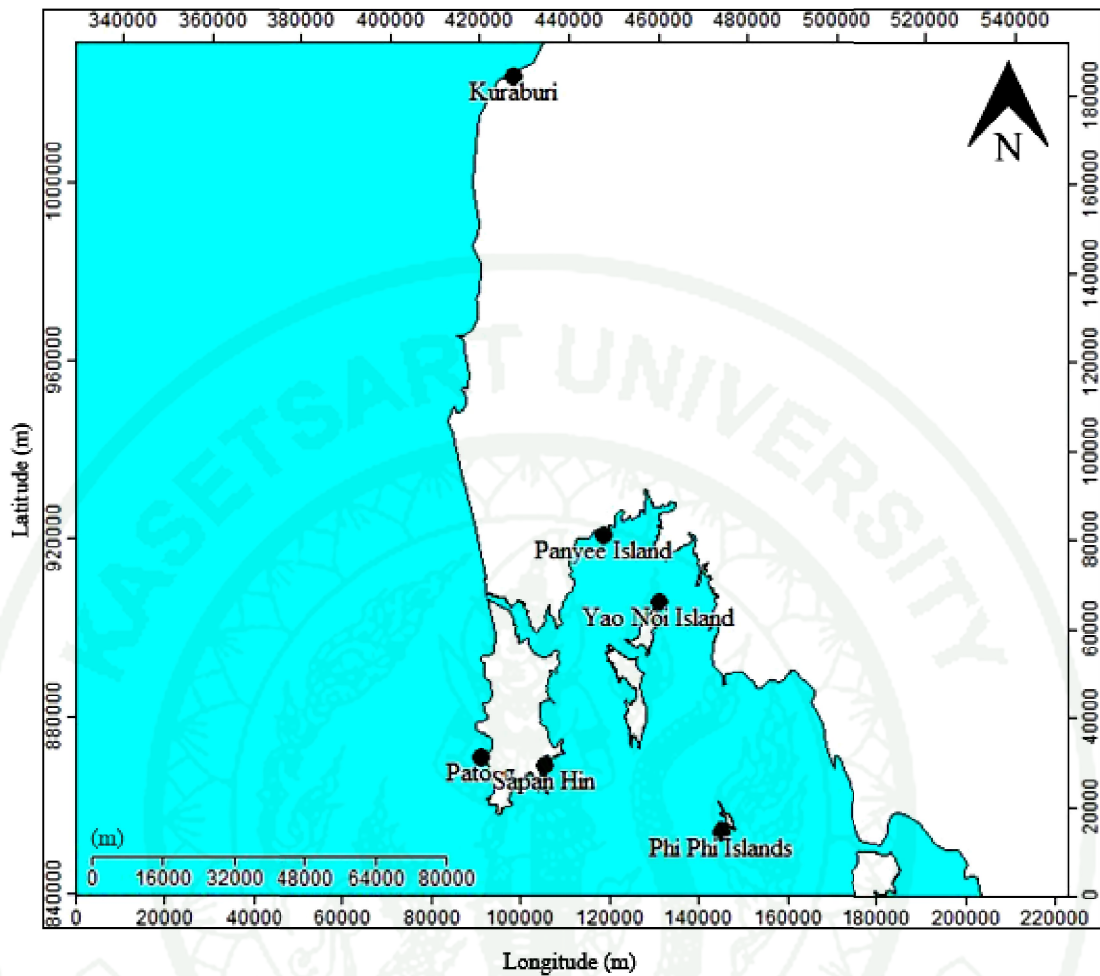


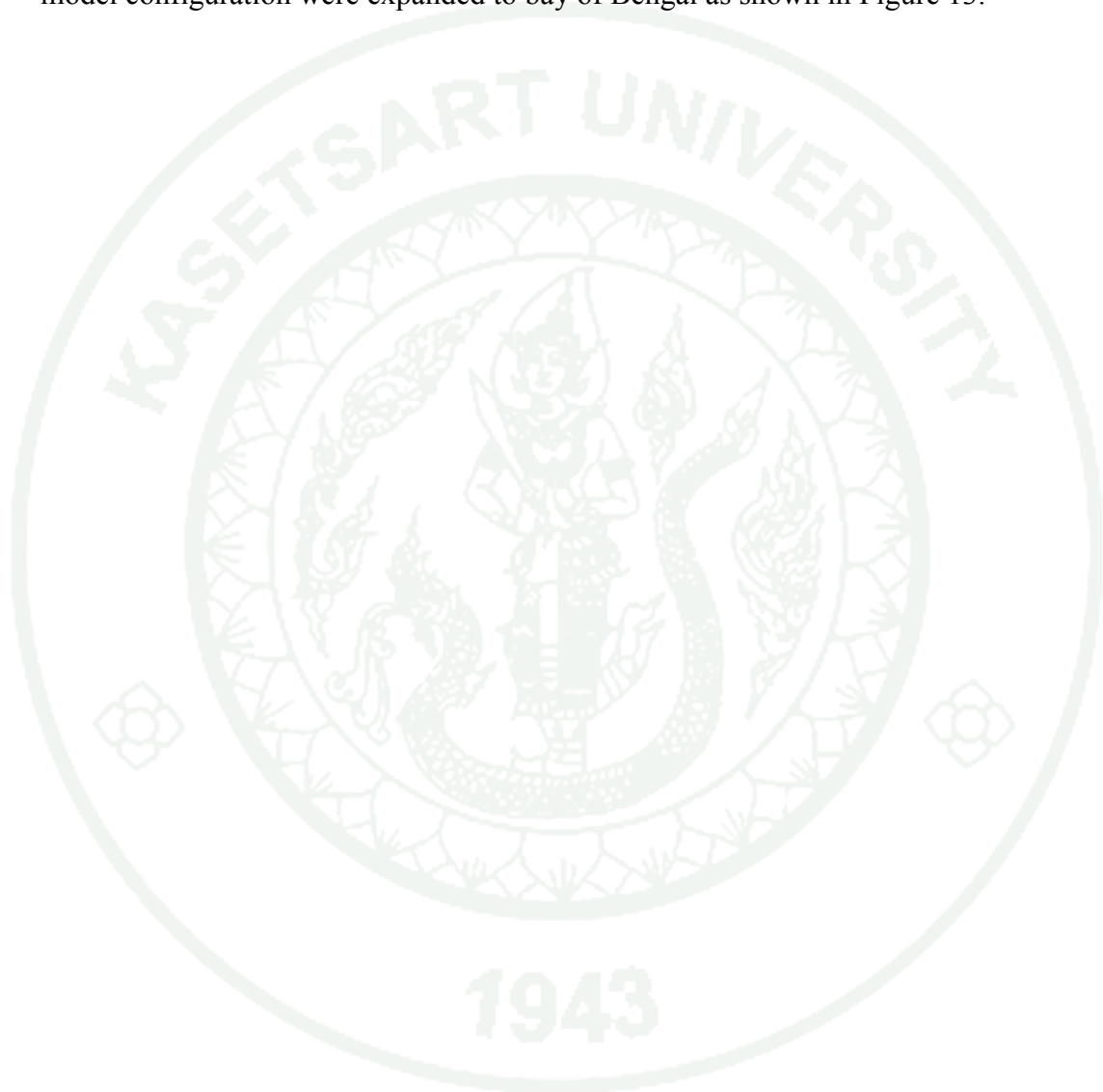
**Figure 11** Study sites for buoy test

## 2. FVCOM and mesh generation

### 2.1 Bathymetry and mesh generation

The area of study is the Andaman Sea which is bounded with Myanmar in the North, South coastal Thailand in the East, the Strait of Malacca and Sumatra island in the South and the Andaman Sea and Nicobar islands in the West as shown in Figure 13. It is located at  $1^{\circ}0'$  North to  $17^{\circ}30'$  North and  $95^{\circ}02'$  East to  $103^{\circ}08'$  East. The computing area is covered  $596,661.16 \text{ km}^2$ .

The Andaman domain was spatially created from Google Earth 7.1.1.1580 (2013). Bathymetry is obtained from The General Bathymetric Chart of the Oceans (GEBCO) 08 grid which is a global 30 arc-second grid as shown in Figure 12. In order to conserve model's stability to be able to simulate for 90 days prediction, model configuration were expanded to bay of Bengal as shown in Figure 13.



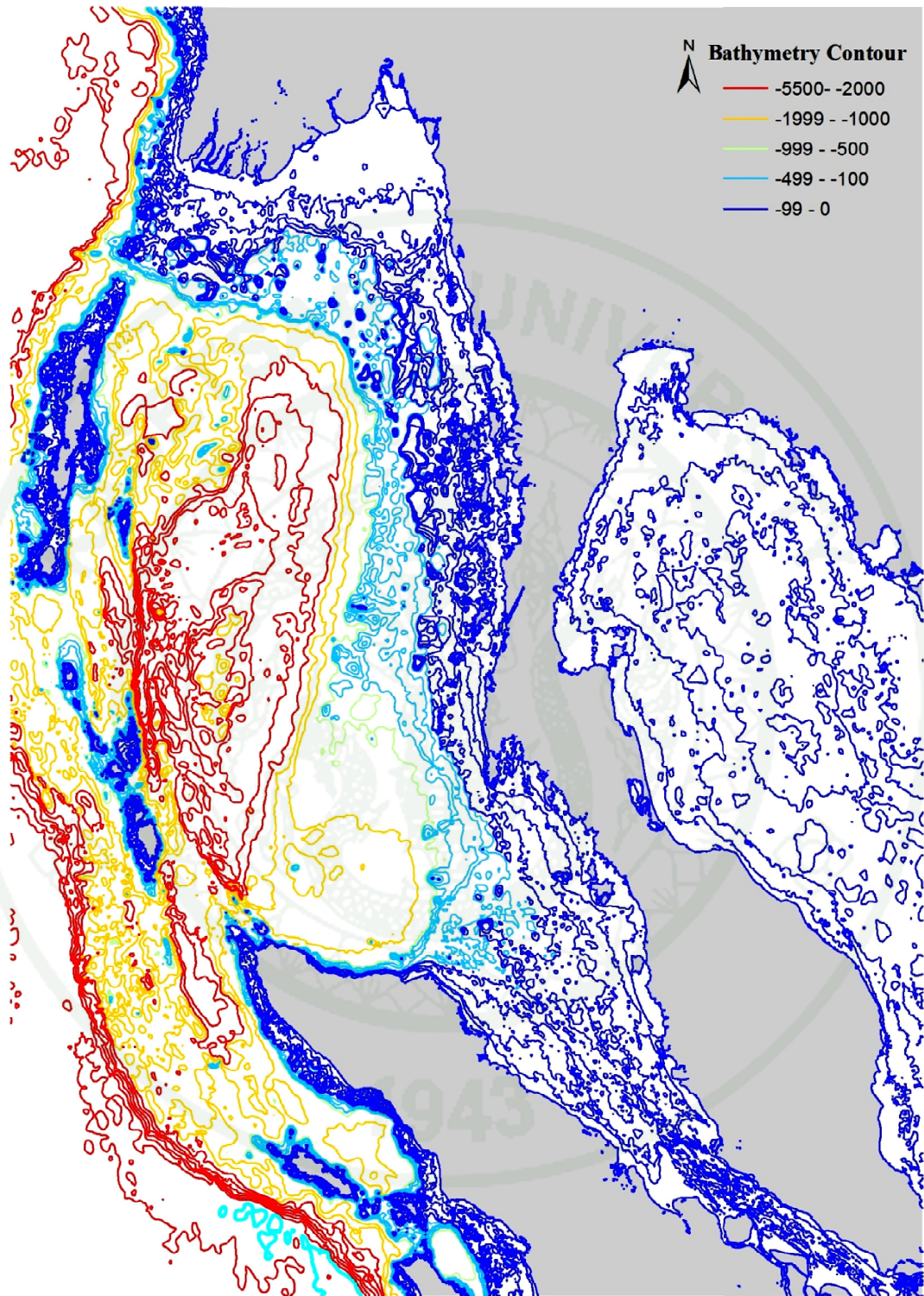


**Figure 12** The topography of the Andaman Sea

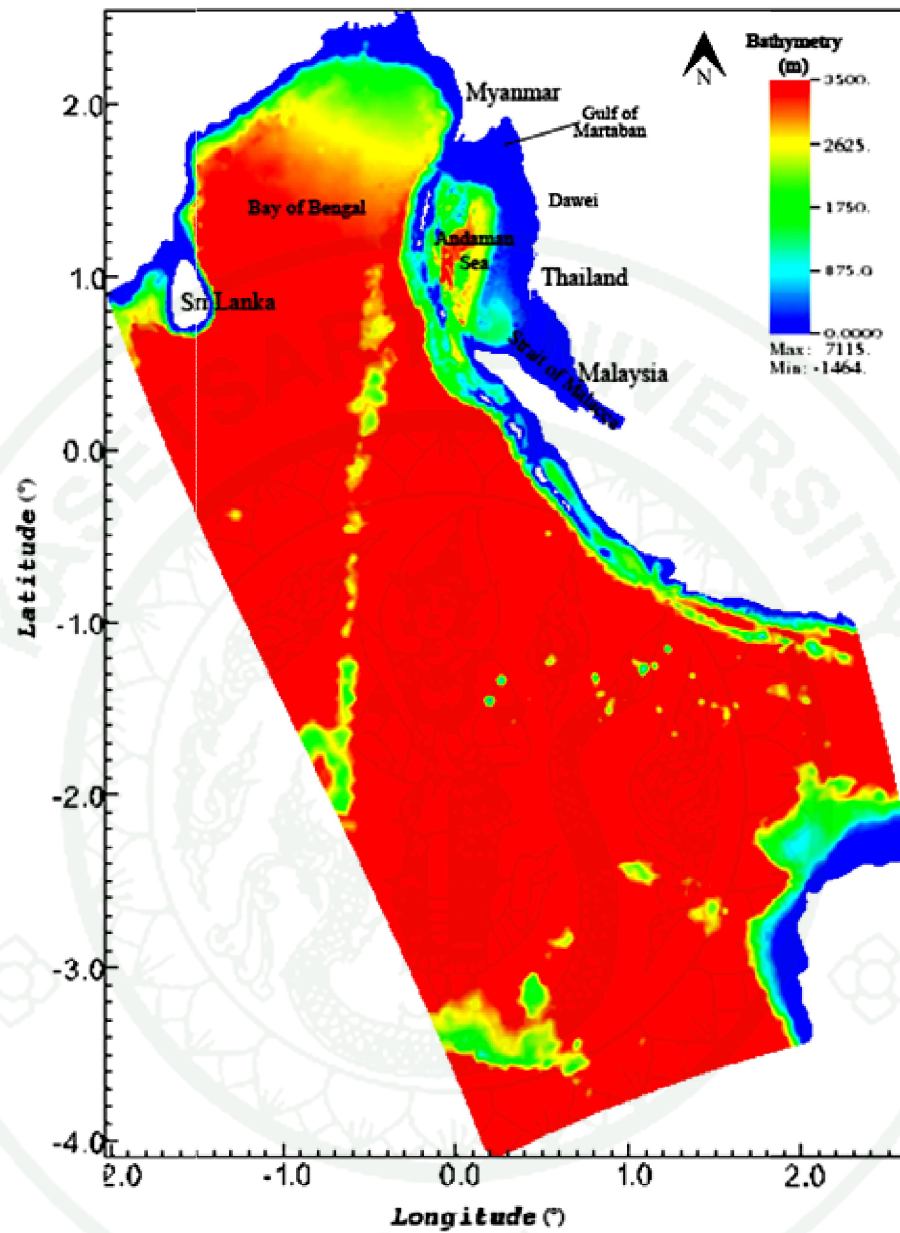


**Figure 13** Model configuration covered the Andaman Sea and bay of Bengal

## 2.2 Model configuration

The unstructured triangular grid is generated within the Andaman domain as shown in Figure 13 by BlueKenue Version 3.3.4. The entire model grid is horizontally composed of 75,365 nodes and 144,897 triangular cells. To create more

finely computing process at the interested study site and shoreline, dense triangular cells were created as shown in Figure 14.

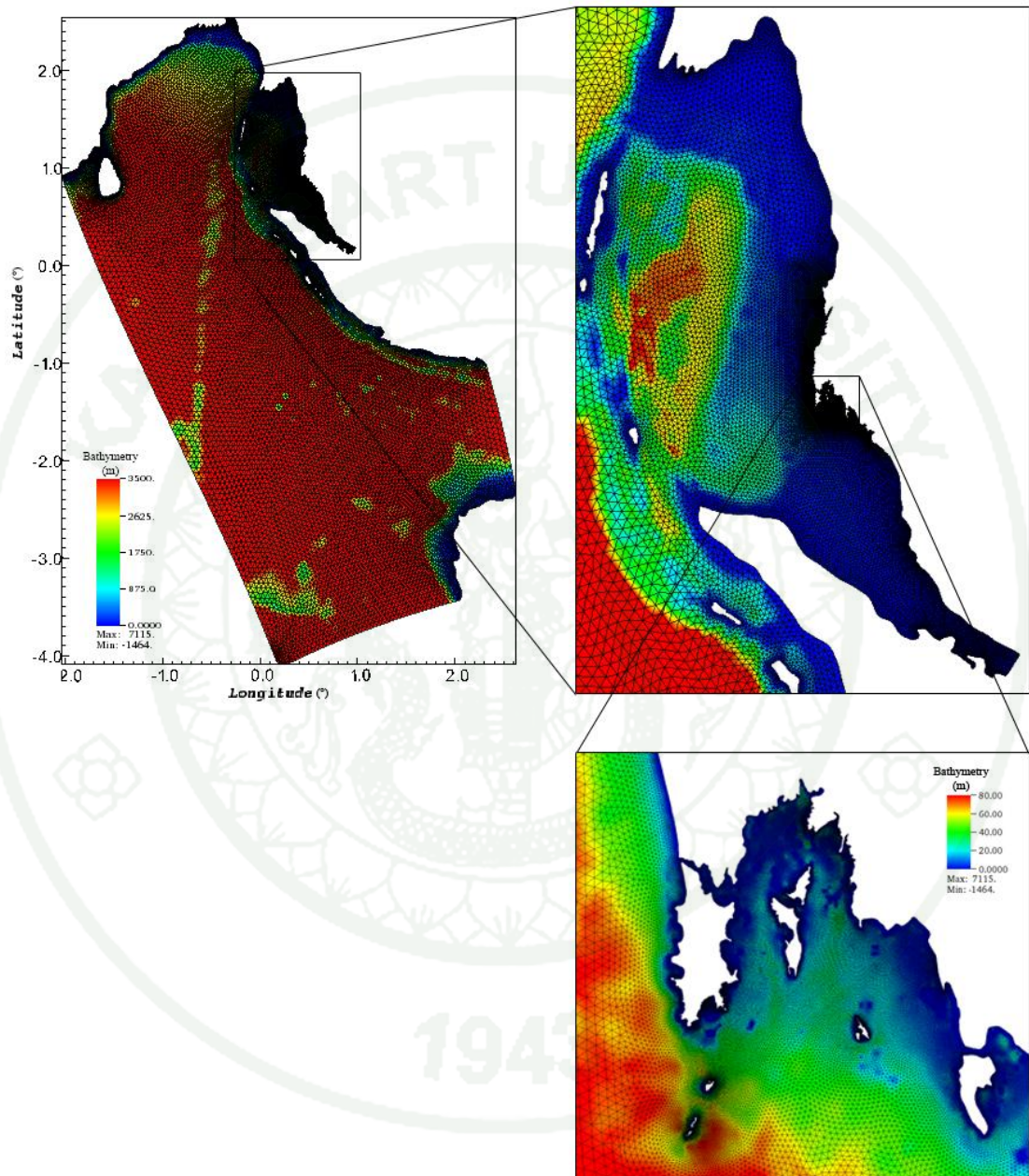


**Figure 14** Study boundary and model configuration

### 2.3 Model forcing and boundary condition

Only open boundary nodes which are located on the boundary line in the sea were selected in order to force tidal amplitude. The tidal circulation has been performed by driving the water elevation at the open boundaries by data obtained from TOPEX 7.2, Tidal Model Driver (TMD) provided by OTIS regional Tidal Solution.

### 2.4 Particle tracking

Particle tracking is based on the prediction of current velocity from FVCOM which calculates the movement of individual particle in space and time. The goal of this technique is to provide visual movement of particle in ocean and estuary. A number of particles were force to leave at the origins according to field's study sites for model verification and in the middle of the ocean for studying movement of particle in general. FVCOM is forced to run three months long based on three case scenarios.

### 2.5 Case scenarios

There are three case scenarios in order to study current pattern in the Andaman Sea and floatable marine litter classified by weather condition as normal weather condition and monsoon seasons. The Andaman Sea is generally influenced by two trading winds throughout the year which are Northeast monsoon and Southeast monsoon. Figure 15 is plotted according to wind direction obtained from Global Forecast System (GFS) during the two monsoons in February and September of 2013 which represents Northeast and Southwest monsoon, respectively. Wind components at 10 m above mean sea level are obtained from GFS Model provided by NOAA Operational Model Archive and Distribution System, as known as NOMADS. Wind components are U (North direction) and V (East direction) with 0.5 degree resolution in global latitude-longitude grid. Therefore, three cases scenarios are categorized as detail below.

### 2.5.1 Tidal dominated condition

Tide is assumed to periodically show the same behavior throughout the year. Tide was simulated for three months including six spring-neap cycle in order to assure computational stability and considered as normal oceanic current without the influence of winds. Tide solution obtained from TOPEX is from 4 January 2013 – 3 March 2013. This scenario represents normal weather condition where the current is dominated solely from tide.

### 2.5.2 Tidal and wind driven during Northeast monsoon

During Northeast monsoon, wind moves from East to West at the coast of Thailand which connected to the Andaman Sea. Tide solution obtained from TOPEX is from 4 January 2013 – 3 March 2013. Likewise, wind components at 10 m obtained from GFS (Figure 15a) are also forced on the same date as tidal amplitude solution. This scenario represents oceanic current in the Andaman Sea during the Northeast monsoon.

### 2.5.3 Tidal and wind driven during Southwest monsoon

The wind moves from West to East and South during Southwest monsoon in the Andaman Sea. Tide solution obtained from TOPEX is from 1 September 2013 – 30 November 2013. In addition, 10-m wind components during the observing time (Figure 15b) are also forced. This case scenario represents oceanic current in the Andaman Sea during the Southwest monsoon.

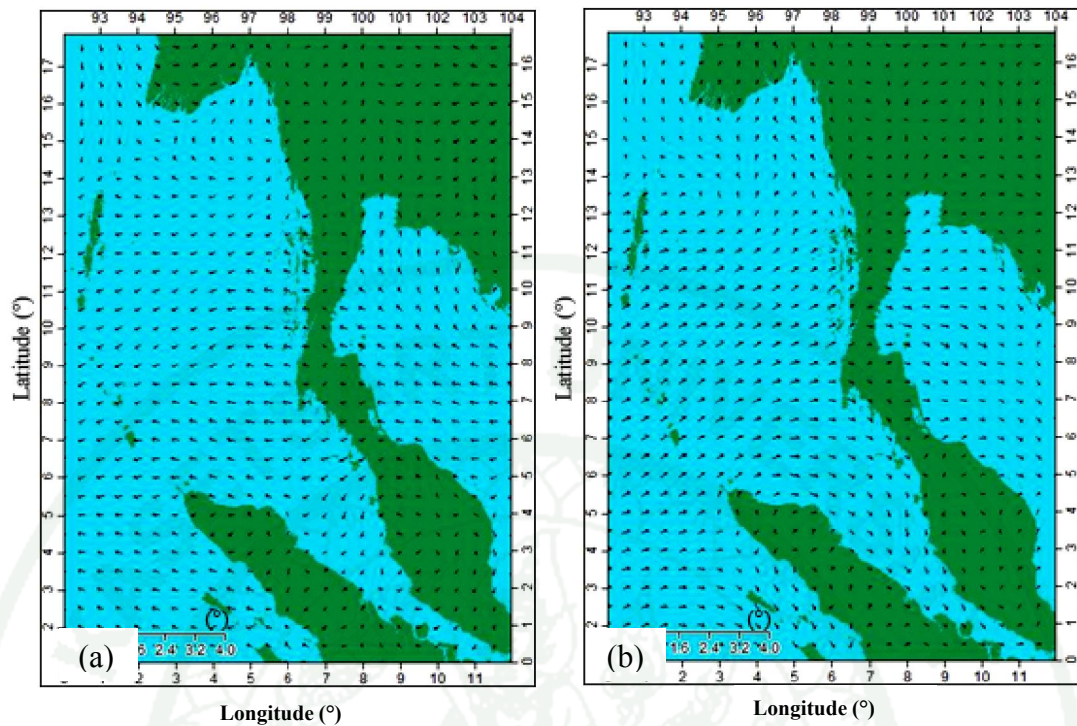


**Figure 15** Winds that influence the Andaman Sea are (a) Northeast monsoon (February, 2013) and (b) Southwest monsoon (September, 2013)

### 3. Discussion and analysis

This session is meant to interpret data obtained from field-site experiment and model's solution for the conclusions of the study.

#### 3.1 Comparison between simulation and observation

The model was forced to estimate and resolve the spring-neap tidal cycle on August 1, 2012 to October 31, 2012 in order to perform Southwest monsoon and on January 1, 2013 to March, 31 2013 in order to perform Northeast monsoon. The first 7 days provide model a ramp-up time and the remaining days are used for data analysis. The water level is compared between observation and simulation for model verification.

There are four stations along the South western Thai coast which is connected to the Andaman Sea. They are Ao Por and Tapao Noi in Phuket, Kuraburi in Phang-Nga and Tarutao in Satul. A gauge was deployed and hourly recorded at Ao Por by Marine Department, while water level was hourly predicted at the other three stations by Hydrographic Department.

Amplitude or water level of tidal solution from FVCOM during mentioned period was compared against observation. There are several indicators that are used to analyze. First, tidal range relative error which is the difference between maximum high tide and low tide to observation in percentage are calculated and compared between simulation and observation. It is reported in percentage of relative error, and the least percentage shows the least error of simulation to observation. Second, a tidal harmonic analysis was determined by the T\_Tide tidal package (Pawlowicz, 2002) and reported in table of differences of tidal amplitudes and phases of each constitutes. Comparison of water level between observation and simulation is also graphically shown in order to observe model validation. Third, histogram of water level difference between observation and simulation is plotted and observe the underestimated and overestimated simulation against observation. Fourth, linear regression of water level between observation (x-axis) and simulation (y-axis) is calculated and plotted in order to determine R-squared which demonstrates relation between simulation and observation.

In addition, particle tracking obtained from solution resolved by FVCOM is horizontally validated against buoy test from study sites, and they are compared for six hours, continuously.

### 3.2 Tidal characteristic and predictive skill

The tidal characteristic during neap tide and spring tide were recorded and reported. In addition, the tidal constituent is used to determine the best description of tide by applying in following equation:

$$F = \frac{K_1 + O_1}{M_2 + S_2} \quad (6)$$

where  $K_1$ ,  $O_1$ ,  $M_2$  and  $S_2$  are amplitude of Luni-solar diurnal, Principal lunar diurnal, Principal lunar and Principal solar, respectively.

Moreover, tidal direction and velocity are observed during different phases of water level of one tidal period, as known as one high tide and one low tide. This is for understanding tidal behavior during a tidal period.

Lastly, FVCOM was use to simulate tidal circulation at the Andaman Sea with fining grid. To estimate computational accuracy, model skill assessment developed by Wilmott (1981) is applied to investigate model's capability in following equation:

$$\text{Skill} = 1 - \frac{\sum_{i=1}^N |X_i - \hat{X}_i|^2}{\sum_{i=1}^N (|X_i - \bar{X}_i| + |\hat{X}_i - \bar{\hat{X}}_i|)^2} \quad (7)$$

where  $X_i$  and  $\hat{X}_i$  are the time series of the observed and modeled variables at gauge station, respectively,  $N$  is the number of observation and an over bar is time mean values. The prefect agreement of observation and model results yields a skill of 1.0, whereas a skill of zero represents the complete disagreement.

### 3.3 Oceanic current pattern in the Andaman Sea

The current in the Andaman Sea is observed in order to have better understanding of current behavior in this region. Current movement in general is reported based upon seasonal differences. Tidal dominated current is reported. In addition, Northeast monsoon lasting from December to June and Southeast monsoon covering July to November in Thailand are, then, observed.

### 3.4 Particle tracking studies based on case scenarios

Particle tracking method is practically used in this study in order to compare those mentioned three case scenarios in the Andaman Sea. Marine particle movement during tidal dominated condition, Northeast monsoon and Southwest monsoon in 90 days are observed and compared in order to investigate the differences of marine particle movement in each individual area based on seasonal condition.

Furthermore, displacement of marine particle between Day 1 and Day 90 is calculated in order to determine the average distance of marine litter in each individual area of different seasonal condition.

## RESULTS AND DISSCUSSION

### Floating buoy experiment

Buoy test was conducted at six different study sites along Andaman coast of southern Thailand. They are Kuraburi, Panyee island and Yao Noi island in Phang-Nga, Patong and Saphan Hin in Phuket and Phi Phi islands in Krabi (Figure 16). Even if buoy test was not conducted covering every part of domain boundary, it was, however, managed to sampling along Thai coast of the Andaman Sea; varied in its locations and environmental features such as land use and adjacent area.

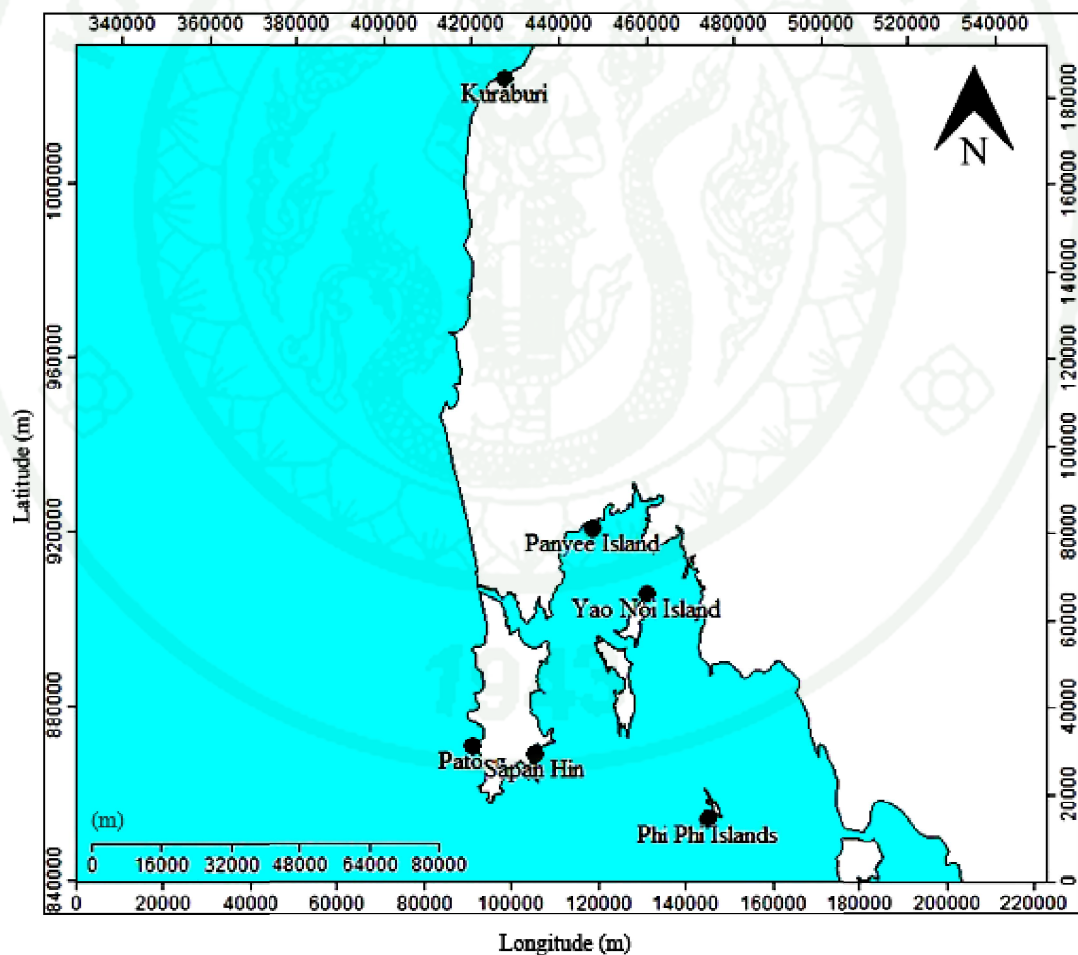


**Figure 16** Study sites for buoy test along the Andaman coast of southern Thailand covering places locating in Phang-Nga, Phuket and Krabi

## 1. Patong beach, Phuket

Patong Beach is located on the Southern of West side of Phuket and is known as famous destination in Phuket because of its beautiful land and underwater sceneries. The exact locations of buoy testing are at Nitrang beach and Paradise beach in Patong beach. Study site is geographically bounded by rocky cave and cliff.

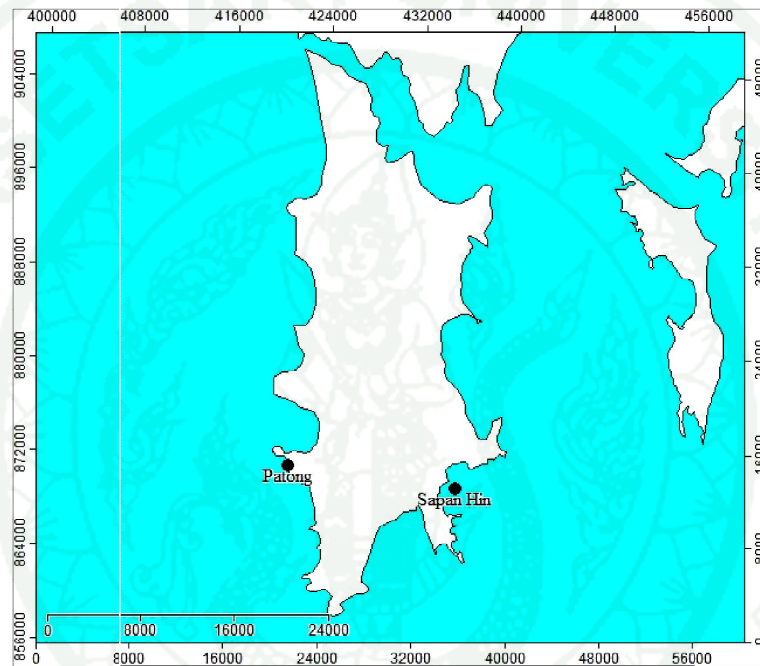


**Figure 17** Buoy test of Western current at Patong beach which located at the Southwest of Phuket.

Daily water level at Patong was assumed by water level at Tapao Noi predicted by Hydrographic Department of the day buoy experiment had been conducted (Figure 18). The experimental period had been conducted from 11 AM – 2 PM, including ebb tide where water level was moving from high water, to mean water and slightly low water (below mean water).

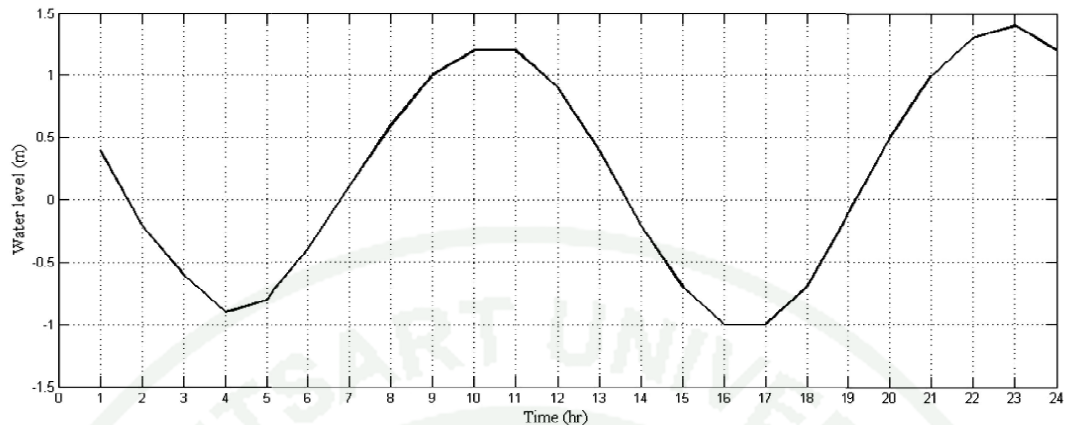


**Figure 18** Daily water level at Patong, Phuket represented by Tapao Noi island on 17<sup>th</sup> November, 2013 (Hydrographic Department)

Many buoys had been floated at various places which are at Nitrang beach, Patong beach. As shown in Figure 19, dots graphically representing buoys with labels of times whereby direction of buoy's movement was demonstrated. A buoy was left for 10 minutes and moved southeasterly as shown in Figure 19a when water level moved from highest water to high water. Meanwhile, Figure 19b showed that buoys moved northwesterly during 1 – 2 PM (including high water level to mean level). In addition, three buoys were tested and moved northwesterly and the North when water level shown as mean water to low water (Figure 19c).

Buoy's velocity was calculated in Table 4. Their velocities were less than 20 cm/s except the fact that a buoy moved much quicker than others for approximately 46 cm/s velocity.



**Figure 19** Floatable buoys at Patong beach at different locations and times where (a) is Buoy 1, (b) is Buoy 2 and (c) is Buoy 3

**Table 4** Buoys observation at Patong Beach and theirs velocities

<b>Buoy</b>	<b>Distance of Buoy (m)</b>	<b>Observation time</b>	<b>Time (min.)</b>	<b>Velocity (cm/s)</b>
1	80.37	11.24-11.56	32	4.19
2	94.02	1.41-1.50	9	17.41
	388.73	1.58-2.12	14	46.28
3	69.04	11.11-11.18	7	16.44
	59.94	1.10-1.28	18	5.55
	115.83	1.33-1.50	17	11.36

## 2. Yao Noi island, Phang-Nga

Yao Noi is located in the middle of Phang-Nga bay along with Yao Yai island, and it is 43 km away from Phang-Nga in the South. Its area is approximately 46.64 km<sup>2</sup>. They are recently well known for eco-tourism where provide cultural education through home-stay. There are many tourist spots especially beaches which lay in the East side of the island, whereas mangrove forest, mud and small scale culture are located in the West side.

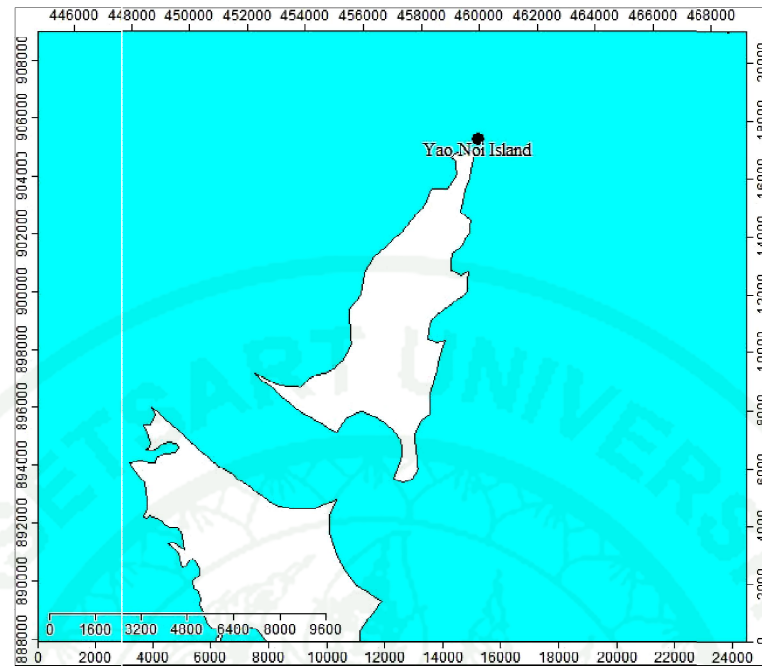


**Figure 20** Buoy test was conducted at the North of Yao Noi island, Phang-Nga bay

Daily water level at Yao Noi island was assumed by water level at Tapao Noi predicted by Hydrographic Department of the day buoy experiment was conducted (Figure 21). The observing time is from 10AM – 3PM including the level water of high tide, highest tide and mean tide. As shown in Figure 21, high tide was displayed at 9 AM – 11 AM and 1 PM – 3 PM, until it reached the highest tide at noon. Mean tide during observing time was shown at 3 PM.

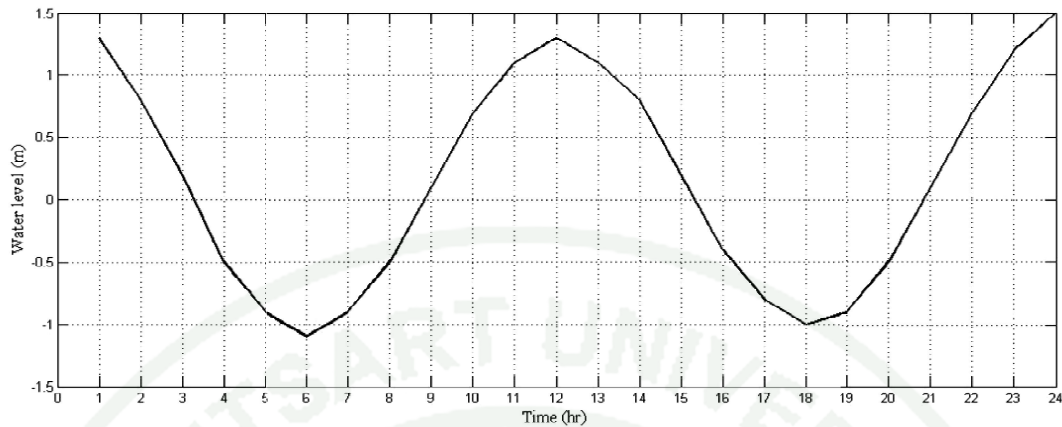


**Figure 21** Daily water level at Yao Noi island, Phang-Nga represented by Tapao Noi island on 20<sup>th</sup> November, 2013 (Hydrographic Department)

Two free buoys were graphically shown in Figure 22a and Figure 22b whereas Figure 22c was buoy weighted with 240 g lead with 50 cm. They were left to continually float on seawater for five hours. Free buoys demonstrated the pattern of movement of going towards Northwest at 10 AM to 12 PM where the tide was flooding. Then, they drastically changed the direction to move southerly until the end of experiment. On the other hand, buoy weighted with lead moved back and forth from East to West during the highest water level (12 PM) and then from West to East after that.

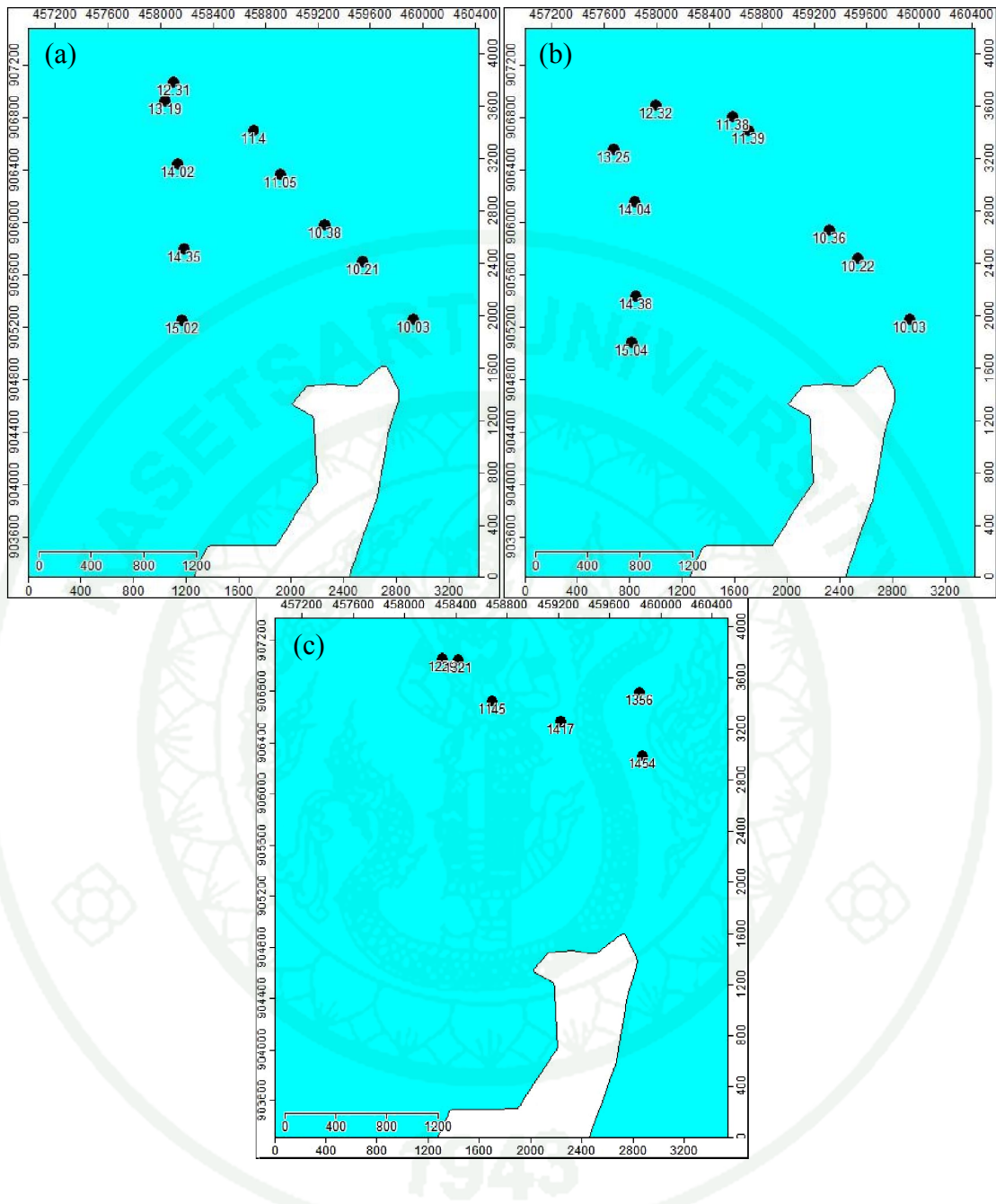


**Figure 22** Floatable buoys at Yao Noi island where (a) is Buoy 1, (b) is Buoy 2 and (c) Buoy 3 which was weighted by 240g lead at 50 cm depth at different times

The velocity of buoy movement in each timing faction was also shown in Table 5. Buoys moved with abating velocity before noon during flooding tide (10 AM – 12 PM) varied from 20 – 50 cm/s. It moved slowly with approximately 25 cm/s

during highest tide. Then as water level decreased, buoy's velocity was increased from 20 – 35 cm/s. Nevertheless, lead weighted buoy also revealed different buoy's movement velocity at different times in the range of 5 – 70 cm/s.

**Table 5** Buoys observation at Yao Noi island and their velocities

Buoy	Distance of Buoy (m)	Observation time	Time (min.)	Velocity (cm/s)
1	590.48	10.03-10.21	18	54.67
	405.31	10.21-10.38	17	39.74
	513.81	10.38-11.05	27	31.72
	399.71	11.05-11.40	35	19.03
	718.16	11.40-12.31	51	23.47
	148.29	12.31-13.19	48	5.15
	498.92	13.19-14.02	43	19.34
	651.06	14.02-14.35	33	32.88
	549.58	14.35-15.02	27	33.92
2	625.3	10.03-10.22	19	54.85
	313.57	10.22-10.36	14	37.33
	1,138.86	10.36-11.38	62	30.61
	729.74	11.39 - 12.32	53	22.95
	469.03	12.32-13.25	53	14.75
	432.55	13.35-14.04	29	24.86
	713.64	14.04-14.38	34	34.98
	363.17	14.38-15.04	26	23.28
3	514.79	11.45-12.29	44	19.50
	131.36	12.29-13.21	52	4.21
	1,439.33	13.21-13.56	35	68.54
	661.26	13.56-14.17	21	52.48
	698.09	14.17-14.54	37	31.45

### 3. Panyee island, Phang Nga

Panyee island is located in the South of Phang-Nga province facing the Andaman Sea at Phang-Nga bay as shown in Figure 23. The fishing village itself relies on fishing industry despite the fact that tourists only visit the place in dry season. The uniqueness of this place is the settlement of household in the sea. Until recently, it became a lunch stop for Phang-Nga bay tour from Phuket, Krabi and Phang-Nga itself.

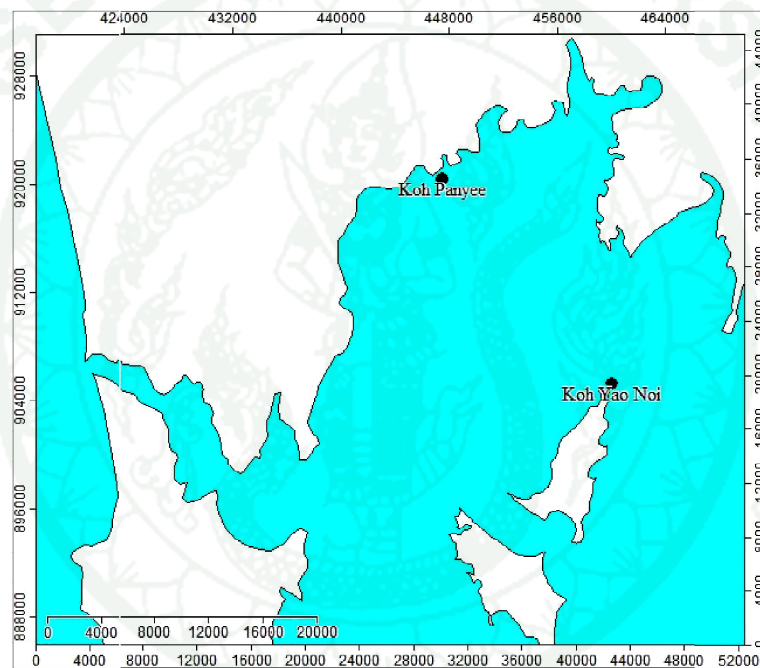


**Figure 23** Buoy test was conducted at Panyee island, located at Phang-Nga bay

Daily water level at Panyee was assumed by water level Tapao Noi predicted by Hydrographic Department on 21<sup>st</sup> November, 2013 (Figure 24). Buoy experiments were done from 10 AM – 5 PM at the place far from and not affected by the mouth of river. At 10 AM, water level demonstrated mean water level and it rose to hit the highest water at 1 PM. Then water level was abated to mean level again at 4.30 PM before it showed and then to low water after that.

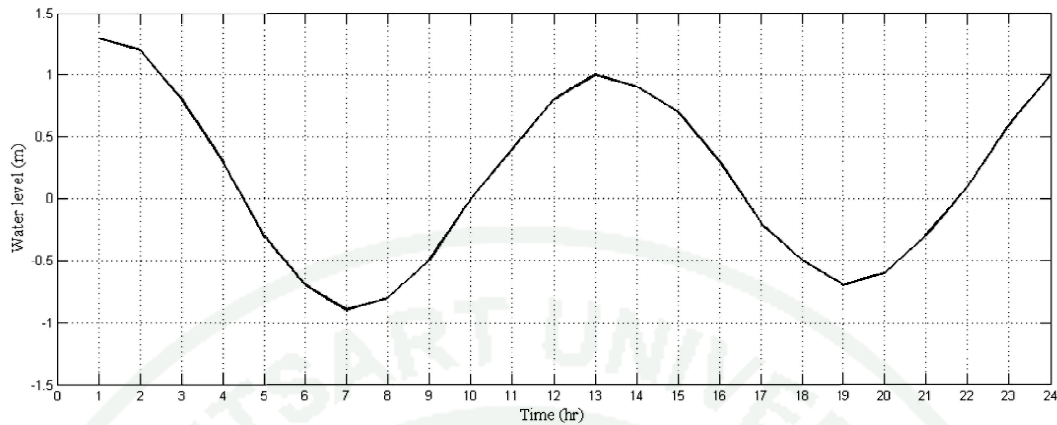


**Figure 24** Daily water level at Panyee island, Phang-Nga represented by Tapao Noi island on 21<sup>st</sup> November, 2013 (Hydrographic Department)

Free buoys were demonstrated by Figure 25a, 25b and 25c, whereas 240 g lead weighted buoy was shown in Figure 25d. All buoys movement commonly revealed the same pattern where it moved southward during early flood tide at 10 – 11 AM (black dots); westward during almost highest water until noon (black dot); and South and southwesterly during ebb tide where water level was decreasing (red dots). Unfortunately, weighted buoy was lost during the experiment, so there was no experiment during ebb tide in the afternoon.

According to Table 6, buoys with and without 240g lead floated on the sea surface with different velocity and it was predicted that a weighted lead buoy moved slower. In the morning as before highest water level at 1 PM, free buoys moved in range between 10 – 60 cm/s, while weighted buoy moved in the range of 15 – 20 cm/s. In the afternoon where water level was decreasing, and buoys' movement velocity even slower than those in the morning in less than 20 cm/s.

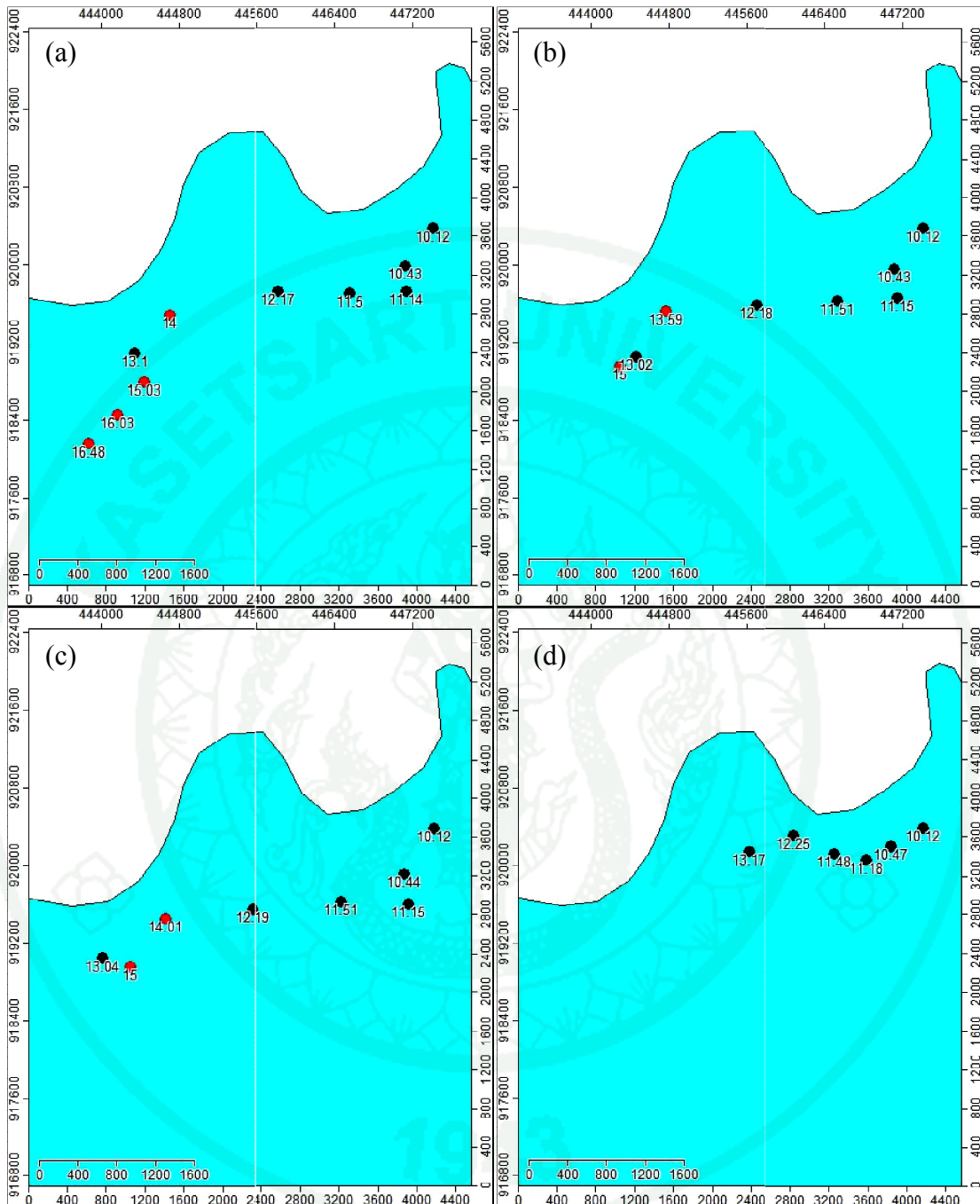


**Figure 25** Floatable buoys at Panyee island where (a) is Buoy 1, (b) is Buoy 2, (c) is Buoy 3 and (d) is Buoy 4 which was weighted by 240g lead at 50 cm depth at different times

**Table 6** Buoy observation at Panyee island and their velocities

<b>Buoy</b>	<b>Distance of Buoy (m)</b>	<b>Observation time</b>	<b>Time (min.)</b>	<b>Velocity (cm/s)</b>
1 (black)	480.34	10.12-10.43	31	25.82
	260.2	10.43-11.14	31	13.99
	581.99	11.14-11.50	36	26.94
	755.37	11.50-12.17	27	46.63
	1,605.64	12.17-13.10	53	50.49
2 (black)	510.03	10.12-10.43	31	27.42
	299.35	10.43-11.15	32	15.59
	619.1	11.15-11.51	36	28.66
	854.79	11.51-12.18	27	52.76
	1,352.91	12.18-13.02	44	51.25
3 (black)	546.44	10.12-10.44	32	28.46
	321.45	10.44-11.15	31	17.28
	696.32	11.15-11.51	36	32.24
	921.09	11.51-12.19	28	54.83
	1,624.78	12.19-13.04	45	60.18
4 (black)	364.51	10.12-10.47	35	17.36
	303.19	10.47-11.18	31	16.30
	344.93	11.18-11.48	30	19.16
	451.94	11.48-12.25	37	20.36
	499.47	12.25-13.17	52	16.01
1 (red)	430.69	15.03-16.03	60	11.96
	414.63	16.03-16.48	45	15.36
2 (red)	721.94	13.59-15.00	61	19.73
3 (red)	614.3	14.01-15.00	59	17.35

#### 4. Phi Phi islands, Krabi

Phi Phi islands are located in Krabi,  $7^{\circ}44'36.51$  North and  $98^{\circ}46'31.68''$  East. They are also located in Phang-Nga bay, 40 km Southeast from Phuket and belong to Krabi province. There are six islands in the group known as Phi Phi islands, and Phi Phi Don is the most well-known island with approximately 9.73 square km as shown in Figure 26. It is one of the most famous tourist destinations because of beautiful beaches and abundant biodiversity.

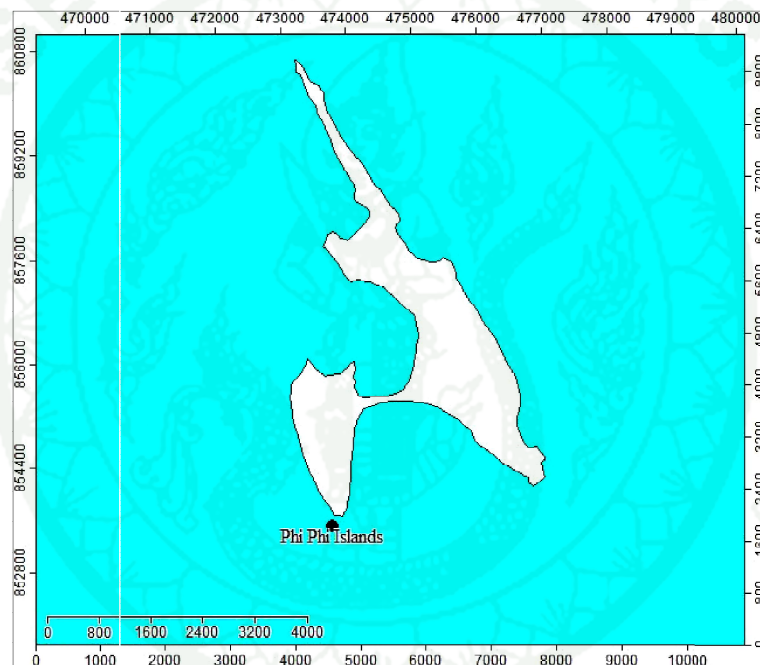


**Figure 26** Buoy test was conducted at Phi Phi Don, the Southwest of Phi Phi island

When buoy experiments were conducted, daily water level at Phi Phi islands calculated by Hydrographic Department was shown in Figure 27 with the assumption that water level at Phi Phi islands can be represented by water level at Tapao Noi island. Three buoys were left floating on the seawater for four hours from 12 – 4 PM in the afternoon. According to daily water level, 12 – 1 PM was flooding tide where low water was increasing to mean water. Then seawater level continually rose until it reached highest water level at 5 PM. However, it was noticeable that the tide was neap tide because tidal range was more or less than 1 m.

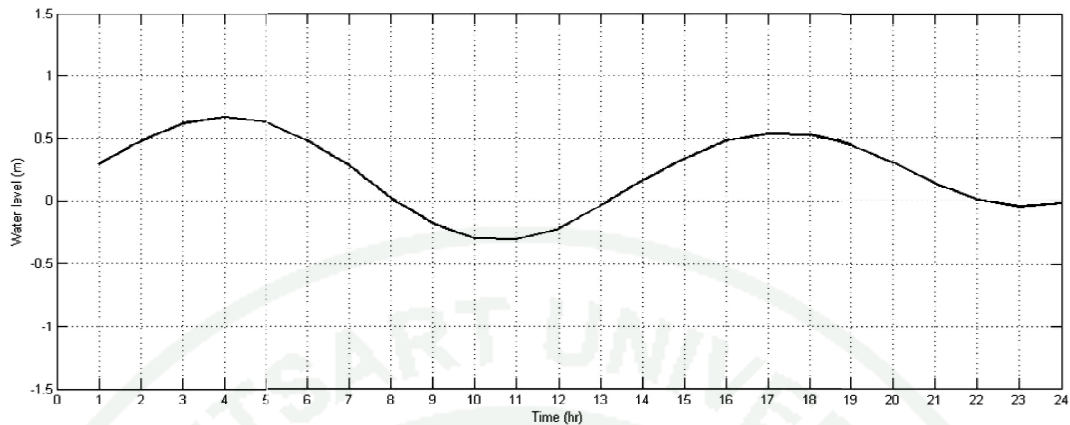


**Figure 27** Daily water level at Phi Phi islands, Krabi represented by Tapao Noi island on 26<sup>th</sup> November, 2013 (Hydrographic Department)

Figure 28 graphically demonstrated movement of three buoys which were left floating on the sea surface. The pattern of buoy movement is from South to North in one direction; however, it should be taken note that the experimental time was when the water was elevated from low water to mean water and to highest water, respectively. There was a buoy moving in the bay. The velocity of buoy movement was in between 25 – 55 cm/s (Table 7). This experiment showed a little error because the recording time is too large and the movement during smaller period of time was not noticed.

**Table 7** Buoys observation at Phi Phi islands and their velocities

Buoy	Distance of Buoy (m)	Observation time	Time (min.)	Velocity (cm/s)
1	3,603.04	12.09-16.11	242	24.81
2	5,579.28	12.09-15.50	176	52.83
3	4,616.95	12.09-16.00	231	33.31



**Figure 28** Three floatable buoys at Phi Phi Don at different time where (a) is Buoy 1, (b) is Buoy 2 and (c) is Buoy 3

## 5. Saphan Hin, Phuket

Saphan Hin is a well known park located in the southern East coast of Phuket, southern coast of the island (Figure 29). There are many households scattered around this area. Geographically, mangrove forest and small fisheries are commonly seen on the East side of Phuket island. Seabed is mostly mud mixed with sand, thus there are many types of seagrasses.

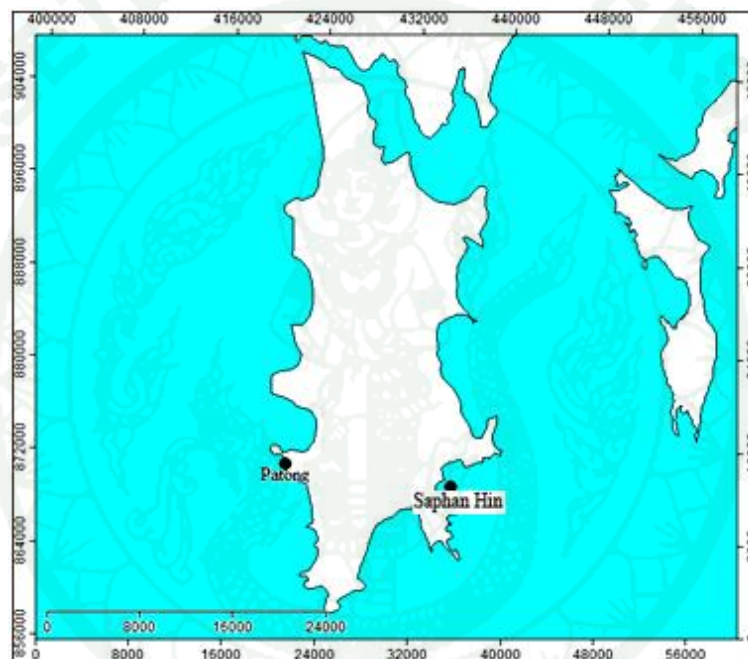


**Figure 29** Buoy test of the eastern current at Saphan Hin which is locate at the Southeast of Phuket

Daily water level at Sapha Hin, Phuket were estimated by Tapao Noi island, less than 5 km away from the study site and was calculated by Hydrographic Department (Figure 30). Buoy experiment were conducted on 28<sup>th</sup> November, 2013 for 6 hours from 9 AM – 3 PM. The observation period covered high water at 9 AM in the morning abating to mean water at 11 AM. Then it was further decreased until it hit lowest water level at 1 PM in the afternoon before it started rising at reached mean water level at 4 PM, as shown in Figure 30.

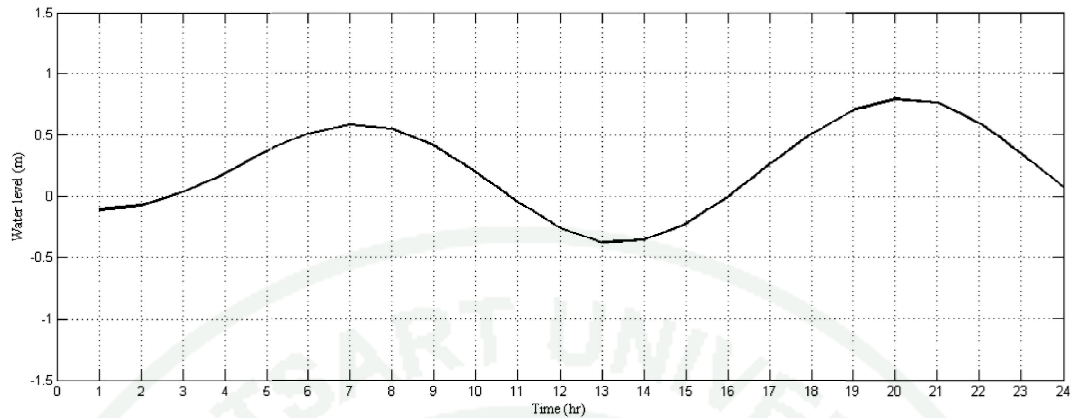


**Figure 30** Daily water level at Saphan Hin, Phuket represented by Tapao Noi island on 28<sup>th</sup> November, 2013 (Hydrographic Department)

Movement of four buoys was entirely graphically shown in Figure 31. All four buoys demonstrated insignificant different result regarding their velocities and directions. As water level decreased from high water to mean water and to low water, buoys moved southward and then it moved westerly during flood tide where water level was elevated.

To sum up, the actual floatable buoys traveled with velocity of 25-40 cm/s as shown in Table 8. Velocity of buoys movement for both directions shown insignificant difference even the flood tide (in the afternoon) was slightly lesser. The experiment displayed an error where buoy was stuck with fishing gears or mud at low tide.

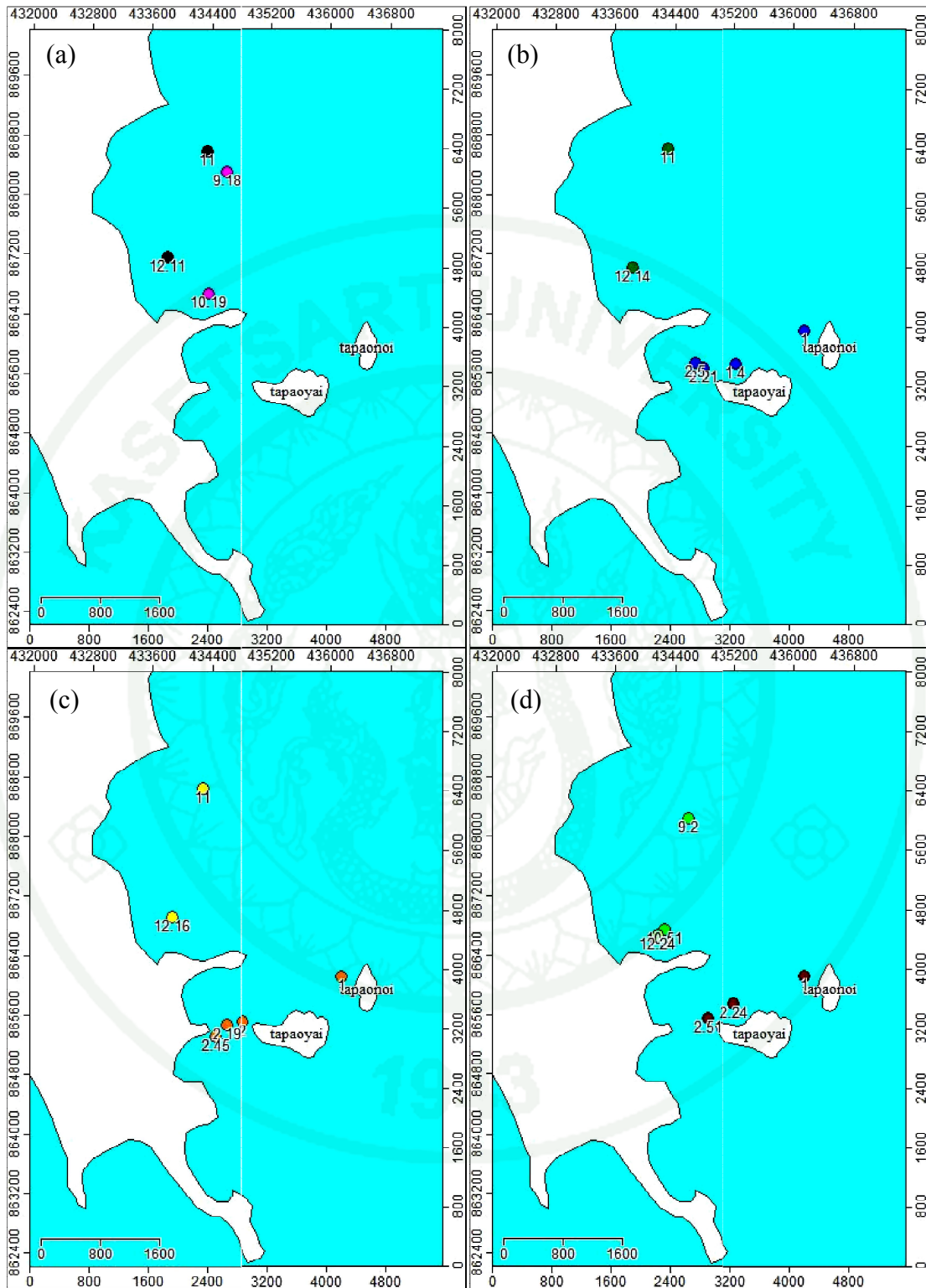


**Figure 31** Four floatable buoys at Sapha Hin at variable time where (a) is Buoy 1, (b) is Buoy 2, (c) is Buoy 3 and (d) is Buoy 4

**Table 8** Buoys observation at Saphan Hin and their velocities

Buoy	Distance of Buoy (m)	Observation time	Time (min.)	Velocity (cm/s)
1 (black)	1,683.55	9.18-10.19	61	46.00
1 (pink)	1,530	11.00-12.11	71	35.92
2 (dark green)	1,665	11.00-12.14	74	37.50
	1,021	1.00-1.40	40	42.54
2 (blue)	444	1.40-2.21	41	18.05
	128	2.21-2.50	29	7.36
3 (yellow)	1,784.50	11.00-12.16	76	39.13
	1,478	1.00-2.00	60	41.06
3 (orange)	219	2.00-2.19	19	19.21
	230	2.19-2.45	26	14.74
4 (light green)	1,547	9.20-10.51	91	28.33
	118.5	10.51-12.24	75	2.63
4 (black)	1,020	1.00-2.24	84	20.24
	400	2.24-2.51	27	24.69

## 6. Kuraburi, Phang-Nga

Kuraburi is located in North of Phang-Nga facing the open Andaman Sea. It accommodates three national parks entitled Similan islands National Park, Sri Phang-Nga National Park and Surin islands National Park. Despite the fact that it is well-known for tourist destination in dry season, small scale aquaculture and fishing industry are also practiced all year round. Anecdotal information from local communities revealed that dugong often visits this area for seagrasses.

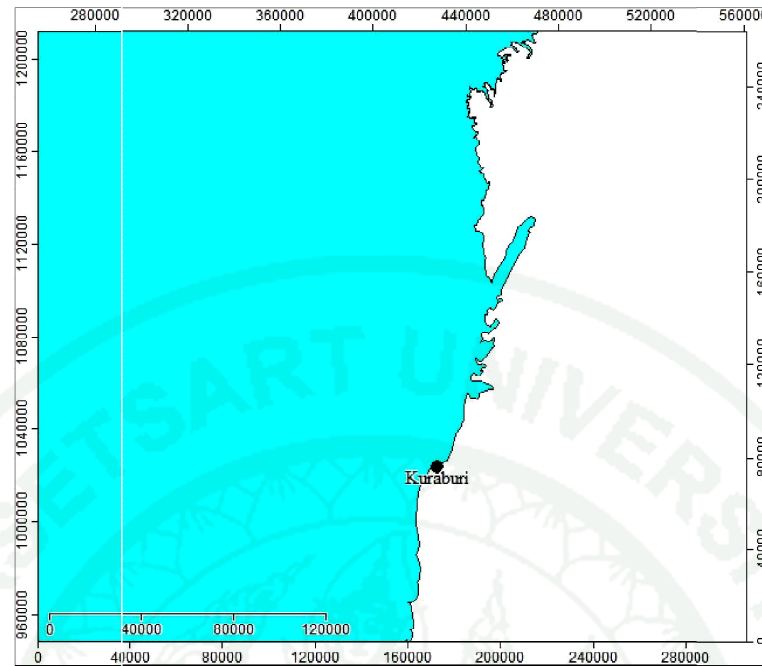


**Figure 32** Buoy test was conducted at the site where is facing open Andaman Sea at Kuraburi, Phang-Nga province

Daily water level at Kuraburi was assumed to be represented by Kuraburi station on 30<sup>th</sup> November, 2013 calculated by Hydrographic Department. The experiment was carried out 10 AM – 2 PM covering highest water level, high water, mean water and low water as shown in Figure 33. Water level demonstrated highest water at 10 AM before it abated by ebb tide and reached water level at 12 PM. Later on, water level continually decreased until it reached lowest water level at 3 PM.

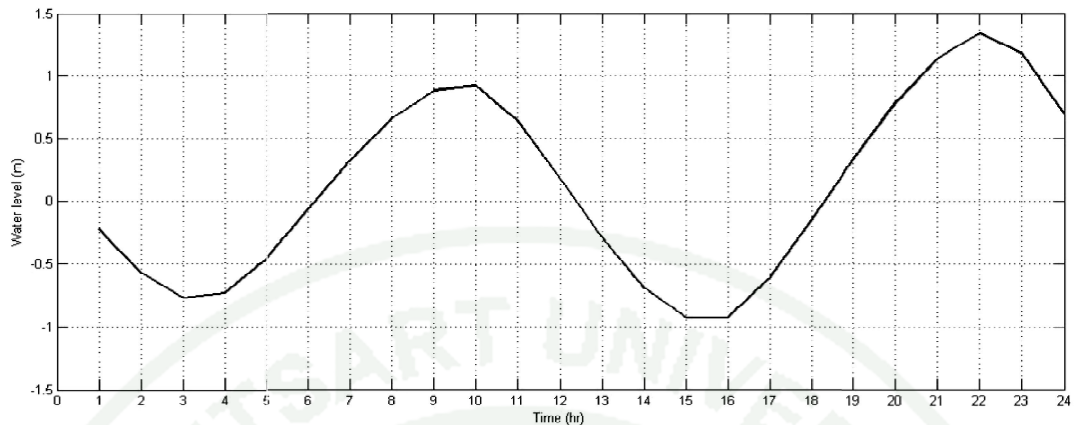


**Figure 33** Daily water level at Kuraburi, Phang-Nga represented by Kuraburi on 30<sup>th</sup> November, 2013 (Hydrographic Department)

Free buoys were graphically shown in Figure 34a, 34b and 34c where 240 g weighted buoy was shown in Figure 34d. All free buoys showed the same movement's direction, while weighted buoy moved differently. Free buoys moved southeasterly when water was decreasing from highest water to mean water level. Meanwhile, weighted buoy moved easterly during high water and southwesterly during low water.

Buoys commonly floated with various velocities of 9 – 30 cm/s for free buoys and 2 – 8 cm/s for weighted buoy as shown in Table 9.

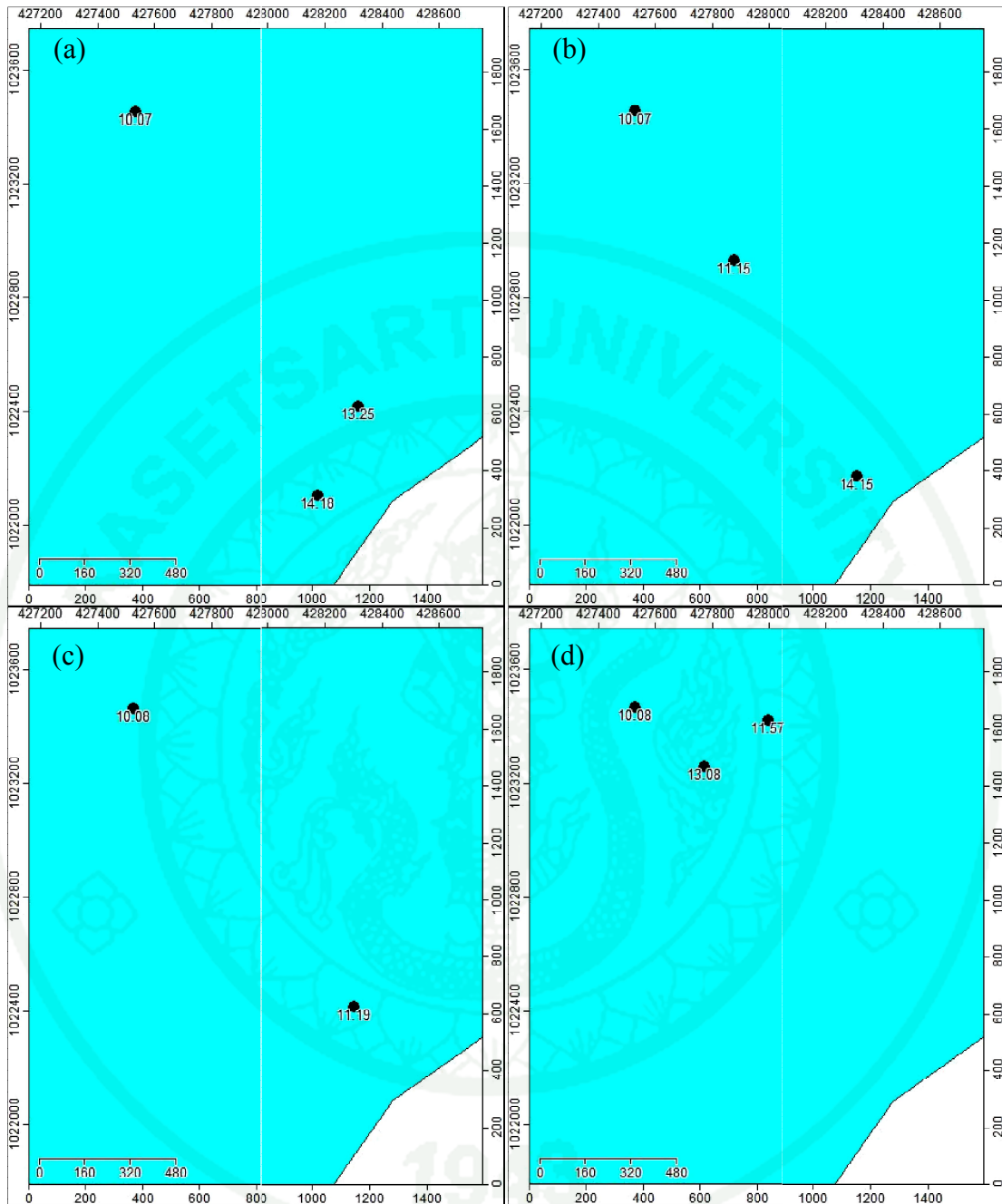


**Figure 34** Floatable buoys in Kuraburi at variable time where (a) is Buoy 1, (b) is Buoy 2, (c) is Buoy 3 and (d) is Buoy 4 which was weighted by 240g lead at 50 cm depth at different times

**Table 9** Buoys observation at Kuraburi and their velocities

Buoy	Distance of Buoy (m)	Observation time	Time (min.)	Velocity (cm/s)
1	1,307.95	10.07-13.25	198	11.01
	346.05	13.25-14.18	53	10.88
2	638.55	10.07-11.15	68	15.65
	895.30	11.15-14.15	180	8.29
3	1,304.83	10.08-11.19	71	30.63
4	468.83	10.08-11.57	109	7.17
	283.47	11.57-13.08	180	2.62

In conclusion, buoy experiment at Patong, Phuket, had disclosed that the floating marine particles were moving with average velocity of 5-45 cm/s. However, the continual longer timing observation would reveal different and different result. In addition, velocity of buoys conducted at Yao Noi island was in the range of 5 - 65 cm/s as well as buoys at Panyee island. Meanwhile at Phi Phi Don island, floating marine particles moved approximately 25-50 cm/s. Buoy experiment at Saphan Hin showed that the particles floating on the sea surface travelled in velocity of 5 - 40 cm/s. Lastly, buoy experiment conducted at Kuraburi were seen travelling with velocity of 5-30 cm/s.

The total buoy experiment continuously conducted for up to 6 hours revealed that the direction of floating marine particles during experimenting hours was influenced by tidal current because they moved in the circle following the rotary current during the tide period. Therefore, the direction of particle movement during maximum 6 hours also based upon the location and tidal current in the areas. This was agreeable to the simulation displayed the movement of 6 hours floating marine particles as tidal dominated. Nevertheless, it should be noted that the longer hour observation would show different result because the buoy was moved in circular direction depending on phase of tidal stage.

## Tidal Validation

Tidal validation is a process where demonstrates the performance of simulation by comparing tidal solution obtained from simulation against observation data. To investigate whether water elevation is performed well by FVCOM, horizontal comparison of water level is analyzed by five means which are 1) tidal range error; 2) tidal harmonic analysis; 3) histogram of water level difference; 4) linear regression of water level and 5) predictive skill. Tidal range error and tidal harmonic analysis were calculated based on 41 day performance including 984 hours; whereas 328 hours were re-sampled for further statistical analysis such as histogram of water level difference, linear regression of water level and predictive skill.

### 1. Tidal range relative error and water level comparison

Tidal range of two spring tides were analyzed its relative error to observation between observation and simulation. Tidal range is vertical difference of between high tide and succeeding low tide. Tidal simulation by FVCOM reveals tidal range relative error of 4.8%, 5.24%, 2.02% and 5.34% at Ao por, Tapao Noi, Kuraburi and Tarutao, respectively. Overall, simulation of tidal range is less than 6% at every station which demonstrates that simulation performs reasonable tidal range.

Comparison of water level at Ao Por, Phuket between observation (black) and simulation is graphically shown in Figure 35.

Overall, tidal solution obtained from model performs overestimated for both high tide and low tide. Unlike spring tide, neap tide period shows more accurate visual tidal elevation.

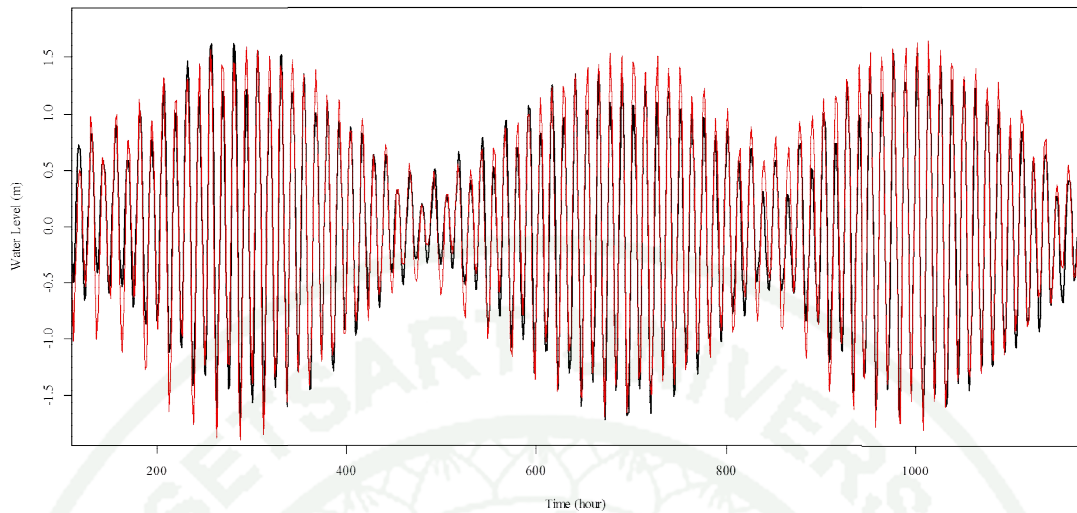


**Figure 35** Comparison of time series tidal elevation at Ao Por for 41 days where black line is observation and red line is simulation

Water level plotted in time series between observation (black) and simulation at Tapao Noi, South East of Phuket, is shown in Figure 36. The visual image casually shows overestimated tidal resolution calculated by FVCOM especially spring tide which probably results in large water level differences.

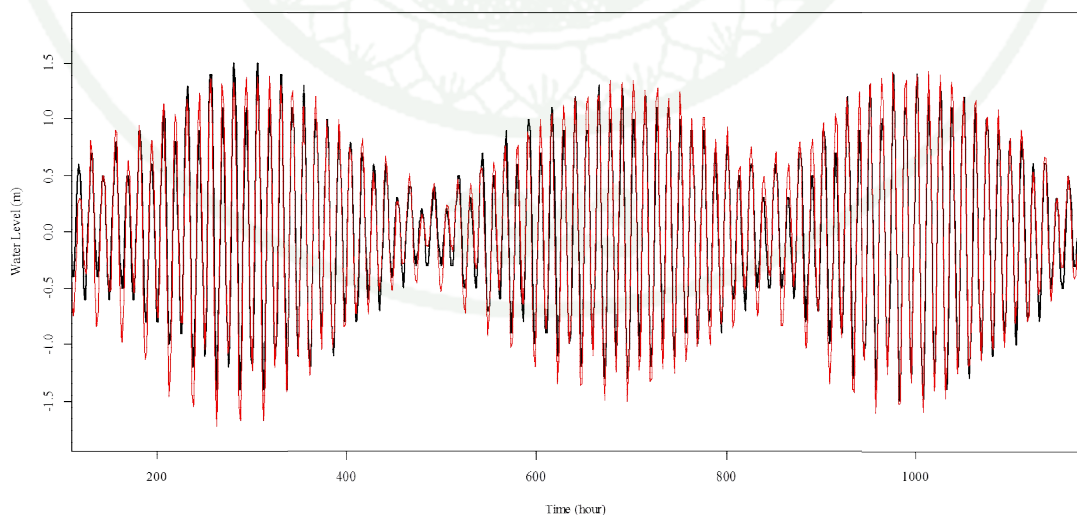


**Figure 36** Comparison of time series tidal elevation at Tapao Noi for 41 days where black line is observation and red line is simulation

Water level of observation and simulation at Kuraburi, Krabi is plotted in time series in Figure 37. It visually demonstrates underestimated tidal resolution at low and high tide during spring tide period; however, overestimate tidal solution can be seen during common low water in regular day basis.

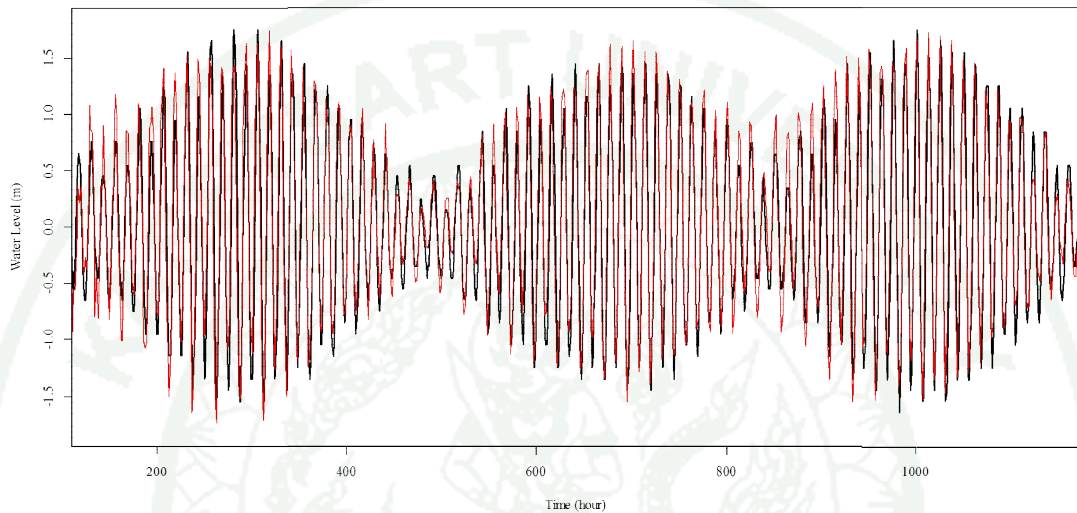


**Figure 37** Comparison of time series tidal elevation at Kuraburi for 41 days where black line is observation and red line is simulation

Water level comparison between tidal observation and simulation by FVCOM at Tarutao, Satul is shown in Figure 38. It occasionally displays overestimated tidal solution during high water and performs underestimated tidal solution for low water.

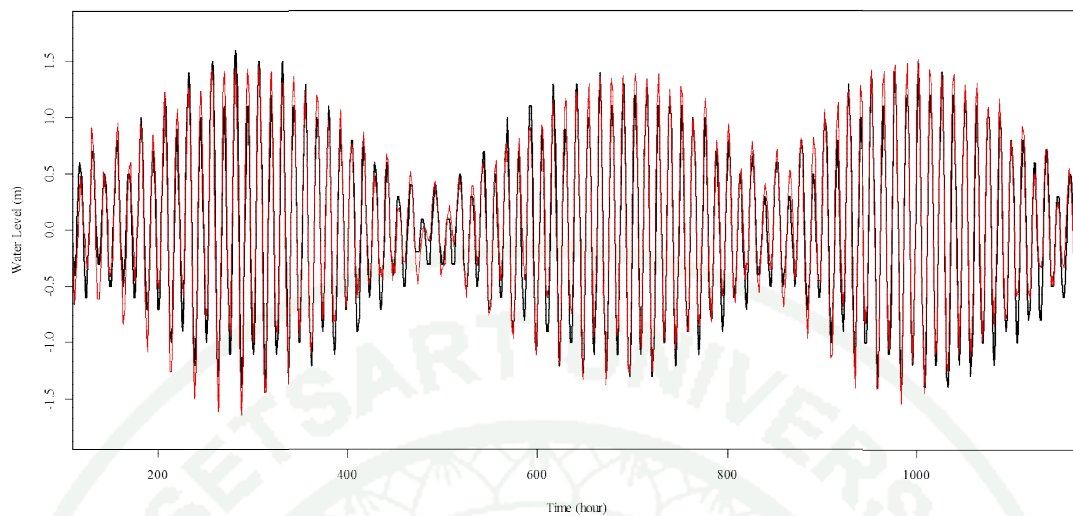


**Figure 38** Comparison of time series tidal elevation at Tarutao for 41 days where black line is observation and red line is simulation

## 2. Tidal harmonic analysis

A tidal harmonic analysis was determined by the T\_Tide tidal package (Pawlowicz *et al.*, 2002) for 41 days in total for both tidal resolution and observed tidal elevation. According to harmonic analysis, tide at four stations along Southern part of Thailand - Ao Por, Tapao Noi, Kuraburi and Tarutao - are dominated by five tidal constituents. They are Principal lunar semidiurnal constituent (M2), Lunar diurnal constituent (K1), Principal solar semidiurnal constituent (S2) and Larger lunar elliptic semidiurnal constituent (N2). Result of tidal harmonic analysis of all station is listed in detailed in Appendix B. Thus, tidal amplitude and phase of those mentioned tidal constituents are reported in Table 10 and Table 11, respectively.

Tidal amplitude difference between observation and simulation at all station is less than 0.1 m (or 10 cm). It is agreeable that major constitutes' amplitude at all station has low percent relative error to observation. Similar results of most major constituents in individual areas are also shown in Global tidal simulation that the tidal amplitude difference is less than 12 cm (Christian *et al.*, 1995). The evidence shown by harmonic analysis, it may conclude that FVSOM has performed well in order to

simulate tidal amplitude which is slightly close to data of tidal amplitude obtained from observation.

**Table 10** Tidal amplitude (m) and its percent reduction difference of harmonic constituents of tidal amplitude

Station	Term	Tidal Constituents' amplitude (m)			
		*M2	*K1	*S2	*N2
Ao Por	Observation	0.93	0.14	0.51	0.17
	Simulation	1.03	0.17	0.52	0.20
	Relative difference (%)	10.68	23.07	0.96	22.32
Tapao Noi	Observation	0.80	0.14	0.43	0.15
	Simulation	0.912	0.16	0.46	0.19
	Relative difference (%)	13.35	19.93	6.56	25.50
Kuraburi	Observation	0.93	0.13	0.51	0.17
	Simulation	0.86	0.14	0.40	0.18
	Relative difference (%)	7.96	6.39	20.97	5.71
Tarutao	Observation	0.82	0.16	0.45	0.14
	Simulation	0.93	0.20	0.50	0.19
	Relative difference (%)	14.03	26.10	11.59	40.16

Tidal phase is also reported in Table 11, as well as tidal phase difference between observation and simulation. Tidal phase shows time difference of tidal occurrence. For the most dominated tidal constituents such M2, tidal phase difference is less 0.61°, 1.99°, 11.06° and 7.04° at Ao Por, Tapao Noi, Kuraburi and Tarutao, respectively. It, therefore, is lagged most at Kuraburi station with approximately 25 minute. The result show that FVCOM has performed well because the phase different is smaller than oceanic simulation that perform by other model at Adriatic Sea which shows the least phase difference of 50° of its most major constituent (Janekovic and Kuzmi, 2005). Based upon tidal phase difference compared between observation and

simulation, phase difference of the most dominated tidal constituent, M2, performs very well with the least phase difference.

**Table 11** Tidal phase (°) and its error statistic of harmonic constituents of tidal elevation

Station	Term	Tidal Constituents' phase (°)			
		*M2	*K1	*S2	*N2
Ao Por	Observation	333.59	298.44	2.76	204.29
	Simulation	332.97	235.77	358.59	214.80
	Difference	0.62	62.67	4.17	10.51
Tapao Noi	Observation	329.85	298.87	358.56	197.84
	Simulation	327.86	233.26	352.71	209.05
	Difference	1.99	65.61	5.85	11.21
Kuraburi	Observation	327.85	298.67	356.89	195.67
	Simulation	316.79	224.42	337.14	197.02
	Difference	11.06	74.25	19.75	1.35
Tarutao	Observation	341.55	302.70	12.69	214.93
	Simulation	340.81	243.67	7.03	221.89
	Difference	0.74	59.03	5.66	6.96

### 3. Histogram of water level difference

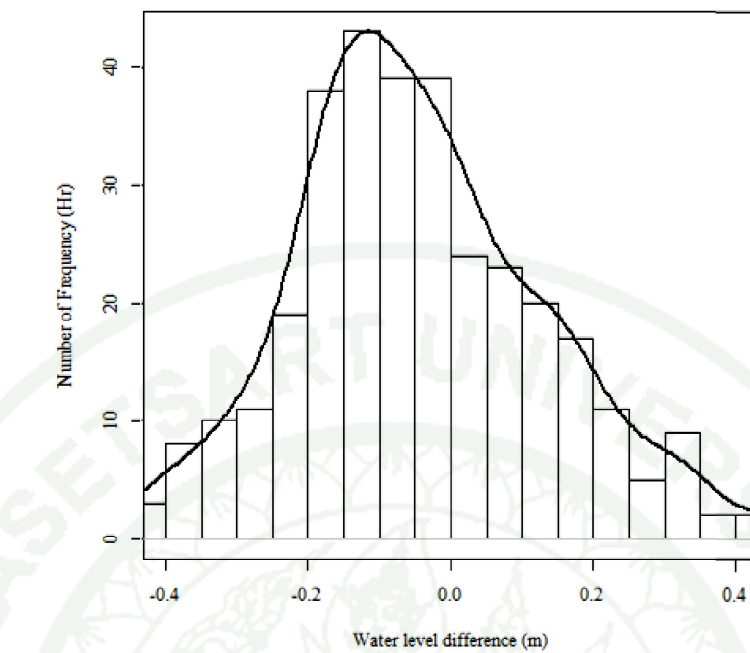
Histogram of water level difference between sampling observation and stimulation at four stations for 328 hours (or 41 days) consists of three spring tides and two neap tides. Difference is calculated by observation deducted with simulation. If difference is equal to zero, water level of simulation performs well against water level of observation. If difference is less than zero, water level of simulation is overestimated. And if difference is greater than zero, water level of simulation is underestimated. Mean of water level difference demonstrates the equal between

simulation and observation. Hence, the more average water level different is close to zero, the more accurate of sampling data.

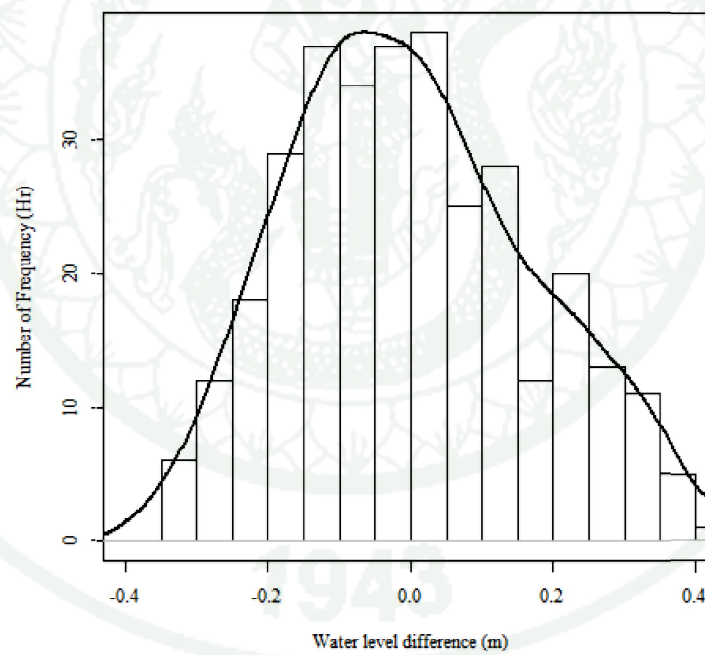
Then difference of water levels are plotted in histogram graph and shown in Figure 39. Overall, water level difference is small at every station. Water level difference at Ao Por is shown in Figure 39a, and average of water difference between simulation and observation is 0.0419 m, which shows that simulation is overestimated. Water level difference at Tapao Noi is shown in Figure 39b. Overall, average of water level difference is 0.0043 m which shows very small overestimated simulation. Water level difference at Kuraburi is shown in Figure 39c, simulation performs the worst among all station because there were many hours that water difference falls to have 40 cm water level difference, and it overall is overestimated average of water level difference of -0.0765 m. Water level difference at Tarutao is shown in Figure 39d, it shows the obvious overestimated calculation with -0.0595 m of average of water level difference. Overall, mean of water level different between observation and simulation at four stations is less than 0.07 m.

To sum up, simulation has overall demonstrated overestimated according to histogram of water level differences between 0 - 20 cm at all stations.

1943

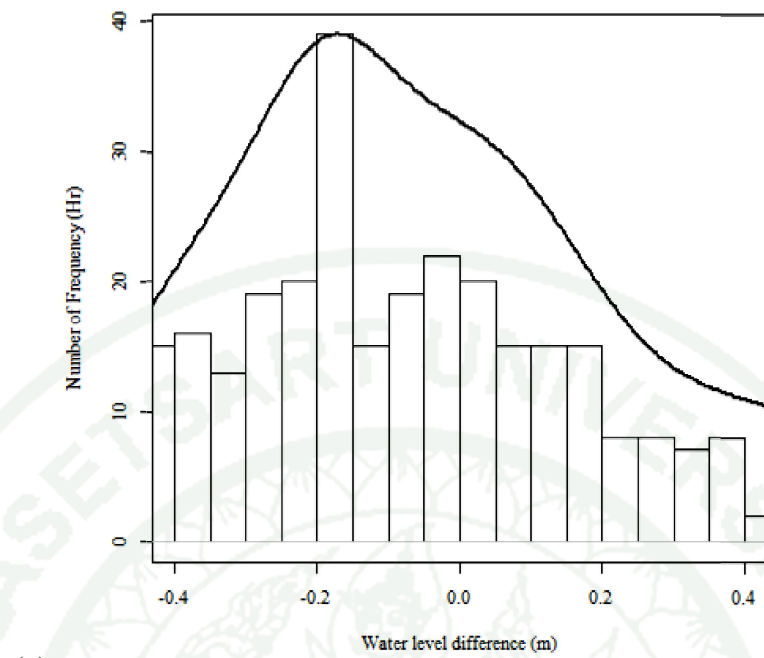


(a)

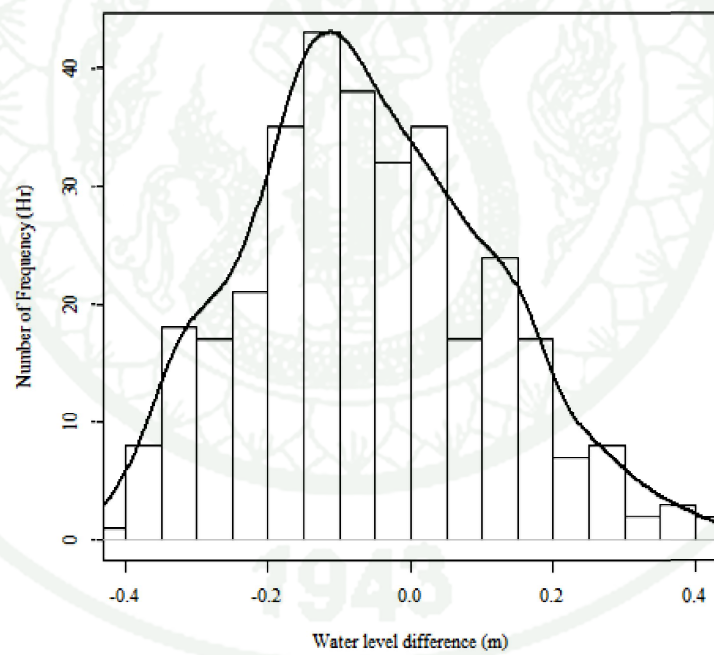


(b)

**Figure 39** Histogram of water level difference between observation and simulation for 328 sampling hours during 41 days at (a) Ao Por, (b) Tapao Noi, (c) Kuraburi and (d) Tarutao



(c)



(d)

**Figure 39** (Continued)

#### 4. Linear regression of water level between observation and simulation

Linear regression of water level between simulation and observation is calculated in order to determine whether water level of those is correlated. Water level of observation and simulation are plotted as x and y coordinates, respectively, for sampling 328 hours during 41 days. Coefficient determination or R squared ( $R^2$ ) explicit how well data point fit the statistic model. It ranges from 0 to 1 where 1 shows a good agreement between observed and modeled data.

Linear regression at four stations is calculated and shown in Figure 40. Overall, all stations show good result of water level between simulation and observation with R squared more than 0.93. The relation of those is linear which indicates that tidal solution would be simulated to have high water if observation shows high water as well. Unlike other three stations, Ao Por station demonstrated disorder data points. This is because observation data is obtained from gauge station. While the other three stations are predicted from data obtained from gauges. Therefore, data points at Tapao Noi, Kuraburi and Tarutao show periodical water level.

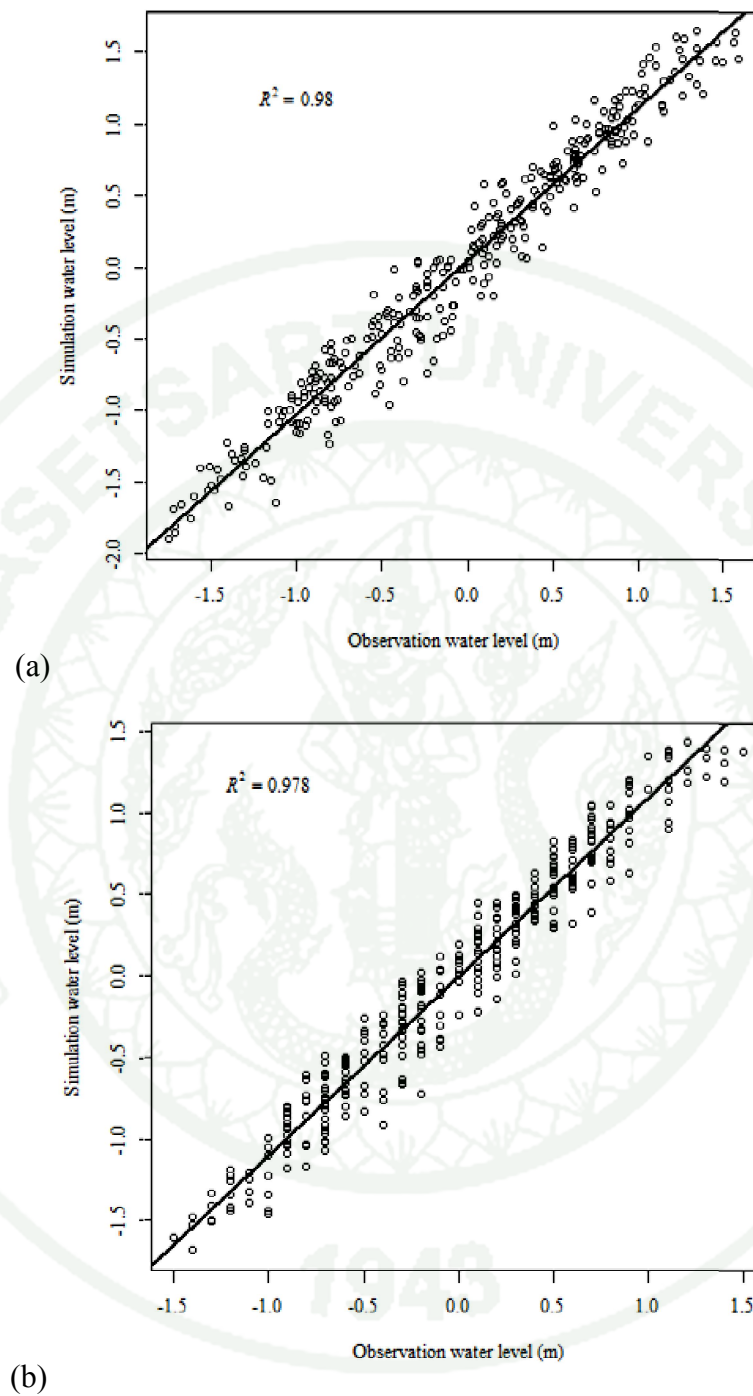
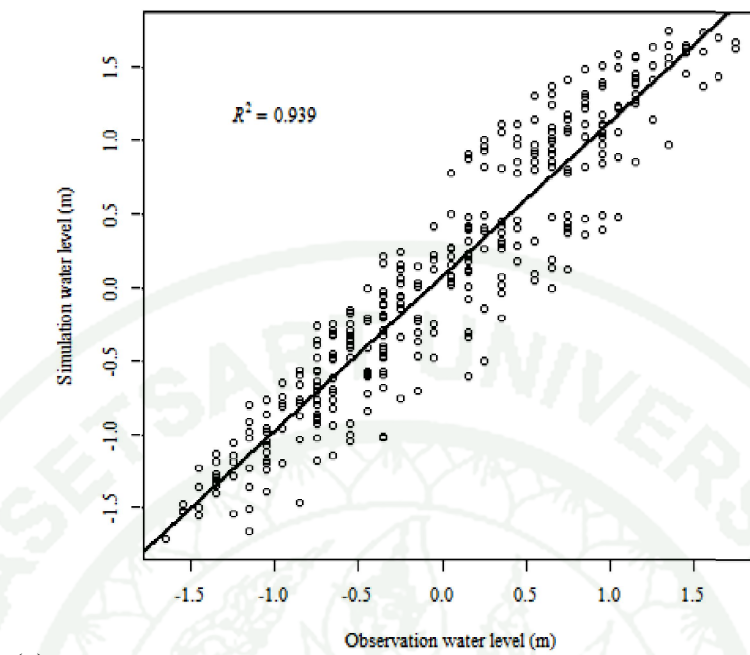
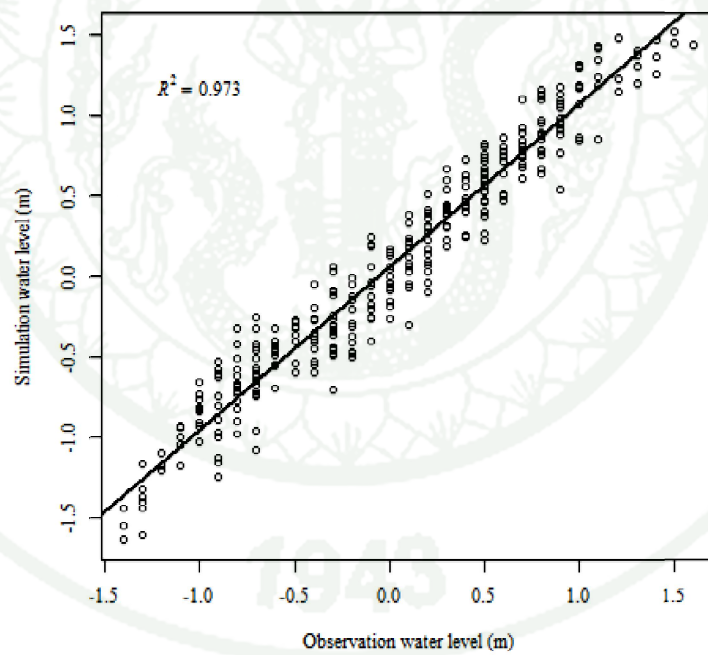


**Figure 40** Linear regression of water level between observation (m) and simulation (m) at (a) Ao Por, (b) Tapao Noi, (c) Kuraburi and (d) Tarutao



(c)



(d)

**Figure 40** (Continued)

## 5. Predictive skill

Based upon calculation of predictive skill of sampling data between simulation and observation; the model yields 0.988, 0.986, 0.964 and 0.984 at Ao por, Tapao Noi, Kuraburi and Tarutao, respectively. It confirms that there is no significant different between four stations in using model to simulate water level. Overall model verification shows that FVCOM has performed a good simulation of water level due to tide.

With all evidence in both statistical analysis and harmonic analysis of water elevation between tidal solution calculated by FVCOM and observation, simulation is agreeable to observation in vertical prediction of water level.

### Current Pattern

#### 1. Tidal characteristic

The tidal constituents of each station were analyzed for tidal description by Form Number. At four stations, tide is majorly dominant by  $M_2$ ,  $S_2$  and  $N_2$  which represent semidiurnal tide and  $K_1$  along with  $O_1$  which represent diurnal tide. Form Number of stations for both observation and simulation is all less than 0.25 (Table 12) which dictates that there is only one major type of tide, namely semidiurnal tide, along western Thai coast of Andaman. Semidiurnal tide presents two high water and two low water dairy with almost equal amplitude. The result is well agreed with hydrodynamic-numerical simulation with HAMSON (Syamsul *et al.*, 2012).

**Table 12** Form number for tidal characteristic at four stations

Stations	Form Number		Tidal characteristic
	Observation	Simulation	
Ao Por	0.125	0.171	Semidiurnal
Tapao Noi	0.150	0.188	Semidiurnal
Kuraburi	0.129	0.181	Semidiurnal
Tarutao	0.173	0.224	Semidiurnal

Semidiurnal is tide where there are two low and two high tides in a day; a period of tide is, thus, approximately 12 hours. Tidal current flows in changing direction throughout a tidal phase in a circular direction. Because of the Earth's clockwise rotation in the North hemisphere, tidal current is circulatory. As shown in Figure 41, water level is the water elevation (m) and velocity is vector of tidal current where length of vector presents current velocity and direction of vector is directional vector of tide. During the high tide where water rises up, tidal current moves northward until it reached maximum high tide. Then the water goes down to mean sea level while it moves northeasterly. At the mean sea level, there is a short period of time where there is no tidal current; so called slack water. Tidal current moves South and Southwest during ebb tide until it reached maximum low tide. Tidal current moves controversy between high tide and low tide. Every hour during the tidal period, speed of the current is varied arising from zero at the time of slack and mean sea level.

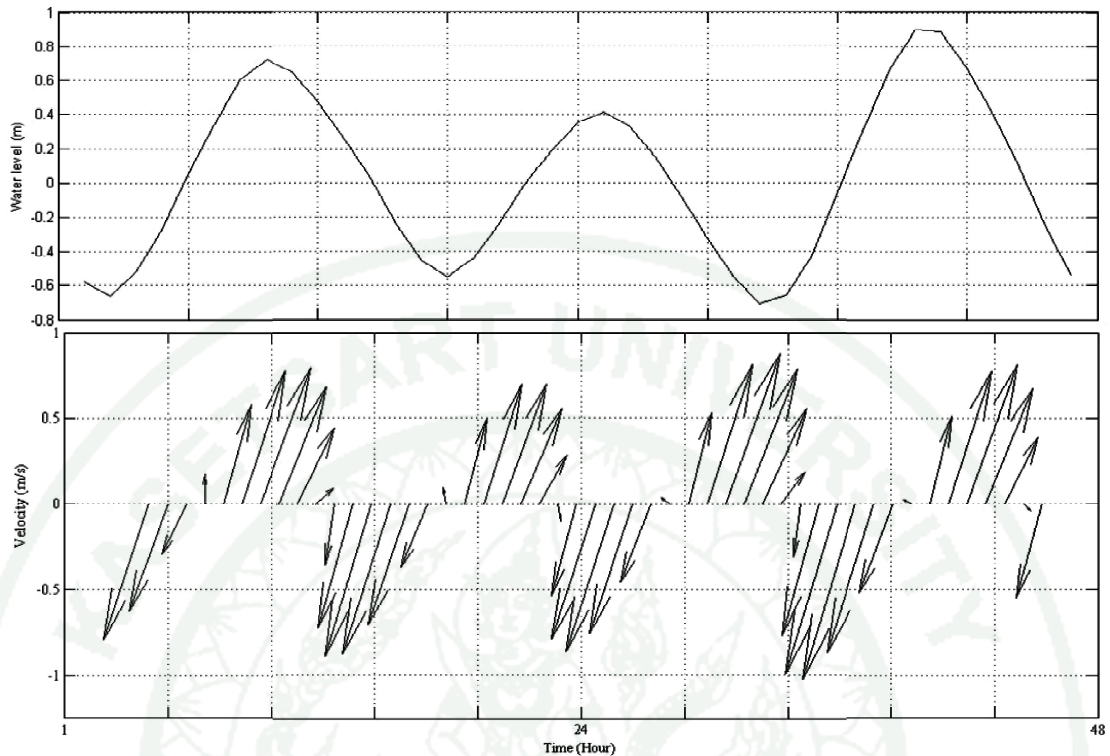


**Figure 41** Tidal rotary current demonstrated its velocity, direction and water level at Saphan Hin, Phuket for four periods of tide.

Dawei in the South West of Myanmar and strait of Malacca are first seen flooded, then the high tide spreads seawards covering gulf of Martaban and Malaysian Peninsula and northwesterly covering Strait of Malacca during flood current (Figure 42a). The high tide is wiped to enter Gulf of Martaban and Strait of Malacca by the mean tide entering from the West of Andaman Sea (Figure 42b). Ebb tide moves from the West of Andaman Sea and Strait of Malacca and there is high water at latitude of  $3-4^{\circ}$  N (Figure 42c). Low water of ebb current flows covering the most part of domain except Gulf of Martaban and Strait of Malacca where there is high water at mentioned latitude (Figure 42d). The high tide at latitude of  $3-4$  where most of the domain covered by low tide moves Southwest and lasted only 4-5 hours before it occurs again when the ebb flood comes.

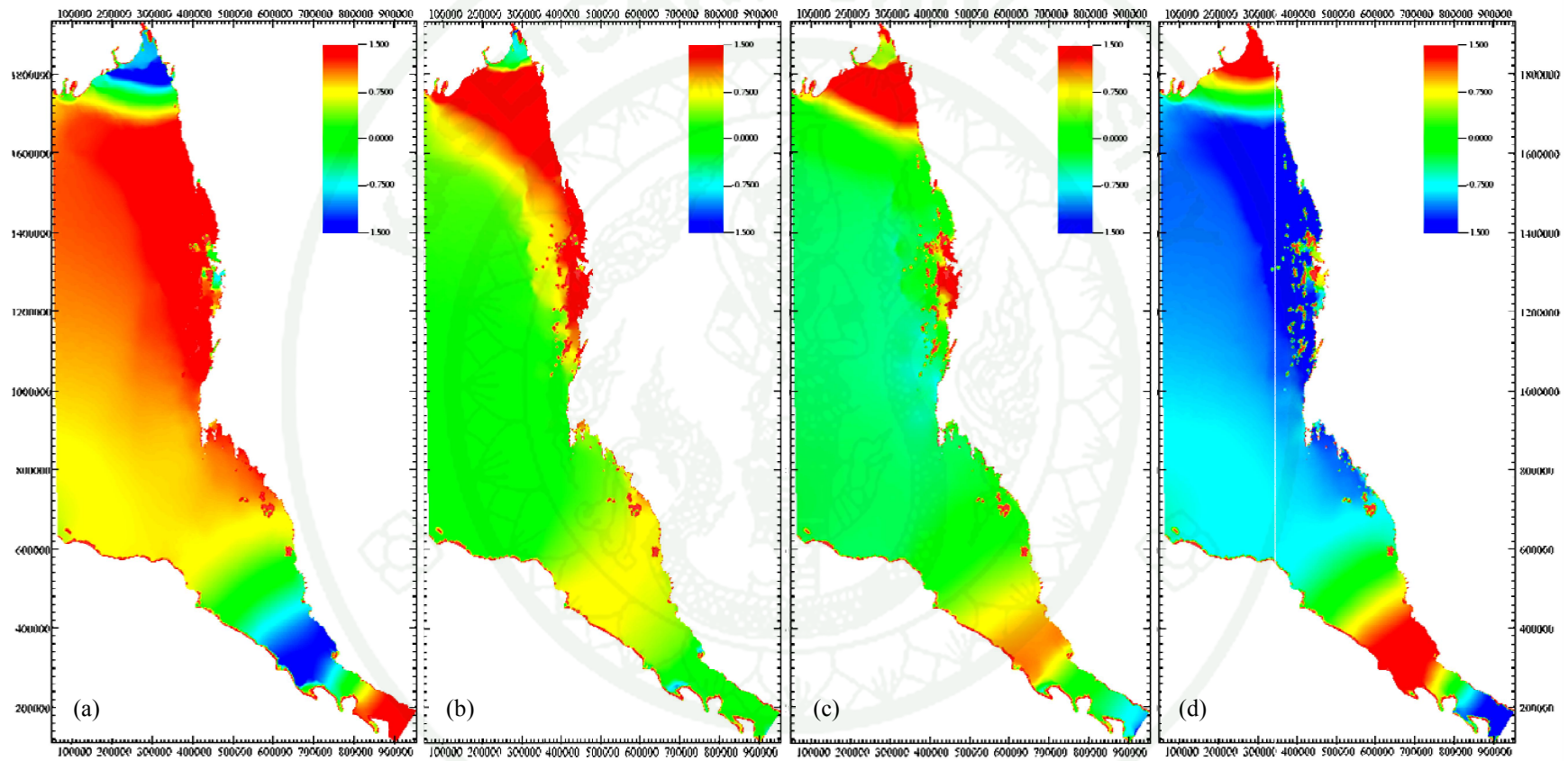


**Figure 42** Sea water level (m) of flood current during (a) high tide and (b) mean tide and ebb current during (c) mean tide and (d) low tide at Phang-Nga bay

## 2. Tidal current pattern

Surface current pattern in Andaman Sea is computed by FVCOM forced by only tidal amplitude at boundary condition. Surface current pattern including velocity and direction is analyzed by one month residual surface current in order to roughly foresee direction of marine particles floating along the sea surface of Andaman Sea driven by tidal dominated condition.

Magnitude of residual surface current resulted from tidal dominated forcing in the Andaman Sea is exhibited in Figure 43a, while that in Phang-Nga bay is shown in Figure 43b. Residual tidal current on the sea surface is nearly zero at distant offshore from coastal zone such at the center of the Andaman Sea. Velocity of residual tidal current is obviously increasing when it is nearer to the shoreline or intertidal zone such coastal zone of Gulf of Martaban, the Andaman and Nibobar islands and the strait of Malacca. Therefore, the residual surface current caused from tide is approximately 0-15 cm/s by overall. At Strait of Malacca, residual surface velocity is 5-30 cm/s which is coherent with HAMSON model forced by tide, wind, salinity and temperature in February (2007) at Malacca Strait (Syamsul *et al.*, 2010). At Phang-Nga bay, residual tidal current is clam except for those areas where is near coastal zone and at shallow water; overall residual surface current velocity is approximately 0 – 20 cm/s. as shown in Figure 43b. The strongest residual tidal surface current is found at Racha islands and Yao islands. The magnitude of tidal residual speed along Thai coastal is less than that simulated by a 2-D vertically-averaged hydrodynamic model (Pornpinatepong, 2005). This is probably due to fo grid size which allows model to capture small magnitude of tidal velocity along near-shore environment.

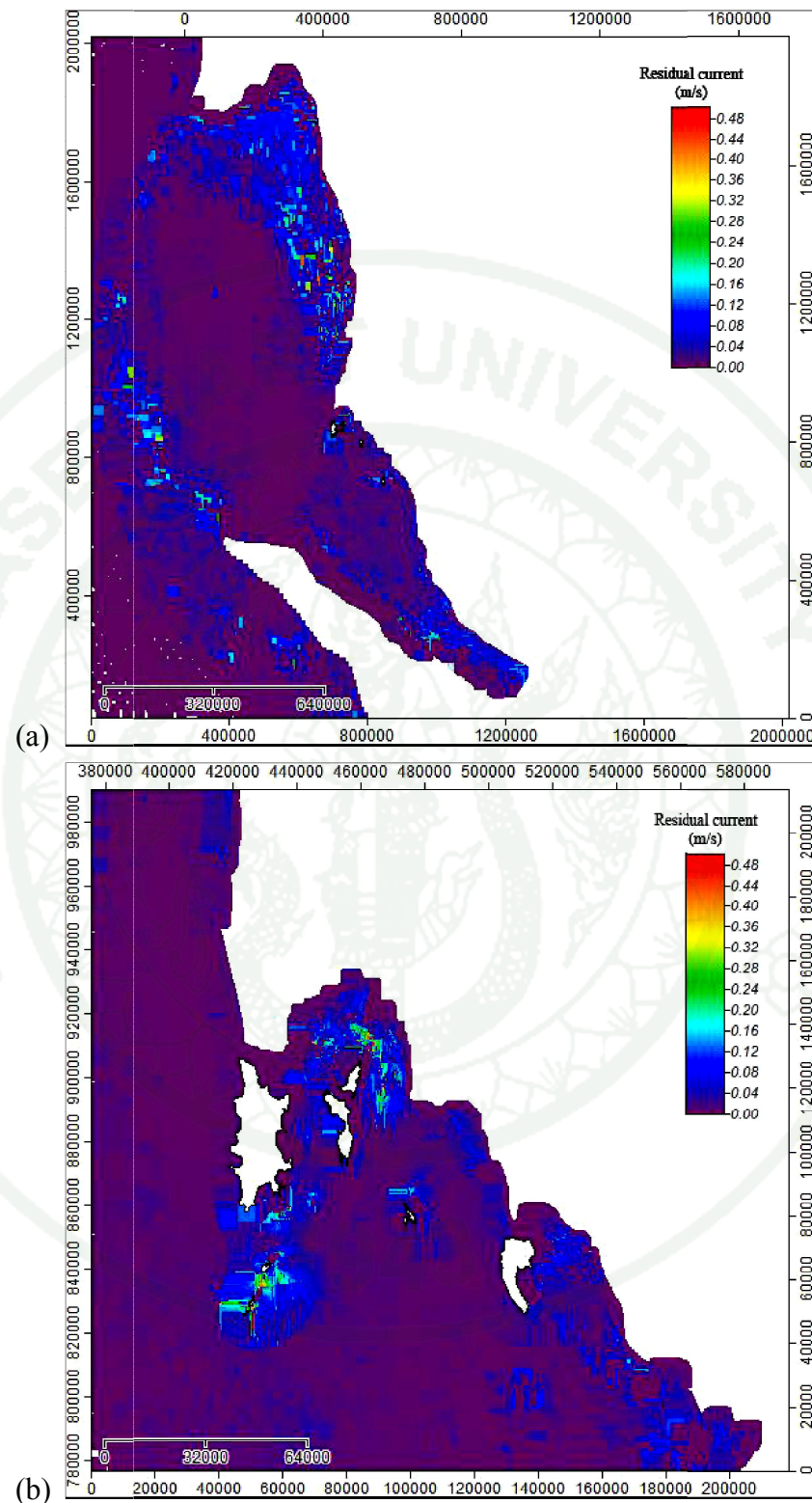


**Figure 43** Magnitude of residual surface current in (a) Andaman Sea and (b) Phang-Nga bay under the tidal dominated condition predicted by FVCOM

Directional vector of residual surface current forced by solely tidal amplitude in the Andaman Sea is shown in Figure 44. Overall observation of residual tidal current on the surface seawater reveals that residual tidal current moves towards various directions. First, it is convincing that residual tidal currents move towards mainland such the southern Myanmar, coastal zone of Thailand, the Malaysian Peninsula and Sumatra island of Indonesia. At the Gulf of Martaban, overall tidal current is moving southerly, whereas that at the center of the Andaman Sea is moving controversially. Meanwhile, residual tidal current at the sea surface moves in the direction of Northwest and Southeast along the geography of the Strait of Malacca.

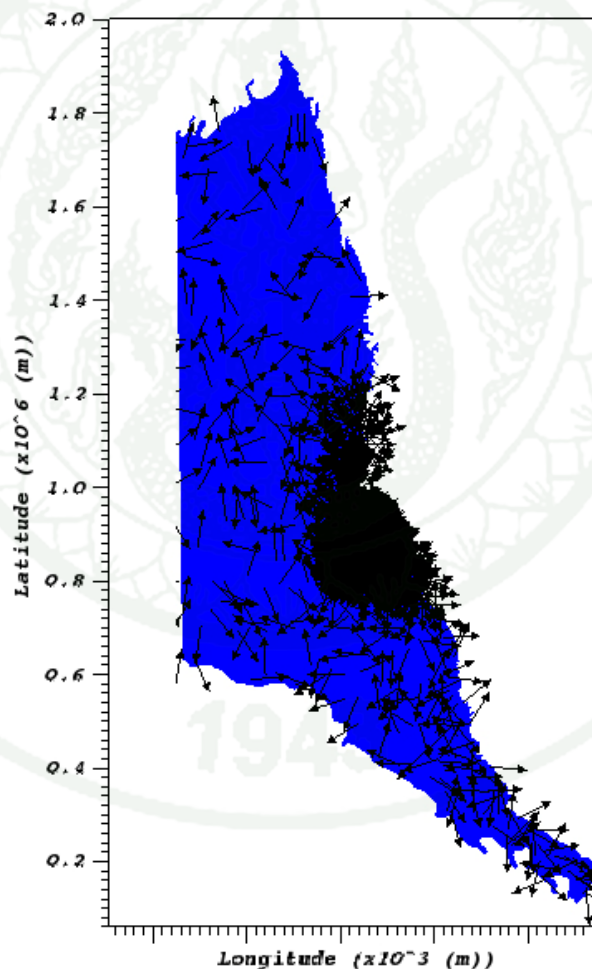


**Figure 44** Directional vector of residual current in Andaman Sea during under tidal dominated condition predicted by FVCOM

Directional vector of residual tidal current at Phang-Nga bay is exhibited in Figure 45. Overall, residual tidal current on the surface seemingly moves southerly along the West coast of Phuket and South of the Phang-Nga bay. However, that in the center of the Phang-Nga bay apparently moves in various directions but it tends to moves landwards to mainland and adjacent islands.

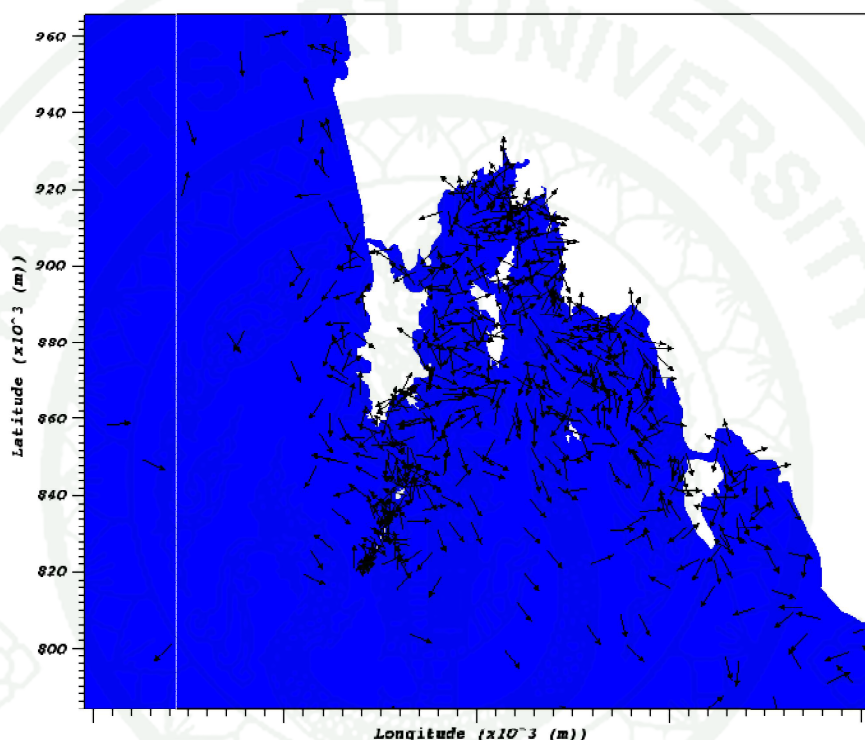


**Figure 45** Directional vector of residual current in Phang-Nga bay under tidal dominated condition predicted by FVCOM

### 3. Current pattern during Northeast monsoon

Surface current pattern in Andaman Sea is computed by FVCOM forced by two major parameters namely tidal amplitude and 10-m wind during Northeast monsoon, 1 January - 31 March, 2013. Surface current pattern including surface current velocity and surface current direction is analyzed by one month residual surface current in order to roughly foresee direction of marine particles floating along

the sea surface of Andaman Sea and represent marine particle transportation during Northeast monsoon.

Magnitude of surface residual current is shown in Figure 46a whereas Phang-Nga bay's is presented in Figure 46b. Overall, surface residual current is nearly zero at the middle of the Andaman Sea, and it is higher at the coastal area of Myanmar, Thailand, Indonesia and Malaysian Peninsula with approximately 5-25 cm/s. At the Strait of Malacca, magnitude of surface residual current is stronger at the coastal of Malaysian Peninsula. The residual surface velocity is 5-15 cm/s. The result from simulation well agrees with (Syamsul *et al.*, 2010) where current in February (2007) at Malacca Strait was simulated by tide, wind, salinity and temperature using HAMSON. In addition, computational solution reveals that magnitude of surface residual current at Myeik is in range of 5-30 cm/s. It is assumed that surface residual current is high because geographical barrier of many small islands. Magnitude of residual surface current in Phang-Nga bay is approximately 5-30 cm/s; stronger residual surface current is presented at the South of Phuket, Racha islands, and the North of Yao Noi island.

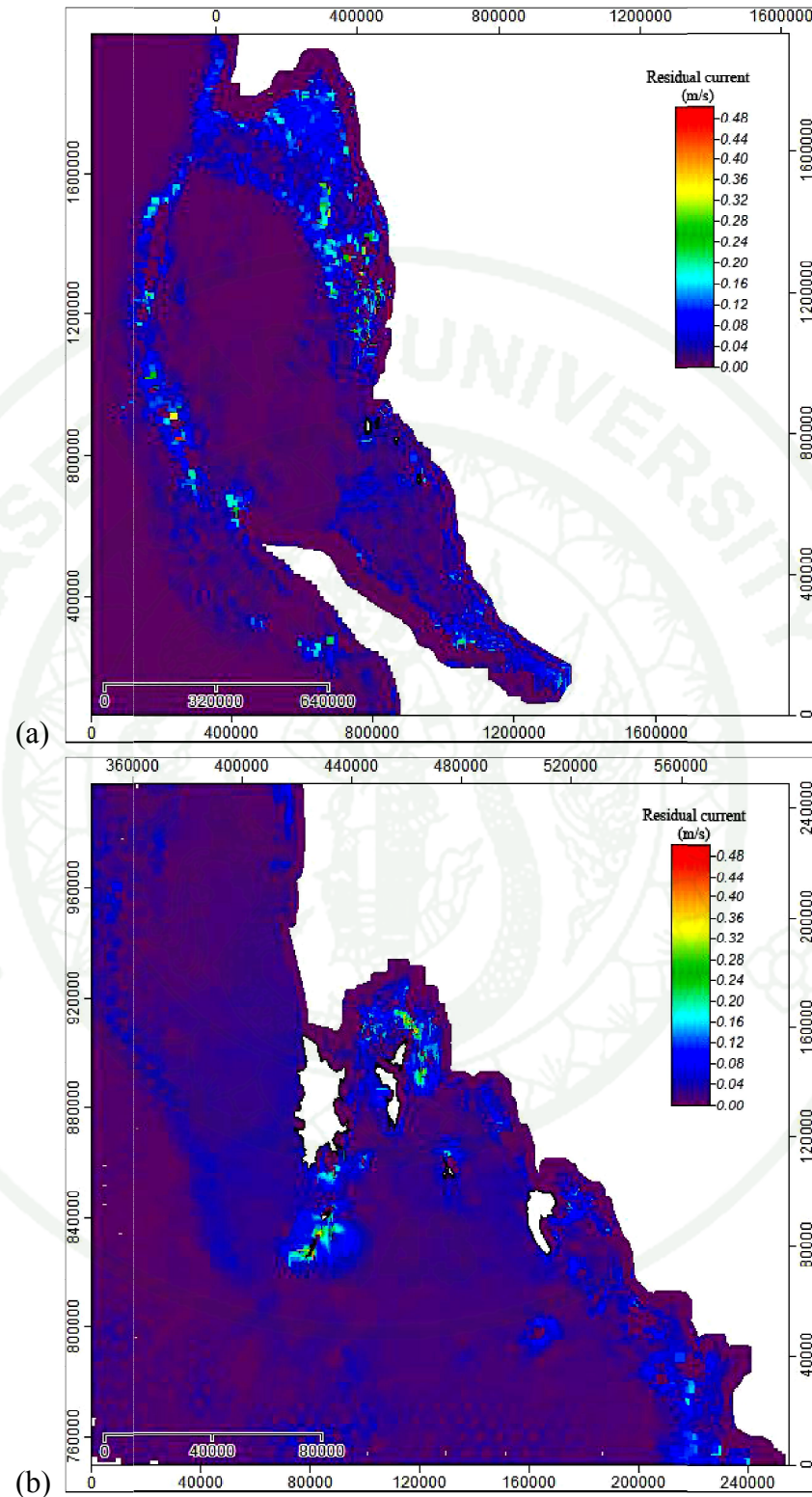


**Figure 46** Magnitude of residual surface current in (a) Andaman Sea and (b) Phang-Nga bay during Northeast monsoon predicted by FVCOM

Directional vector of residual surface current during Northeast monsoon in Andaman Sea is displayed in Figure 47. Overall, residual surface current seems to moves out of Andaman Sea to the West, heading to Andaman and Nicobar islands and to the South, heading to the Strait of Malacca. Furthermore, residual surface current along the coastline moves landwards. At Gulf of Martaban, Myanmar, residual surface current moves down South out of the gulf, while that in Myeik moves westwards. Along coastal zone of Thailand, the current moves out of Phang-Nga bay to the Northwest direction. At the Strait of Malacca, the current has a tendency to move down out of Andaman Sea, along with the coastal geography of the Strait of Malacca.

Directional vector of residual surface current in Phang-Nga bay is clearly presented in Figure 48. It evidently shows the movement of residual surface current which dictates to the movement of marine particles on sea surface in this area. Along the coastline of Phang-Nga province down to East Phuket, the current moves seawards to the open Andaman Sea. The current also moves out of Phang-Nga bay at the South of Phuket and South of Racha islands. There are many dynamic movements in Phang-Nga bay amongst Phuket, Yao islands and mainland. Residual surface current tends to move down from South of Phang-Nga province to East coast of Phuket and Yao islands. In addition, residual surface current also moves seawards from mainland and along the coast in the East of Phang-Nga bay. In addition, residual surface current at Lanta Yai island tends to moves North and Northwest along the coast of mainland and to Phi Phi islands. Lastly, residual surface current convinced to move southwards out of the bay.

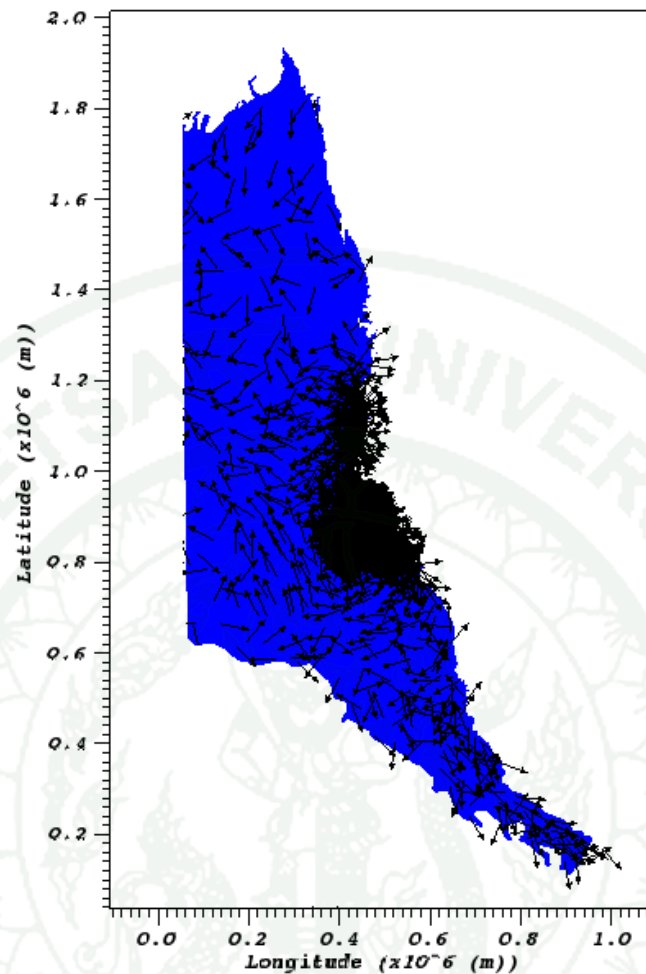


**Figure 47** Directional vector of residual current in the Andaman Sea during Northeast monsoon predicted by FVCOM

Direction of residual surface current dictates the movement of marine particles in individual areas because this acts as a vehicle that drives any marine litter to various places. It is evidently conclusive that some particles will stuck at the coastal zone of mainland and islands, while most of them tend to move out of the bay in the East and South.

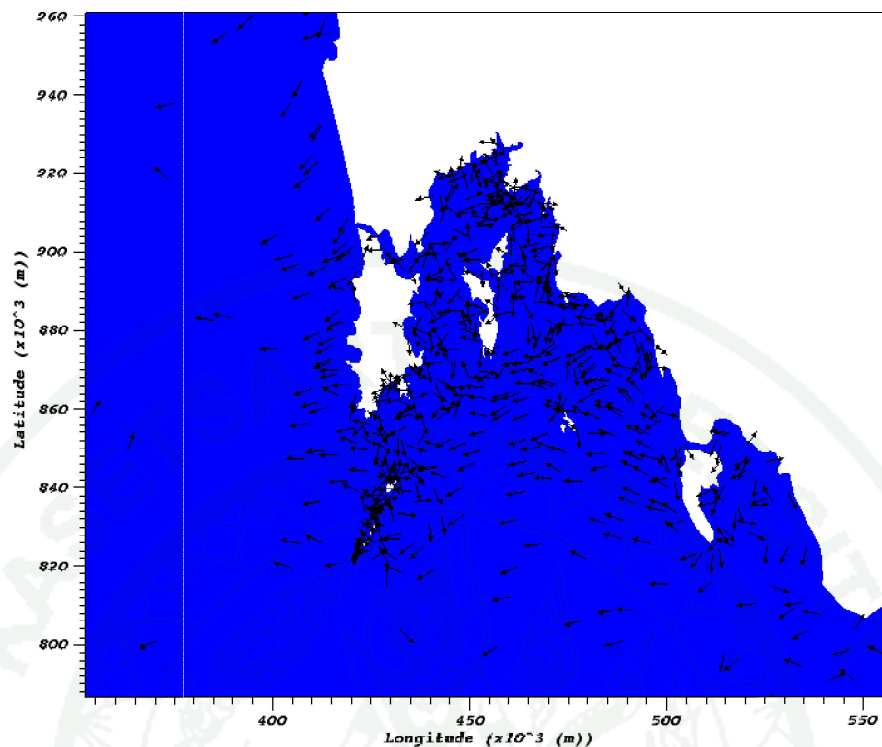


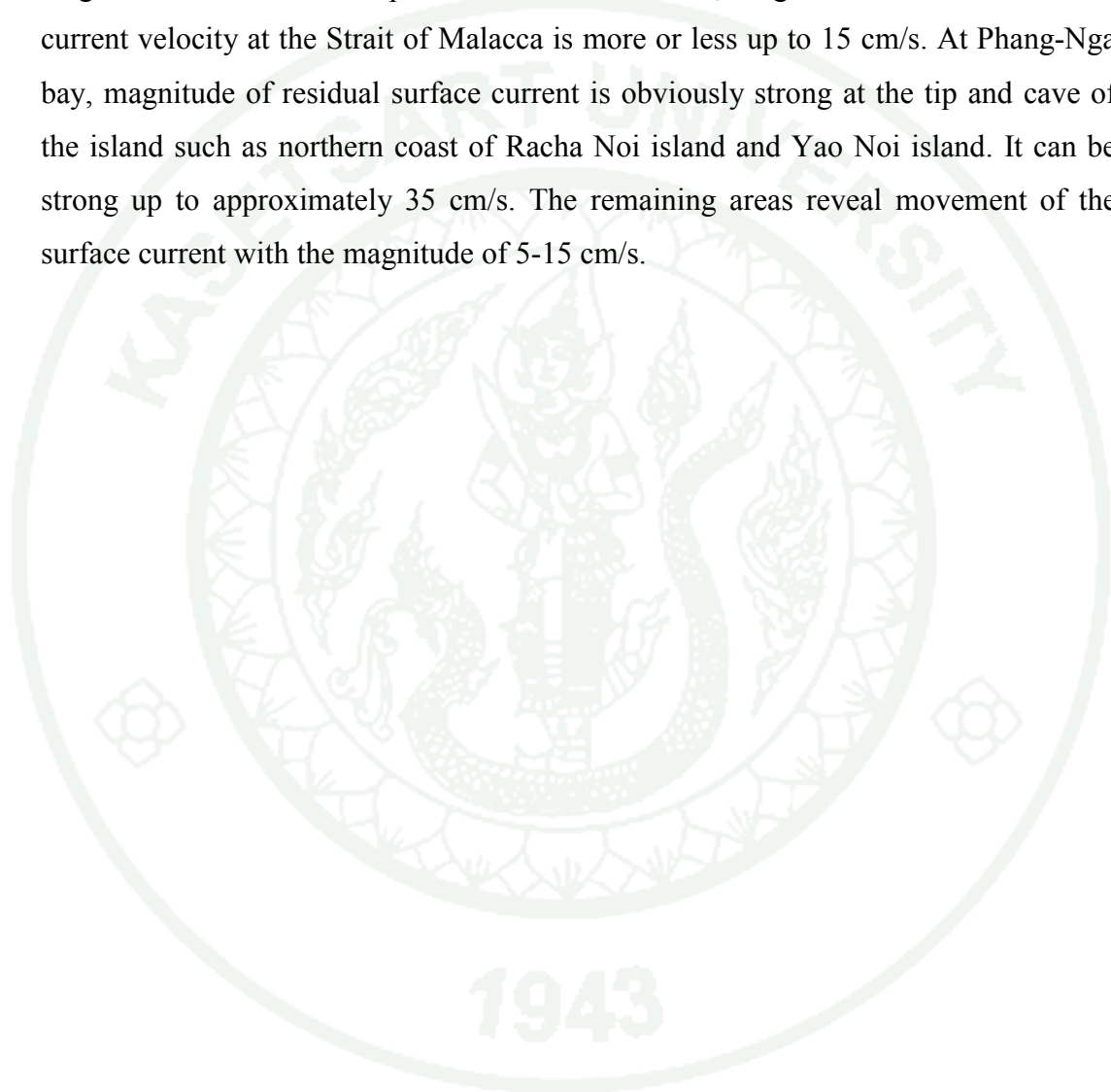
**Figure 48** Directional vector of residual current in Phang-Nga bay during Northeast monsoon predicted by FVCOM

#### 4. Current pattern during Southwest monsoon

Surface current pattern in Andaman Sea is computed by FVCOM forced by two major parameters namely tidal amplitude and 10 m wind during Southwest monsoon, 1 September - 30 November, 2013. Surface current pattern including surface current velocity and surface current direction is analyzed by one-month residual surface current in order to roughly foresee direction of marine particles floating along the sea surface of Andaman Sea and represent marine particle transportation during Southwest monsoon.

Magnitude of current velocity during Southwest monsoon in Andaman Sea and Phang-Nga bay are demonstrated in Figure 49a and 49b, respectively. Likewise, magnitude of residual current at the center of the Andaman Sea is slightly calm whereas that at adjacent islands and shallow water tend to have stronger residual

current magnitude. The residual current magnitude of the Andaman Sea during Southwest monsoon is in the range of 0-35 cm/s. At the Myeik area, oceanic bathymetry is complex because of various levels of bathymetry that results in smaller of water channel; it, then, causes in stronger current's velocity. Residual current magnitude in this area is up to 30 cm/s. In addition, magnitude of residual surface current velocity at the Strait of Malacca is more or less up to 15 cm/s. At Phang-Nga bay, magnitude of residual surface current is obviously strong at the tip and cave of the island such as northern coast of Racha Noi island and Yao Noi island. It can be strong up to approximately 35 cm/s. The remaining areas reveal movement of the surface current with the magnitude of 5-15 cm/s.



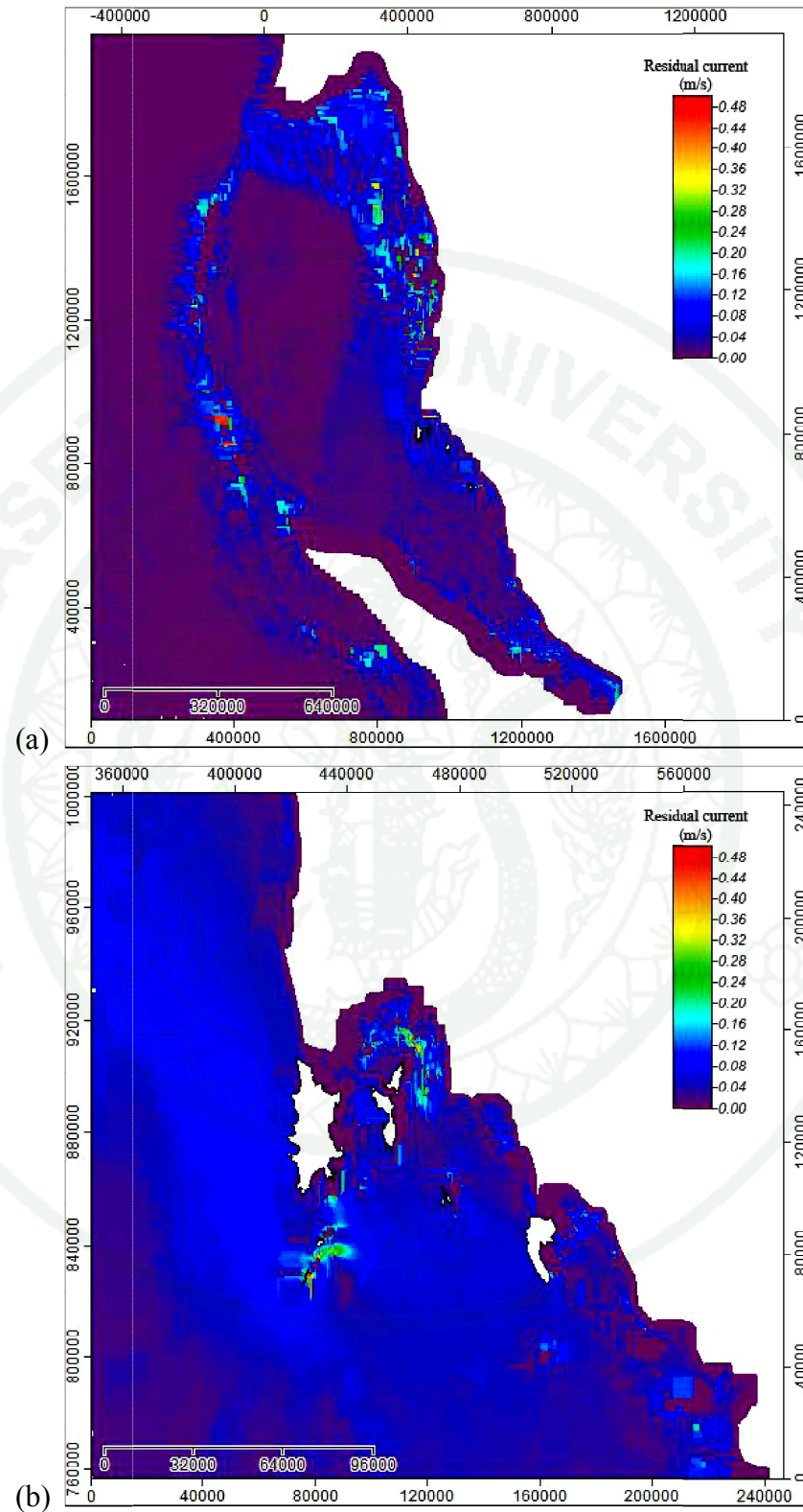


**Figure 49** Magnitude of residual surface current in (a) the Andaman Sea and (b) Phang-Nga bay during Southwest monsoon predicted by FVCOM

The directional vector of surface residual current of the Andaman Sea is shown in Figure 50; it demonstrated that the surface residual current at the center of the sea move from West side of the sea to the South during Southwest monsoon. At the same time, surface current at the Gulf of Martaban seems to have both moving landwards and seawards. And at the Strait of Malacca, residual current seems to move landwards and along the strait to the South out of the Andaman Sea.

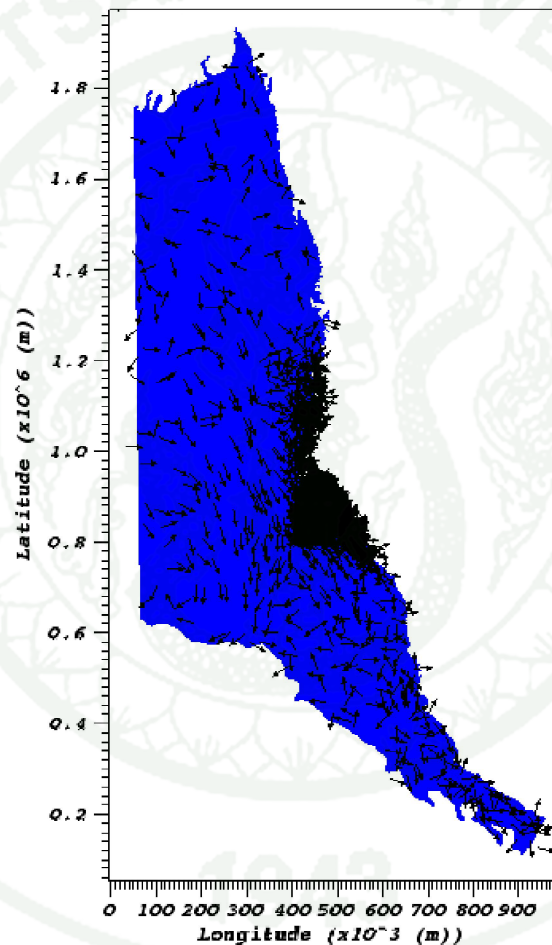


**Figure 50** Directional vector of residual current in the Andaman Sea during Southwest monsoon predicted by FVCOM

At Phang-Nga bay, the directional vector of residual surface current reveals that the current reaches Phang-Nga bay from Northwest direction as shown in Figure 51, getting inside the bay at the South of Phuket and continues heading easterly before

it goes southward once it hits mainland. Some residual current gets inside the bay and moves southward.

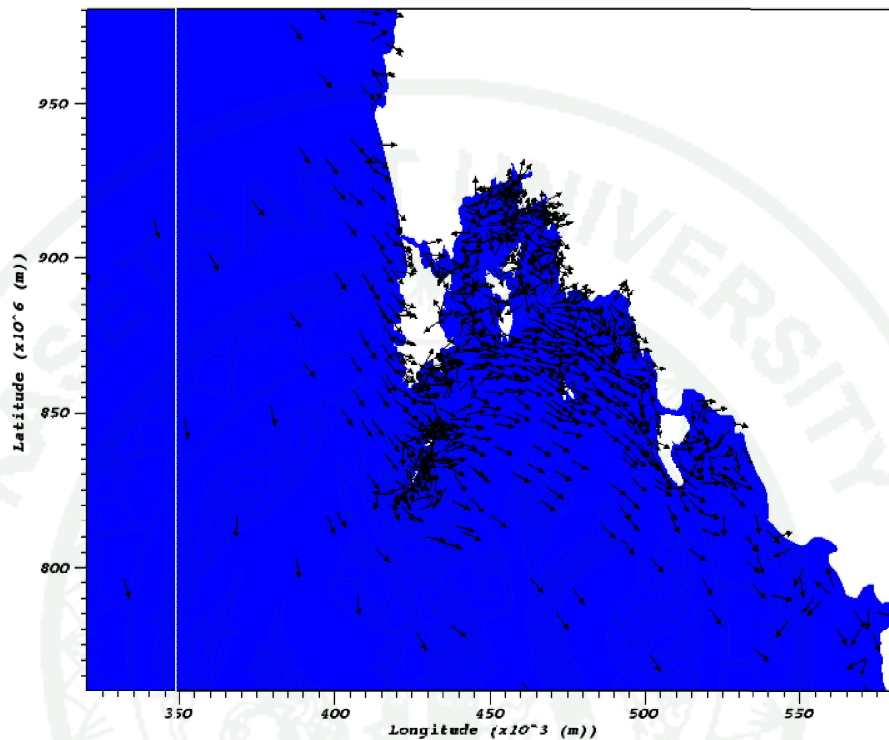


**Figure 51** Directional vector of residual current in Phang-Nga during Southwest monsoon predicted by FVCOM

### Marine particle transport

Particle tracking method is carried out in this study in order to trace transportation of marine litter during three case scenarios; tidal dominated condition, Northeast monsoon and Southwest monsoon in the Andaman Sea. Particle is assumed to be floating marine particle or litter which is driven along with the current in individual areas on sea surface, and its density is equal to marine's density. Current pattern in the Andaman Sea is simulated by FVCOM and based upon hydrological physics of marine towards various parameters such bathymetry, meteorological data and so on. FVCOM is forced by tidal elevation at open boundary and non-uniform 10

m wind of two mentioned monsoons at every element. It represents marine litter transportation within 90 day time under those three case scenarios.

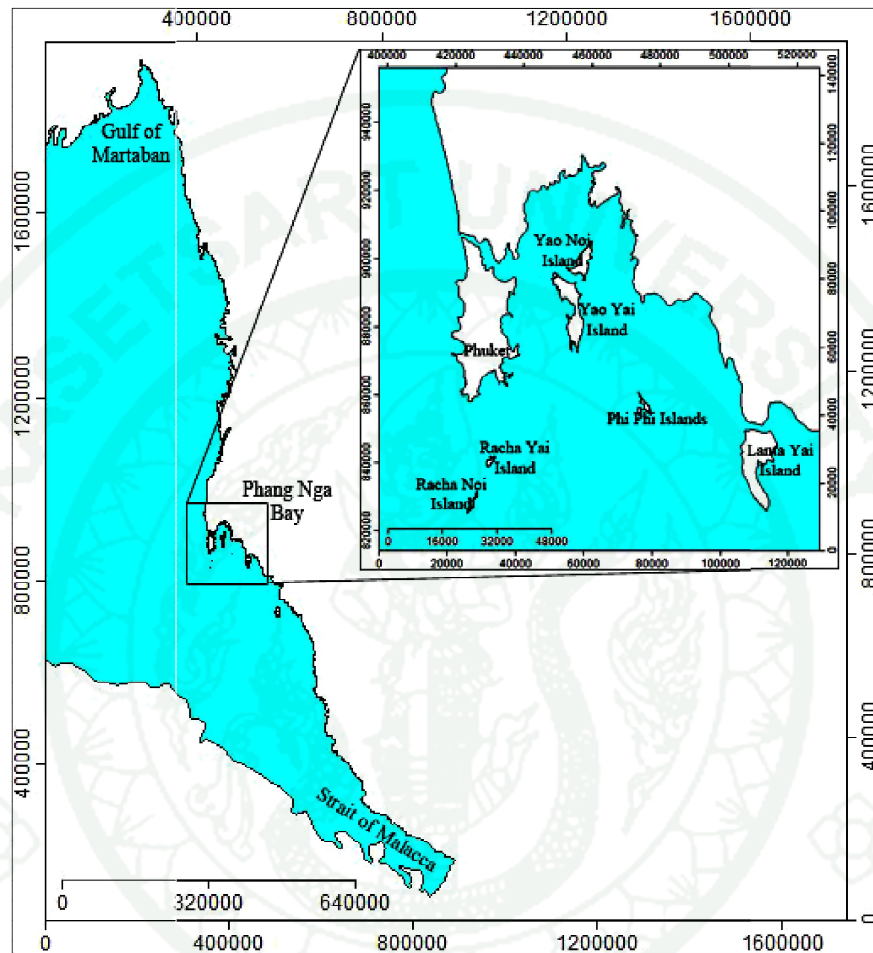


**Figure 52** Locations of tracing marine litter movement in the Andaman Sea

In addition, particle is observed its movement in both on-shore (near shore environment) and off shore. On-shore origins along coastal line of important areas are coastal line of mainland connected to the Andaman Sea in southern of Thailand, Phuket, Phi Phi islands, Racha Yai island, Racha Noi island, Yao Noi island, Yao Yai island and Lanta island as shown in Figure 52. And off shore is particularly in Phang-Nga bay.

## 1. Phang-Nga bay

This section overall reports the observation of marine litter in Phang-Nga bay where is bounded by Phuket in the East, Phang-Nga in the North and Krabi in the West. Marine litters are originated from seven different places of Phang-Nga bay which are coastal line of mainland (red dots), Phuket (orange dots), Yao islands (green dots), Phi Phi Don island (light blue dots), Racha Yai island (purple dots), Racha Noi island (blue dots) and Lanta Yai island (yellow dots) as shown in Figure 53a.

### Scenario 1: Tidal dominated condition

Figure 53b demonstrates movement of marine particle based on tidal driven. Marine particle under this scenario is solely scatter due to tidal drive in Phang-Nga bay. Overall, floating marine litters did not tend to travel in a long distance except for some marine particles originated from Phuket, Yao islands and Racha islands. Yao islands received some marine particles that were sourced from coastal mainland and Phuket; simultaneously, marine particle originated from Yao islands also travelled to Phuket and the coastal line of mainland.

### Scenario 2: Northeast monsoon

During the Northeast monsoon season, some marine litter remains at or along the coastal line of the origins (Figure 53c). Some marine litters from coastal mainland manage to reach islands and some from islands also travelled to other islands and coastal of mainland as well. However, it is conclusive that there are far so many marine litters that remain travelling in the sea or off shore within the observation time, and they are from every observed sources of marine litters in Phang-Nga bay. Particles originated in each area will be reported in detailed further. A number of marine litters at the origins in Day 90 are much lessened than Day 1, and they were overall scattered in Phang-Nga bay even if some were spread out of Phang-Nga bay in the direction of East and West sides.

### Scenario 3: Southwest monsoon

Overall, floating marine particles have a tendency to move southerly during Southwest monsoon as presented in Figure 53d. During this season, marine particles originated at Phuket (orange dots) were all moving eastwards to Yao islands, Phi Phi islands and Lanta Yai island. At the same time, particles at Yao islands (green dots) were also moving easterly to coastal line of mainland and Phi Phi islands. However, Phi Phi islands originated floating marine litters (light blue dots) that tended to travel locally; there were a few particles that were moving out of the island. Particles from Lanta Yai island (yellow dots) were spread out to South, Southwest and Southeast directions. Some of them were stuck at estuary zone of the coastal line of mainland in the southern part of Thailand. The source of the origin that seemed to have less movement of particle was coastal line of the mainland. Particles from coastal line facing the open Andaman Sea were slightly moving down South to West coast of Phuket. Meanwhile, floating marine particles sourced from the coastal line of mainland bounding to the Phang-Nga bay were moving down South to Yao islands and Lanta Yai island. Lastly, it was convincing that floating marine particles at Racha Noi island (blue dots) and Racha Yai island (purple dots) island tended to travel in a large scale during Southwest monsoon. They obviously headed to East and Southeast direction, and some particles at Racha Noi island travelled to coastal zone of Racha Yai island.

Tidal forcing only moved particle movement in Phang-Nga bay to travel in a small range in the center of the bay and out of the bay to the Andaman Sea in the South. However oceanic current under seasonal condition of Northeast monsoon apparently drove floating marine particles to both West and South direction. To those marine particle movements under Northeast monsoon travelling to South direction was relatively in the same boundary. Movement of marine particles in Southwest monsoon revealed different movement because all particles originated around Phang-Nga bay were moving to the center of the bay and to the South in the long distance. A few particles were even managed to reach offshore of Langkawi, Malaysia.

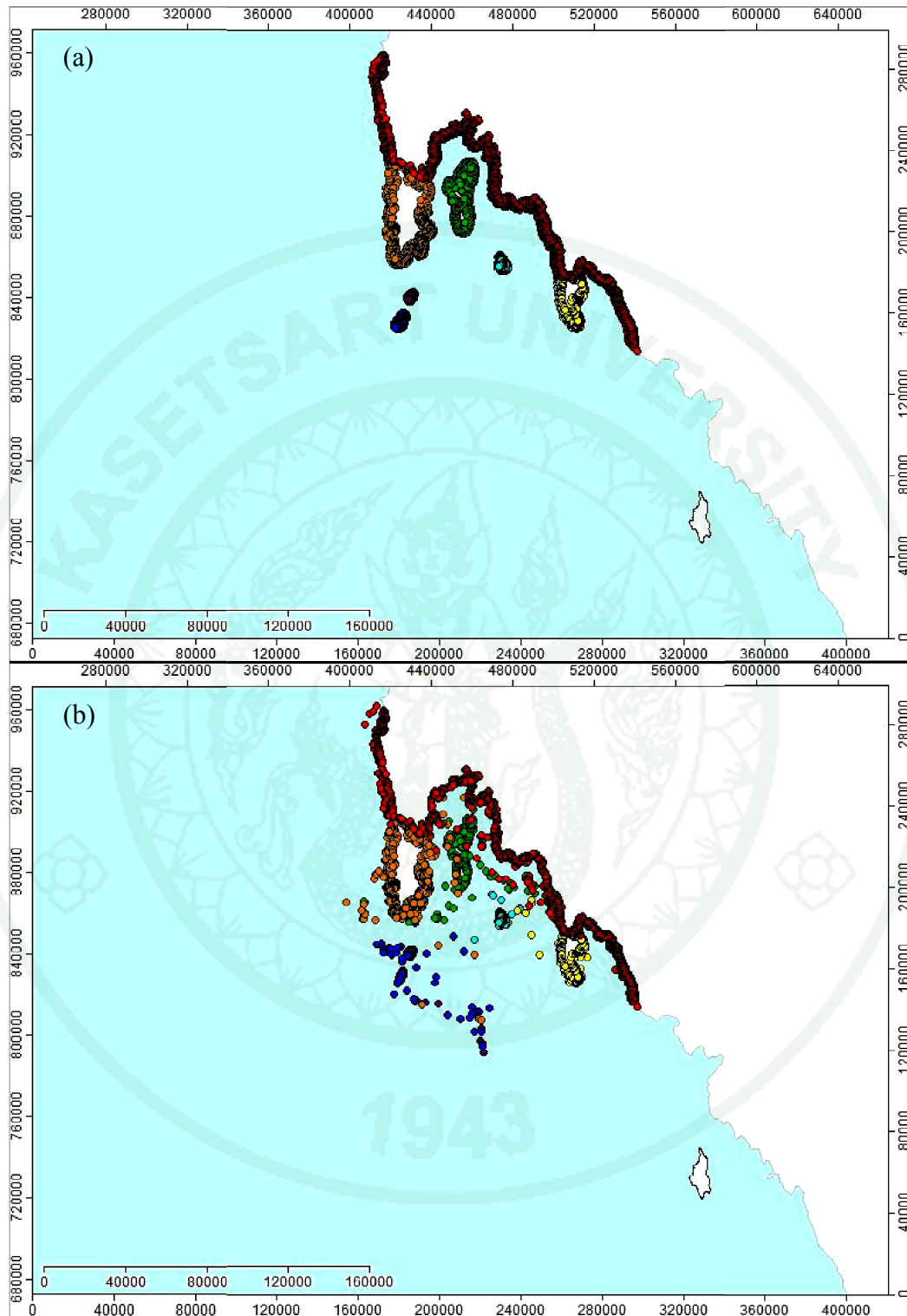


**Figure 53** Transportation of marine litters in Phang-Nga bay between (a) Day 1 and Day 90 under the condition of (b) tidal dominant, (c) Northeast monsoon and (d) Southwest monsoon

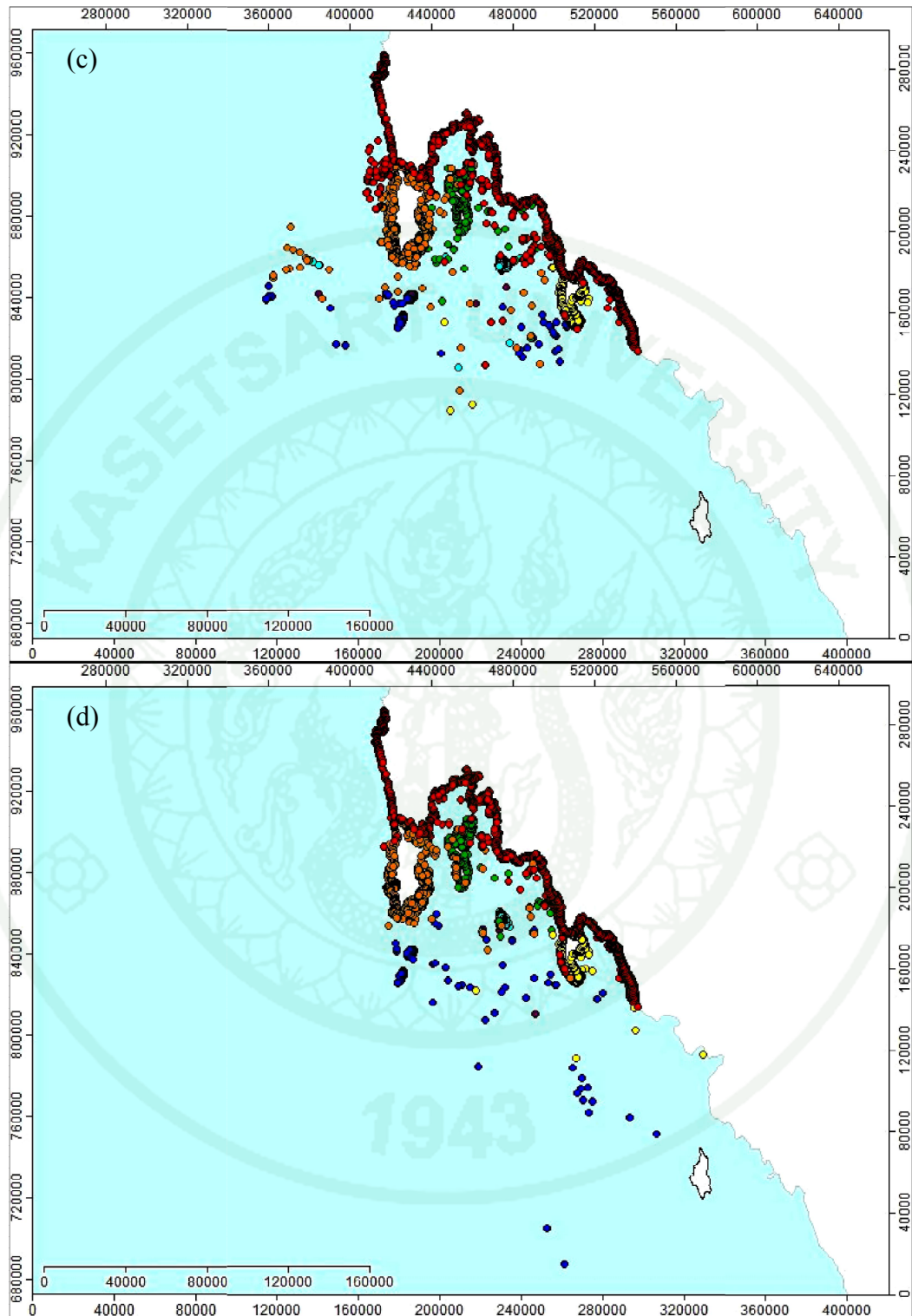


Figure 53 (Continued)

Displacement of marine particles in Phang-Nga bay of three different scenarios was overall summarized in Table 13 and histogram of marine particle displacement was profiled in Figure 56. It was overall summarized that marine litters originated onshore of places around Phang-Nga bays was able to travel farthest approximately 160 km within 90 days. Even if the farthest distance of particle displacement was significantly different, yet mean displace was relatively indifferent. As shown in Figure 54, displacement of floating marine litter in three different scenarios had a similarly dispersing histogram even if tidal forcing consistently drove marine particle in the range of 50-75 km more than those in coupled with 10-m wind.

Considering displacement of marine litter at sea surface, tide combined with wind during two different monsoons had more capability to drive marine litters to go farther. In addition, mean displacement of marine litters was slightly the same. It, therefore, could be concluded that 10-m wind, overall, enhanced current to drive floating marine litters to travel far. In addition, significant farthest displacement between with and without wind forcing proved that wind coupled with tide was able to move some floating marine litters in a large scale.

**Table 13** Displacement profile of marine particles at Phang-Nga bay

Scenario	Displacement (m)		
	Min	Mean	Max
Tidal dominated	10	8,204 ± 17,394	62,270
Northeast monsoon	10	11,170 ± 11,721	115,000
Southwest monsoon	10	10,600 ± 19,272	163,400

Particle displacement during Northeast monsoon occupied range of travelling up to 75 km, whereas that under Southwest monsoon covered longer range over 100 km from the origins. And lastly, tide was dominant to scatter floating marine litter up to 50 km.

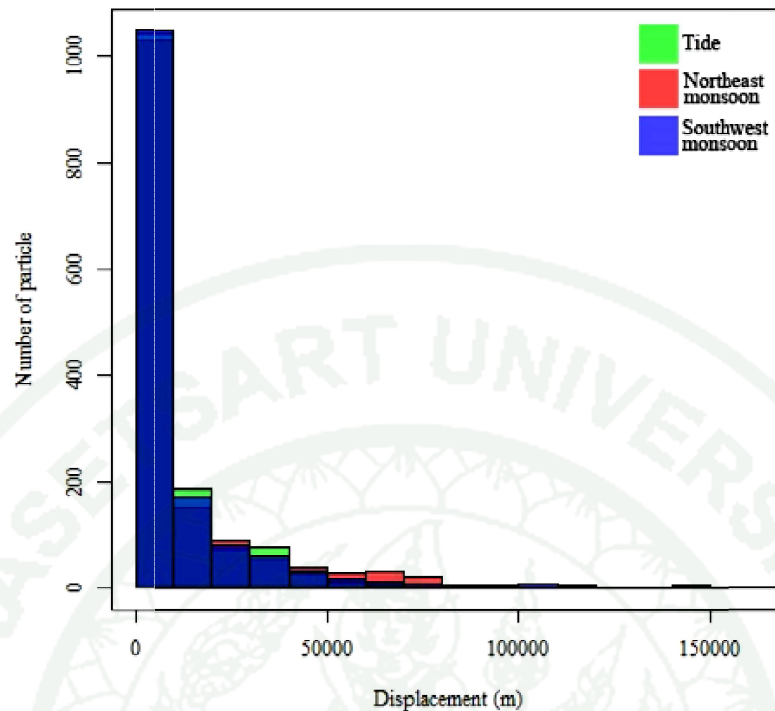


**Figure 54** Histogram of particle displacement (m) at Phang-Nga bay in three case scenarios

## 2. Coastal line of mainland

Coastal line of mainland connected to the Andaman Sea of southern part of Thailand was consisted of West of Phang-Nga province facing open the Andaman Sea, North of Phang-Nga bay and West of Krabi province. As shown in Figure 55, marine litters are originated from five different places which were the West of Phang-Nga province (purple dots), North of Phang-Nga bay (red dots), top of West Krabi (yellow dots), middle of West Krabi (green dots) and low West Krabi (blue dots). They represented marine litters from mainland and its transportation in the Andaman Sea during tidal dominated condition, Northeast monsoon and Southwest for 90 days.

### Scenario 1: Tidal dominated condition

Overall, tide seems to move particles from coastal line of the mainland in only small distance except for those particles originated from the North of Phang-Nga bay (red and yellow dots). They tended to move southerly reaching the center of the bay where situated Yao islands (Figure 55b). Surprisingly, some of which were also brought to estuary zone of the mainland in the middle of West coast Krabi. Meanwhile, particles from the middle of West Krabi (green dots) were moving closer to the land, especially at the areas where located the mouth of river and small islands. Lastly, floating marine litters at lower part of West Krabi (blue dots) tended to only move along the coast due to tidal driving.

### Scenario 2: Northeast monsoon

Figure 57a displayed the starting time, whereas Figure 55c demonstrates final observation time. Marine litters from West of Phang-Nga province facing the open Andaman Sea (purple dots) tended to move southward to Phuket and some remained at and along the shore line; however, it did not seem to reach shoreline of Phuket with approximately 6 km away. Nevertheless, marine particles at North Phang-Nga bay (blue dots) mostly travelled along the coastal line and accumulated at the right side of the observed area. Furthermore, particles from the left side of North Phang-Nga bay moved southerly to and pass Phuket to the sea while those at the right side of observed area floated to Yao islands. They travelled around Yao Noi island and possibly reached its shore line because the origin was only 10 km away from its destination. Particles from top of West Krabi (blue dots) seemed to perform the most dynamic among all observed origins. Most of them moved southerly out of the origin and left only some floating along the shore line. Surprisingly, there were some marine litters at Phi Phi Don island originated from the top of West Krabi, and some of which was travelled even farther in the South. Particles originated from middle of West Krabi (green dots) tended to move along the coastal zone and accumulated at around the estuary. There were only some particles which travelled to the West of its origin for few kilometers and to Lanta Yai islands. Lastly, marine litters from lower part of

West Krabi (orange dots) seemed to rarely move out; they remained along the coastal zone and accumulated at estuary areas along the coastal line.

### Scenario 3: Southwest monsoon

Marine particles originated from the coastal line of mainland had a tendency to move in small range during Southwest monsoon (Figure 55d). Those originated at West coast of Phang-Nga province (purple dots), they only moved down South to Phuket and reached its coastal zone and beaches. However, particles originated at North of Phang-Nga bay (red dots) seemed to have longer transportation because they travelled to Yao islands and the middle of West Krabi and some moved along the coastal line and at the estuary zone of the source. Marine litters sourced at upper coastal of Krabi (yellow dots) were brought to center of Phang-Nga bay at Yao Noi island, around the island. Some particles were driven far to middle of West coast of Krabi. Some particles originated at the middle of West coast of Krabi (green dots) were scattered to Lanta Yai island and along the coastal zone the southern part. Lastly, particles originated from lower of West coast of Krabi seemed to move closer to the mainland.

Considering movement of marine litters under three case scenarios, the result showed that tide forcing drove marine particles only in a small range; which was similar to rang of those under Southwest monsoon. In addition, some particles which were driven far from the origins under tide condition were brought closer to the origins or easterly during Southwest monsoon. However, particle movement under Northeast monsoon showed significantly different because most of them were scatter in the West of the origins. This was because wind blows from Northeast to Southwest during this monsoon.

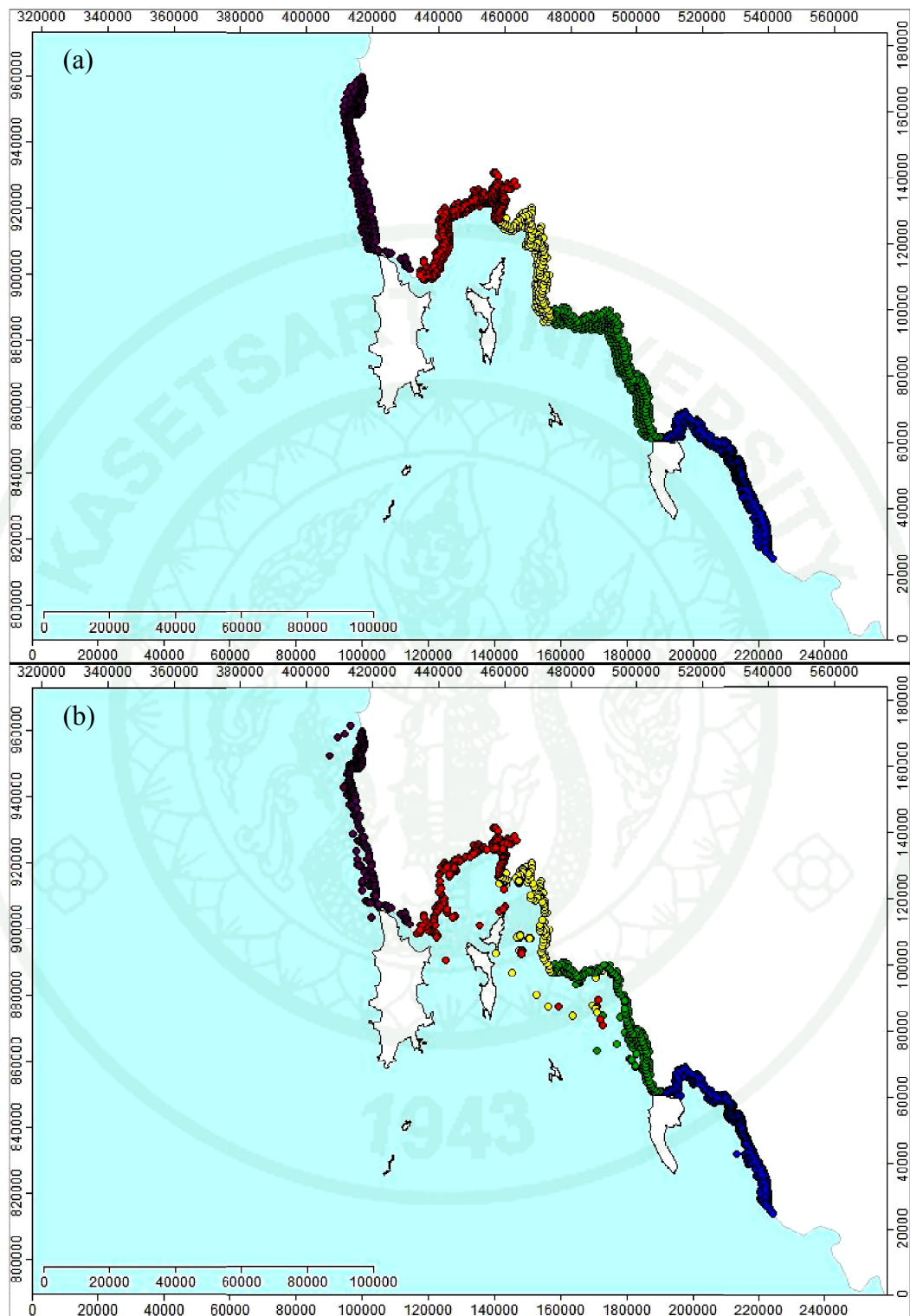


**Figure 55** Transportation of marine at coastal line of mainland between (a) Day 1 and Day 90 under the condition of (b) tidal dominant, (c) Northeast monsoon and (d) Southwest monsoon

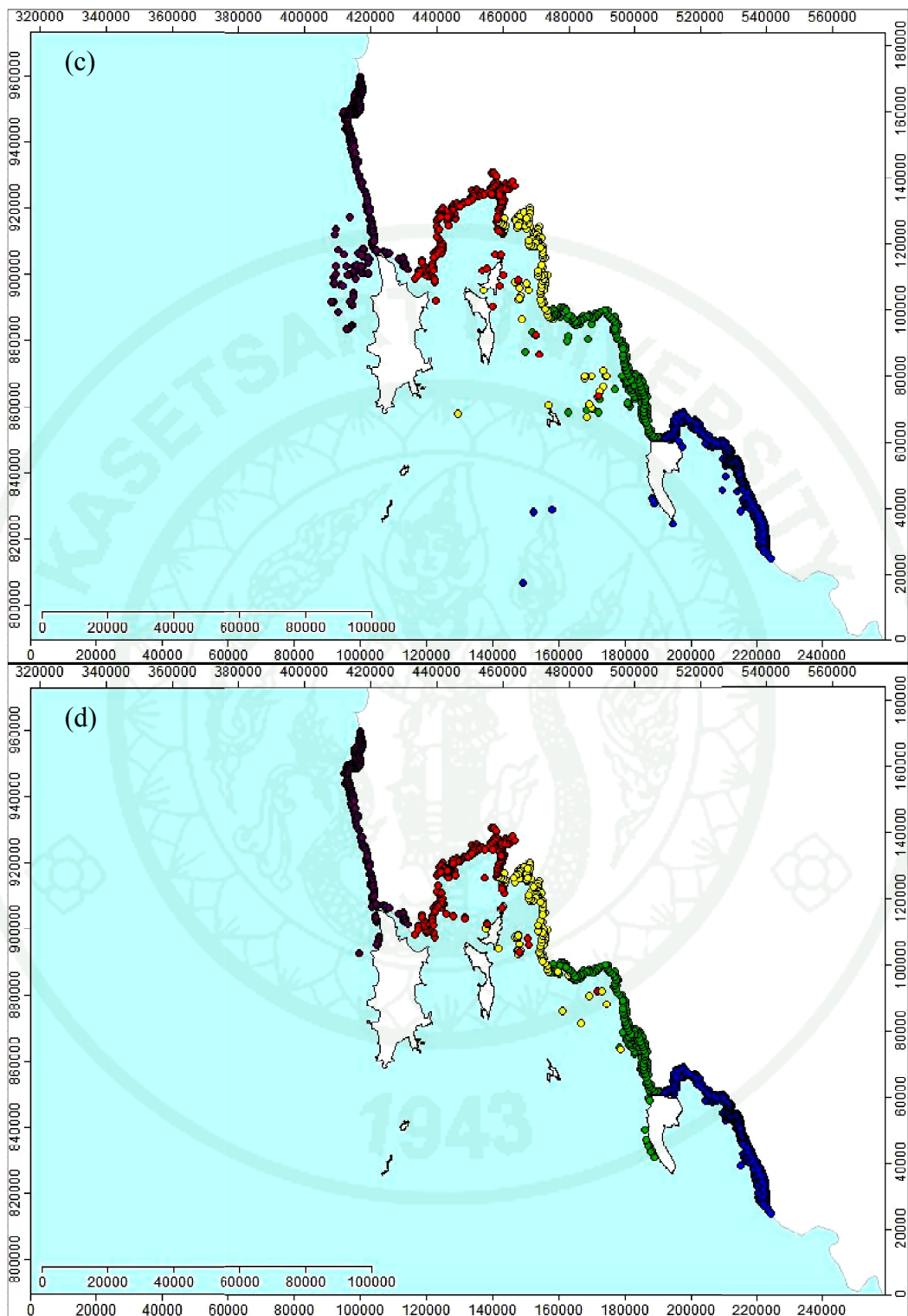


Figure 55 (Continued)

Displacement of marine particle originated from coastal line of mainland of three different scenarios was fully summarized in Table 14 and histogram of marine particles displacement was profiled in Figure 56. It was proved that Northeast monsoon drove floating marine litter originated from coastal line of mainland in a long distance with longest displacement and the whole set of marine particles. Among all, tidal forcing had the least displacement of particles but it could drive floating particles in a longer distance than those driven in Southwest monsoon.

**Table 14** Displacement profile of marine particles originated from coastal line of mainland

Scenario	Displacement (m)		
	Min	Mean	Max
Tidal dominated	10	5,507 ± 13,338	61,540
Northeast monsoon	10	9,561 ± 9,015	71,510
Southwest monsoon	10	6,418 ± 8,769	53,530

Histogram of particle displacement also illustrated that only some particles were able to travel in a long distance of more than 30 km from coastal line origin in the monsoon. But tidal forcing allowed them to float along in a various ranges with only a few particles. Considering all case scenarios, most particles under mentioned three cases were mostly allowed to travel in the range of 10-50 km within 90 days.

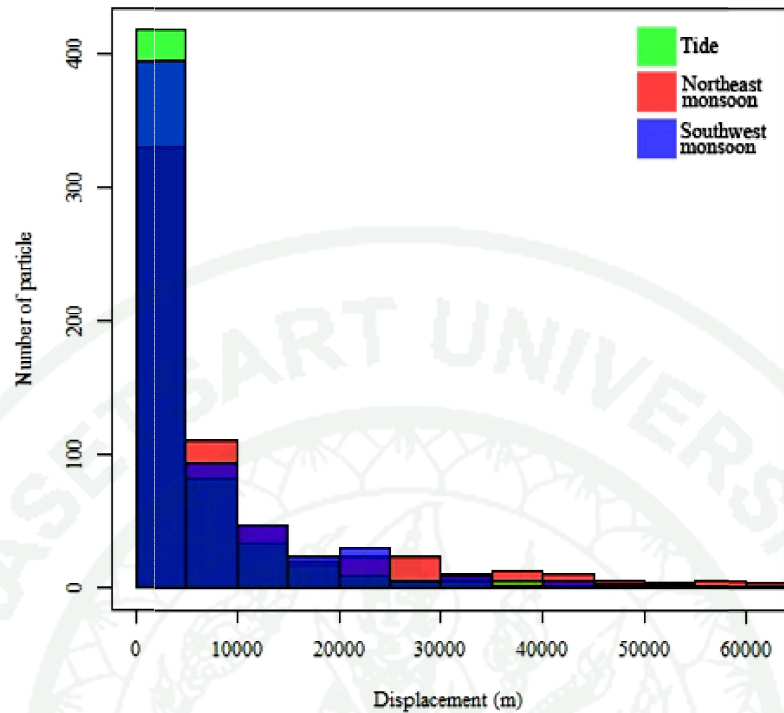


**Figure 56** Histogram of particle displacement (m) at coastal line of mainland in three case scenarios

Paths of marine litters originated from the coastal of mainland under tidal condition, Northeast monsoon and Southwest monsoon were shown in Figure 57a, Figure 57b and Figure 57c, respectively. In tidal condition, most of litters originated from coastal mainland were not distributed away from the origins. Meanwhile, Northeast monsoon drove marine litter at Kuraburi down to North of Phuket and arrived within several weeks. And for all seasons, litters at the coastal of Phang-Nga bay were distributed out the origins reaching the Yao islands even if marine litter movement during Southwest monsoon showed slightly different movement pattern.

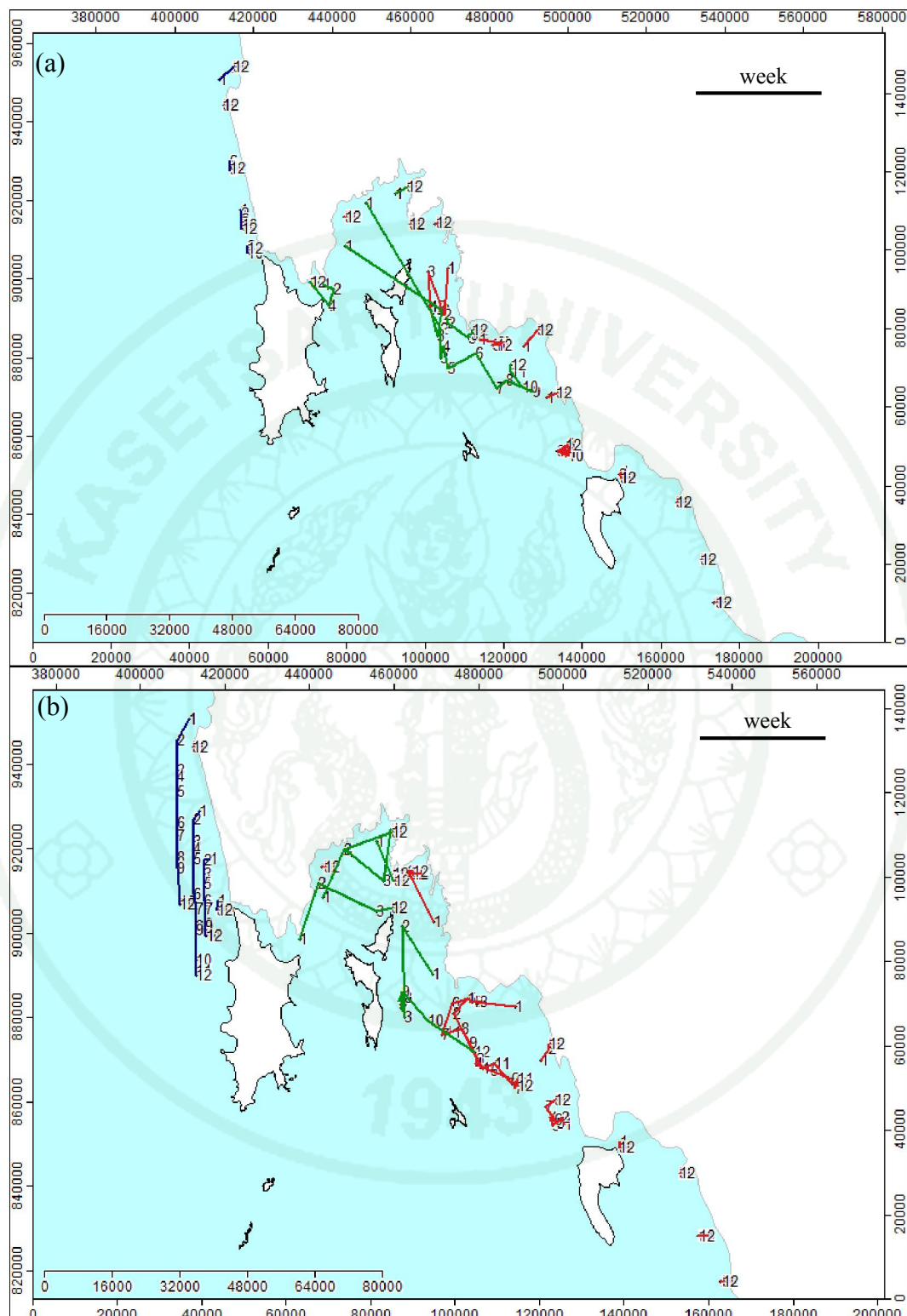


**Figure 57** Transportation path of marine litters originated from the coastal of Phang-Nga bay under the condition of (a) tidal dominant, (b) Northeast monsoon and (c) Southwest monsoon

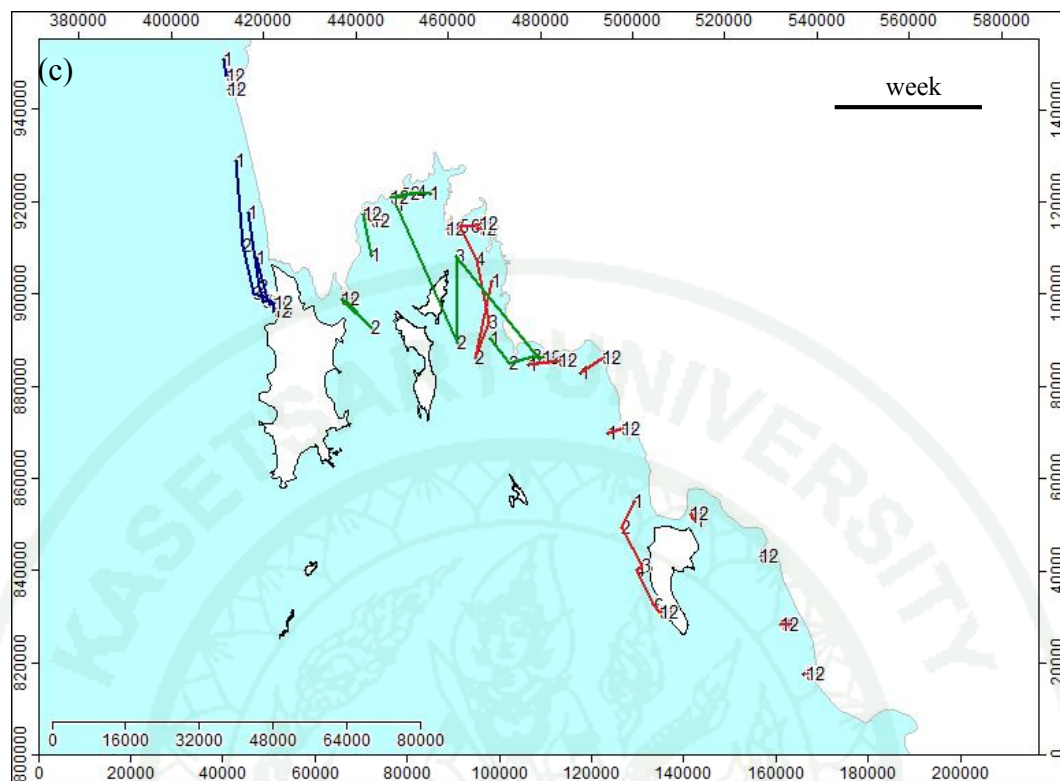


**Figure 57 (Continued)**

### 3. Phuket

Particles were originated from eight different observed sites along coastal line of Phuket which were Northwest (brown dots), West at Patong bay (purple dots), Southwest at Kata beaches (blue dots), South at Promthep cave (blue dots), Lon island (green dots), Panwa cave (yellow dots), East (orange dots) and North of Phuket (red dots) as shown in Figure 58.

#### Scenario 1: Tidal dominated condition

Demonstrated in Figure 58b, many dynamic movements of marine particles could be seen at particles originated from South at Promthep cave (blue dots), Panwa cave (yellow dots) and East (orange dots) of Phuket. Floating litters originated from Promthep cave were tidally driven into three directions; westward moving to the West coast, eastward heading to Yao islands and southward. Litters originated from Panwa

cave (yellow) had a tendency to move in the same direction as those in Promthep which were heading to West, East and South direction. Nevertheless, marine particles from Panwa cave and adjacent areas seemed to travel farther to mainland, East coast of Phuket and Yao islands. Meanwhile particles originated from the East coast of Phuket only moved easterly to Yao islands and coastal of mainland.

#### Scenario 2: Northeast monsoon

Figure 58c demonstrated that density of particles at the origins was obviously lessened; overall, particles from Phuket were apt to scatter out of the observed sites in various directions. Particles originated from Northwest (brown dots) displayed the least dynamic of marine litters, they only moved downward along the coastline and compiled at Mai Khao and Bang Tao beaches. There were a few particles that travelled to Kata beach area, about 6-7 km away from shoreline. Like Northwest origin, particles at Patong bay (Purple dots) hardly showed movement except some that moved out and float within the original bay. Marine litters from Kata beaches (blue dots), meanwhile, moved westerly out of Phuket approximately 50 km during 90 days, and a few particles were moved to Patong bay. Particles originally from the South of Phuket (light blue dot) evidently spread out to various directions both to the sea and other beaches. Furthermore, they were able to travel to other sites such as Patong beach, Kata beaches, Lon islands, Panwa cave and Yao Noi island. Particles at South Phuket near Lon island were almost moved out even though some are stuck at around Lon island. They inclined to travel southerly, easterly and northeasterly, and they also travelled to the East side of Phanwa cave and Phuket. Yet some particles moved along shoreline to Promthep cave and Kata beaches. Marine litters originally from Panwa cave had a tendency to scatter seawards in various directions like those from Promthep cave. Some particles were stuck at Lon island, around Yao Noi island and near mainland which was 7 km away from top of West Krabi. Marine litters from East side of Phuket (orange dots) generally moved seawards into Phang-Nga bay except for a few particles that moved southerly. Some particles managed to reach Yao Yai island, Yao Noi island and shoreline of South of Phang-Nga province. Some particles also moved close to its shoreline and compiled at the caves of unique

geometry. Lastly marine litters originated from North of Phuket (red dots) were scattered to shoreline of South of Phang-Nga Province and moved close to its original coastal line.

### Scenario 3: Southwest monsoon

Floating marine particles originated at Phuket were all moved easterly heading to the center of Phang-Nga bay (Figure 58d). Scattered particles from Phuket were from the South such as Promthep cave (light blue dots), Southeast coast such as Panwa cave (yellow dots) and East coast (orange dots). Particles at Panwa cave and adjacent areas were dispersed in a long scale reaching Yao islands, Phi Phi islands, Lanta Yai island and each coastal line of mainland within 90 days of transportation. Some particles originated at the East coast of Phuket (orange dots) were travelling to Yao islands-Yao Yai's West coast and North of Phang-Nga bay. At the same time, floating marine litters at the West coast of Phuket got closer to mainland because the wind blew from West to East during Southwest monsoon. In addition, particles at the North of Phuket (red dots) tended to move up North.

Considering floating marine litter movement under three case scenarios; they provided different movement pattern regarding the direction of particle dispersion and origins that allowed particles to transport. Under tidal force, particles originated at both sides of Phuket were scattered out of the origins, especially those in the South and East sides of Phuket. In addition, particle movement during Northeast monsoon tended to disperse out of the origins in many directions including West, South and East sides. Controversially, particle movement under Southwest monsoon was obviously dispersed only in the East side in the center of Phang-Nga bay.

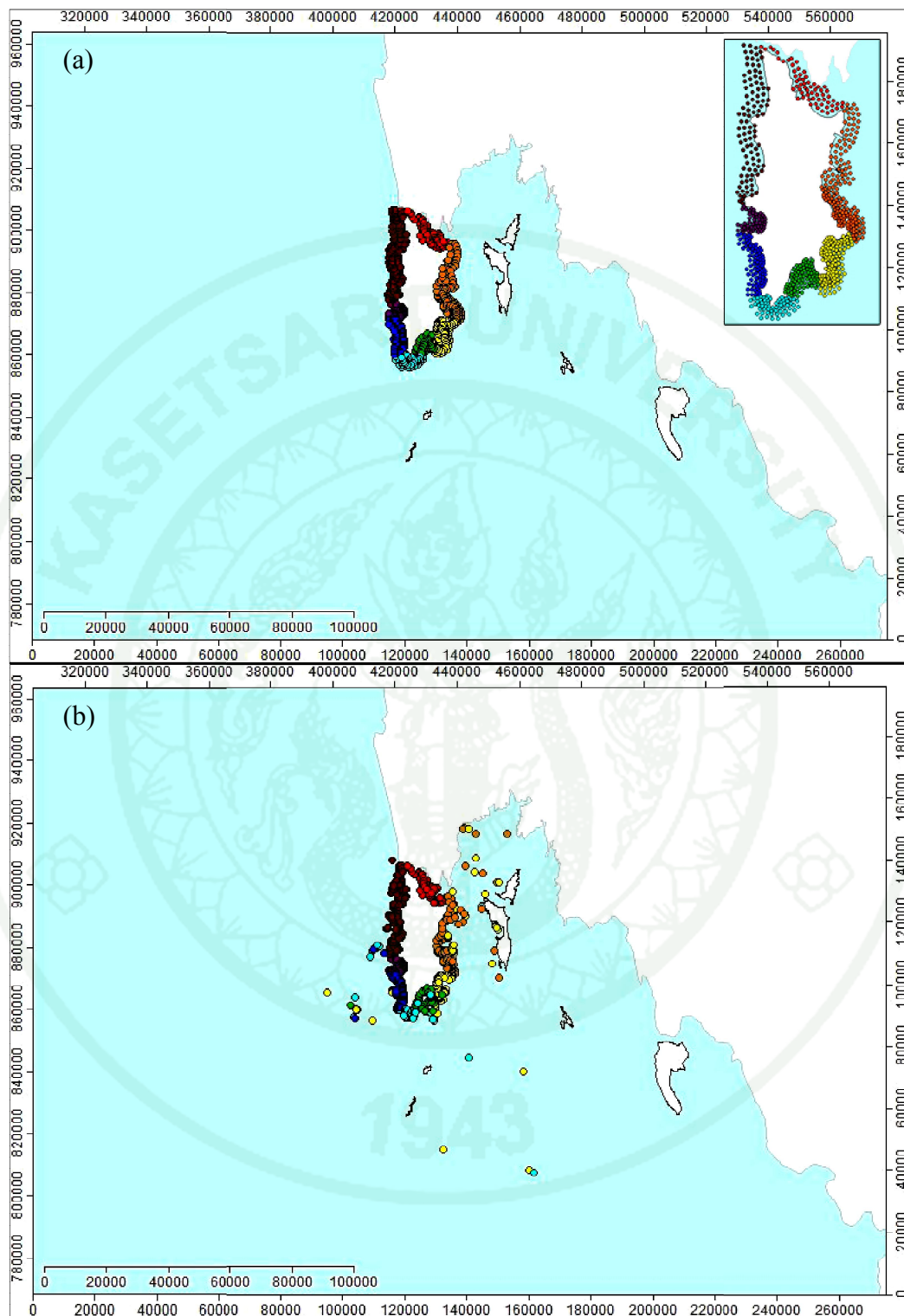


**Figure 58** Transportation of marine litters at Phuket between (a) Day 1 and Day 90 under the condition of (b) tidal dominant, (c) Northeast monsoon and (d) Southwest monsoon

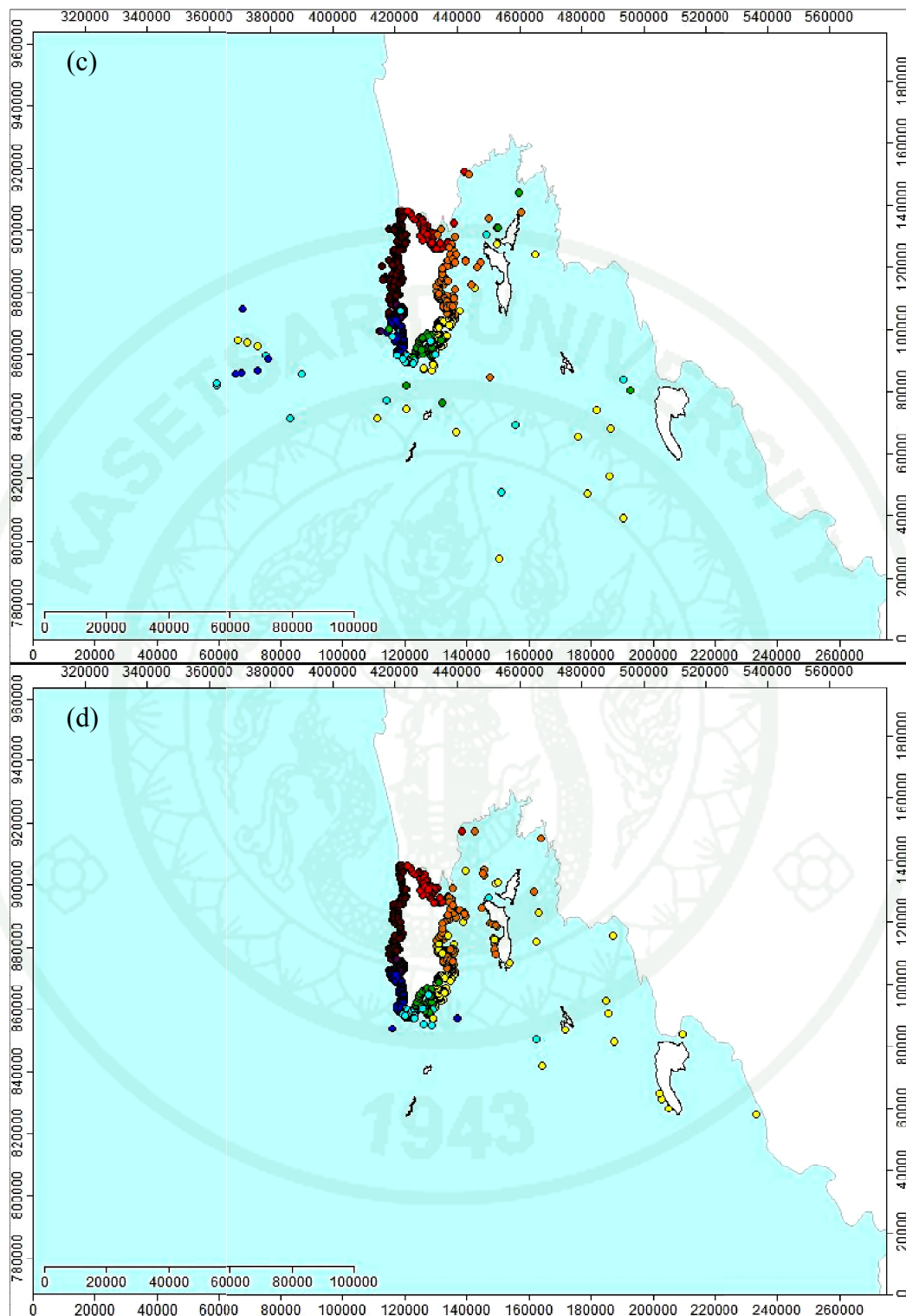


Figure 58 (Continued)

Displacement of marine particle originated from Phuket of three different scenarios was summarized in Table 15 and histogram of marine particle displacement was showed in Figure 59. According to statistical analysis of particle displacement, it was convincing that particles were moving in longest distance during Southwest monsoon with more or less than in 7 km average and the maximum of 105 km. Overall displacement of particles under tidal force and Northeast monsoon was relatively insignificant, but wind during Northeast monsoon affected surface current velocity which drive floating particle in a longer distance.

**Table 15** Displacement profile of marine particles originated from Phuket

Scenario	Displacement (m)		
	Min	Mean	Max
Tidal dominated	10	2,068 ± 15,527	62,270
Northeast monsoon	10	2,279 ± 11,165	83,280
Southwest monsoon	10	7,645 ± 13,351	106,200

Histogram of particle displacement was shown in Figure 61 represented length of particle dispersion from the origin of Phuket. Current under Northeast monsoon drove the surface current to move particles in a large range of displacement up to 70 km, whereas those were moved apparently up to 45 km during tidal dominant. Lastly, particles dominantly moved under Southwest monsoon in the range up to 80 km.

Random samplings of marine litter were chosen to represent marine litter originated at the different coast of the island and locations. To study the route of litters' transportation, path of the litter starting from the origins (Week 1) to the destination (Week 12) were drawn. The path distributions of litters originated from the coastal of mainland under the condition of tide both Northeast monsoon and Southwest monsoon are shown in Figure 60a, Figure 60b and Figure 60c, respectively.

Under the tidal condition, marine litters originated from the West coast of Phuket were not able to travel far from the coast during observed 12 weeks. On the other hand, marine litters originated from the East coast of Phuket travelled to the Yao islands. In addition, litters originated from the south of the island, such as Promthep cave, Lon island and Panwa cave, travelled far during Week 1 to Week 3. Sampled litters at the West coast of Phuket under the Northeast monsoon did not travel in a long distance except the sample originated at Kata beaches that were driven out of the origin during Week 1 to Week 5. Marine litters at the East coast of Phuket were driven to the Yao islands by reaching at Yao Yai island at within 8 weeks. Lastly, marine litters originated from East coast of Phuket under the Eastern monsoon displayed that they reached Lanta Yai island at within 8 weeks and arrived coastal of mainland within 5 weeks.

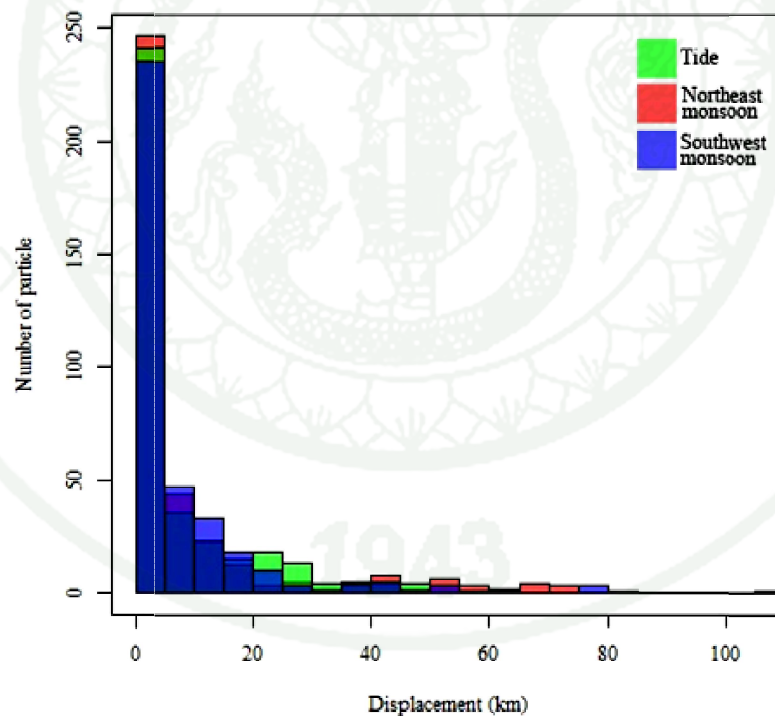


**Figure 59** Histogram of particle displacement (m) at Phuket in three case scenarios

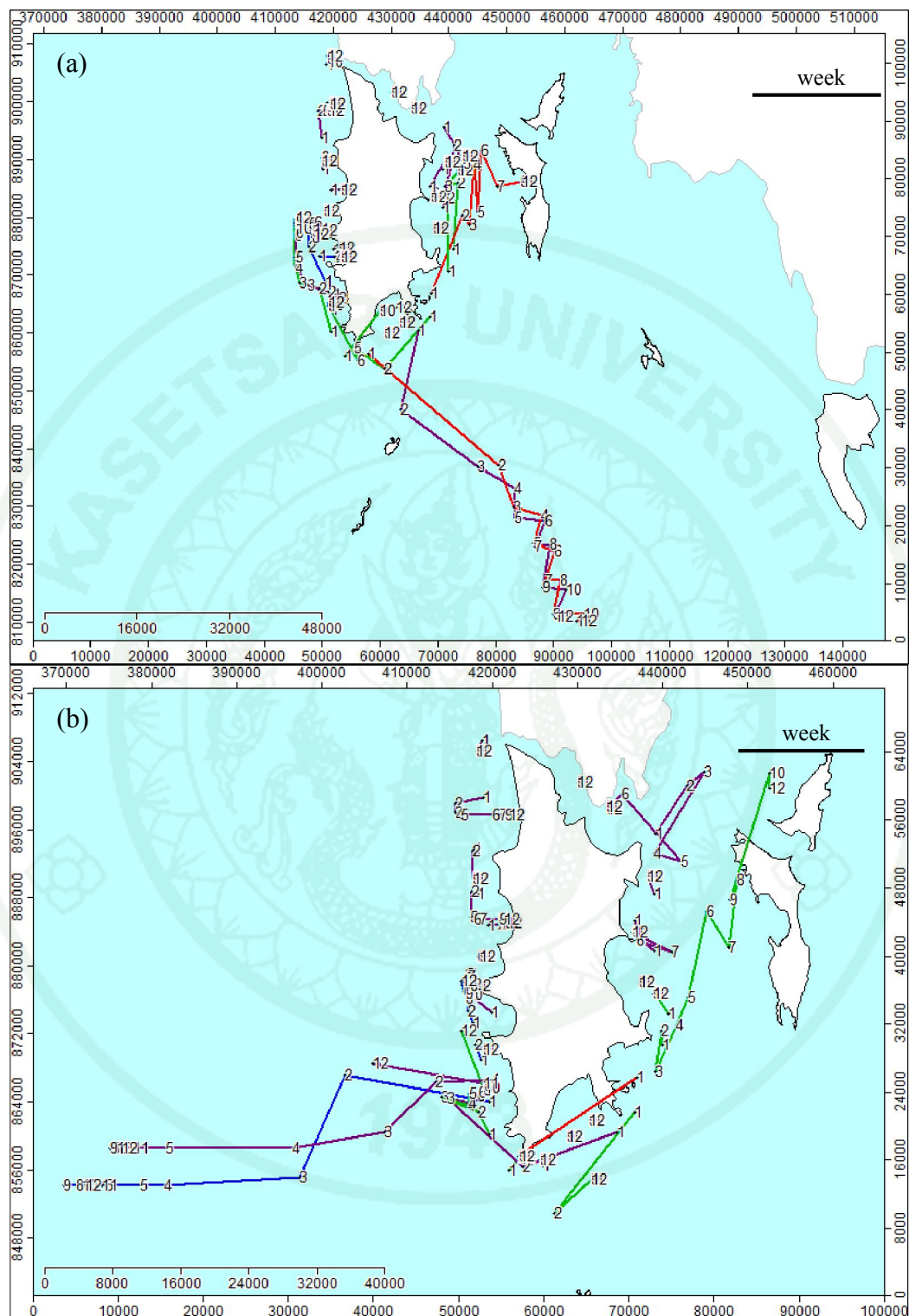


**Figure 60** Transportation path of marine litters originated from Phuket under the condition of (a) tidal dominant, (b) Northeast monsoon and (c) Southwest monsoon

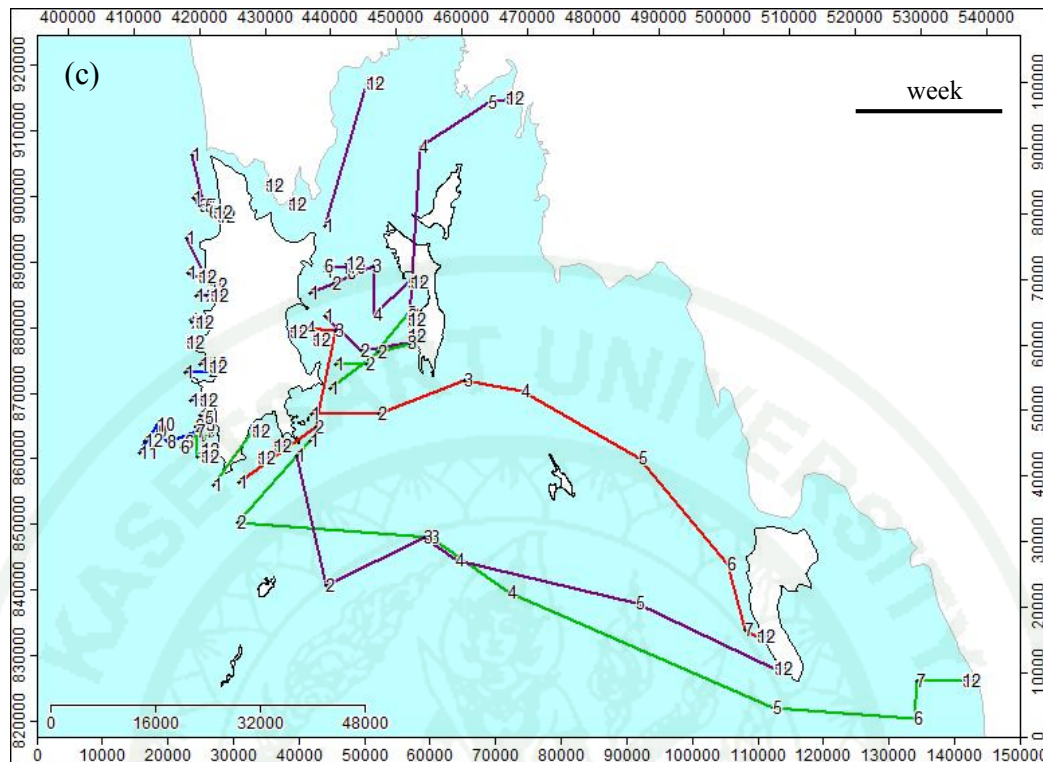


**Figure 60** (Continued)

#### 4. Yao islands

Yao islands was consisted of two islands namely Yao Noi island and Yao Yai island. They were located in the middle of Phang-Nga bay which was predictably that particles originated from these areas would be spread within the bay. The observed sites were classified into six sites which are West of Yao Yai island (light blue dots), South of Yao Yai island (purple dots), East of Yao Yai island (blue dots), North of Yao Yai island and South of Yao Noi island (red dots), West of Yao Noi island (yellow dots) and East of Yai Noi island (orange dots) as shown in Figure 61.

##### Scenario 1: Tidal dominated condition

Overall, floating marine litters were scattered all over the Phang-Nga bay; to East coast of Phuket and to coastal line of the mainland in the North and the East side (Figure 61b). This proved that tide was able to drive particles from Yao Yai island to

Yao Noi island. By tidal driven, floating marine litters originated from the West of Yao Yai island (light blue dots) were mostly heading northerly to South of the Phang-Nga province, while some of them were arriving at the East coast of Phuket and West coast of Yao Noi island. At the same time, particles sourced at the West coast of Yao Noi island (yellow dots) seemed to only move in a small distance. For those from South of Yao Yai island (purple color), they tended to travel to the South of Phuket according to the direction of current during ebb tide. Particles originated from the East coast of Yao islands (orange and blue dots) had a tendency to be tidally driven to the East side heading coastal line of the mainland. Locally, particles from the East coast of Yao Yai island (blue dots) were moving to East coast of Yao Noi island, meanwhile some particles from the East coast of Yao Noi island (orange dots) were transported to coastal mainland at the North of the bay and the other side of the island. Lastly, floating marine litters in between Yao Yai and Yao Noi islands (red dots) were moving along the shape of the strait between the islands Northwest and Southeast directions.

#### Scenario 2: Northeast monsoon

It was predicted that marine litters originated from West side of Yao Yai island (light blue dots) were distributed southerly, westerly to Phuket and northerly to South of Phang-Nga province and West side of Yao Noi island (Figure 61c). It was also graphically displayed that particles that reached East Phuket (Ao Por) and South of Phang-Nga province were the influence of estuary zone and geographical barrier. A few particles that were driven southerly seemed to travel farther. Particles at the space between Yao Yai and Yao Noi islands (red dots) also spread out but only in East and West directions to Phuket and to mainland of Krabi, respectively. Some also seemed floating around Yao Noi island. However, particles originally from West side of Yao Noi island (yellow dots) seemed to have least dynamic because they solely moved and accumulated along the original shoreline with particles that presented that there might be a possibility that marine litters originated from this area could travel far southward. Furthermore, marine litters originated from East side of Yao Noi island (orange dots) were driven to North, East and South directions to shoreline of Phang-Nga and Krabi

Province and Phi Phi islands, in the South. However, marine litters originally from East of Yao Yai island (blue dots) demonstrated the obvious result that they could scatter to their East, South and West directions. Some particles moved to Krabi shoreline, Phi Phi islands, Phanwa cave and Promthep cave in Phuket and the open Andaman Sea. Lastly, particles originally from South of Yao Yai island moved southwesterly and reached South Phuket and westerly to East Phuket.

### Scenario 3: Southwest monsoon

Floating marine litters were moved from the origin from Yao islands all around the bay in every direction especially to the East direction (Figure 61d). Particles originated from the West coast of Yao Yai island (light blue dots) were dispersed to the North reaching mainland of South Phang-Nga province and West coast of Yao Noi island, to the West arriving East coast of Phuket and to the South moving out of Phang-Nga bay and facing the open Andaman Sea. Meanwhile, floating marine litters originated from the West coast of Yao Noi island (yellow dots) were hardly found far from the origin. They were moving along the coastal zone and a few of them were travelled to mainland in the East of the bay. Particles sourced from the East coast of Yao Noi island (orange dots) were travelling in the North-East direction to mainland of Krabi province and to Southeast direction heading to mainland and Phi Phi island. In addition, some particles from the East coast of Yao Yai island (blue dots) were chiefly moving to the East and reach the middle zone of mainland. Particles from the South of Yao islands (purple dots) were dispersed southwesterly for a long distance and reached the middle coast Krabi and Lanta Yai island. Lastly, particles, sourced from the area in between Yao Noi and Yao Yai island (red dots), were brought along the shape of the geology to Southeast direction; some of them were reaching southern part of Yao Noi island and northern part of Yao Yai island.

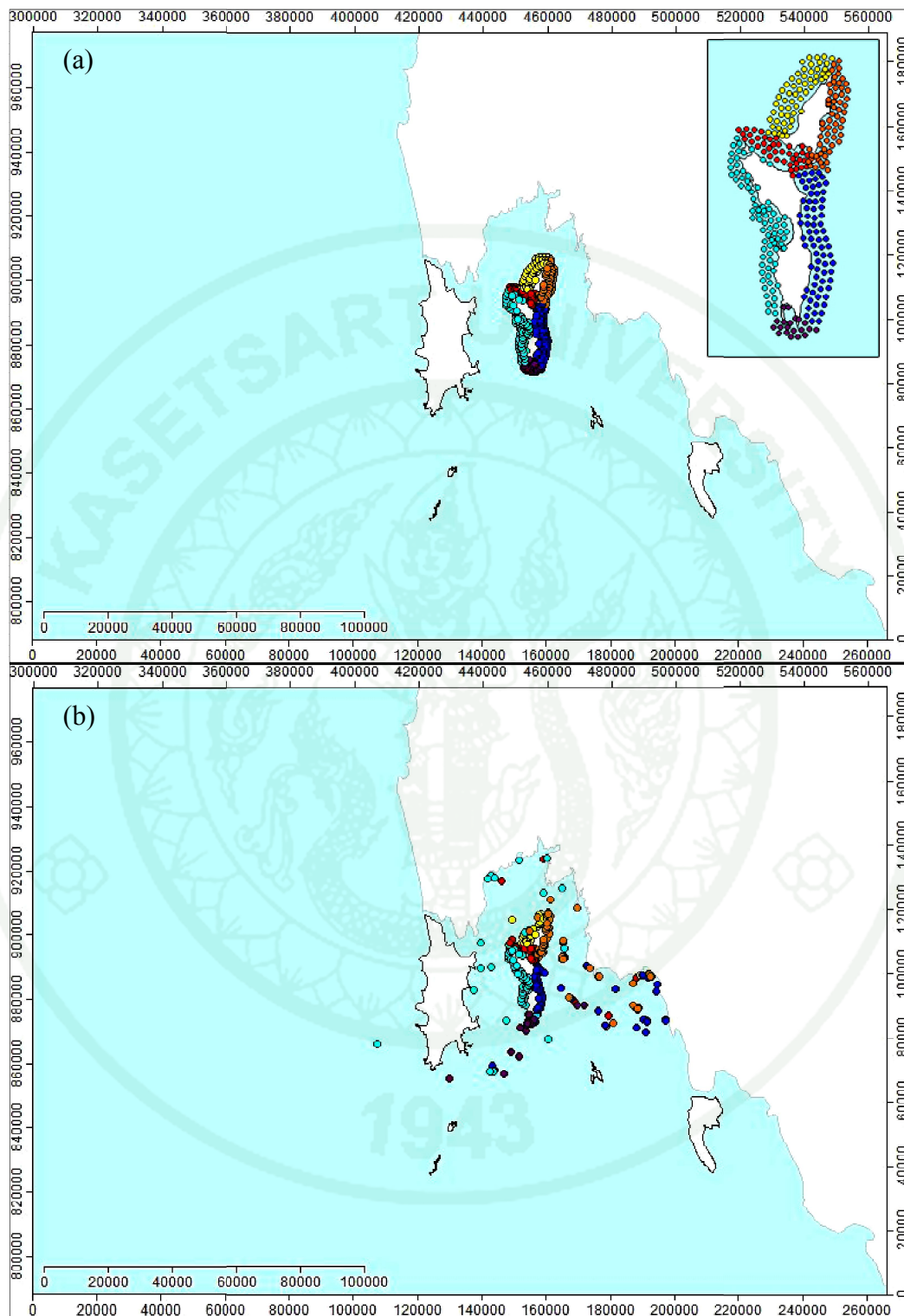


**Figure 61** Transportation of marine litters at Yao islands between (a) Day 1 and Day 90 under the condition of (b) tidal dominant, (c) Northeast monsoon and (d) Southwest monsoon

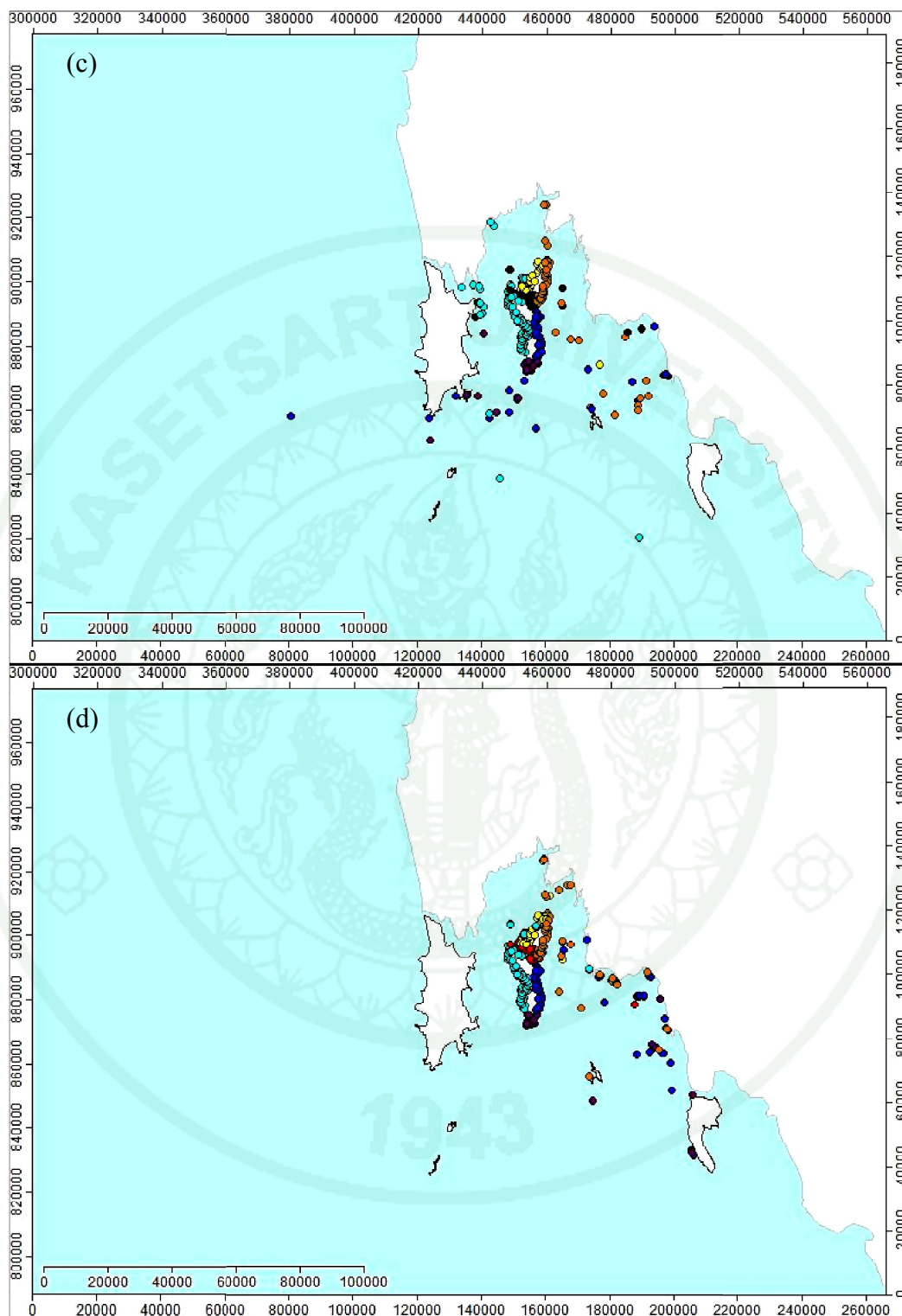


**Figure 61** (Continued)

To sum up, Tidal dominated current had dispersed floating marine litters originated at Yao islands in all directions around the Phang-Nga bay; a few particles that were moved out to West side of the bay to the open Andaman Sea. Sea surface current during Northeast monsoon had the tendency to bring particles in this area to travel in the same direction as tidal dominated current, yet it was in the longer distance. Nevertheless, particles movement under Southwest monsoon showed significantly difference regarding dispersion direction; particles were only moved to the East and Southeast of origin.

Displacement of marine particles originated from Yao islands of three different scenarios was fully summarized in Table 16 and histogram of marine particles displacement was profiled in Figure 62. Current forced by tide had wholly driven floating marine litters as similar to that under Northeast monsoon; wind in Northeast monsoon had driven particles in farther displacement. Particles in Southwest monsoon seemed to travel farthest with 15 km average and 66 km maximum, yet particles in Northeast monsoon could drive particles far up to 81 km.

**Table 16** Displacement profile of marine particles originated from Yao islands

Scenario	Displacement (m)		
	Min	Mean	Max
Tidal dominated	10	12,640 ± 14,812	47,290
Northeast monsoon	30	11,700 ± 13,087	81,110
Southwest monsoon	10	15,000 ± 16,364	66,020

Histogram of particle displacement at Yao islands under three case scenarios indicated that current under tidal condition was able to dominantly drive floating marine particles in the distance up to 35 km within 90 days, whereas current in Northeast monsoon drove particles locally. In addition, current in Southwest monsoon was prominently drive marine litter far up to 50 km.

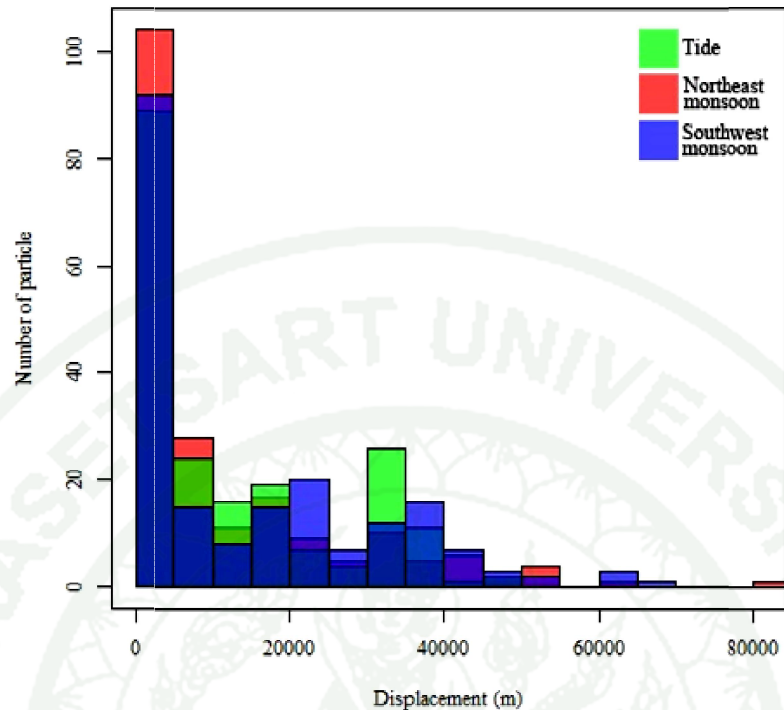


**Figure 62** Histogram of particle displacement (m) at Yao islands in three case scenarios

Sampled litters were randomly chosen to represent the path of marine litters originated at the Yao islands during 12 weeks as shown in Figure 63. The paths of litters under tidal condition showed the direction of tidal flow in the Phang-Nga bay. Some litters reached the coastal of mainland at Week 12 and presented more dynamics at the East side of the Yao islands (Figure 63a). For the Northeast monsoon, litters at the West coast of Yao island arrived Phuket within 5 weeks, and some were moving to the south of the origins (Figure 63b). For the Southwest monsoon, litters originated at the West coast of Yao islands rarely moved out while those at the East coast moved easterly and reached the mainland within 4 weeks and also reached Lanta Yai island within 6 weeks, more or less (Figure 63c).

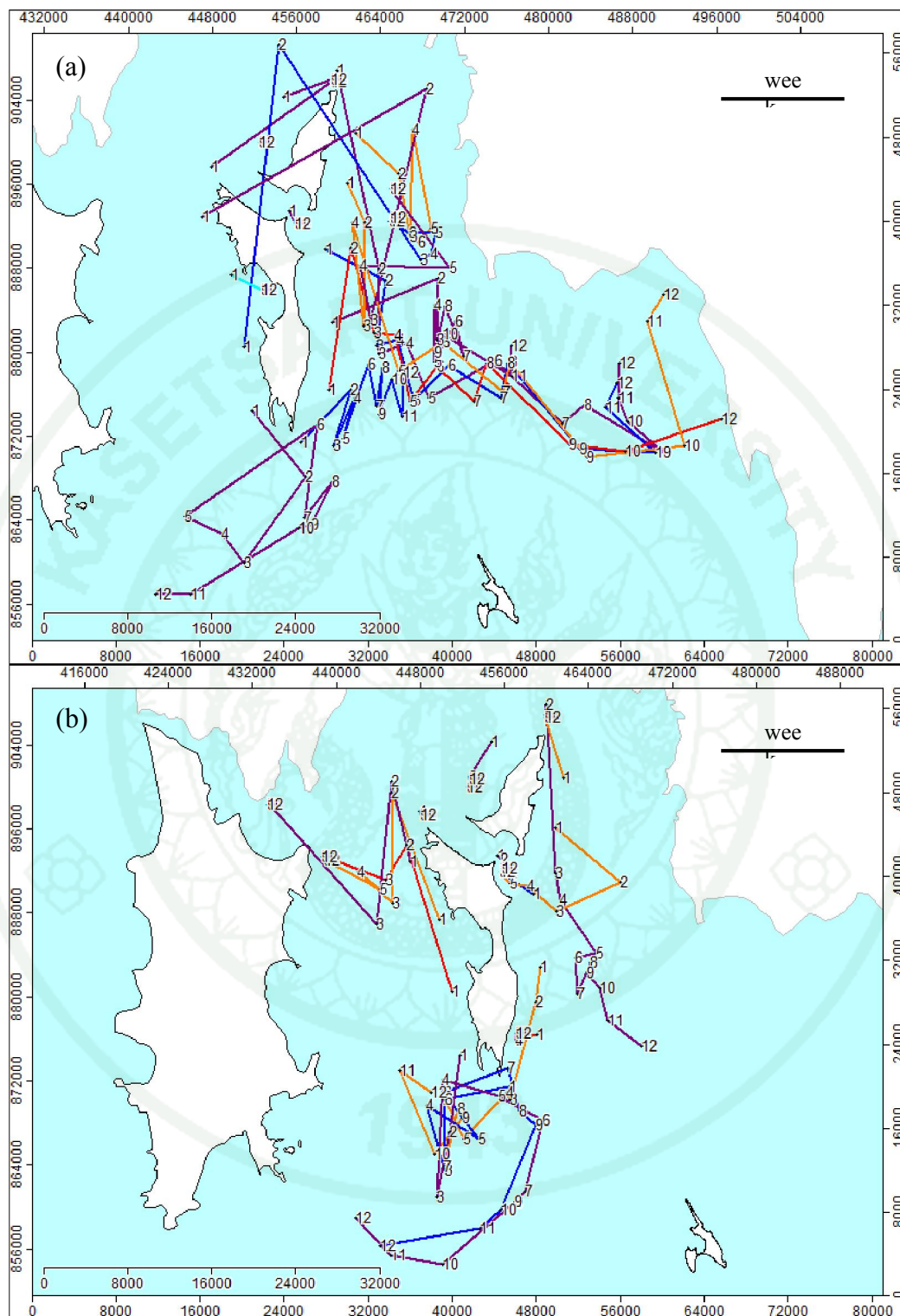


**Figure 63** Transportation path of marine litters originated at Yao islands under the condition of (a) tidal dominant, (b) Northeast monsoon and (c) Southwest monsoon

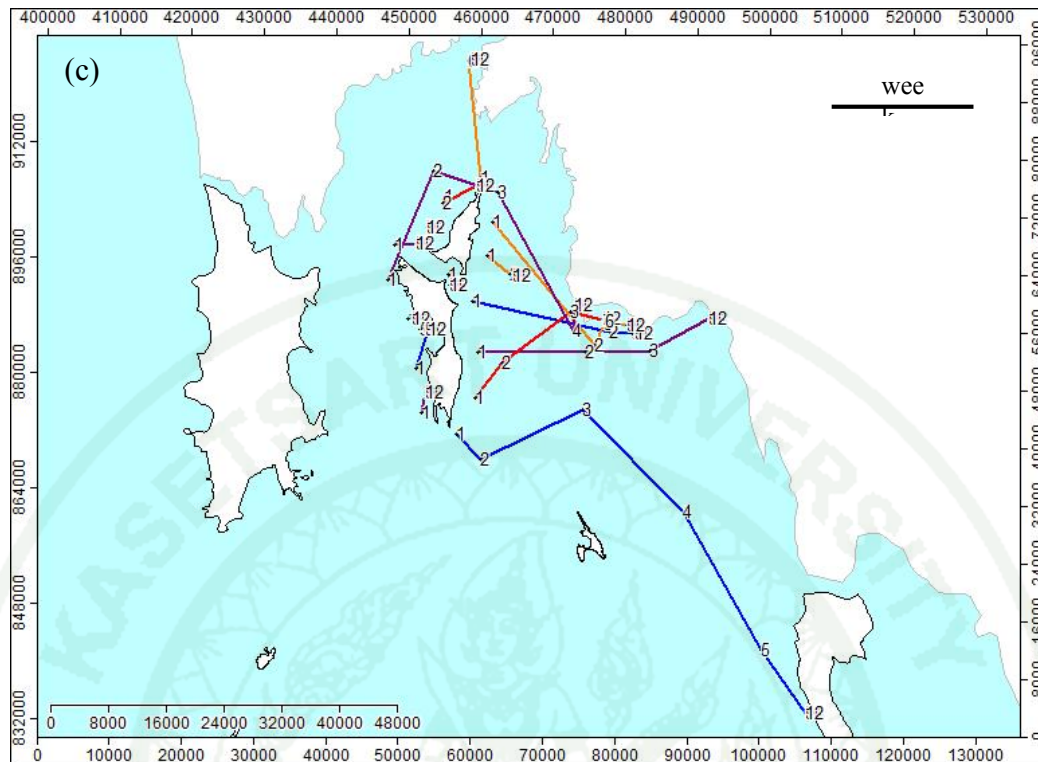


**Figure 63** (Continued)

### 5. Phi Phi islands

Phi Phi islands are composed of many islands around this area, but a major well-known island is called Phi Phi Don island as shown in Figure 64. Marine litters was observed around this island and separated into three sites which were West side (orange dots), East side (light blue dots) and South (purple dots) of Phi Phi Don island. Particle tracking revealed by FVCOM for 90 days showed that particles originated from this island was freely scattered out of the island in slightly far distance every directions with longest distance of 100 km during 90 days.

#### Scenario 1: Tidal dominated condition

Tide only drove particles originated from Phi Phi Don islands in the Northeast-Southwest direction, as shown in Figure 66b. All particles at every sides of the island had a tendency to move in the mentioned direction. Surprisingly, there were

some particles originated at the East coast managed to travel along the coast and reached West coast of the islands. Particles at both West and East coasts could travel to the coastal line of the mainland.

#### Scenario 2: Northeast monsoon

Not only moving out of the island, but a few particles also moved from one side to another side of the island (Figure 64c). Particle originated from East side (light blue dots) of the island had a tendency to scatter to every direction: northward to Yao islands; eastward to mainland, Krabi shoreline; southward floating into the sea and; westward to the open Andaman Sea and to West side of Phi Phi Don island. However, marine litters originated from South of this island (purple dots) tended to travel to West and to South farther than to East direction, and a few particles also reached West side of the island. Particles originated at West side of the island (orange dots) were moving westward to the open Andaman Sea, northward to reach Yao islands and eastward to mainland – Krabi shoreline.

#### Scenario 3: Southwest monsoon

During Southwest monsoon, particles originated from Phi Phi islands were rather travelling around the island and local zone as shown in Figure 64d. There were only a few particles that travelled seawards to Lanta Yai island, and they were from the West and South coasts of the Phi Phi Don island. In addition, floating marine litters from the South (purple dots) of the island were able to reach North tip of the island.

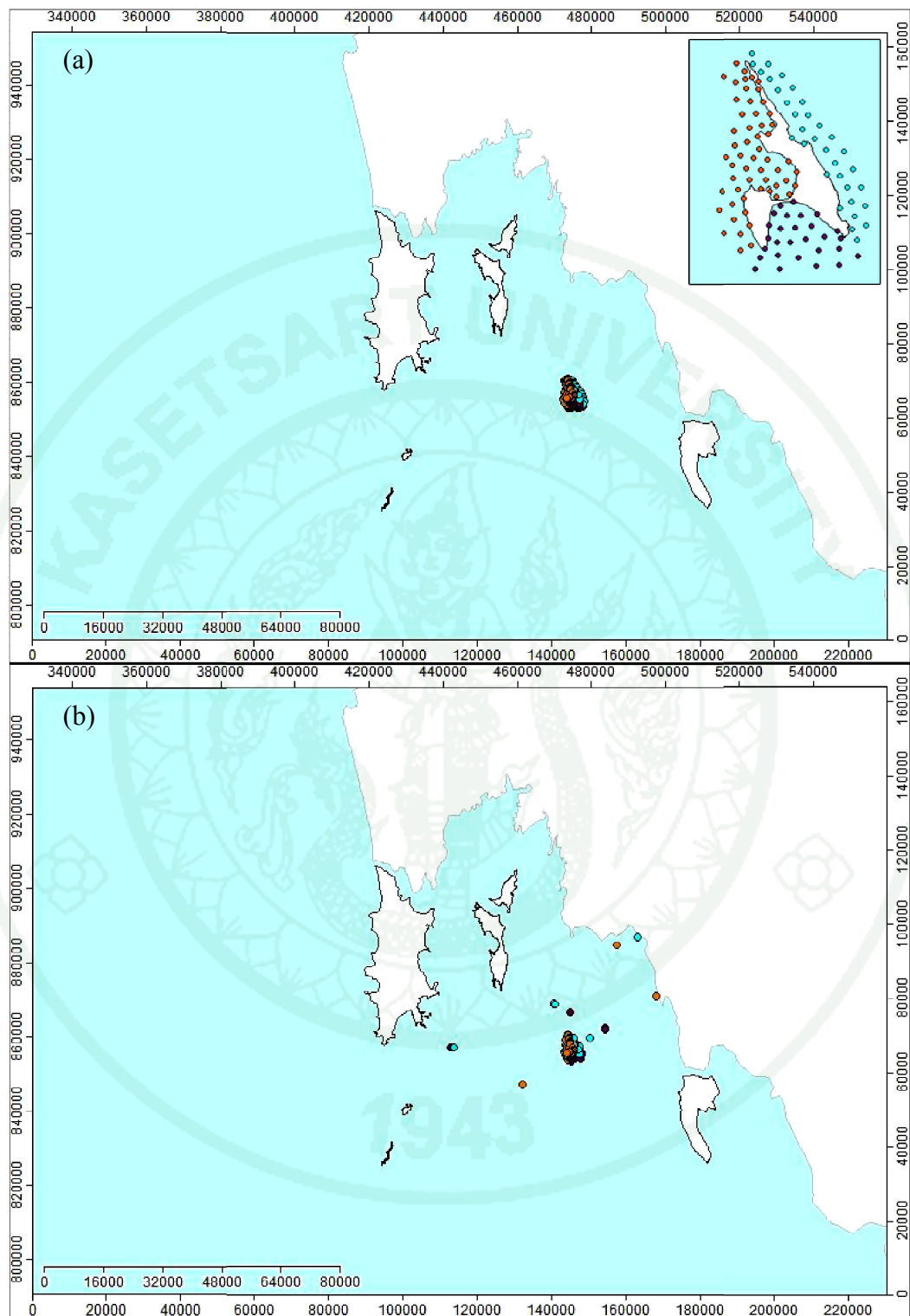


**Figure 64** Transportation of marine litters at Phi Phi islands between (a) Day 1 and Day 90 under the condition of (b) tidal dominant, (c) Northeast monsoon and (d) Southwest monsoon

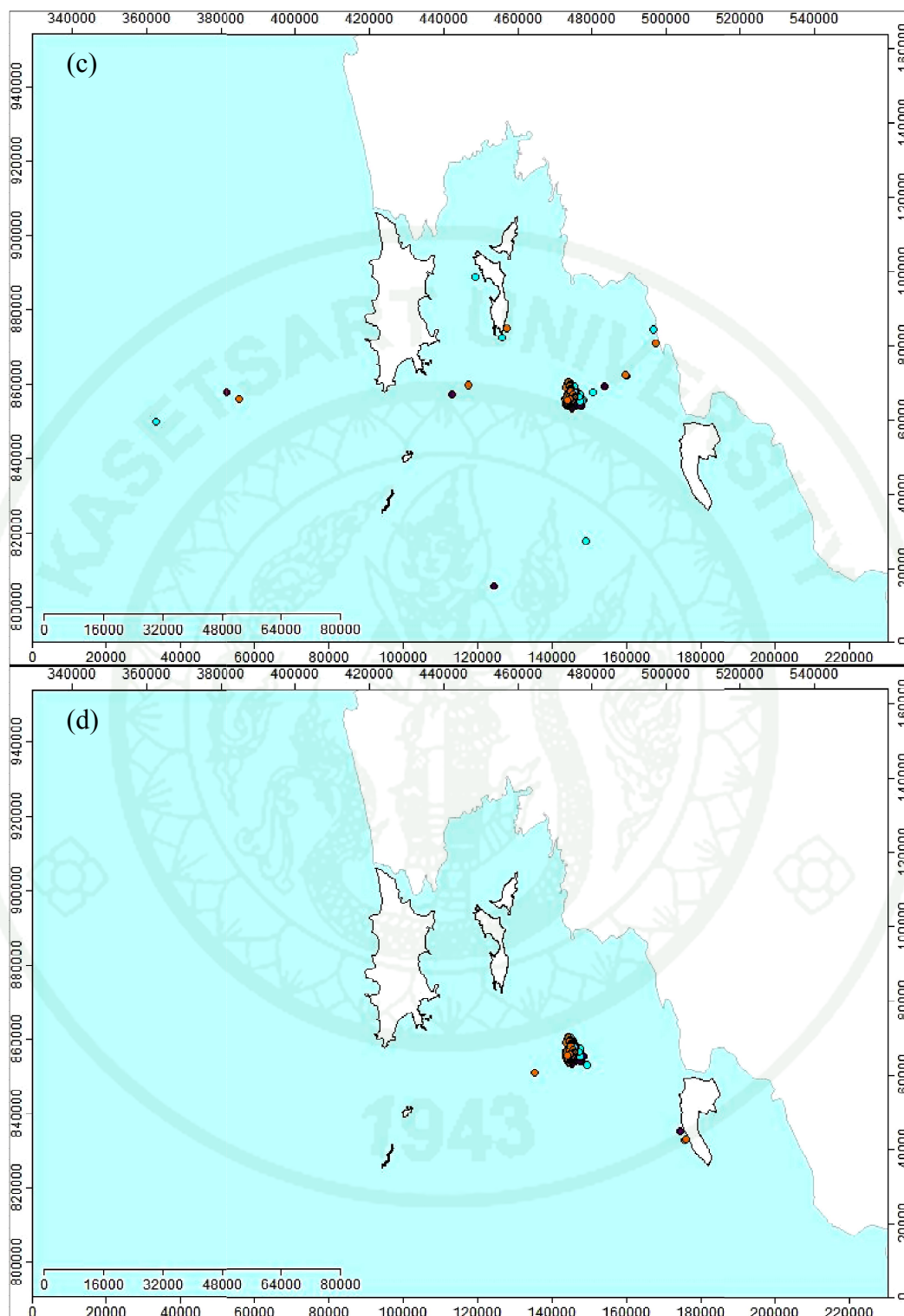


Figure 64 (Continued)

Floating marine litters were moving in Northeast and Southwest direction during tidal dominated condition while that in Northeast monsoon were brought to West and East plane but the distance was longer than that under tidal condition. Lastly, particles were mostly travelling along the coastal zone during Southwest monsoon.

Displacement of marine particles originated from Phi Phi islands of three different scenarios was summarized in Table 17 and histogram of marine particle displacement was profiled in Figure 65. Commonly, particle displacements of tidal dominated condition and Southwest monsoon had similar length of dispersion, whereas current in Northeast monsoon drove particles farther than others. In addition, maximum particle displacement under tidal forcing was as nearly as that under Northeast monsoon. However, particles from Phi Phi island were able to travel in long distance in Northeast monsoon up to approximately 115 km.

**Table 17** Displacement profile of marine particles originated from Phi Phi islands

Scenario	Displacement (m)		
	Min	Mean	Max
Tidal dominated	10	7,895 ± 28,418	33,430
Northeast monsoon	10	17,570 ± 10,065	115,000
Southwest monsoon	30	6,656 ± 12,922	42,470

Histogram of particle displacement of floating marine litters originated from Phi Phi Don island indicated that tidal current commonly drove particles far up to 35 km. Meanwhile, current during Southeast monsoon dominantly caused particles to move locally up to 35 km. Lastly, particle dispersion in Northeast monsoon seemed to scatter in the large scale and longer duration than other scenarios.

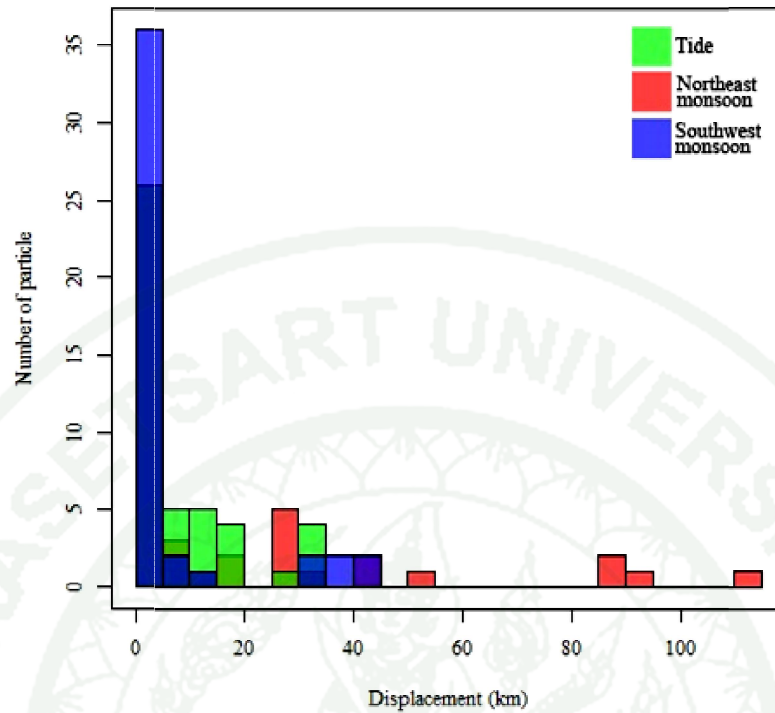


**Figure 65** Histogram of particle displacement (m) at Phi Phi islands in three case scenarios

Path of marine litter transportation originated from Phi Phi islands were sampled and shown in Figure 66 under three conditions which are (a) tidal condition, (b) Northeast monsoon and (c) Southwest monsoon. Under the tidal condition, the litters went back and forth but not be able to reach mainland within 12 weeks' time (Figure 66a). For Northeast monsoon, path of some marine litters dispersed in many directions. Some litters reached Racha islands within 7 weeks and moved out of the islands while some litters arrived at Yao Yai island (Figure 66b). For Southwest monsoon, paths of marine litters went to the East direction to Lanta Yai island within 5 weeks. In addition, the litters originated at the South of the Phi Phi islands were moved out of the island to the North and were driven back to the other side of the origin (Figure 66c).

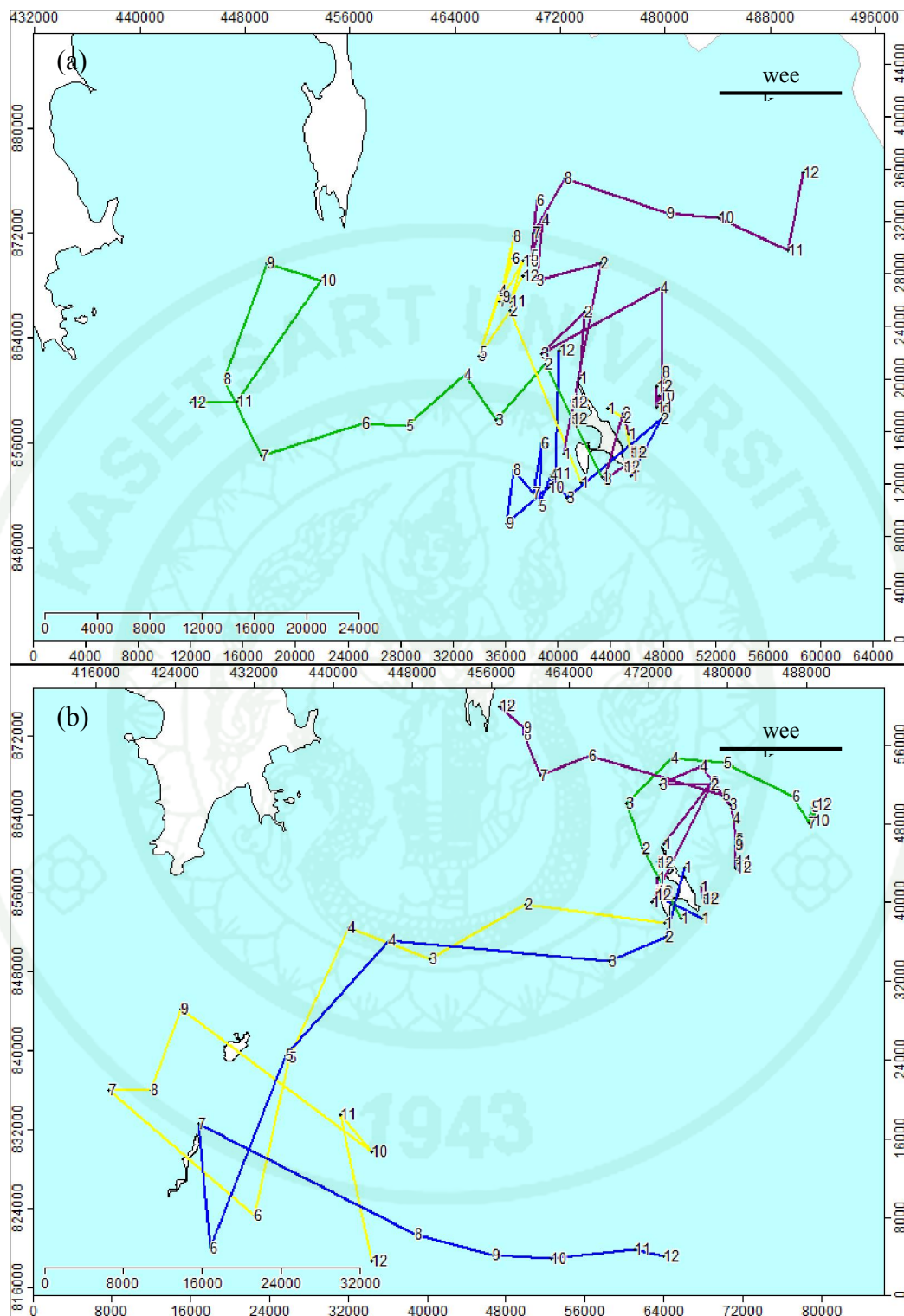


**Figure 66** Transportation path of marine litters originated from Phi Phi islands under the condition of (a) tidal dominant, (b) Northeast monsoon and (c) Southwest monsoon

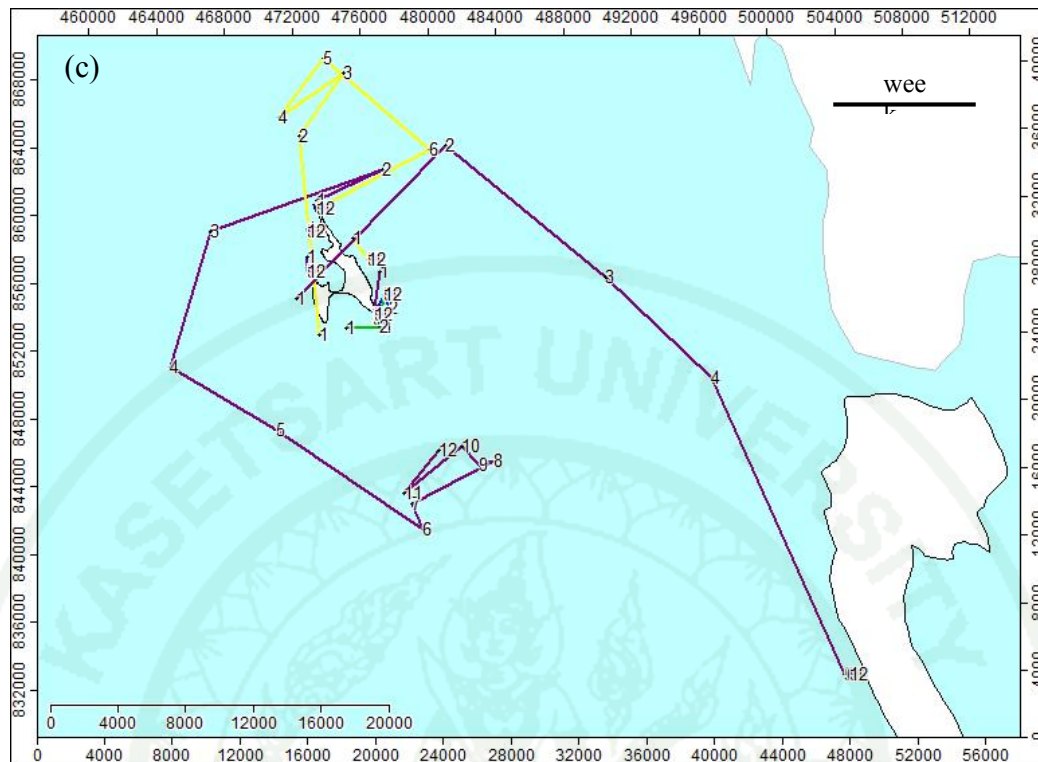


**Figure 66** (Continued)

## 6. Racha Yai island

Racha Yai island is located in the South of Phuket. Particles originated from this island were monitored at three observatory sites of the island which were North (purple dots), West (orange dots) and East (light blue dots) as shown in Figure 67.

### Scenario 1: Tidal dominated condition

Basically, floating marine litters originated from Racha Yai island were tidally moved to Northwest and Southeast directions (Figure 67b). Locally, those particles originated from the West coast (orange dots) were rarely moved. Unlike particles at West coast, those from North (purple dots) and East (light blue dots) coast tended to travel in long distance in Northeast-Southwest directions. In addition, marine litters from North coast could reach South coast, and particles from East coast could reach

North coast. However, particles originated from the North coast of the island seemed to travel farthest.

#### Scenario 2: Northeast monsoon

Particle tracking by FVCOM for 90 days revealed that most particles were distributed to East and West side, and a few particles moved northward (Figure 67c). Particles originated from North (purple dots) spread out in nearly the same distance towards West, North and East direction. They reached South of Phuket as they moved northerly, reached the open Andaman Sea as they moved to the East and freely floated to off shore of Phang-Nga bay near Phi Phi islands and Lanta Yai island as they moved to the East. Likewise, particles originated from East side (blue dots) of the island floated to the same direction as those from North of the island, but they seemed to move farther to the East. However, particles originally from West side (orange dots) of the island tended to remain at the origin.

#### Scenario 3: Southwest monsoon

Particles originated from Racha Yai island were moving in long distance, especially to the South in the open Andaman Sea (Figure 67d). Floating marine litters that were originated from the West coast of the island (orange dots) tended to travel locally. Meanwhile, particles from the North side (purple dots) and East coast (light blue dots) of the island had a tendency to disperse out of the island. Some of them were moving to East direction heading to Phi Phi islands, whereas a few particles were travelling to South of the bay in a long distance.

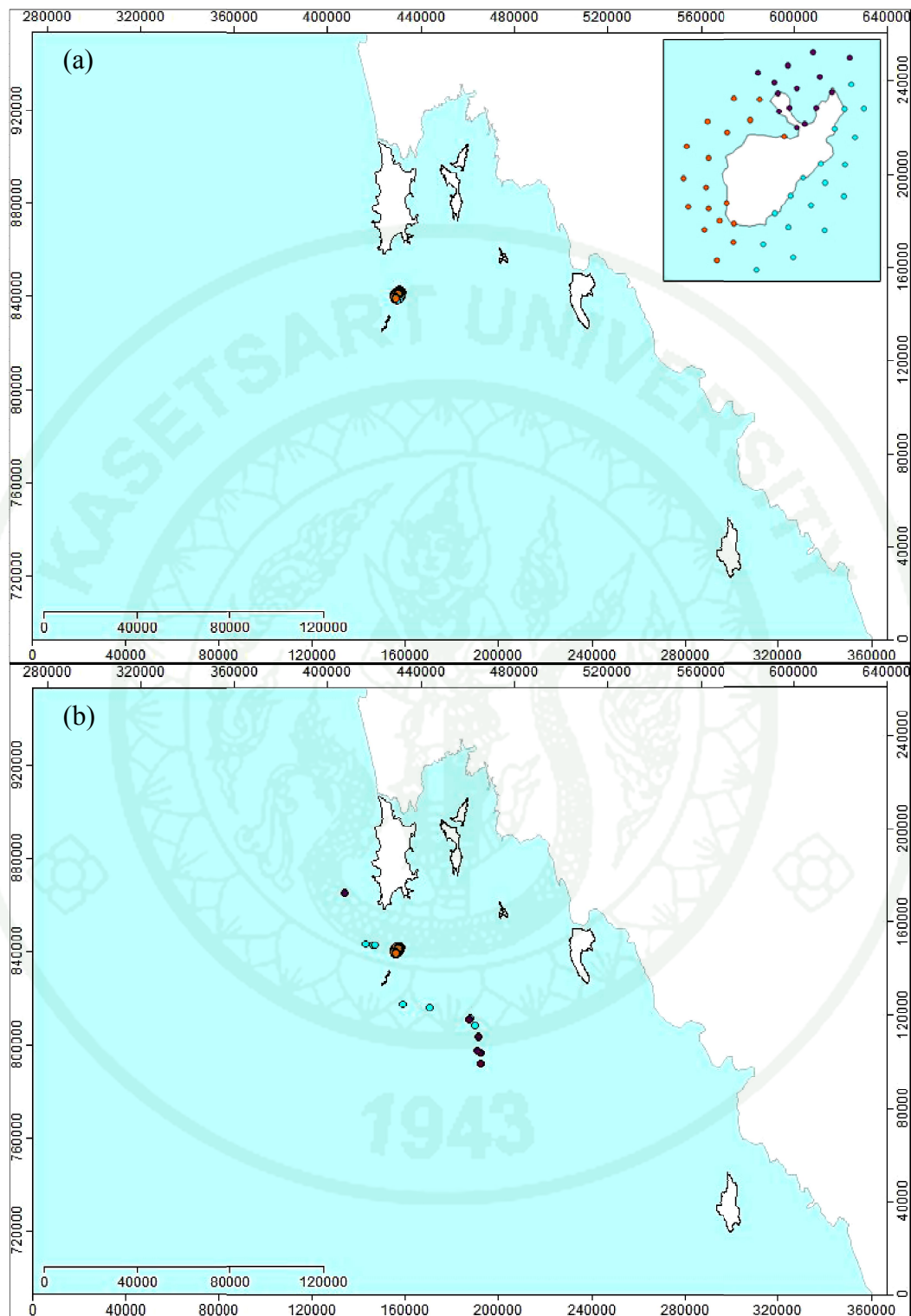


**Figure 67** Transportation of marine litters at Racha Yai island between (a) Day 1 and Day 90 under the condition of (b) tidal dominant, (c) Northeast monsoon and (d) Southwest monsoon

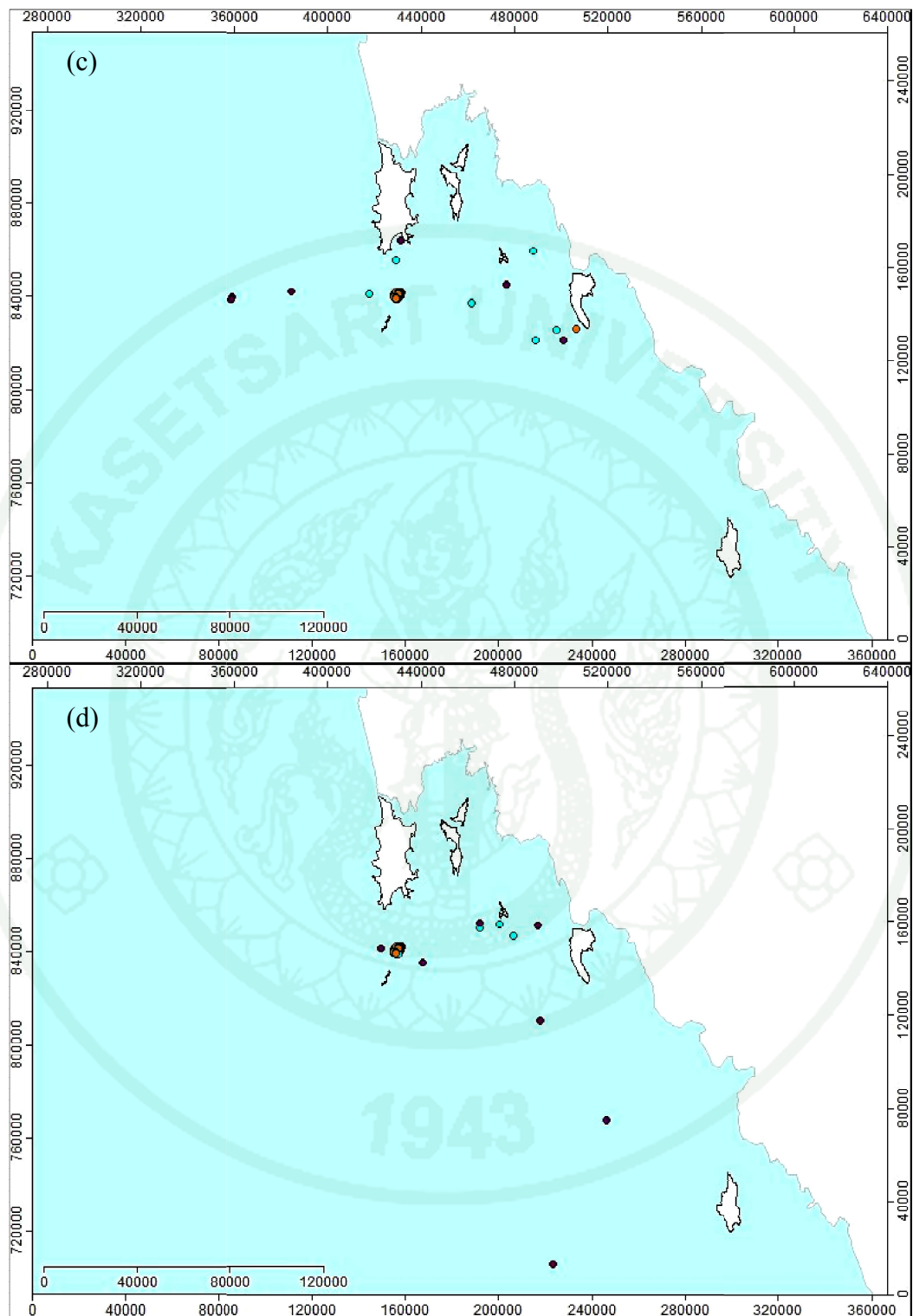


Figure 67 (Continued)

Particles movement of three case scenarios showed different pattern and direction of marine litter dispersion. Direction of marine litters floating caused by tidal current was in the Northwest and Southeast direction. In addition, current in Northeast monsoon seemed to disperse floating marine litters to the West and East direction whereas those in Southwest monsoon had a tendency to take floating marine to the direction of East and Southeast.

Displacement of marine particles originated from Racha Yai island at three different scenarios was overall summarized in Table 18 and histogram of marine particles displacement was profiled in Figure 68. According to statistic, particle displacement under three case scenarios, the farthest particle dispersion occurred during Southeast monsoon with approximately 150 km from the origin, but particles moved farthest during Northeast monsoon.

**Table 18** Displacement profile of marine particles originated from Racha Yai island

Scenario	Displacement (m)		
	Min	Mean	Max
Tidal dominated	10	26,980 ± 28,134	61,400
Northeast monsoon	10	43,000 ± 22,279	78,440
Southwest monsoon	10	34,780 ± 44,284	152,300

Histogram had demonstrated that tidal current dominantly took along floating marine particles more or less at the range up to 55 km while particle displacement travelled up to 75 km. Overall, most floating marine particles rather travelled locally at the range up to 50 km; there were a few particles that were carried in a long distance by current under Southwest monsoon.

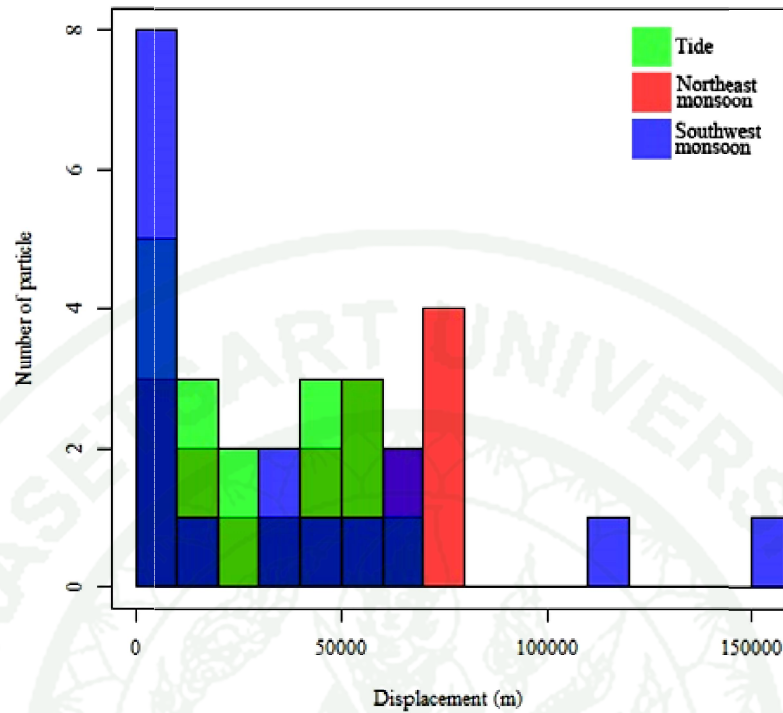


**Figure 68** Histogram of particle displacement (m) at Racha Yai island in three case scenarios

Marine litters were randomly sampled in order to represent the path of litters' transportation under tidal condition (Figure 69a), Northeast monsoon (Figure 69b) and Southwest monsoon (Figure 69c). The tidal condition drove marine litters to drive in the zigzag line into the southeast direction. In Northeast monsoon, litters moved to Lanta Yai island and almost reached there within 12 weeks' time. In addition, some samples moved to the open ocean. On the other hand, Southwest monsoon drove some marine litters to the Southeast of the origin and almost reached Tarutao island.

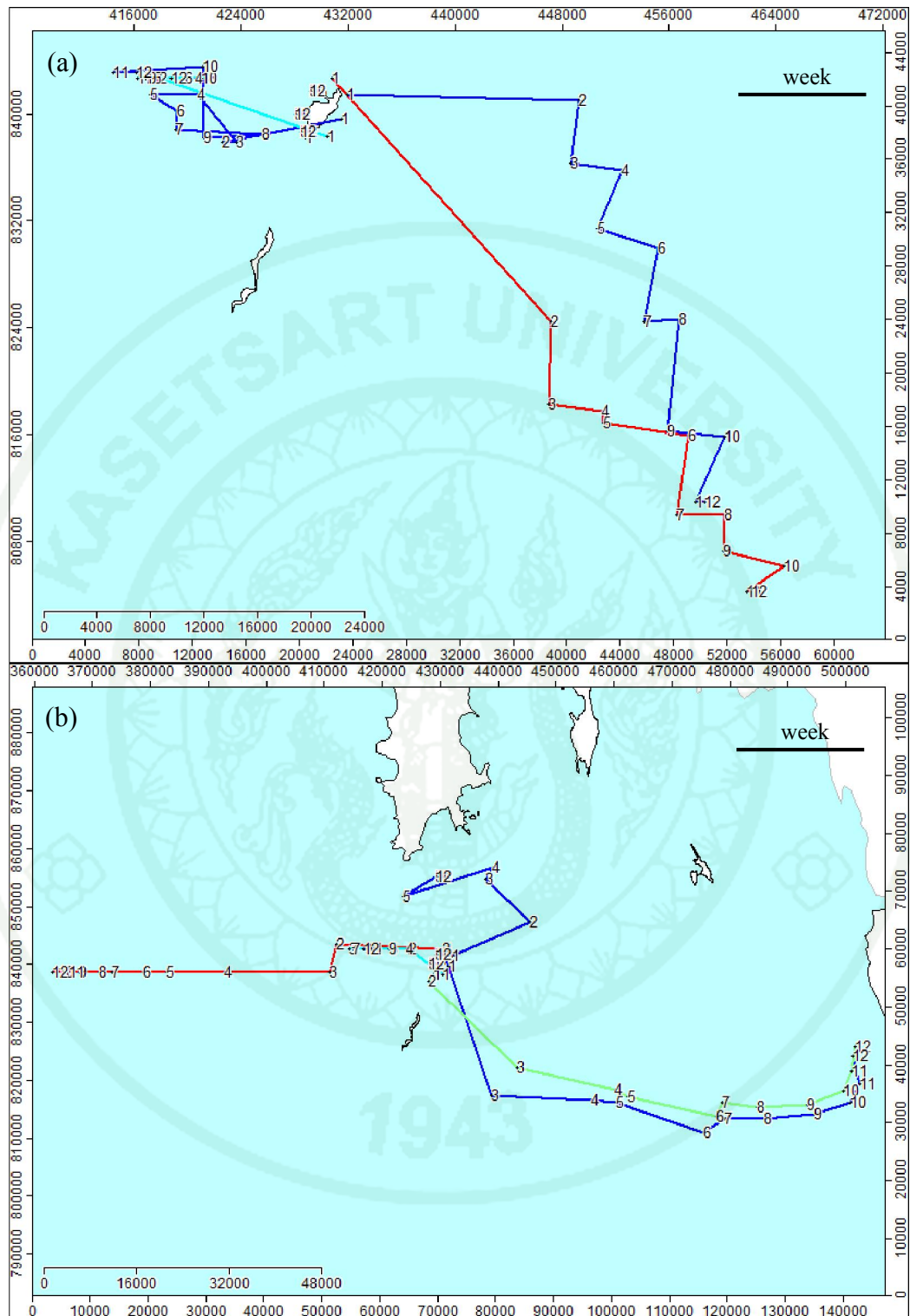


**Figure 69** Transportation path of marine litters originated from Racha Yai island under the condition of (a) tidal dominant, (b) Northeast monsoon and (c) Southwest monsoon

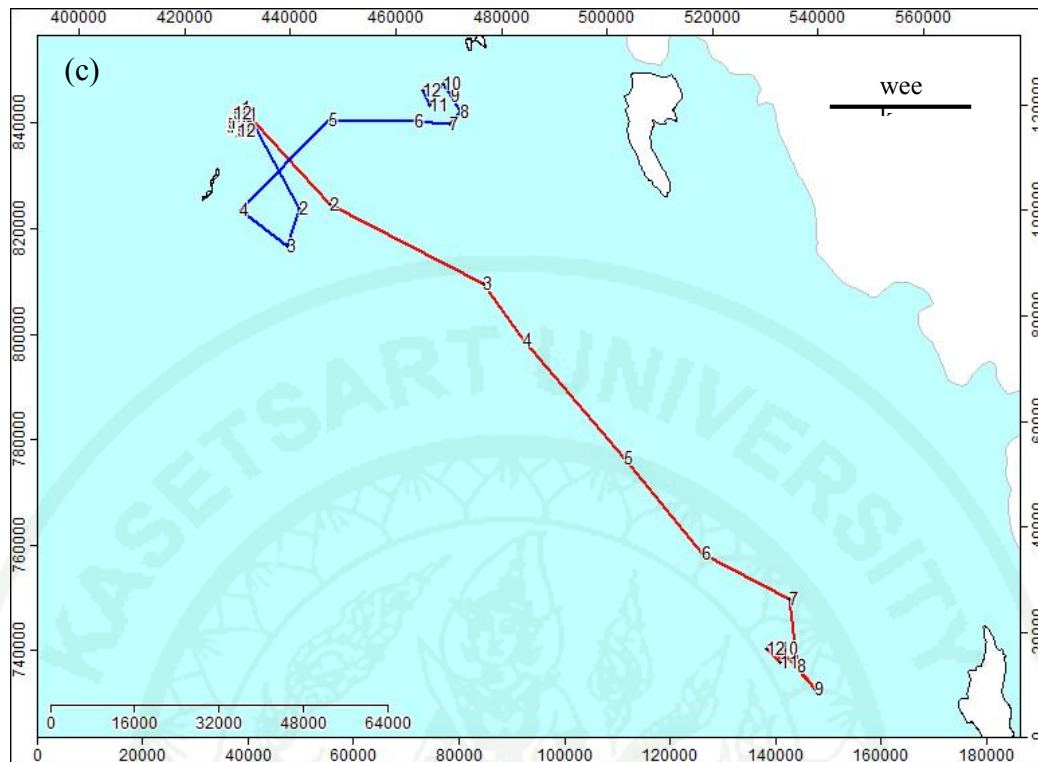


**Figure 69** (Continued)

## 7. Racha Noi island

Racha Noi island is located down South of Phuket and Racha Yai island. Tracking of particles originated from this island for 90 days revealed many dynamic movements which were distributed in long distance to many directions. Four observatory sites were established around Racha Noi island and assigned as sources of marine litters: upper West (red dots), lower West (yellow dots), upper East (purple dots) and East bottom (blue dots) as shown in Figure 70a.

### Scenario 1: Tidal dominated condition

Particles around the island had a tendency to move towards the North, East and Southeast directions (Figure 70b). Locally, particles originated from East coast (purple and blue dots) of the island were able to reach West coast of the island, while particles at the West coast seemed to head Easterly. Floating marine litters at the East

top of the island were likely to be able to reach West, South and East coast of Phuket island and South coast of Racha Yai island. Marine litters from the upper West (red dots) of the island tended to stay at the source more than those from the other sources. Some marine litters from this source even travelled seaward in a long distance in the Northwest-Southeast direction.

#### Scenario 2: Northeast monsoon

Particles originated from this island rather moved towards East and West (Figure 70c). Particles sourced from upper West (red dots) of the island were rather heading to the West of the island in more or less at the distance of 65 km, and to North reaching Racha Yai island. Controversially, particles from lower West (yellow dots) travelled to North and East side. Meanwhile, particles originated at upper East (purple dots) of the island moved to every direction but travel farther in East-West direction. Last but not least, particles from lower East (blue dots) of the island locally moved to West side of the island and travelled in a long distance towards the East as well.

#### Scenario 3: Southwest monsoon

Particles originated from Racha Noi island were dispersed to the North, East and Southeast of the origin (Figure 70d). Racha Yai island was the place where received floating marine particles from all origins around Racha Noi island. Almost all particles originated from the lower West coast (yellow dots) were moving out and scattering around the island along the coastal line, Racha Yai island in the North, coastal of mainland in the East of the origin and offshore in Southeast direction. Meanwhile, some particles originated from the upper West coast (red dots) were scattered out to the East and Southeast, leaving most particles floating at the coastal zone of the origin. Floating marine litters from the East coast of Racha Noi island (blue and purple dots) were floating towards North, East and Southeast.

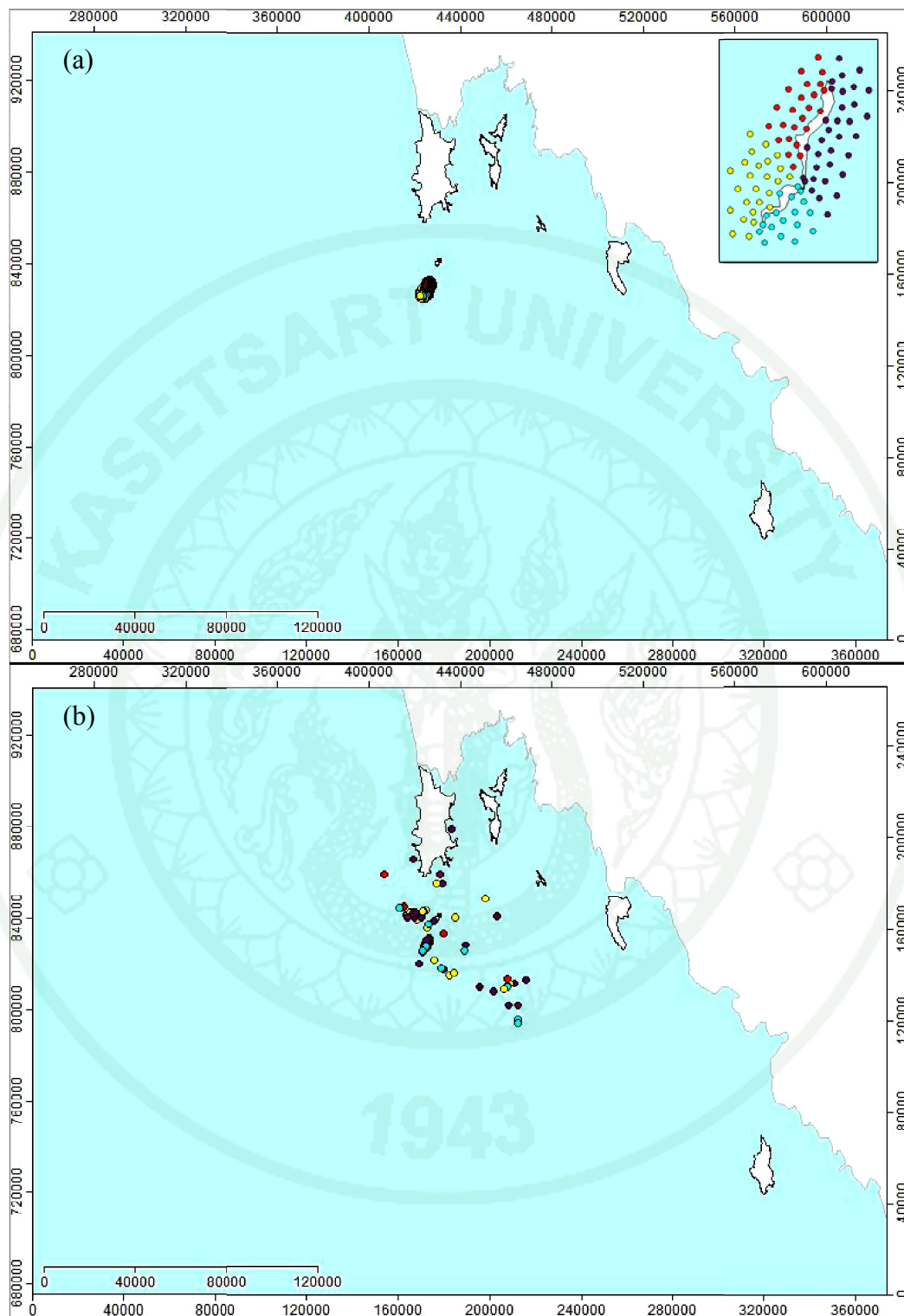


**Figure 70** Transportation of marine litters at Racha Noi island between (a) Day 1 and Day 90 under the condition of (b) tidal dominant, (c) Northeast monsoon and (d) Southwest monsoon

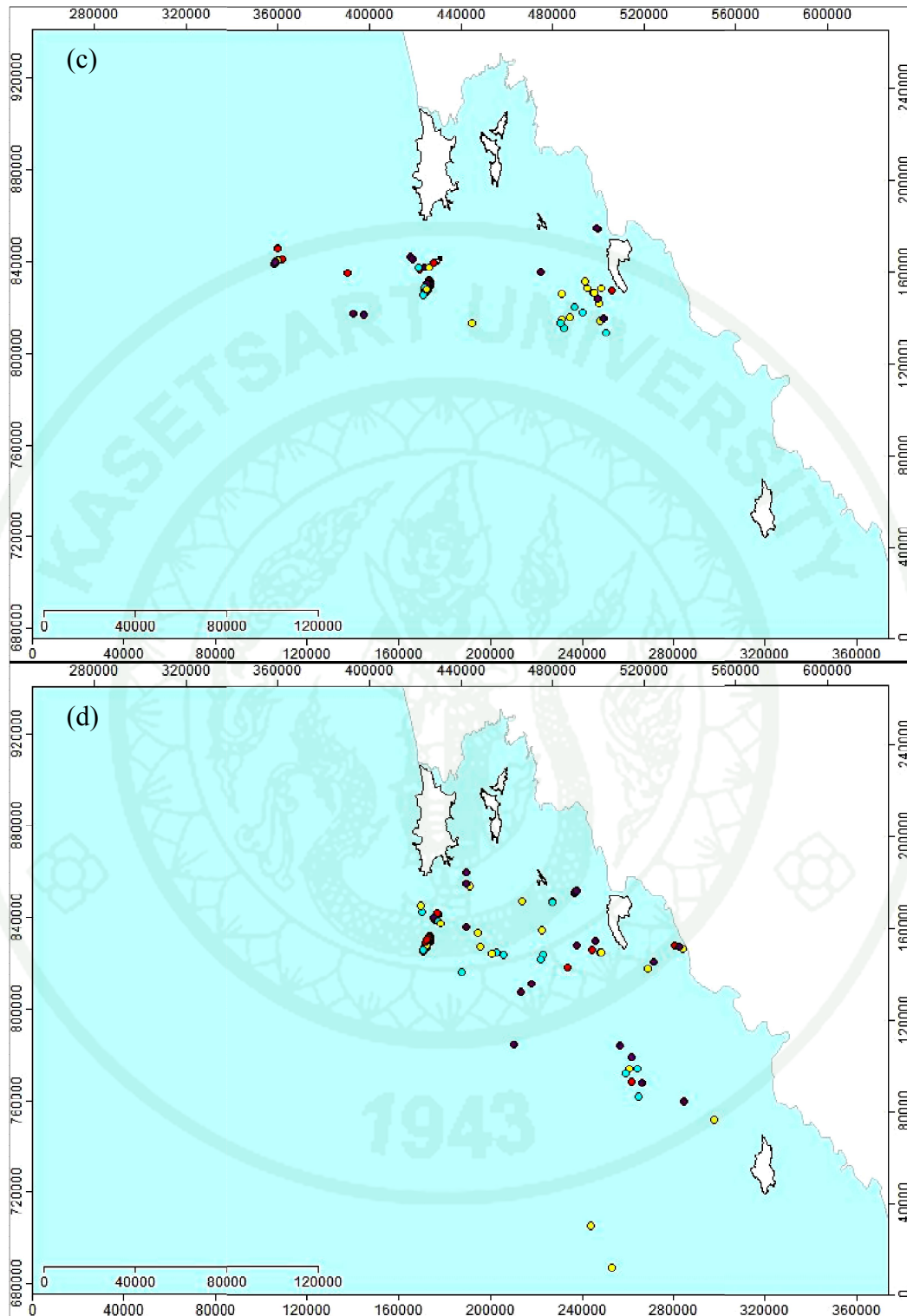


**Figure 70** (Continued)

Movement of marine particles caused by tidal dominant was showed that floating marine litters mostly travelled in long distance to the North of the origin, to the East and then down to the Southeast of the island. However, current caused by Northeast monsoon tended to bring particles on the surface to East and West directions and slightly moved to North reaching Racha Yai island. Particles originated from Racha Noi island under Southwest monsoon were likely taken to the East and Southeast of the origin.

Displacement of marine particles originated from Racha Noi island in three different scenarios was detailed summarized in Table 19 and histogram of marine particle displacement was profiled in Figure 71. Monsoons had absolutely brought floating marine litters farther than tidal force, according to statistic analysis of marine particle displacement. Surprisingly, minimum particle displacement during Southwest monsoon went more or less far up to 90 m, and particles were driven far up to 163 km.

**Table 19** Displacement profile of marine particles originated from Racha Noi island

Scenario	Displacement (m)		
	Min	Mean	Max
Tidal dominated	10	18,750 ± 31,671	51,730
Northeast monsoon	10	29,920 ± 14,381	81,810
Southwest monsoon	92	53,660 ± 44,866	163,400

It was obviously seen in the histogram of particle displacement that particles were scattered in the large scale during Southeast monsoon; whereas, current under Northeast monsoon was prominently cover in the rage of 50-75 km. Meanwhile, tidal was dominant to carry particles on the sea surface at the rage of 25-50 km.

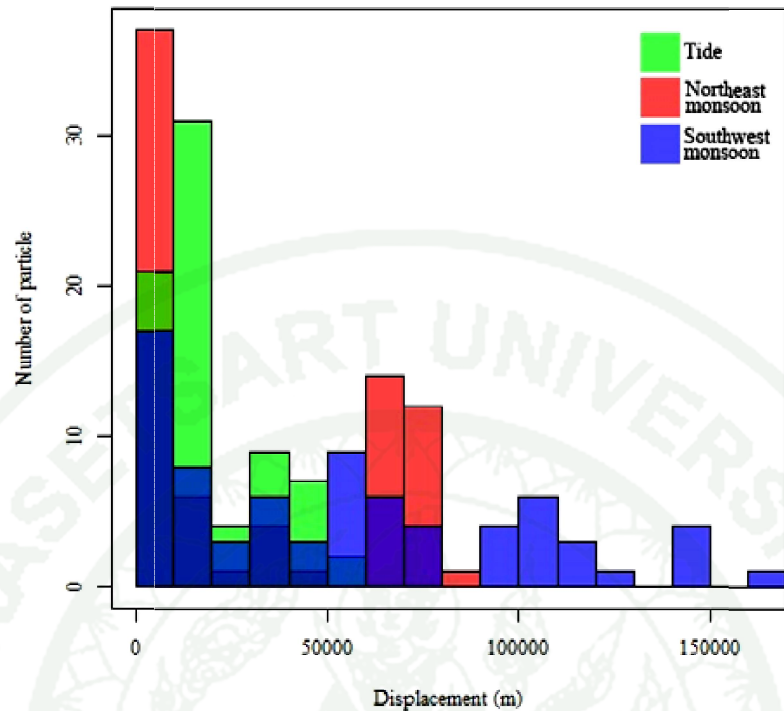


**Figure 71** Histogram of particle displacement (m) at Racha Noi island in three case scenarios

Marine litters originated from Racha Noi island were randomly selected to represent path of marine litters' transportation to show the origin (Week 1) and its destination (Week 12). Path of marine litter distribution under the tidal condition was shown in Figure 72a which showed the moving of litters that were moved back and forth according to tidal flow. Some marine litters arrived nearby Racha Yai island within few week. The distance of marine litter under tidal condition was not far but in various directions. However, the movement of marine litters under Northeast monsoon was shown in Figure 72b and under the Southwest was shown in Figure 72c. Marine litters were driven to both East and West side in Northeast monsoon; it was potentially reached Lanta Yai island at Week 12. In addition, most of the marine litters showed the same path direction in Southwest monsoon which was going to the Southeast side.

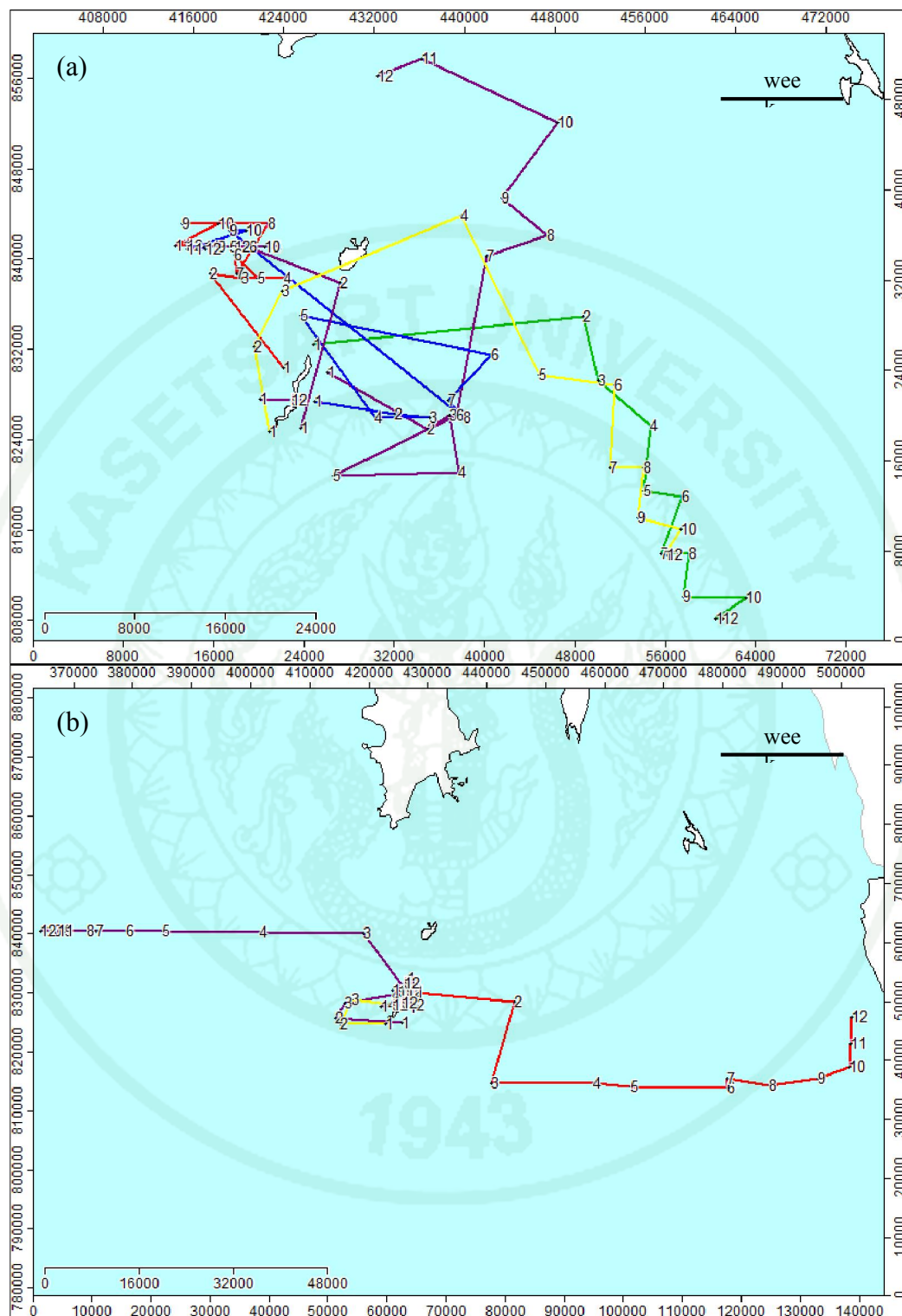


**Figure 72** Transportation path of marine litters originated from Racha Noi island under the condition of (a) tidal dominant, (b) Northeast monsoon and (c) Southwest monsoon

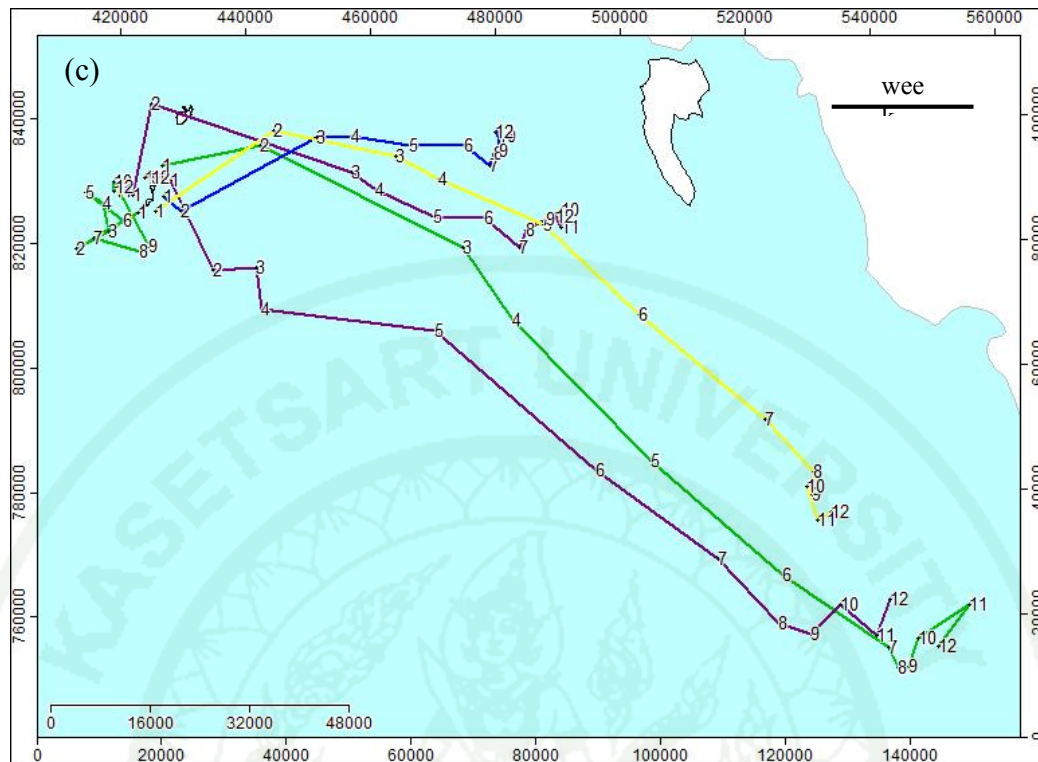


**Figure 72 (Continued)**

## 8. Lanta Yai island

Lanta Yai island is located adjacent to mainland, Krabi shoreline. Observatory sites of particle tracking around Lanta Yai island was established at four different sites as West coast (purple dots), North coast (blue dots), upper East (yellow dots) and lower East (red dots) as shown in Figure 73a.

### Scenario 1: Tidal dominated condition

Floating marine litters originated from Lanta Yai island seemed to be driven northward and northwestward (Figure 73b). Particles sourced from the West coast (purple dots) as well as those sourced from the lower East (red dots) moved to the West coast before further travel seaward within Phang-Nga bay.

### Scenario 2: Northeast monsoon

Particles originated from Lanta Yai island are slightly moved while comparing with other locations (Figure 73c). There were some particles which were driven to move further in longer distance. However, marine litters originated from the North (blue dots) of the island tended to move closer to the shoreline. Likewise, particles at lower East (red dots) tended to move landward, while one particle tended to travel to the West side of the island. Moreover, particles sourced at upper East (yellow dots) of the island only had little movement. Particles at the West coast (purple dots) of the island displayed apparent dynamic movement of marine litters on such a way that most of them float North to reach shoreline of Krabi mainland, and a few of them were scattered away from the origin in westerly and southwesterly.

### Scenario 3: Southwest monsoon

Particles from the West coast (purple dots) of Lanta Yai island were mostly travelling along the coast and moving landward (Figure 73d). At the same time, particles originated from the lower East coast of the island (red dots) were driven easterly to mainland and estuary zone as well as down South. Floating marine litters at the upper East coast of the island were scattered in short distance from the origin.

To conclude, three case scenarios revealed different pattern of particle dispersion of particles originated from Lanta Yai island. Tidal current tended to move particles from Lanta Yai island towards North and reached coastal of mainland. However, particles were transported to East and South directions during Southwest monsoon; most of them rather travelled along the coast. Lastly, particles from Lanta Yai island had a tendency to spread out far to North reaching mainland and southwesterly.

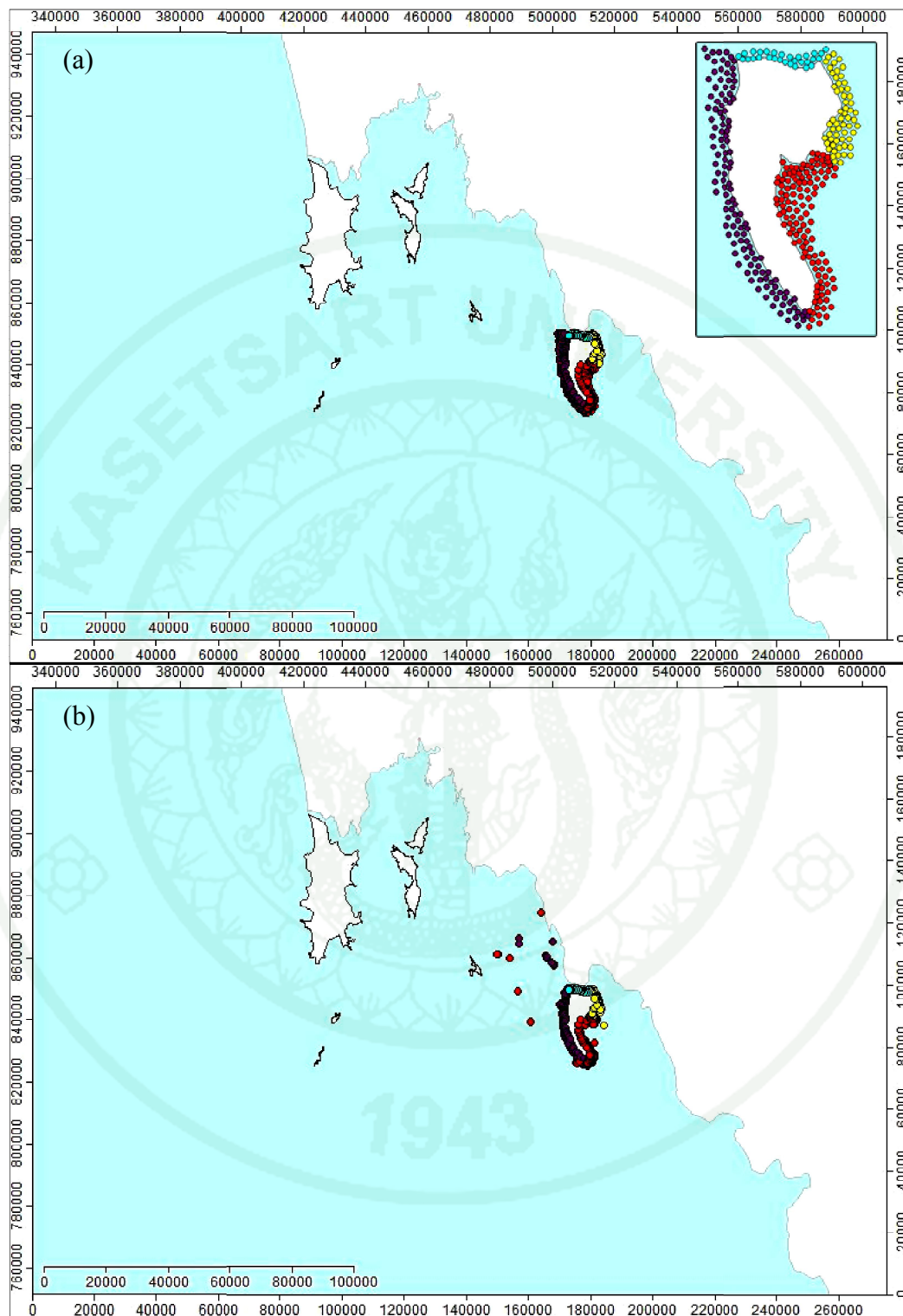


**Figure 73** Transportation of marine litters at Lanta Yai island between (a) Day 1 and Day 90 under the condition of (b) tidal dominant, (c) Northeast monsoon and (d) Southwest monsoon

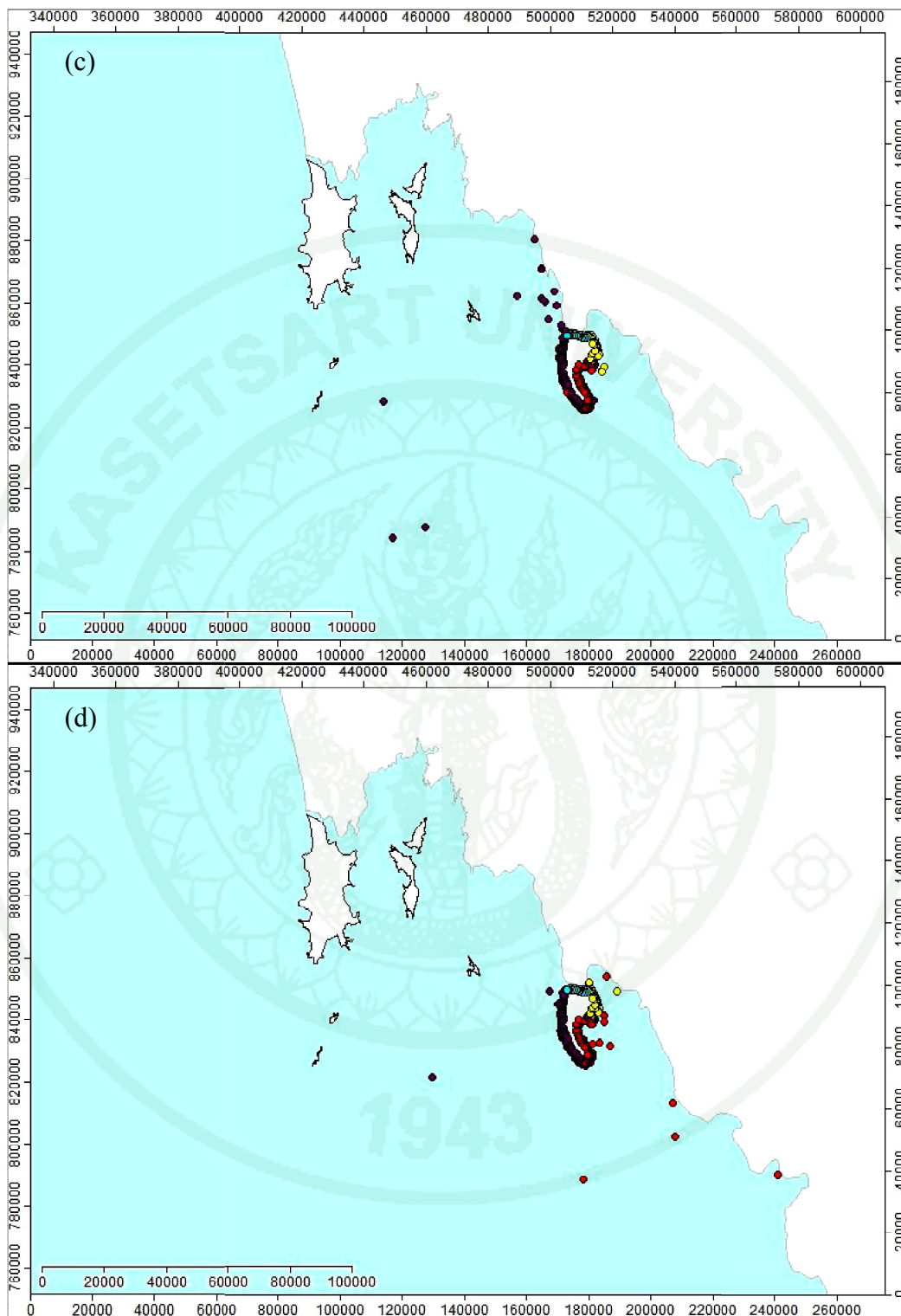


Figure 73 (Continued)

Displacement of marine particles originated from Lanta Yai island in three different scenarios was summarized in Table 20 and histogram of marine particle displacement was showed in Figure 74. Particle displacement during Southwest monsoon seemed to spread out in the least distance compared to other scenarios, but they were moved far up to 70 km which was nearly the farthest length of displacement of particles during Northeast monsoon.

**Table 20** Displacement profile of marine particles originated from Lanta Yai island

Scenario	Displacement (m)		
	Min	Mean	Max
Tidal dominated	10	7,352 ± 12,390	51,720
Northeast monsoon	10	7,493 ± 11,387	72,380
Southwest monsoon	10	5,145 ± 9,783	70,170

Histogram demonstrates that particle displacement during Southwest monsoon dominantly covered displacement of 0-15 km within 90 days. However, tidal current seemed to dominate in a longer range from 15 – 30 km. Particle displacement during Northeast monsoon tended to dominate at the range of 20 km.

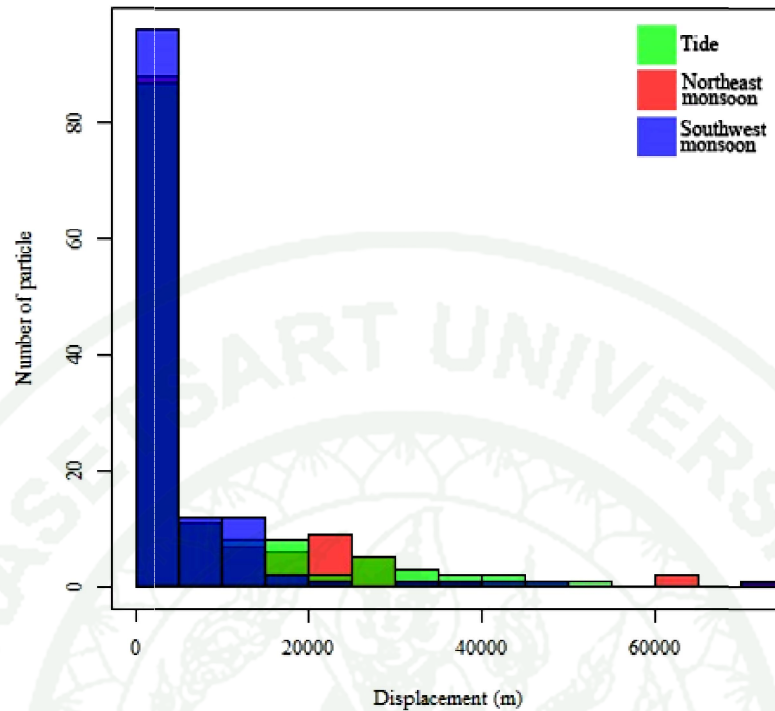


**Figure 74** Histogram of particle displacement (m) at Lanta Yai island in three case scenarios

Marine litters originated from Lanta Yai island were randomly selected to represent the distribution path of marine litters. Path of marine litter transport under showed that the litters at the east side rarely moved. Meanwhile, some litters at the west coast were moving up north and arrived at the coastal of mainland in a few weeks (Figure 75a). The distribution of marine litters under the Northeast monsoon showed that the litters at the west coast of the island moved to both seawards and landwards to coastal of mainland (Figure 75b). For the Southwest monsoon, the litters at the west coast of the island showed that the litter moved along the coast; some sample at the lower Lanta Yai island moved seawards as shown in Figure 75c.

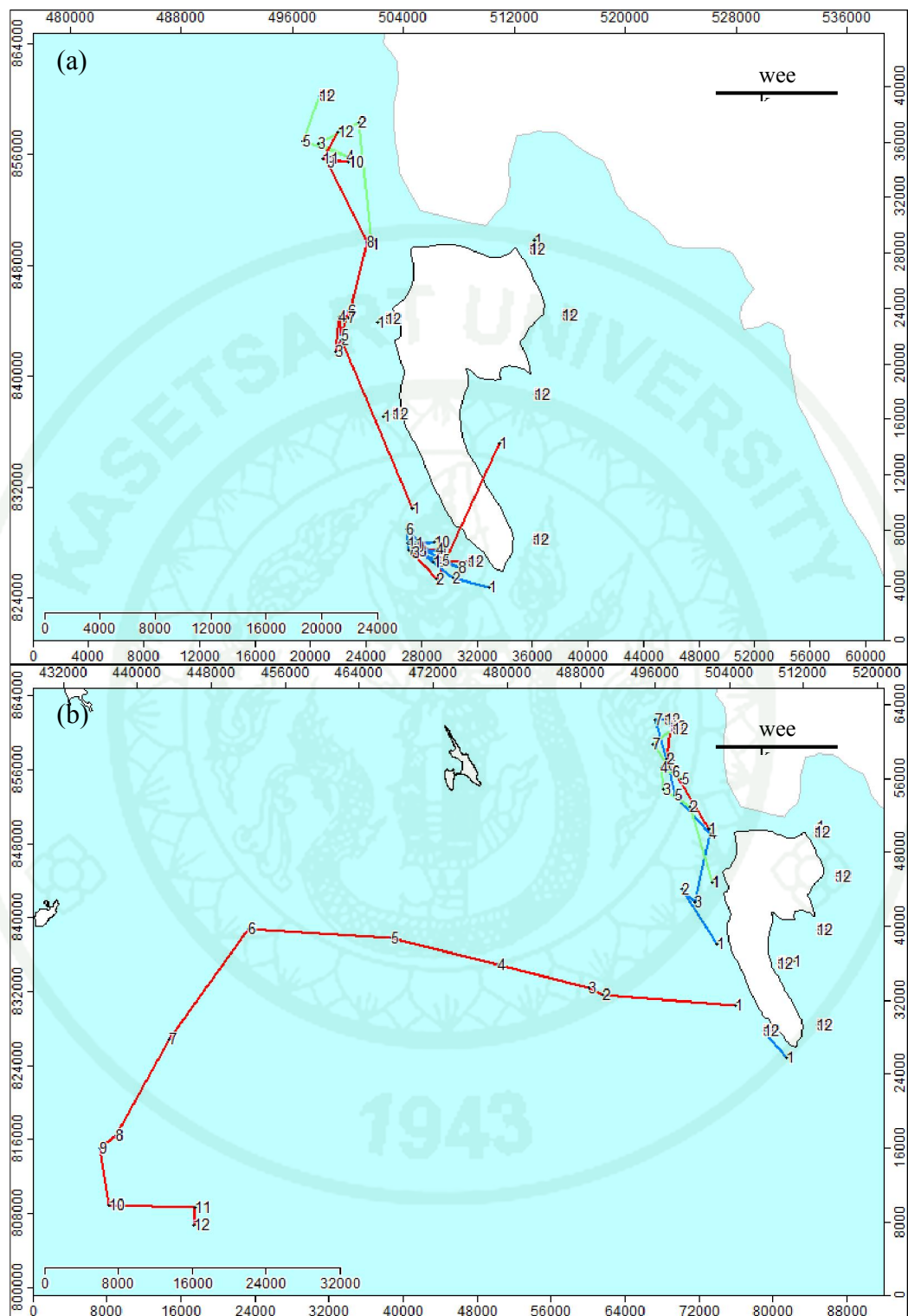


**Figure 75** Transportation path of marine litters originated at Lanta Yai island under the condition of (a) tidal dominant, (b) Northeast monsoon and (c) Southwest monsoon

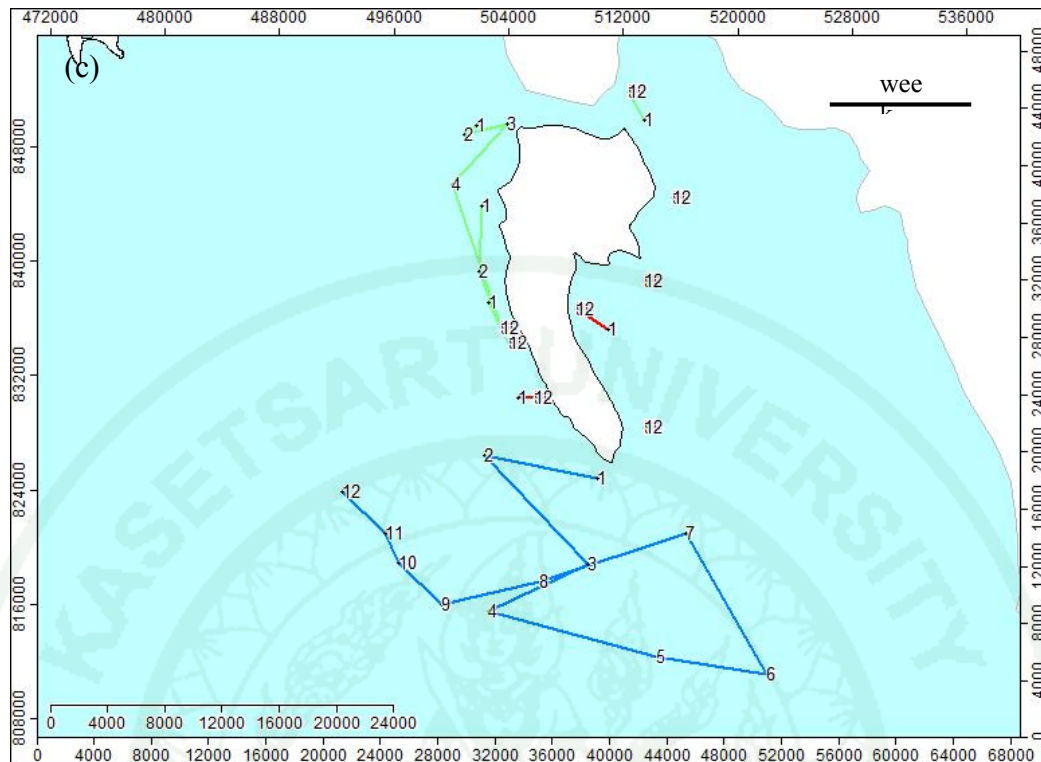


**Figure 75 (Continued)**

## 9. Offshore

According to Figure 55, there were many marine particles driven in offshore environment at Phang-Nga bay; therefore, marine litters originated offshore were traced and observed for 90 days during tidal dominated condition, Northeast monsoon and Southwest monsoon. At Phang-Nga bay, there were eight offshore sites presenting dense particles i.e. West coast of Phuket (purple dots), around Racha Yai island (blue dots), offshore between Phuket and Yao islands (green), South of Yao islands (light blue dots), offshore between Yao islands and mainland (red dots), North of Phi Phi island (maroon dots), South of Lanta Yai island (yellow dots) and offshore between Lanta Yai island and mainland (orange dots) as shown in Figure 76a.

### Scenario 1: Tidal dominated condition

Floating marine litters originated from offshore of Phuket's West coast (purple dots) had only a slight change due to tidal driving; they went seaward in a short distance (Figure 76b). At the same time, marine particles from offshore of Racha Yai island (blue dots) tended to move to all directions except to the South and Southwest. Particles from the South of Yao islands (light blue dots) were driven by tide in the East-West direction to reach the South cave of Phuket and Yao Yai island, but there were some particles driven to the North and reached mainland in the North of the bay. Floating marine particles from offshore between Phuket and Yao islands (green dots) were moving northerly to reach mainland at the North of the bay and to the West coast of both Yao Noi and Yao Yai islands. Those offshore particles between Yao islands and mainland (red dots) moved northerly and easterly; most of them were stuck at the estuary zone despite the fact that a few of them tended to reach the West coast of Yao Noi island. Moreover, particles from the North of Phi Phi island (red dots) tended to move landward to the North and reach coastal line of mainland's estuary zone. In addition, some of them moved to the Southwest to Phi Phi islands and even farther to the West. Meanwhile floating marine litters at the South of Lanta Yai island (yellow dots) seemingly travelled to the West then North and South directions. Lastly, marine particles at the offshore between Lanta Yai island and mainland (orange dots) were both moving landward and seaward. Those moving landward were stuck at the estuary zone while those moving seaward were out to the Andaman Sea and continue moving to the North-South direction.

### Scenario 2: Northeast monsoon

Marine litters offshore of West coast of Phuket (purple dots) had a tendency to travel further seaward to the East (Figure 76c). Meanwhile, particles offshore around Racha Yai island (blue dots) rather moved out seaward. There were only a few particles that travelled closer to the beach, whereas the others tended to continually move either East or West direction. Some particles from this area even reached Lanta Yai island. The similar marine litter movement behavior was repeated to particles

originated offshore between Phuket and Yao island (green dots) and South of Yao islands (light blue dots). They seemed to move in North-South direction and compiled at East coastal zone of Phuket, mouth of rivers in South of Phang-Nga province and West coast of Yao Yai and Yao Noi islands. In addition, it was evidently shown that some particles from this area moved to the South of eastern coast of Yao Yai island, whereas particles at the South of Yao Yai island (light blue dots) were brought to South cape of Phuket and entering into the open Andaman Sea. Particle movement originated from offshore between Yao islands and mainland (red dots) tended to spread out to every direction; they reached coastal zone of Yao islands, estuaries of Krabi province and even South of Yao Islands. In addition, particles originated from North of Phi Phi islands (red dots) also scattered out in various directions. Some of those travelled to coastal line of mainland, reaching Phi Phi islands, arriving East of Yao Yai islands and East of Phuket. Particles originated offshore of South of Lanta Yai island (yellow dots) were brought westward and southwestward. There was only few particles having a capability of travelling along the coast of Lanta Yai island facing Phang-Nga bay. Particles originated offshore between Lanta Yai island and mainland dispersed out and travelled to various places. Some particle evidently reached coastal zone of Lanta Yai island and mainland Krabi and Trang provinces, and remained floating at the South of Phang-Nga bay.

### Scenario 3: Southwest monsoon

During Southwest monsoon, particles from offshore of West Phuket (purple dots) were brought to coastal line of West Phuket, and taken the farthest to Lanta Yai island as shown in Figure 76d. In addition, particles offshore between the East coast of Phuket and West coast of Yao islands (green dots) were all moving easterly reaching West coast of Yao islands and some parts of mainland. Likewise, particles originated from the South of Yao islands (light blue dots) were brought northerly reaching West coast of Yao islands, easterly to mainland, southeasterly to Phi Phi islands and Lanta Yai island and to the South of the bay at the open Andaman Sea. At the same time, particles offshore between Yao islands and mainland (red and maroon dots) were dispersed to the East direction arriving coastal mainland, especially around

estuary zone in the middle of West coast of Krabi, and some of them are travelled to Phi Phi islands and Lanta Yai island. Floating marine litters offshore of Racha Yai island were dispersed towards West and arrived Phi Phi islands, Lanta Yai island and the coastal zone of mainland. In addition, some of them were also scattered in the Southeast of the origins and floating in the open Andaman Sea in quite a distance from the origin. Floating particles offshore of South of Lanta Yai island (yellow dots) were scattered to the Southeast arriving coastal line of mainland around estuary zone and to the South in the open Andaman Sea. Lastly, particles from the offshore between Lanta Yai island and mainland (orange dots) were brought to coastal zone of the mainland and the East coast of Lanta Yai island. Some particles were scattered out to the West of Phang-Nga bay and the open Andaman Sea in the South.

To conclude, tidal current dispersed floating marine particles originated offshore in Phang-Nga bay in only a certain distance, and there were many floating marine litters that remained travelling in the sea. Moreover, particles from offshore of Phang-Nga bay under three case scenarios were reaching coastal zone of many areas. In addition, particle movement under Northeast monsoon was seen to arrive at the East coast of Phuket. However, particles floating offshore were seen all over the place at the West coast of Phuket, Yao island and coastal mainland as well as Lanta Yai island. Besides, particles travelling during Southwest monsoon were also found at the South of Phang-Nga bay.

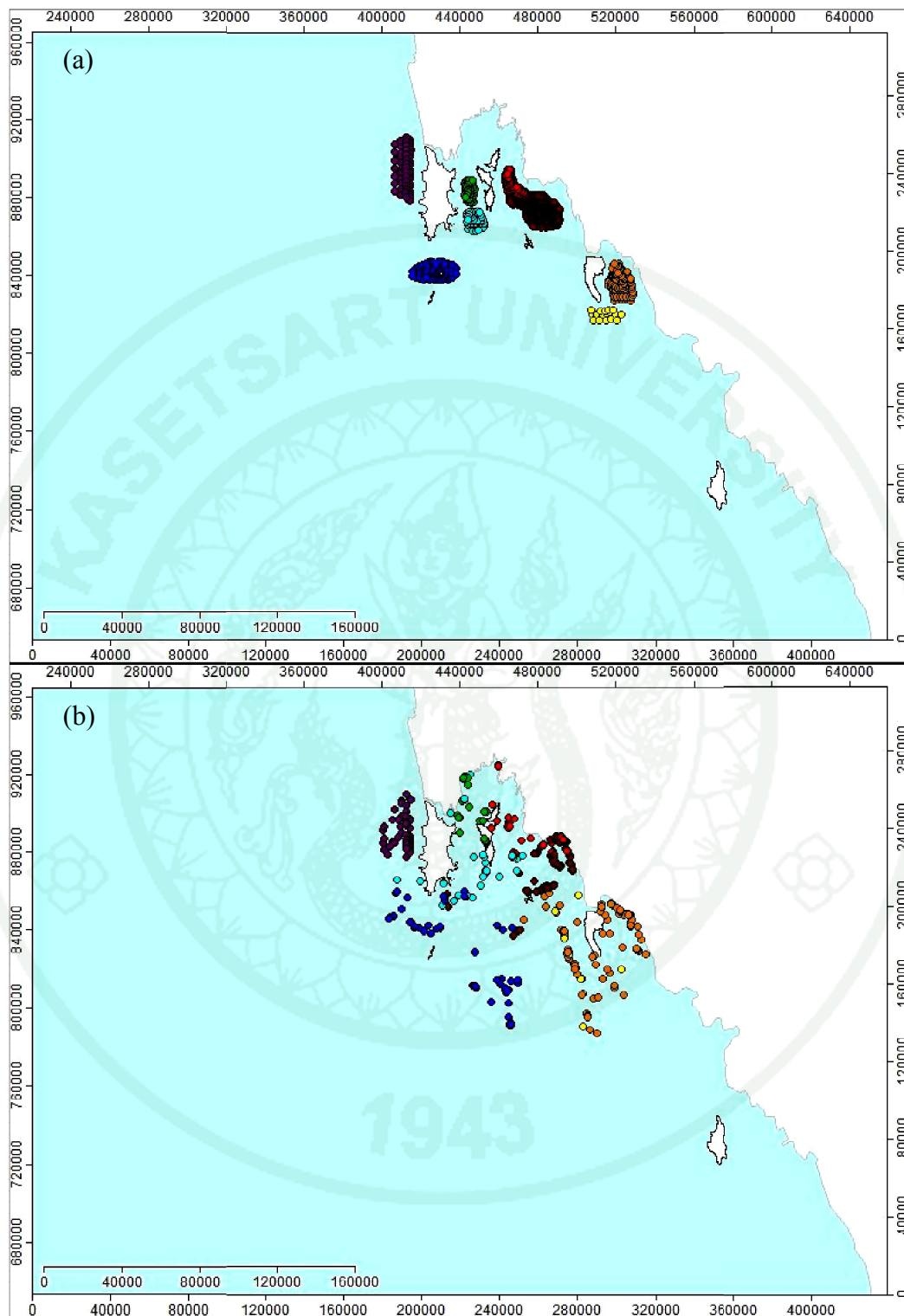


**Figure 76** Transportation of marine litters at offshore between (a) Day 1 and Day 90 under the condition of (b) tidal dominant, (c) Northeast monsoon and (d) Southwest monsoon

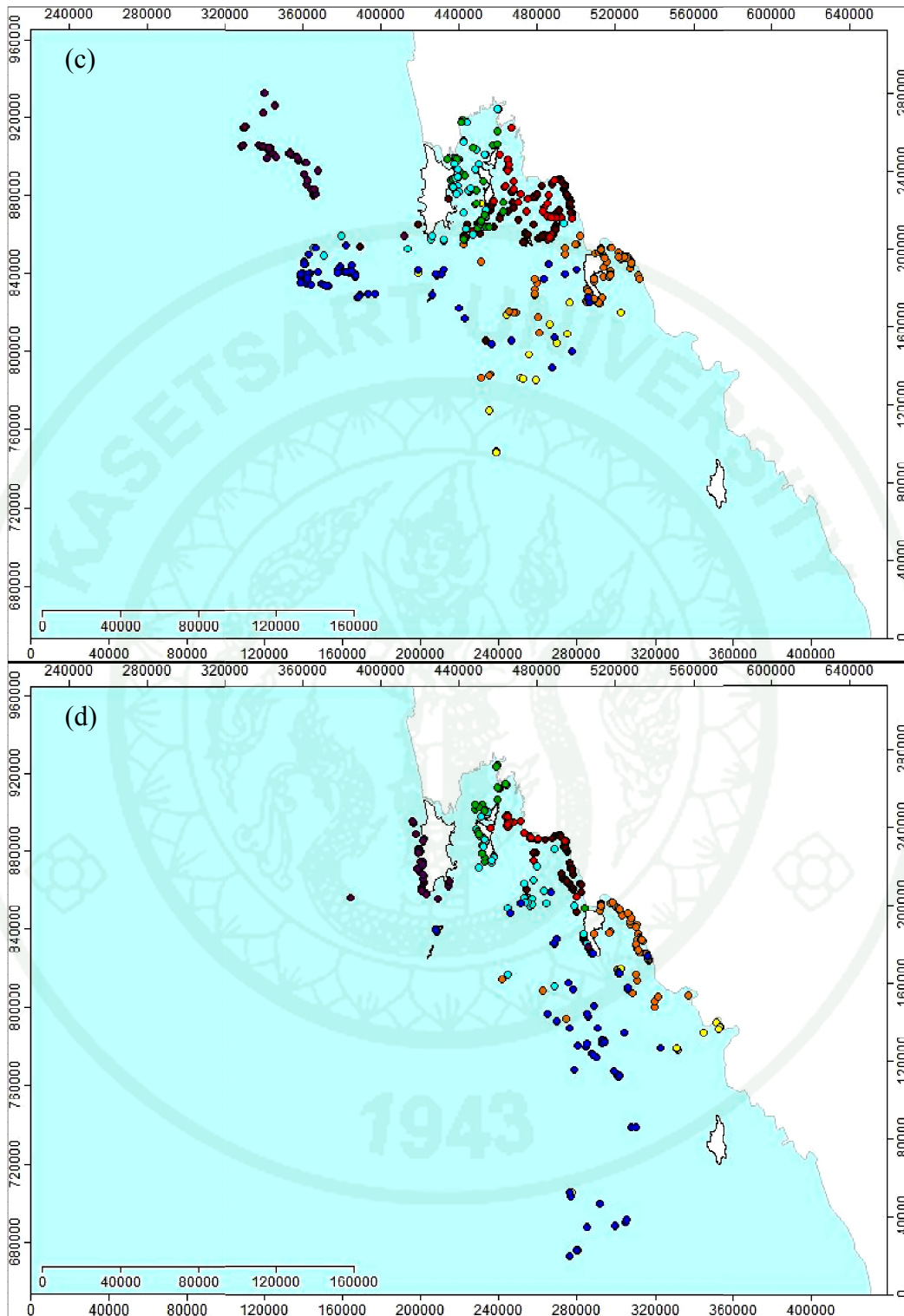


Figure 76 (Continued)

Displacement of marine particles originated offshore at three different scenarios was summarized in Table 21 and histogram of marine particle displacement was profiled in Figure 77. Particle displacement showed that most particles during Southwest monsoon were dispersed farther than those in Northeast monsoon and normal tidal condition.

**Table 21** Displacement profile of marine particles originated offshore

Scenario	Displacement (m)		
	Min	Mean	Max
Tidal dominated	50	17,560 ± 22,830	66,770
Northeast monsoon	50	29,470 ± 13,628	102,700
Southwest monsoon	50	40,890 ± 43,864	187,000

As shown in histogram of particle displacement, particles during tidal dominated condition and Northeast monsoon were relatively scattered up to 75 km. Particle displacement during Northeast monsoon dominantly occupied the range of 40- 75 km, whereas tidal condition chiefly covered up to 25 km of dispersion. Lastly, particle scattered during Southwest monsoon prominently covered large scale movement and long distance travel.

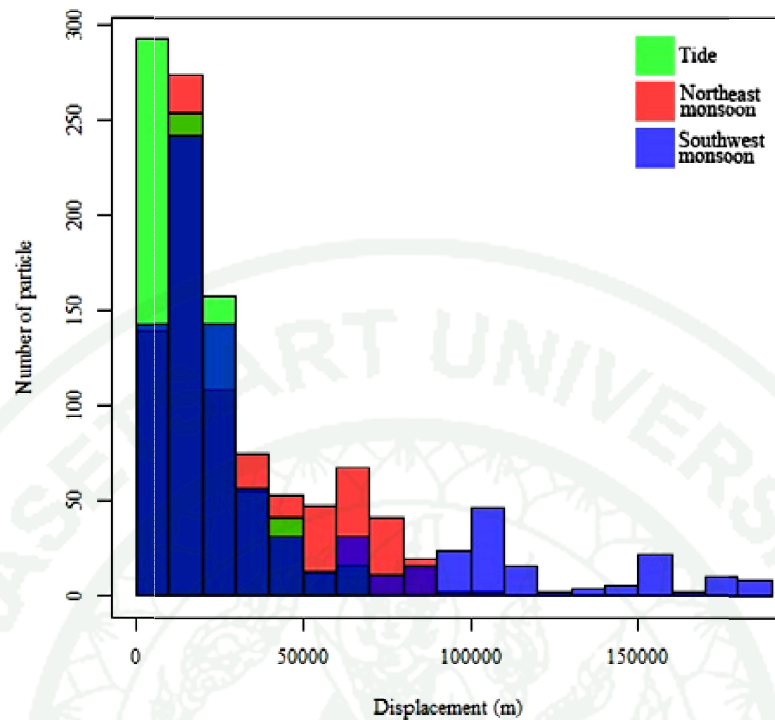


**Figure 77** Histogram of particle displacement (m) at Offshore of Phang-Nga bay at three case scenarios

Litters in offshore environment were randomly selected to represent the marine litter left floating or originated at offshore as shown in Figure 80. Path of the marine litters' transportation under tidal condition showed that marine litters at the west coast of Phuket were not moved much. Litters originated from the other areas in offshore moved in zigzag line due to tidal flow (Figure 78a). Moreover, the marine litter originated from offshore under the Northeast monsoon showed the long distance to the West direction for those originated from West Phuket, Racha Yai island and Lanta Yai island (Figure 78b). For Southwest monsoon, litters originated from all observed locations at offshore moved in the same direction which is southeast from the origins as shown in Figure 78c. Litters originated from west of Phuket and Yao islands arrived shoreline of Phuket and Yao islands within a few weeks.

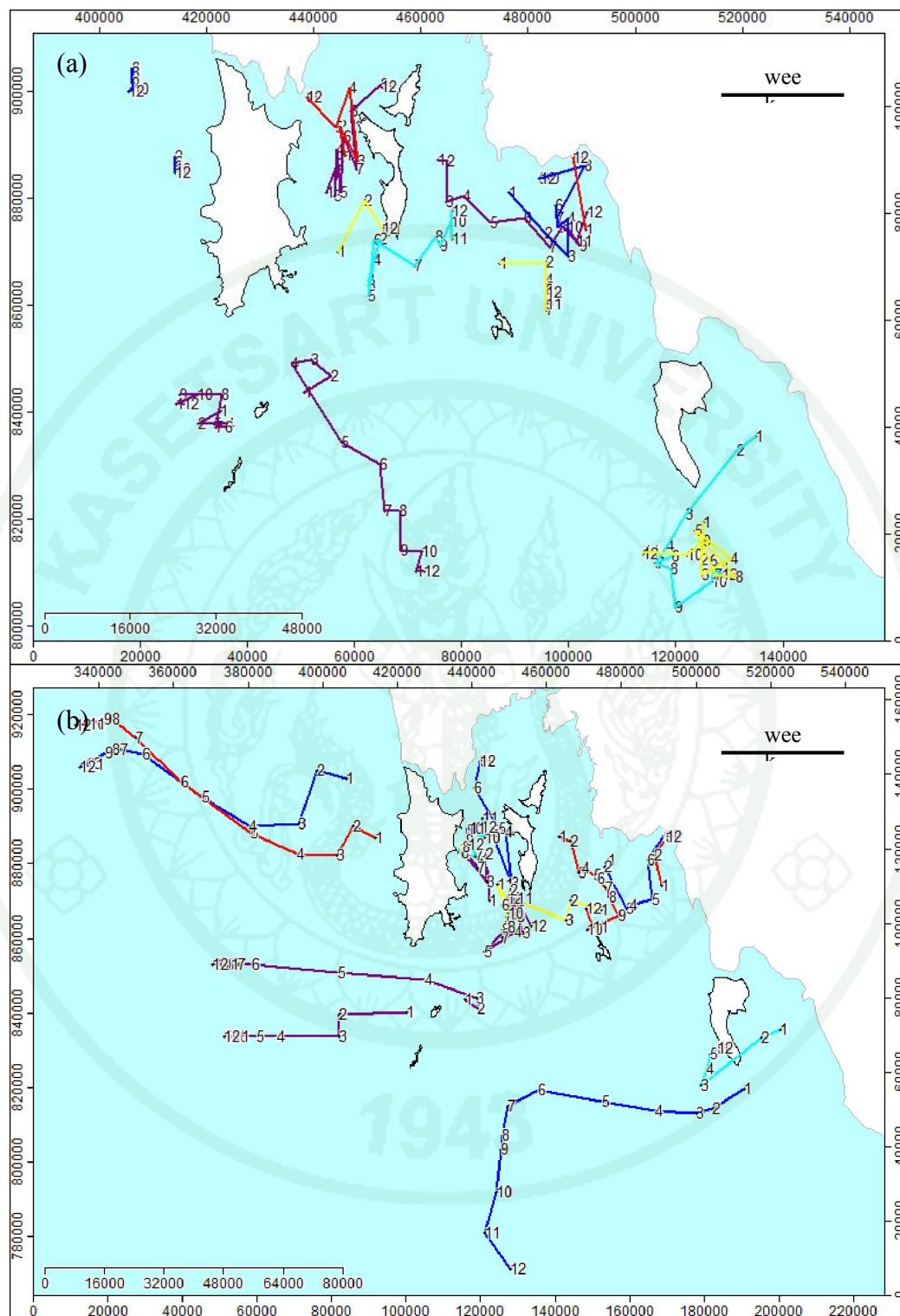


**Figure 78** Transportation path of marine litters originated from offshore of Phang-Nga bay under the condition of (a) tidal dominant, (b) Northeast monsoon and (c) Southwest monsoon

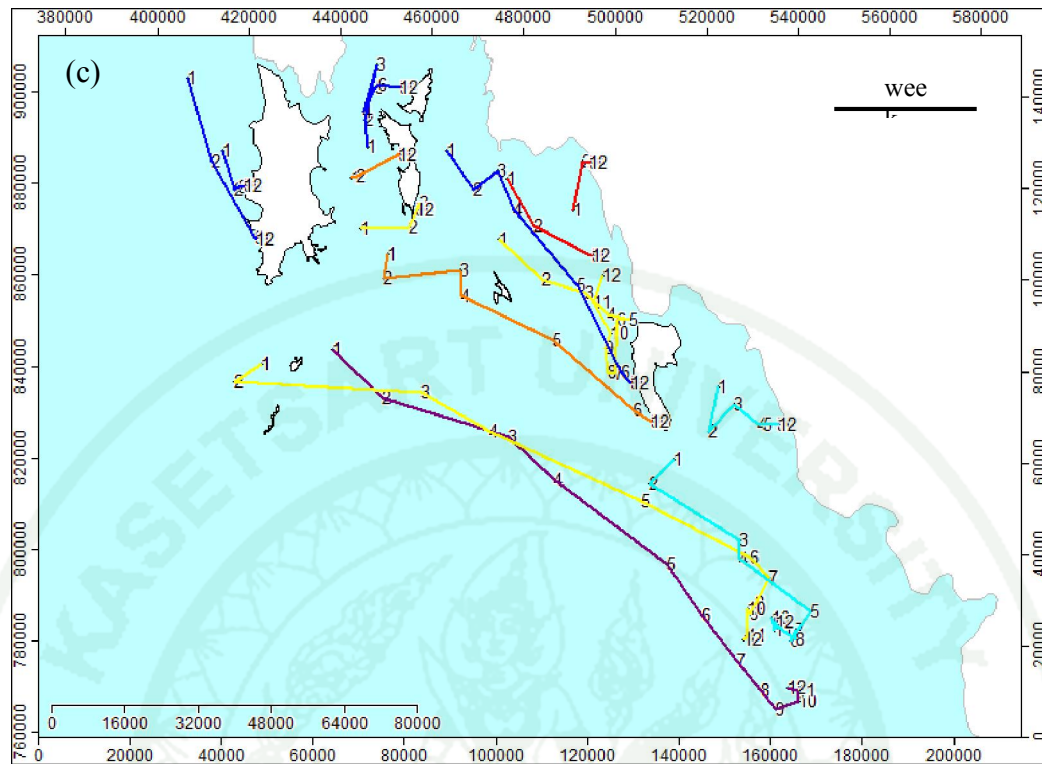


Figure 78 (Continued)

## CONCLUSION AND RECOMMENDATIONS

### Conclusion

As the study of oceanic circulation in order to trace marine particle movement on the sea surface of the Andaman Sea simulated by FVCOM, performance of the simulation is validated by using water elevation and velocity and direction of buoy test obtained from field trip, thus, the strategic results of this study are as followed:

#### 1. Floating buoy experiment

Buoy experiment at Patong, Phuket, had disclosed that the floating marine particles were moving with average velocity of 5-45 cm/s. In addition, velocity of buoys conducted at Yao Noi island was in the range of 5 - 65 cm/s as well as buoys at Panyee island. Meanwhile at Phi Phi Don island, floating marine particles moved approximately 25-50 cm/s. Buoy experiment at Saphan Hin showed that the particles floating on the sea surface travelled in velocity of 5 - 40 cm/s. Lastly, buoy experiment conducted at Kuraburi were seen travelling with velocity of 5-30 cm/s.

The total buoy experiment continuously conducted for up to 6 hours revealed that the direction of floating marine particles during experimenting hours was influenced by tidal current because they moved in the circle following the rotary current during the tide period. Therefore, the direction of particle movement during maximum 6 hours also based upon the location and tidal current in the areas. This was agreeable to the simulation displayed the movement of 6 hours floating marine particles as tidal dominated.

#### 2. Tidal validation

Tidal simulation by FVCOM revealed tidal range relative error of 4.8%, 5.24%, 2.02% and 5.34% at Ao por, Tapao Noi, Kuraburi and Tarutao, respectively. The tidal constitute dominated in these areas were M2, K1, S2 and N2 with less than

15% relative error to observation of tidal elevation. In addition, tidal harmonic analysis revealed that phase difference was less than  $12^\circ$  for most major tidal constituents which was lagged approximately 25 minutes. Histogram of water elevation error between calculation and simulation showed that in most cases water elevation error was in the range of 0-20 cm, for both overestimated and underestimated results. And all result of linear regression between observed and simulation water level showed that all stations held R-squared more than 0.93. Lastly, predictive skill of model performance was entirely more than 0.96. With all solid evidences evaluating model performance, simulation was agreeable to observation in prediction of water level.

### **3. Current pattern**

Current pattern was studied under three case scenarios which were tidal dominated condition, current in Southeast monsoon and current in Southwest monsoon. The results showed that 10-m winds under the monsoon strengthened the velocity of current solely driven by tide. Tidal dominated had current velocity of approximately 0-25 cm/s; however, current in Northeast monsoon and Southwest monsoon was 0-35 cm/s. Direction of residual current under three scenarios were also different; tide had random direction based upon location; oceanic current moved out of the Andaman Sea to the West during Northeast monsoon and; current entering the Andaman Sea from the West during Southwest monsoon.

### **4. Marine particle transportation**

It was overall summarized that marine litters originated onshore of places around Phang-Nga bays were able to travel farthest approximately 160 km within 90 days and those originated offshore were able to travel up to 187 km. During 90 day observation, floating marine litters from onshore or mainland could be driven to reach other islands or areas elsewhere and some remaining particles were left floating offshore too. Likewise, particles originated offshore were dispersed to reach mainland or onshore as well.

### **Recommendations**

1. The future study can be investigation of marine litters in other areas especially along the coast of the Andaman Sea where big cities are located such as Langkawi, Penang and Myeik.

2. Marine litter survey study and particle tracking method such as GPS and other tracking tools for long distance floating marine particles are recommended.

3. It was found that marine litters transport in different seasons varied especially where the origin and destination of the particles based upon current circulation. Therefore, waste management plan and policy should be done carefully especially to those vulnerable areas such tourist destinations and areas where living habitats for abundant economic fisheries and endangered species.

4. Model should also be improved and verified by observed current velocity for further study because marine litter transport is based upon the velocity of current. The more accurate velocity simulation would greatly assure the accuracy of litters' transportation.

## LITERATURE CITED

- Absornsuda, S. 1977. **The Physical Oceanography in The Andaman Sea During The Two Monsoon Seasons**. Marine Science Department, Chulalongkorn University.
- Anthony, C., E. Adler, J. Barbière, Y. Cohen, S. Evans, S. Jarayabhand, L. Jeftic, R. Jung, S. Kinsey, E.T. Kusui, I. Lavine, P. Manyara, L. Oosterbaan, M.A. Pereira, S. Sheavly, A. Tkalin, S. Varadarajan, B. Wenneker and G. Westphalen. 2009. **UNEP/IOC Guidelines on Survey and Monitoring of Marine Litter**. United Nations Environment Programme/Intergovernmental Oceanographic Commission.
- Catherine, C.F. and K. Sherman. 2010. **Trash Travels: From Our Hand to the Sea, Around the Global, and Through Time**. Available source: [http://act.oceanconservancy.org/images/2010ICCRReportRelease\\_pressPhotos/2010\\_ICC\\_Report.pdf](http://act.oceanconservancy.org/images/2010ICCRReportRelease_pressPhotos/2010_ICC_Report.pdf), April 10, 2014.
- Changsheng, C. 2013. **Lecture-1: FVCOM-An unstructured grid Finite-Volume Community Ocean Model**. Department of Fisheries Oceanography, School for Marine Science and Technology, University of Massachusetts- Dartmouth.
- Changsheng, C., H. Huang, R.C. Beardsley, Q. Xu, R. Limeburner, G.W. Cowles, Y. Sun, J. Qi and H. Lin. 2011 Tidal dynamics in the Gulf of Maine and New England Shelf: An application of FVCOM. **Journal of Geophysical Research**. 116.
- Changsheng, C., R.C. Beardsley and G. Cowles. 2006. An Unstructured Grid, Finite Volume Coastal Ocean Model Fvcom System. **Oceanography**. 19.

- Changsheng, C., R.C. Beardsley and G. Cowles. 2006. **An Unstructured Grid, Finite-Volume Coastal Ocean Model FVCOM User Manual (2 Ed)**. Department of Fisheries Oceanography, School for Marine Science and Technology, University of Massachusetts- Dartmouth.
- Chen, L., Z. Qijie, L. Mingguang, S. Jinyu and L. Wenbo. 2009. Litter dynamics and forest structure of the introduced *Sonneratia caseolaris* mangrove forest in Shenzhen, China. **Estuarine, Coastal and Shelf Science**. 85 (2): 241-246.
- Christian, L.P., M. Genco and F. Lyard. 1995. Modeling and Predicting Tides over the World Ocean. **Coastal and Estuarine Studies**. 47: 175-201.
- Courtney, A. **Plastic Marine Debris: An in-depth look**. Available source: [www.MarineDebris.noaa.gov](http://www.MarineDebris.noaa.gov), April 25, 2014.
- Department of Marine and Coastal Resource (DMCR). 2014. **Marine Litter Pick-up**. Available Source: <http://www.dmcg.go.th/Thailandcoastalcleanup/>, March 28, 2014.
- Dubravko, J. and L. Wang. 2009. **Application of Unstructured-Grid Finite Volume Coastal Ocean Model (FVCOM) to the Gulf of Mexico Hypoxic Zone**. Department of Oceanography and Coastal Sciences, Louisiana State University.
- Edyvane, K.S., A. Dalgetty, P.W. Hone, J.S. Higham and N.M. Wace. 2004. Long-term marine litter monitoring in the remote Great Australian Bight, South Australia. **Mar Pollut Bull**. 48 (11-12): 1060-1075.
- Elodie, M., K. Maamaatuaiahutapu and V. Taillandier. 2009. Floating marine litter surface drift: Convergence and accumulation toward the South Pacific subtropical gyre. **Marine Pollution Bulletin**. 58: 1347-1355.

- Fredrik, M. and C. Folke. 1999. ANALYSIS Ecological goods and services of coral reef ecosystems. **Ecological Economics** 29: 215-233.
- Greenfins. 2007. **Trash Sea**. Available Source: [http://www.greenfins-thailand.org/uploads/news/40/trash\\_sea.pdf](http://www.greenfins-thailand.org/uploads/news/40/trash_sea.pdf), Anugust 13, 2013.
- Guoqi, H., Z. Ma, B.D. Young, M. Foreman and N. Chen. 2011. Simulation of three-dimensional circulation and hydrography over the Grand Banks of Newfoundland. **Ocean Modelling**. 40: 199-210.
- Iván, A.H. and M. Thiel. 2009. Floating marine litter in fjords, gulfs and channels of southern Chile. **Marine Pollution Bulletin** 58: 341-350.
- James, P.T. 1990. **The Seasonal Circulation of the Upper Ocean in the bay of Bengal**. Ph.D. Thesis, The Florida State University.
- Janekovic, I. and K. Carl. 2005. Numerical simulation of the Adriatic Sea principal tidal constituents. **Annales Geophysicae**. 23: 3207-3218.
- Jose, G.B.D. 2002. The pollution of the marine environment by plastic litter: a review. **Marine Pollution Bulletin** 44: 842-852.
- Katie, R. 1992. **Tide on Trash: A Learning Guide on Marine Debris**. United States Environmental Protection Agency.
- Kazushiro, A. and A. Isobe. 2007. Application of Finite Volume Coastal Ocean Model to Hindcasting the Wind-Induced Sea-Level Variation in Fukuoka bay. **Journal of Oceanography**. 63: 333-339.
- Lebreton, L.C.M., S.D. Greer and J.C. Borrero. 2012. Numerical modelling of floating litter in the world's oceans. **Marine Pollution Bulletin**. 64: 653-661.

- Lianyuan, Z., C. Chen and F.Y. Zhang. 2004. Development of water quality model in the Satilla River Estuary, Georgia. **Ecological Modelling**. 178: 457-482.
- Martin, S.A. 2011. Trash Talking: Exploring Marine Debris on the Andaman Coast, Thailand. **Thailand Surfrider**. 6: 48 - 50.
- Maximenko, N. 2011. **Where Will the Debris from Japan's Tsunami Drift in the Ocean**. The International Pacific Research Center.
- Michelle, A., A. Walters, D. Santillo and P. Johnstin. **Plastic Debris in the World's Oceans**. Greenpeace.
- Pablo, D., R. Bastida, M. Dassis, G. Giardino, M. Gerpe and D. Rodríguez. 2011. Plastic ingestion in Franciscana dolphins, *Pontoporia blainvillei* (Gervais and d'Orbigny, 1844), from Argentina. **Marine Pollution Bulletin**.
- Pawlowicz, R., B. Beardsley and S. Lentz. 2002. Classical tidal harmonic analysis including error estimates in MATLAB using T\_TIDE. **Computers and Geosciences**. 28: 929-937.
- Pawlowicz, R., B. Beardsley and S. Lentz. Classical tidal harmonic analysis including error estimates in MATLAB using T\_TIDE. **Computers and Geosciences**. 28: 929-937.
- Pramote, S., B. Kjerfve and S. Khokiattiwong. 1994. Numerical Model of Tidal Circulation in Phangnha bay, Thailand. **Phuket mar . biol. Cent. Res. Bull.** 59: 65-81.
- Praween, L. **Oceanographic Features with Biological Indication in the Andaman Sea, Thailand**. Phuket Marine Biological Center.

Robert, H.W., R. He and L. Zheng. 2004. **Model the West Florida Shelf Circulation with POM, ROMS and FVCOM: Inter-Comparisons Gauged Against in-situ Data**. HYCOM Workshop.

Somkiat, K. 2010. **General Oceanographic Status of Andaman Sea On SEAFDEC**. Phuket Marine Biological Center.

Somkiat, K., P. Limpsaichol and S. Petpiroon. 1991. Oceanographic Variation in Phangnga bay, Thailand under monsoonal effects. **Phuket mar . biol. Cent. Res. Bull.** 55: 43-76.

Stevenson, C. 2011. **Plastic Debris in the California Marine Ecosystem: A Summary of Current Research, Solution Efforts and Data Gaps**. University of Southern California Sea Grant.

Syamsul, R., I. Setiawan, T. Iskandar and Y. Ilhamsyah. 2010. Currents Simulation in the Malacca Straits by Using Three-Dimensional Numerical Model. **Sians Malaysiaa.** 39 (4): 519-524.

Syamsul, R., P. Damm, M.A. Wahid, J. Sundermann, Y. Ilhamsyah and T.I. Muhammad. 2012. General Circulation in the Malacca Strait and Andaman Sea: A Numerical Model Study. **Americal Journal of Environmental Science.** 8 (5): 479-488.

The United States Environmental Protection Agency (EPA). 2002. **Assessing And Monitoring Floatable Debris**. United States Environmental Protection Agency.

Tom, P. 2010. **The Social & Economic Effect of Marine Litter**. Available Source: [http://www.dorsetforyou.com/media/pdf/q/i/The\\_Social\\_\\_Economic\\_Effect\\_of\\_Marine\\_Litter\\_-\\_Kimo\\_UK\\_-\\_Tom\\_Piper.pdf](http://www.dorsetforyou.com/media/pdf/q/i/The_Social__Economic_Effect_of_Marine_Litter_-_Kimo_UK_-_Tom_Piper.pdf), April 15, 2014.

Topçu, E. N., A.M. Tonay, A. Dede, A.A. Öztürk and B. Öztürk. 2013. Origin and abundance of marine litter along sandy beaches of the Turkish Western Black Sea Coast. **Marine Environmental Research**. 85: 21-28.

United Nation of Environmental Program (UNEP). 2005. **Marine Litter: An analytical overview**. United Nation of Environmental Program.

United Nation of Environmental Program, UNEP. 2009. **Marine Litter: A global Challenge**. United Nation of Environmental Program.

Wang, J. and Y. Shen. 2010. Modeling oil spills transportation in seas based on unstructured grid, finite-volume, wave-ocean model. **Ocean Modelling**. 35 (4): 332-344.

Wilmott, C. 1981. On the validation of models. **Physical Geography**. 2: 184-194.

World Society for the Protection of Animals (WSPA). 2012. **Untangled Marine litter: a global picture of the impact on animal welfare and of animal-focused solutions**. World Society for the Protection of Animals, Butterworth.

World Wildlife Fund (WWF). **Andaman Sea ecoregion**. WWF International Corals

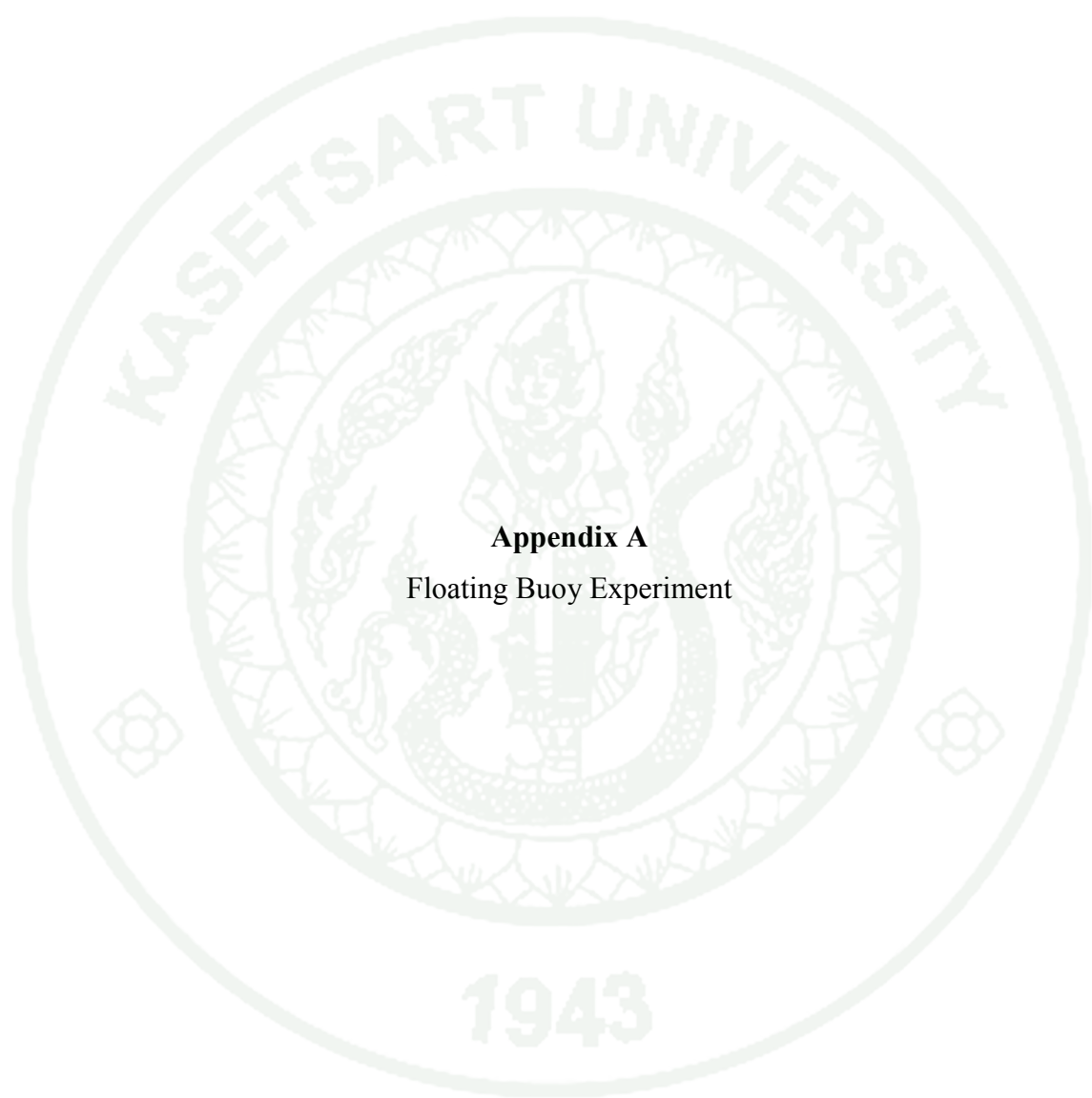
Wyrski, K. 1973. Physical Oceanography of the Indian Ocean. **The biology of the Indian Ocean**. (2): 18-37.

Xing, Y., A. Congfang and J. Sheng. 2013. A three-dimensional hydrodynamic and salinity transport model of estuarine circulation with an application to a macrotidal estuary. **Applied Ocean Research**. 39: 53-71.

Zheng, L. and W.H. Robert. Rookery bay and Naples bay circulation simulations: Applications to tides and fresh water inflow regulation. **Ecological Modelling**. 221 (7): 986-996.



**APPENDICES**



**Appendix A**  
Floating Buoy Experiment



**Appendix Figure A1** Buoy was left freely floating on sea surface



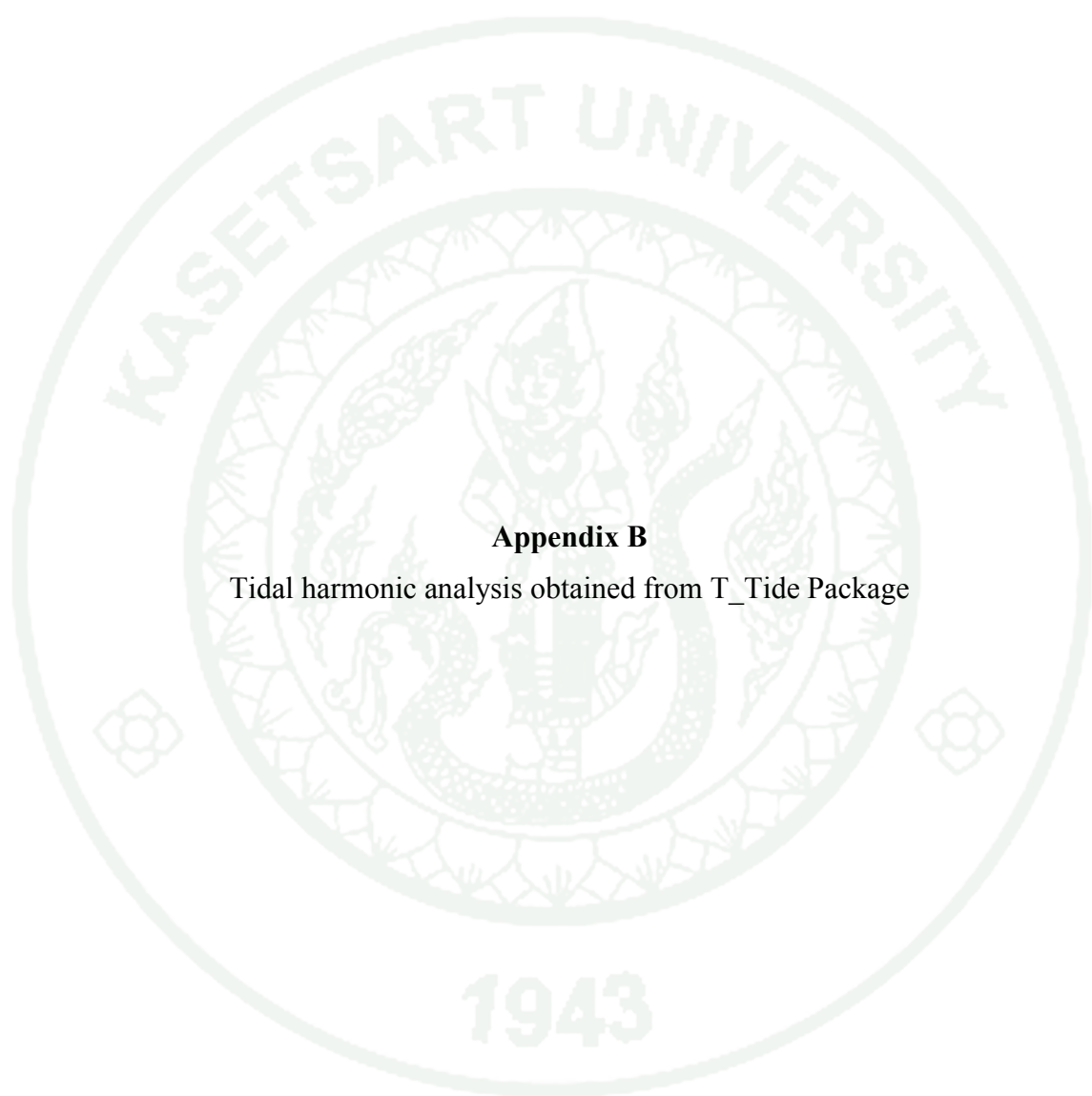
**Appendix Figure A2** Buoy was driven and stuck at the fishing gears in coastal zone



**Appendix Figure A3** Buoy reached the muddy land during low tide



**Appendix Figure A4** Buoys were stuck on rocky cave during current driven



**Appendix B**

Tidal harmonic analysis obtained from T\_Tide Package

**Observation at Ao Por**

nobs = 985, ngood = 985, record length (days) = 41.04

var(x)= 0.64427 var(xp)= 0.64024 var(xres)= 0.0041074

percent var predicted/var original= 99.4 %

**Appendix Table B1** Tidal amplitude and phase with 95% CI estimates of observation data at Ao Por station

Tide	Frequency	Amplitude	Amplitude error	Phase	Phase error	snr
*MM	0.0015122	0.0322	0.019	209.68	33.57	3
*MSF	0.0028219	0.0436	0.019	248.45	23.38	5
ALP1	0.0343966	0.0033	0.004	89.53	91.33	0.7
2Q1	0.0357064	0.0039	0.004	270.12	78.13	0.82
*Q1	0.0372185	0.0069	0.005	236.36	37.15	2
*O1	0.0387307	0.0453	0.004	25.71	5.85	1.1e+02
NO1	0.0402686	0.0044	0.005	292.09	59.91	0.88
*K1	0.0417807	0.1361	0.004	298.44	2.00	1e+03
*J1	0.0432929	0.0127	0.004	38.96	22.97	8.6
*OO1	0.0448308	0.0123	0.004	13.72	21.99	8.1
*UPS1	0.046343	0.0055	0.005	136.85	39.46	1.3
*EPS2	0.0761773	0.0192	0.018	258.30	58.43	1.1
*MU2	0.0776895	0.0616	0.022	31.92	19.11	7.8
*N2	0.0789992	0.1685	0.020	204.29	6.98	73
*M2	0.0805114	0.9324	0.019	333.59	1.29	2.3e+03
*L2	0.0820236	0.0498	0.020	289.08	23.06	6.2
*S2	0.0833333	0.5111	0.020	2.76	2.27	6.4e+02
*ETA2	0.0850736	0.0196	0.018	235.00	54.15	1.2
*MO3	0.1192421	0.0122	0.004	23.91	24.85	9.4
M3	0.1207671	0.0039	0.004	135.95	71.79	0.94

Appendix Table B1 (Continued)

<b>Tide</b>	<b>Frequency</b>	<b>Amplitude</b>	<b>Amplitude error</b>	<b>Phase</b>	<b>Phase error</b>	<b>snr</b>
*MK3	0.1222921	0.0353	0.005	355.26	7.42	49
*SK3	0.1251141	0.0187	0.004	25.97	14.39	18
MN4	0.1595106	0.0084	0.012	10.11	96.11	0.52
*M4	0.1610228	0.0262	0.012	124.48	28.93	4.5
SN4	0.1623326	0.0099	0.011	51.69	80.45	0.74
*MS4	0.1638447	0.0347	0.014	145.17	22.19	6.6
S4	0.1666667	0.0083	0.012	253.68	100.74	0.51
*2MK5	0.2028035	0.0049	0.004	153.76	60.46	1.5
*2SK5	0.2084474	0.0052	0.005	145.68	52.54	1.2
2MN6	0.2400221	0.0017	0.002	100.13	74.34	0.72
*M6	0.2415342	0.0036	0.002	211.99	39.05	2.5
*2MS6	0.2443561	0.0054	0.002	241.41	23.25	6
*2SM6	0.2471781	0.0034	0.002	265.92	38.15	1.9
*3MK7	0.2833149	0.0015	0.001	53.00	47.62	1.3
M8	0.3220456	0.0012	0.001	191.16	85.51	0.67

**Simulation at Ao Por**

nobs = 657, ngood = 657, record length (days) = 41.06

var(x)= 0.76365 var(xp)= 0.76173 var(xres)= 0.0022868

percent var predicted/var original= 99.7 %

**Appendix Table B2** Tidal amplitude and phase with 95% CI estimates of simulation data at Ao Por

Tide	Frequency	Amplitude	Amplitude error	Phase	Phase error	snr
*MM	0.0015122	0.0131	0.003	123.47	17.07	17
*MSF	0.0028219	0.0221	0.004	58.49	10.46	29
ALP1	0.0343966	0.0015	0.004	319.49	186.74	0.15
2Q1	0.0357064	0.0028	0.004	106.06	118.72	0.48
*Q1	0.0372185	0.0186	0.005	171.36	18.22	12
*O1	0.0387307	0.0974	0.006	315.40	3.60	2.4e+02
NO1	0.0402686	0.0052	0.005	290.34	69.06	0.91
*K1	0.0417807	0.1675	0.005	235.77	2.09	9.3e+02
*J1	0.0432929	0.0028	0.005	215.73	113.47	0.36
*OO1	0.0448308	0.0084	0.006	100.42	40.51	2.3
*UPS1	0.046343	0.0015	0.004	110.70	187.89	0.11
*EPS2	0.0761773	0.0082	0.017	293.57	110.68	0.24
*MU2	0.0776895	0.0303	0.019	64.68	39.88	2.5
*N2	0.0789992	0.2061	0.020	214.80	5.58	1e+02
*M2	0.0805114	1.0320	0.021	332.97	1.05	2.4e+03
*L2	0.0820236	0.0104	0.016	257.90	114.94	0.45
*S2	0.0833333	0.5160	0.019	358.59	2.25	7.4e+02
*ETA2	0.0850736	0.0207	0.017	253.48	53.44	1.4
*MO3	0.1192421	0.0097	0.008	112.20	55.80	1.5
M3	0.1207671	0.0066	0.007	213.74	71.90	0.82

Appendix Table B2 (Continued)

<b>Tide</b>	<b>Frequency</b>	<b>Amplitude</b>	<b>Amplitude error</b>	<b>Phase</b>	<b>Phase error</b>	<b>snr</b>
*MK3	0.1222921	0.0158	0.008	254.33	31.84	4.2
*SK3	0.1251141	0.0028	0.007	180.43	140.01	0.15
MN4	0.1595106	0.0148	0.003	342.92	9.96	30
*M4	0.1610228	0.0096	0.003	124.49	15.21	13
SN4	0.1623326	0.0065	0.003	13.24	26.20	6.5
*MS4	0.1638447	0.0331	0.003	132.30	4.00	1.3e+02
S4	0.1666667	0.0100	0.003	161.34	16.74	12
*2MK5	0.2028035	0.0032	0.004	358.62	68.32	0.83
*2SK5	0.2084474	0.0009	0.002	179.54	176.09	0.12
2MN6	0.2400221	0.0012	0.002	124.95	133.59	0.25
*M6	0.2415342	0.0025	0.003	108.90	82.15	0.75
*2MS6	0.2443561	0.0047	0.003	211.01	40.74	2
*2SM6	0.2471781	0.0021	0.003	291.32	90.13	0.55
*3MK7	0.2833149	0.0039	0.003	108.89	42.23	1.6
M8	0.3220456	0.0042	0.004	205.43	59.13	1

1943

**Observation Kuraburi**

nobs = 985, ngood = 985, record length (days) = 41.04

var(x)= 0.64742 var(xp)= 0.64481 var(xres)= 0.0026649

percent var predicted/var original= 99.6 %

**Appendix Table B3** Tidal amplitude and phase with 95% CI estimates of observation data at Kuraburi station

Tide	Frequency	Amplitude	Amplitude error	Phase	Phase error	snr
*MM	0.0015122	0.0272	0.006	147.01	11.13	22
*MSF	0.0028219	0.0407	0.006	66.41	7.95	50
ALP1	0.0343966	0.0015	0.004	356.43	161.32	0.16
2Q1	0.0357064	0.0006	0.004	173.55	206.61	0.025
*Q1	0.0372185	0.0035	0.004	172.22	81.25	0.73
*O1	0.0387307	0.0511	0.005	17.38	5.46	1.2e+02
NO1	0.0402686	0.0034	0.005	218.39	75.88	0.58
*K1	0.0417807	0.1345	0.005	298.67	2.05	8.2e+02
*J1	0.0432929	0.0081	0.004	58.96	33.02	3.3
*OO1	0.0448308	0.0061	0.005	26.78	46.74	1.6
*UPS1	0.046343	0.0009	0.003	314.98	185.48	0.085
*EPS2	0.0761773	0.0146	0.021	199.15	100.70	0.47
*MU2	0.0776895	0.0654	0.025	53.98	22.27	6.8
*N2	0.0789992	0.1662	0.027	195.67	9.30	37
*M2	0.0805114	0.9344	0.026	327.85	1.34	1.3e+03
*L2	0.0820236	0.0574	0.024	253.29	28.52	5.6
*S2	0.0833333	0.5070	0.025	356.89	2.63	4.2e+02
*ETA2	0.0850736	0.0267	0.026	267.01	60.47	1
*MO3	0.1192421	0.0112	0.004	94.23	23.66	6.8
M3	0.1207671	0.0011	0.003	54.18	168.81	0.14

Appendix Table B3 (Continued)

<b>Tide</b>	<b>Frequency</b>	<b>Amplitude</b>	<b>Amplitude error</b>	<b>Phase</b>	<b>Phase error</b>	<b>snr</b>
*MK3	0.1222921	0.0117	0.004	17.68	18.66	7.3
*SK3	0.1251141	0.0074	0.004	8.86	30.01	2.8
MN4	0.1595106	0.0074	0.009	274.37	72.16	0.71
*M4	0.1610228	0.0247	0.009	4.53	22.90	7.4
SN4	0.1623326	0.0071	0.010	266.31	76.91	0.49
*MS4	0.1638447	0.0367	0.010	53.84	16.10	14
S4	0.1666667	0.0104	0.010	153.44	57.76	1.1
*2MK5	0.2028035	0.0014	0.003	326.20	127.14	0.25
*2SK5	0.2084474	0.0027	0.003	152.82	67.24	0.8
2MN6	0.2400221	0.0039	0.004	133.71	70.60	0.98
*M6	0.2415342	0.0070	0.004	295.74	35.31	2.9
*2MS6	0.2443561	0.0154	0.004	318.34	17.64	13
*2SM6	0.2471781	0.0142	0.005	230.31	19.16	9.8
*3MK7	0.2833149	0.0008	0.002	178.88	173.32	0.11
M8	0.3220456	0.0025	0.003	310.27	110.50	0.51

1943

**Simulation Kuraburi**

nobs = 657, ngood = 657, record length (days) = 41.06

var(x)= 0.52552 var(xp)= 0.51731 var(xres)= 0.0070942

percent var predicted/var original= 98.4 %

**Appendix Table B4** Tidal amplitude and phase with 95% CI estimates of simulation data at Kuraburi station

Tide	Frequency	Amplitude	Amplitude error	Phase	Phase error	snr
*MM	0.0015122	0.0069	0.005	115.38	42.75	1.9
*MSF	0.0028219	0.0201	0.005	43.07	14.30	15
ALP1	0.0343966	0.0019	0.004	298.93	140.38	0.18
2Q1	0.0357064	0.0025	0.004	97.52	125.51	0.31
*Q1	0.0372185	0.0186	0.006	155.53	17.27	8.7
*O1	0.0387307	0.0856	0.005	304.43	3.80	2.9e+02
NO1	0.0402686	0.0033	0.005	238.10	101.76	0.52
*K1	0.0417807	0.1431	0.005	224.42	2.44	7.3e+02
*J1	0.0432929	0.0016	0.004	1.66	166.01	0.18
*OO1	0.0448308	0.0058	0.006	107.83	54.93	0.96
*UPS1	0.046343	0.0026	0.004	95.34	127.08	0.34
*EPS2	0.0761773	0.0059	0.011	240.82	119.10	0.28
*MU2	0.0776895	0.0114	0.013	48.76	63.54	0.72
*N2	0.0789992	0.1757	0.016	197.02	5.09	1.2e+02
*M2	0.0805114	0.8600	0.014	316.79	1.11	3.5e+03
*L2	0.0820236	0.0073	0.012	213.31	117.45	0.37
*S2	0.0833333	0.4007	0.013	337.14	2.21	9.3e+02
*ETA2	0.0850736	0.0087	0.012	218.47	91.04	0.53
*MO3	0.1192421	0.0105	0.007	85.20	36.53	2.1
M3	0.1207671	0.0018	0.004	256.95	181.31	0.19

Appendix Table B4 (Continued)

<b>Tide</b>	<b>Frequency</b>	<b>Amplitude</b>	<b>Amplitude error</b>	<b>Phase</b>	<b>Phase error</b>	<b>snr</b>
*MK3	0.1222921	0.0004	0.005	168.14	254.04	0.0078
*SK3	0.1251141	0.0007	0.005	177.49	243.55	0.025
MN4	0.1595106	0.0048	0.004	329.68	52.95	1.5
*M4	0.1610228	0.0167	0.004	115.87	12.51	17
SN4	0.1623326	0.0019	0.003	356.54	121.96	0.31
*MS4	0.1638447	0.0086	0.004	113.52	28.09	4.2
S4	0.1666667	0.0031	0.003	315.72	81.24	0.83
*2MK5	0.2028035	0.0045	0.004	242.18	71.84	1.1
*2SK5	0.2084474	0.0016	0.003	27.83	154.42	0.26
2MN6	0.2400221	0.0030	0.017	169.62	242.88	0.032
*M6	0.2415342	0.0050	0.019	345.45	189.49	0.066
*2MS6	0.2443561	0.0107	0.023	65.08	125.42	0.21
*2SM6	0.2471781	0.0095	0.020	281.47	129.55	0.23
*3MK7	0.2833149	0.0039	0.004	357.07	60.95	1.2
M8	0.3220456	0.0010	0.006	353.67	211.57	0.031

**Observation Tapao Noi**

nobs = 985, ngood = 985, record length (days) = 41.04

var(x)= 0.48012 var(xp)= 0.47717 var(xres)= 0.0023973

percent var predicted/var original= 99.4 %

**Appendix Table B5** Tidal amplitude and phase with 95% CI estimates of observation data at Tapao Noi Station

Tide	Frequency	Amplitude	Amplitude error	Phase	Phase error	snr
*MM	0.0015122	0.0115	0.006	82.99	32.26	3.8
*MSF	0.0028219	0.0063	0.006	177.59	58.28	1.2
ALP1	0.0343966	0.0015	0.004	123.56	167.03	0.18
2Q1	0.0357064	0.0018	0.004	265.95	123.62	0.19
*Q1	0.0372185	0.0040	0.005	196.11	74.75	0.59
*O1	0.0387307	0.0492	0.005	4.48	6.11	1.1e+02
NO1	0.0402686	0.0043	0.005	127.59	72.62	0.68
*K1	0.0417807	0.1360	0.005	298.87	2.20	7.3e+02
*J1	0.0432929	0.0094	0.005	71.06	31.25	3.7
*OO1	0.0448308	0.0058	0.005	2.62	59.15	1.3
*UPS1	0.046343	0.0003	0.004	142.55	255.39	0.0091
*EPS2	0.0761773	0.0114	0.016	268.92	82.59	0.52
*MU2	0.0776895	0.0398	0.015	38.28	23.18	7.3
*N2	0.0789992	0.1478	0.017	197.84	6.02	77
*M2	0.0805114	0.8051	0.016	329.85	1.22	2.5e+03
*L2	0.0820236	0.0327	0.017	257.58	25.67	3.8
*S2	0.0833333	0.4301	0.017	358.56	2.04	6.7e+02
*ETA2	0.0850736	0.0206	0.015	249.45	41.82	1.9
*MO3	0.1192421	0.0059	0.005	12.05	56.05	1.4

Appendix Table B5 (Continued)

<b>Tide</b>	<b>Frequency</b>	<b>Amplitude</b>	<b>Amplitude error</b>	<b>Phase</b>	<b>Phase error</b>	<b>snr</b>
M3	0.1207671	0.0033	0.005	69.49	87.67	0.52
*MK3	0.1222921	0.0094	0.005	358.24	32.72	3.5
*SK3	0.1251141	0.0136	0.006	338.17	23.35	5
MN4	0.1595106	0.0024	0.004	18.55	128.20	0.4
*M4	0.1610228	0.0130	0.005	104.77	19.71	8.2
SN4	0.1623326	0.0031	0.005	352.23	90.39	0.42
*MS4	0.1638447	0.0091	0.005	153.28	29.28	3.9
S4	0.1666667	0.0008	0.003	310.41	197.65	0.07
*2MK5	0.2028035	0.0019	0.002	246.55	74.97	0.83
*2SK5	0.2084474	0.0026	0.003	216.35	69.07	0.92
2MN6	0.2400221	0.0019	0.003	67.14	110.23	0.41
*M6	0.2415342	0.0029	0.003	260.17	61.13	0.83
*2MS6	0.2443561	0.0022	0.003	204.25	89.01	0.63
*2SM6	0.2471781	0.0014	0.003	323.41	124.86	0.26
*3MK7	0.2833149	0.0004	0.003	276.80	247.42	0.016
M8	0.3220456	0.0008	0.003	68.01	172.73	0.083

1943

**Simulation Tapao Noi**

nobs = 657, ngood = 657, record length (days) = 41.06

rayleigh criterion = 1.0

var(x)= 0.60173 var(xp)= 0.59967 var(xres)= 0.0016844

percent var predicted/var original= 99.7 %

**Appendix Table B6** Tidal amplitude and phase with 95% CI estimates of simulation data at Tapao Noi Station

Tide	Frequency	Amplitude	Amplitude error	Phase	Phase error	snr
*MM	0.0015122	0.0055	0.003	132.89	34.19	2.8
*MSF	0.0028219	0.0087	0.003	97.81	23.15	6.3
ALP1	0.0343966	0.0008	0.004	277.53	217.07	0.043
2Q1	0.0357064	0.0019	0.005	119.65	173.06	0.18
*Q1	0.0372185	0.0192	0.006	164.76	18.61	10
*O1	0.0387307	0.0953	0.006	312.17	3.33	2.6e+02
NO1	0.0402686	0.0040	0.006	293.86	98.80	0.49
*K1	0.0417807	0.1631	0.006	233.26	2.07	7.7e+02
*J1	0.0432929	0.0019	0.004	237.57	169.13	0.2
*OO1	0.0448308	0.0081	0.006	111.07	38.72	1.7
*UPS1	0.046343	0.0012	0.004	105.83	177.94	0.083
*EPS2	0.0761773	0.0052	0.012	274.78	145.51	0.19
*MU2	0.0776895	0.0185	0.017	54.54	58.43	1.2
*N2	0.0789992	0.1855	0.018	209.05	5.32	1.1e+02
*M2	0.0805114	0.9126	0.018	327.86	1.07	2.7e+03
*L2	0.0820236	0.0079	0.013	246.38	109.00	0.39
*S2	0.0833333	0.4583	0.018	352.71	2.03	6.4e+02
*ETA2	0.0850736	0.0150	0.016	245.50	69.69	0.93
*MO3	0.1192421	0.0097	0.007	106.65	43.03	2.1

Appendix Table B6 (Continued)

<b>Tide</b>	<b>Frequency</b>	<b>Amplitude</b>	<b>Amplitude error</b>	<b>Phase</b>	<b>Phase error</b>	<b>snr</b>
M3	0.1207671	0.0051	0.006	204.37	81.26	0.76
*MK3	0.1222921	0.0096	0.006	238.95	41.17	2.2
*SK3	0.1251141	0.0027	0.005	165.40	103.61	0.29
MN4	0.1595106	0.0077	0.001	339.48	7.04	76
*M4	0.1610228	0.0103	0.001	174.02	5.04	1.5e+02
SN4	0.1623326	0.0028	0.001	17.34	19.48	9.1
*MS4	0.1638447	0.0176	0.001	148.35	2.70	3e+02
S4	0.1666667	0.0032	0.001	162.06	16.24	13
*2MK5	0.2028035	0.0005	0.001	9.34	135.22	0.22
*2SK5	0.2084474	0.0004	0.001	155.80	127.90	0.18
2MN6	0.2400221	0.0011	0.002	118.17	122.69	0.36
*M6	0.2415342	0.0008	0.002	218.60	134.70	0.14
*2MS6	0.2443561	0.0018	0.002	276.86	75.47	0.61
*2SM6	0.2471781	0.0028	0.002	334.86	52.76	1.4
*3MK7	0.2833149	0.0020	0.001	120.34	35.87	2.3
M8	0.3220456	0.0017	0.002	219.36	81.99	0.61

1943

**Observation Tarutao**

nobs = 985, ngood = 985, record length (days) = 41.04

rayleigh criterion = 1.0

var(x)= 0.5027 var(xp)= 0.50041 var(xres)= 0.0022893

percent var predicted/var original= 99.5 %

**Appendix Table B7** Tidal amplitude and phase with 95% CI estimates of observation data at Tarutao Station

Tide	Frequency	Amplitude	Amplitude error	Phase	Phase error	snr
*MM	0.0015122	0.0269	0.009	105.58	18.30	9.3
*MSF	0.0028219	0.0197	0.008	340.43	21.44	6.8
ALP1	0.0343966	0.0022	0.004	10.27	148.50	0.27
2Q1	0.0357064	0.0049	0.005	6.66	59.09	0.97
*Q1	0.0372185	0.0073	0.005	205.12	43.31	1.8
*O1	0.0387307	0.0580	0.006	2.28	5.10	93
NO1	0.0402686	0.0073	0.005	135.92	42.80	2.1
*K1	0.0417807	0.1617	0.005	302.70	2.02	1e+03
*J1	0.0432929	0.0079	0.006	79.60	36.77	2.1
*OO1	0.0448308	0.0088	0.005	29.74	33.43	3.1
*UPS1	0.046343	0.0005	0.004	286.85	226.11	0.019
*EPS2	0.0761773	0.0218	0.019	277.49	48.25	1.3
*MU2	0.0776895	0.0603	0.019	50.22	20.10	10
*N2	0.0789992	0.1387	0.020	214.93	8.27	46
*M2	0.0805114	0.8192	0.019	341.55	1.56	1.8e+03
*L2	0.0820236	0.0454	0.021	292.93	28.68	4.9
*S2	0.0833333	0.4538	0.022	12.69	2.81	4.2e+02
*ETA2	0.0850736	0.0286	0.021	270.21	44.45	1.8
*MO3	0.1192421	0.0008	0.002	238.19	188.54	0.1

Appendix Table B7 (Continued)

<b>Tide</b>	<b>Frequency</b>	<b>Amplitude</b>	<b>Amplitude error</b>	<b>Phase</b>	<b>Phase error</b>	<b>snr</b>
M3	0.1207671	0.0045	0.003	122.72	35.00	1.8
*MK3	0.1222921	0.0004	0.002	344.24	216.62	0.035
*SK3	0.1251141	0.0074	0.003	336.61	21.25	5.4
MN4	0.1595106	0.0007	0.004	62.04	225.01	0.029
*M4	0.1610228	0.0094	0.006	93.07	40.12	2.2
SN4	0.1623326	0.0037	0.006	88.90	112.69	0.4
*MS4	0.1638447	0.0098	0.007	140.14	45.46	2.2
S4	0.1666667	0.0036	0.006	220.50	103.47	0.36
*2MK5	0.2028035	0.0018	0.003	319.85	140.22	0.39
*2SK5	0.2084474	0.0018	0.003	230.38	119.09	0.31
2MN6	0.2400221	0.0048	0.003	195.36	37.71	2.6
*M6	0.2415342	0.0016	0.002	61.89	104.71	0.46
*2MS6	0.2443561	0.0038	0.003	107.19	43.88	1.6
*2SM6	0.2471781	0.0018	0.003	152.15	90.31	0.4
*3MK7	0.2833149	0.0007	0.002	135.20	170.42	0.17
M8	0.3220456	0.0047	0.004	328.19	49.28	1.3

1943

**Simulation Tarutao**

nobs = 657, ngood = 657, record length (days) = 41.06

rayleigh criterion = 1.0

var(x)= 0.66332 var(xp)= 0.66035 var(xres)= 0.002461

percent var predicted/var original= 99.6 %

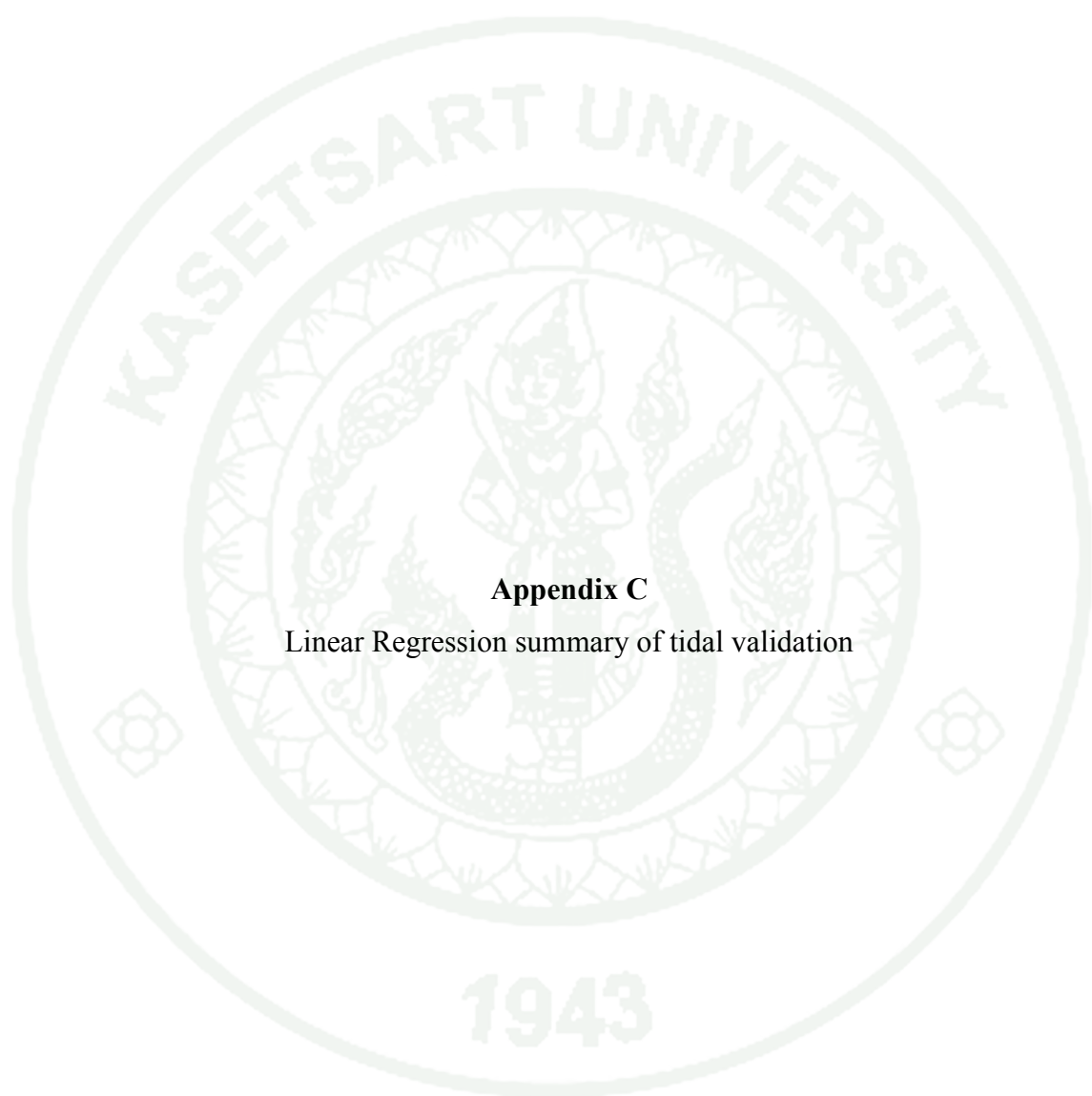
**Appendix Table B8** Tidal amplitude and phase with 95% CI estimates of simulation data at Tarutao Station

Tide	Frequency	Amplitude	Amplitude error	Phase	Phase error	snr
*MM	0.0015122	0.0061	0.005	128.82	41.41	1.7
*MSF	0.0028219	0.0093	0.004	99.35	25.85	4.8
ALP1	0.0343966	0.0026	0.005	325.24	144.45	0.25
2Q1	0.0357064	0.0045	0.006	130.64	86.86	0.6
*Q1	0.0372185	0.0215	0.008	170.66	19.75	7.7
*O1	0.0387307	0.1188	0.008	321.34	3.02	2.5e+02
NO1	0.0402686	0.0075	0.007	308.88	58.98	1.2
*K1	0.0417807	0.2039	0.007	243.67	2.05	8.6e+02
*J1	0.0432929	0.0047	0.006	206.64	75.47	0.57
*OO1	0.0448308	0.0125	0.007	111.76	30.32	2.9
*UPS1	0.046343	0.0024	0.006	111.30	140.54	0.19
*EPS2	0.0761773	0.0093	0.016	293.27	108.01	0.32
*MU2	0.0776895	0.0297	0.020	57.90	38.38	2.3
*N2	0.0789992	0.1944	0.022	221.89	5.82	80
*M2	0.0805114	0.9341	0.022	340.81	1.22	1.8e+03
*L2	0.0820236	0.0100	0.015	265.53	112.08	0.45
*S2	0.0833333	0.5064	0.019	7.03	2.09	6.9e+02
*ETA2	0.0850736	0.0202	0.022	254.22	54.57	0.85
*MO3	0.1192421	0.0099	0.007	147.39	37.28	2

Appendix Table B8 (Continued)

<b>Tide</b>	<b>Frequency</b>	<b>Amplitude</b>	<b>Amplitude error</b>	<b>Phase</b>	<b>Phase error</b>	<b>snr</b>
M3	0.1207671	0.0056	0.006	233.02	75.74	0.85
*MK3	0.1222921	0.0066	0.006	232.22	53.86	1.1
*SK3	0.1251141	0.0029	0.006	171.32	118.74	0.27
MN4	0.1595106	0.0079	0.005	36.00	34.23	2.7
*M4	0.1610228	0.0345	0.004	186.45	7.83	69
SN4	0.1623326	0.0052	0.005	87.64	50.50	1.2
*MS4	0.1638447	0.0259	0.005	188.56	10.65	30
S4	0.1666667	0.0038	0.004	231.01	81.16	0.94
*2MK5	0.2028035	0.0058	0.004	309.70	41.31	2.1
*2SK5	0.2084474	0.0007	0.002	312.99	192.89	0.075
2MN6	0.2400221	0.0096	0.006	323.97	36.80	2.8
*M6	0.2415342	0.0141	0.007	87.73	23.63	4.2
*2MS6	0.2443561	0.0224	0.006	127.43	15.17	16
*2SM6	0.2471781	0.0119	0.006	149.19	28.67	3.5
*3MK7	0.2833149	0.0023	0.002	100.02	54.86	1.5
M8	0.3220456	0.0009	0.001	269.01	117.16	0.44

1943



**Appendix C**

Linear Regression summary of tidal validation

### 1. Comparison of water level between observation and simulation at Ao Por

**Appendix Table C1** Residuals of tidal elevation linear regression between observation and simulation at Ao Por

Minimum	1 <sup>st</sup> Quadrant	Median	3 <sup>rd</sup> Quadrant	Maximum
-0.53585	-0.09802	0.02467	0.11869	0.42756

**Appendix Table C2** Coefficients of tidal elevation linear regression between observation and simulation at Ao Por

	Estimate	Standard Error	t value	Pr(> t )
Intercept	0.043907	0.009623	4.563	7.15e-06 ***
Observation	1.066387	0.011968	89.102	< 2e-16 ***

Significant codes: 0 '\*\*\*' 0.001 '\*\*' 0.01 '\*' 0.05 '.' 0.1 ' ' 1

Residual standard error: 0.1744 on 327 degrees of freedom  
 Multiple R-squared: 0.9604,  
 Adjusted R-squared: 0.9603  
 F-statistic: 7939 on 1 and 327 DF  
 p-value: < 2.2e-16

## 2. Comparison of water level between observation and simulation at Tapao Noi

**Appendix Table C3** Residuals of tidal elevation linear regression between observation and simulation at Tapao Noi

Minimum	1st Quadrant	Median	3rd Quadrant	Maximum
-0.84400	-0.17700	0.03025	0.19877	0.67254

**Appendix Table C4** Coefficients of tidal elevation linear regression between observation and simulation at Tapao Noi

	Estimate	Standard Error	t value	Pr(> t )
Intercept	0.07652	0.01699	4.505	9.27e-06 ***
Observation	1.04811	0.02115	49.564	< 2e-16 ***

Significant codes: 0 '\*\*\*' 0.001 '\*\*' 0.01 '\*' 0.05 '.' 0.1 ' ' 1

Residual standard error: 0.3081 on 327 degrees of freedom

Multiple R-squared: 0.8825

Adjusted R-squared: 0.8822

F-statistic: 2457 on 1 and 327 DF

p-value: < 2.2e-16

### 3. Comparison of water level between observation and simulation at Kuraburi

**Appendix Table C5** Residuals of tidal elevation linear regression between observation and simulation at Kuraburi

Minimum	1 <sup>st</sup> Quadrant	Median	3 <sup>rd</sup> Quadrant	Maximum
-0.50643	-0.10700	0.01482	0.13346	0.33504

**Appendix Table C6** Coefficients of tidal elevation linear regression between observation and simulation at Kuraburi

	Estimate	Standard Error	t value	Pr(> t )
Intercept	-0.003650	0.008975	-0.407	0.684
Observation	1.092458	0.013004	84.012	<2e-16 ***

Significant codes: 0 '\*\*\*' 0.001 '\*\*' 0.01 '\*' 0.05 '.' 0.1 ' ' 1

Residual standard error: 0.1628 on 327 degrees of freedom

Multiple R-squared: 0.9557

Adjusted R-squared: 0.9556

F-statistic: 7058 on 1 and 327 DF

p-value: < 2.2e-16

#### 4. Comparison of water level between observation and simulation at Tarutao

**Appendix Table C7** Residuals of tidal elevation linear regression between observation and simulation at Tarutao

Minimum	1 <sup>st</sup> Quadrant	Median	3 <sup>rd</sup> Quadrant	Maximum
-0.46518	-0.11216	0.01394	0.11647	0.42682

**Appendix Table C8** Coefficients of tidal elevation linear regression between observation and simulation at Tarutao

	Estimate	Standard Error	t value	Pr(> t )
Intercept	0.059374	0.009392	6.322	8.48e-10 ***
Observation	1.013135	0.013292	76.221	< 2e-16 ***

Significant codes: 0 '\*\*\*' 0.001 '\*\*' 0.01 '\*' 0.05 '.' 0.1 ' ' 1

Residual standard error: 0.1703 on 327 degrees of freedom

Multiple R-squared: 0.9467

Adjusted R-squared: 0.9466

F-statistic: 5810 on 1 and 327 DF

p-value: < 2.2e-16

## CURRICULUM VITAE

**NAME** : Ms. Rungtip Junlah

**BIRTH DATE** : March 28, 1990

**BIRTH PLACE** : Loei, Thailand

<b>EDUCATION</b>	<b>:</b>	<b><u>YEAR</u></b>	<b><u>INSTITUTE</u></b>	<b><u>DEGREE/DIPLOMA</u></b>
		2012	Mahidol University	B.Sc. (Hons) (Environmental science and technology)

**POSITION** : -

**WORK PLACE** : -

**SCHOLARSHIP** : Tokyo Institute of Technology (TAIST-Tokyo Tech). 2012-2014